VOLUME XLVIII NUMBER 8, PART I

THE
JOURNAL OF GEOLOGY

November-December 1940

THE THEORY OF GROUND-WATER MOTION

M. KING HUBBERT
Columbia University

ABSTRACT

The existing analytical treatments of ground-water flow have mostly been founded upon the erroneous conception, borrowed from the theory of the flow of the ideal frictionless fluids of classical hydrodynamics, that ground-water motion is derivable from a velocity potential. This conception is in conformity with the principle of the conservation of matter but not with that of the conservation of energy. In the present paper it is shown that a more exceptionless analytical theory results if a potential whose value at a given point is defined to be equal to the work required to transform a unit mass of fluid from an arbitrary standard state to the state at the point in question is employed. Denoting this function by Φ, it is shown that the differential equation of fluid flow in an isotropic medium is given by $\mathbf{q} = -\sigma \operatorname{grad} \Phi$, where $\mathbf{q}$ is the flow vector whose magnitude is equal to the volume of fluid crossing a unit of area normal to the flow direction in unit time, and σ a specific conductivity parameter depending upon both the properties of the fluid and the medium. This is an expression of Darcy's law and is physically, as well as mathematically, analogous to Ohm's law in electricity and leads to the same deductions in analogous situations.

It is shown that $\sigma = k\rho/\eta$, where k is the permeability parameter depending upon the geometrical properties of the medium only and ρ and η are the density and viscosity, respectively, of the fluid.

The remainder of the paper is devoted to deducing the consequences of Darcy's law as just expressed, with particular regard for the practical problems of ground-water hydrology.

INTRODUCTION

Since the pioneer experiments of Darcy[1] on the flow of water through filter sands, a succession of important analytical treatments have appeared in which the flow of ground water has been discussed

[1] Henry Darcy, *Les Fontaines publiques de la ville de Dijon* (Paris: Victor Dalmont, 1856).

as a problem in field theory of mathematical physics. Outstanding among these analytical treatments is the now almost classical study of Slichter[2] and the recent treatments of Dachler[3] and of Muskat.[4]

While the importance of these and similar works cannot be overestimated, they have all fallen short in one or more important respects of the goal of establishing a theory of ground-water motion which is both free from internal contradictions and in conformity with all the fundamental principles of physics which ground-water motion must satisfy. In these treatments ample precaution has been taken not to violate the principle of the conservation of matter, but much less care has been exercised with respect to the equally inviolable first and second laws of thermodynamics.

In the present paper an attempt will be made to establish the theory of ground-water motion upon such a basis that the deduced consequences will be in more complete conformity with the principles of physics than has been the case heretofore. In doing this the entire subject will have to be re-examined from first principles because the contradictions to be avoided are inherent in the fundamental conceptions employed. The results we shall achieve will, in the main, resemble those of the existing treatments, but significant differences will arise where the neglect of energy relationships is nonallowable.

The present treatment will, as far as possible, be logically complete; yet the reader may occasionally feel the need for amplification of fundamental principles that can here be discussed only briefly. For this he is referred to standard treatises of potential theory, thermodynamics, hydrodynamics, dynamic meteorology, heat conduction, and electrodynamics. While many treatises of these various subjects exist, among those that the author has employed extensively are: Planck, *Theory of Heat* and *Thermodynamics;* Gibbs, "On the Equilibrium of Heterogeneous Substances" (in *Collected Works*); Kellogg, *Foundation of Potential Theory;* Coffin, *Vector Analysis;*

[2] C. S. Slichter, "Theoretical Investigation of the Motion of Ground Water," *19th Ann. Rept. U.S. Geol. Surv.*, Part II (1897–98), pp. 295–384.

[3] Robert Dachler, *Grundwasserströmung* (Vienna: J. Springer, 1936).

[4] Morris Muskat, *Flow of Homogeneous Fluids through Porous Media* (New York: McGraw-Hill, 1937).

Ewald, Pöschl, and Prandtl, *The Physics of Solids and Fluids;* Prandtl and Tietjens, *Hydro- and Aerodynamics* (2 vols.); V. Bjerknes, "Dynamic Meteorology and Hydrography" (*Carnegie Inst. Wash. Pub. 88* [1911]); Abraham and Becker, *Classical Electricity and Magnetism;* Page and Adams, *Principles of Electricity.*

For the geological background of ground-water hydrology no better source exists than the publications of the Division of Ground Water of the United States Geological Survey, particularly Meinzer, "The Occurrence of Ground Water in the United States with a Discussion of Principles" (*U.S. Geol. Surv. Water-Supply Paper 489* [1923]). A recent treatment of the same subject is Tolman, *Ground Water.*

THE DARCY EXPERIMENT

The general problem of ground-water motion is principally this: Suppose we are given the complete geometry (at least statistically) of an underground region extending from the earth's surface to some arbitrary depth, and we know the rate of the flow of water across the boundary of the region at all points, what is the nature of the flow at every point in its interior? A variation of this problem that is commonly encountered in practice consists in being given the geometry and the state of flow throughout a region in space and being required to anticipate the changes in the flow system which will result from certain specified alterations to be imposed upon it.

Stated thus broadly, both these problems appear formidable, and indeed are so until we develop certain necessary relationships which will enable us to deal with them. In order to acquire the necessary analytical tools for use in more general problems, we arbitrarily choose a simple flow system which we investigate exhaustively. Having done this, we then shall return with the knowledge thus gained to problems of a more complex nature.

The motion of ground water differs from the more familiar problems of fluid flow in that in this case the flow, instead of occurring in open basins or channels, takes place through an intricately branched network of open spaces interpenetrating a skeletal solid framework. There are, therefore, two distinct and essential elements to every such flow problem: the properties of the fluid, and the properties

of the solid framework or *medium*. The flow properties of the fluid are sufficiently determined for most purposes by its viscosity, η, and its density, ρ.

The two more important properties of the medium are its *porosity* and its *permeability*. The porosity, ϵ, may be defined as the ratio of the free space, or voids, to the total volume. In rocks this ranges from zero to more than 50 per cent. The permeability of the medium pertains to the facility with which fluids flow through it. For the present only a qualitative definition is possible. Of two media through which the same fluid is made to flow under identical conditions, we may say that the one through which the flow is more rapid has the greater permeability. A medium may be said to be *isotropic* with respect to permeability if it is equally permeable to flow in all directions.

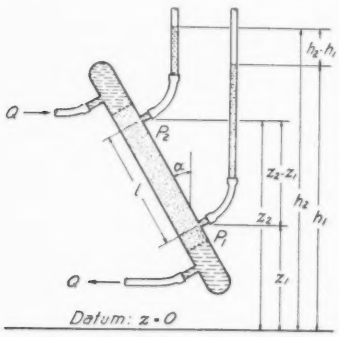

FIG. 1.—Apparatus for studying the flow of liquid through a permeable material.

Now, to begin our analysis, we choose a region of space occupied by a medium which is homogeneous and isotropic with respect to porosity and permeability. We assume, moreover, that the solid framework is insoluble and chemically inert with respect to the fluid passing through it, and ideally rigid. For the region to be investigated we choose a volume whose shape is that of a right circular cylinder of cross-sectional area A and length l, where both A and l are large, compared with the small irregularities or grain-size of the medium. We require that the flow through the volume be rectilinear and in a direction parallel to the axis of the cylinder.

These conditions may be approximately realized experimentally if we construct the apparatus shown in Figure 1. This consists of a large metal cylinder mounted so as to pivot about a horizontal axis perpendicular to its own axis. The mid-section of the cylinder between two screens is filled with sand or other suitable granular material of uniform grade. The ends of the cylinder are closed, but near

each end inlet and outlet hose connections are attached. At points P_1 and P_2 in the same axial line and distance l apart two manometer openings are tapped into the mid-section filled with the permeable material. By means of flexible rubber tubing these are connected with permanently mounted open-topped manometers.

We choose a standard datum of elevation above which the elevations of the points P_1 and P_2 are z_1 and z_2, respectively. We let the angle of tilt of the large cylinder be α, where α is zero when the cylinder is vertical with P_2 above P_1.

Water is made to flow through the system at a total discharge rate of Q units of volume per unit of time. It rises to elevations h_1 and h_2 above the standard datum in the two manometer tubes terminated at P_1 and P_2, respectively.

We now wish to investigate the relations among the several variables of the system. We adopt the convention that the total discharge, Q, is positive when the flow is directed from P_1 to P_2, and negative when from P_2 to P_1. By varying Q we establish the following relationships: When

$$\left.\begin{array}{llll} Q = 0, & h_2 = h_1 & \text{or} & h_2 - h_1 = 0, \\ Q > 0, & h_2 < h_1 & \text{or} & h_2 - h_1 < 0, \\ Q < 0, & h_2 > h_1 & \text{or} & h_2 - h_1 > 0. \end{array}\right\} \tag{1}$$

We also observe that this relationship is one of proportionality and that

$$Q \propto -(h_2 - h_1). \tag{2}$$

We next investigate the effect of changing the angle of tilt α. Letting Q remain constant, we tilt the system so that α assumes all possible values from zero to 180°, and we discover that the results expressed by equations (1) and (2) are in nowise influenced by the value of α, being exactly the same whether the system is upright, inclined, horizontal, or upside down.

Two other important variables of the system whose effects require investigation are the area of cross section A and the length l. This could be done by rebuilding the apparatus and varying first A and then l; but to do so is hardly necessary, since the answers are implicit in the experiment already described.

Consider first the variation of A. Since the direction of the flow is axial, no change will be produced if we insert a thin axial partition dividing the cylinder into two halves of area $A/2$ each and discharge $Q/2$ in each half. In this case the manometer readings, which remain unchanged, are registering the flow in only one-half of the system. Still further partitioning would give us a series of n equal parallel tubes, each conducting water at a rate Q/n, with still no change in the manometer readings, although only the flow Q/n in a tube whose cross section is A/n is being recorded. From this it is clear that a reduction in cross section of the flow system has no influence on the manometer readings provided the discharge across that area is varied at the same rate. This leads us to the conclusion that it is the ratio Q/A which must be kept constant if the manometer readings are not to vary. The total discharge divided by the cross-sectional area is obviously equal to the discharge per unit of area or to the *specific discharge* q. Consequently,

$$\frac{Q}{A} = q \propto -(h_2 - h_1) \tag{3}$$

or, for a given value of the manometer readings,

$$Q = qA\ , \tag{4}$$

where the specific discharge, q, is the constant of proportionality.

In a similar manner we investigate the effect of varying the length l between the bases of the two manometer tubes. The height difference $h_2 - h_1$ is the reaction to the discharge q through the length l. Since the flow is uniform over every cross section of the system, then for length dl there must correspond a fall in h, of dh, such that

$$\frac{dh}{dl} = \frac{h_2 - h_1}{l}\ , \tag{5}$$

and these quantities must be proportional to q. Or, if $(h_2 - h_1)$ is kept constant,

$$Q \propto \frac{1}{l}\ . \tag{6}$$

Now, if we combine the results of equations (2)–(6) into a single expression, we obtain

$$Q = -KA \cdot \frac{h_2 - h_1}{l}; \tag{7}$$

or, by employing the specific discharge q and the differential expression dh/dl,

$$q = \frac{Q}{A} = -K \cdot \frac{dh}{dl}, \tag{8}$$

where K is a constant of proportionality.

With the exception of the variation of the angle of tilt, α, which, as we have seen, produces no effect, the experiment just described is essentially that performed originally by Henry Darcy, whose results are better expressed in his own words:

> Ainsi, en appelant e l'eppaiseur de la couche de sable, P la pression atmosphérique, h la hauteur de l'eau sur cette couche, on aura $P + h$ pour la pression a laquelle sera soumise la base superieure; saient, de plus, $P \pm h_0$ la pression supportié par la surface inferieure, k un coefficient dependant de la perméabilité de la couche, q le volume débité, on a
>
> $$q = k \frac{s}{e} [h + e \pm h_0]$$
>
> qui se réduit à
>
> $$q = k \frac{s}{e} [h + e], \quad \text{quand} \quad h_0 = 0,$$
>
> au lorsque la pression sous le filtre est equal à la pression atmosphérique.[5]

Darcy explains elsewhere that s is the area of cross section. Although the language employed is necessarily somewhat archaic by present standards, it seems clear that his standard datum from which the manometer heights were measured was the lower base of his filter sand. Then $h + e$ is the height in the upper manometer, and h_0 that in the lower, this being either positive or negative, depending upon whether or not a vacuum was employed. It is clear, therefore, that the results announced by Darcy are entirely in accord with those expressed by equations (7) and (8)—a relationship which appropriately has come to be known as "Darcy's law."

[5] *Op. cit.*, pp. 570 ff.

Darcy also noted, significantly, that the relationship was no longer valid for fluid velocities greater than 10–11 cm/sec.

THE PHYSICAL SIGNIFICANCE OF DARCY'S LAW

The relationships embodied in equation (8) form the necessary basis upon which any analytical theory of ground-water motion must rest; but the method of obtaining this equation has been empirical, and, expressed in this primitive form, the equation is of slight usefulness because it expresses only what we have learned already and gives us no insight into the deeper mechanism of fluid flow.

What determines the direction of the fluid flow in the first place? What would be the effect if we changed from a finer to a coarser sand? How would the flow rate be altered if we changed the viscosity or the density of the fluid? These and other similar ones are questions that equation (8) does not answer; yet they are questions to which it is highly important that answers be known.

Let us consider first the question of what determines the direction of the fluid motion, that is, whether the flow in Figure 1 is to be directed from P_1 to P_2 or from P_2 to P_1. We obviously cannot say that elevation is the determining factor, because, as we have seen already, if the flow is initially from a higher to a lower elevation, an inversion of the system changes the flow from a lower to a higher elevation without affecting in the slightest degree either its rate or the readings of the manometers.

If it is not elevation, perhaps it is the fluid pressure that is the determining factor in the flow, with the flow always directed away from regions where the pressure is higher and toward those where it is lower. In fact, the great majority of all writers upon this subject have stated that this is so, and many have employed equations of the form

$$q = -K' \cdot \frac{dp}{dl} \tag{9}$$

as a statement of Darcy's law, presumably under the impression that equations (8) and (9) are physically equivalent statements.

Whether or not this is so may readily be determined in the following manner: At any point P in a flow system whose elevation

above the standard datum is z, we terminate a manometer tube in which the liquid rises to a height h above the datum. The pressure at the point P is determined by the height of the liquid column above P and is given by

$$p = \rho g(h - z) + p_0 , \tag{10}$$

where p is the pressure, ρ the density of the liquid, g the acceleration due to gravity, and p_0 the pressure of the atmosphere. Now, if we apply equation (10) to the points P_1 and P_2 of Figure 1, we obtain

$$\left.\begin{aligned} p_1 &= \rho g(h_1 - z_1) + p_0 , \\ p_2 &= \rho g(h_2 - z_2) + p_0 , \end{aligned}\right\} \tag{11}$$

and the difference between the pressures at the two points is

$$p_2 - p_1 = \rho g(h_2 - h_1) - \rho g(z_2 - z_1) . \tag{12}$$

Now we already know that as $(h_2 - h_1) \to 0$, $q \to 0$; but in that case p_1 is less than p_2 by the quantity $\rho g(z_2 - z_1)$, which gives us a case where the flow is zero when one of the two pressures is greater than the other. Next, suppose we make h_2 slightly greater than h_1, which will correspond to flow from P_2 to P_1, but still not great enough for $(h_2 - h_1)$ to equal $(z_2 - z_1)$. In this case the pressure p_2 will still be less than p_1, and we shall have flow from a region of lower to one of higher pressure. Then if we invert the system by rotation through 180° about a horizontal axis, the pressure at P_2 will become greater than that at P_1 without the rate of flow or the manometer reading being changed. Consequently, we must conclude that a liquid can with equal facility be made to flow from a region of higher to one of lower pressure, or from a region of lower to one of higher, quite arbitrarily.

To investigate equation (9) we need only to express equation (12) differentially:

$$\frac{dp}{dl} = \rho g \cdot \frac{dh}{dl} - \rho g \cdot \frac{dz}{dl} . \tag{13}$$

But

$$\frac{dz}{dl} = \cos \alpha \,, \tag{14}$$

so that when we insert this into equation (13) we obtain

$$\frac{dp}{dl} = \rho g \cdot \frac{dh}{dl} - \rho g \cos \alpha \,. \tag{15}$$

When this is substituted into equation (9), it gives

$$q = -K' \rho g \left(\frac{dh}{dl} - \cos \alpha \right), \tag{16}$$

which is manifestly not equivalent to equation (8) under any condition except when the second term, that of cos α, is negligible, compared with the first. This is only true either when cos α is approximately zero, corresponding to nearly horizontal flow, or when dh/dl is very large, compared with unity, the maximum value of cos α.

In the experiment of Figure 1, and in ground-water motion in general, the direction of flow may have any inclination from vertical to horizontal, so that the assumption of cos $\alpha = 0$ is not tenable. Moreover, dh/dl is ordinarily very much smaller than unity, the maximum value of cos α. Hence, in problems of ground-water flow, equation (9) is not only not equivalent to Darcy's law, as expressed by equation (8), but is not even a valid approximation to it. Consequently, the employment of equation (9) or any equivalent statement wherein the rate of flow is assumed to be proportional to the pressure gradient, when dealing with ground-water problems, is to be ruled out on the grounds of being physically erroneous.

When dealing with the flow of gases, on the other hand, dh/dl, or its equivalent, may be large, compared with cos α, in which case the employment of equation (9) becomes an allowable approximation.

What, then, does determine the direction of the flow? What we still seek to find is some physical quantity, capable of measurement at every point in a flow system, whose properties are such that the flow always occurs from regions in which the quantity has higher values to those in which it has lower, regardless of the direction in

space. What we have demonstrated so far is that neither elevation nor pressure is such a quantity.

Formally, the manometer height h satisfies this condition entirely, but to adopt it empirically without further investigation would be like reading the length of the mercury column of a thermometer without knowing that temperature was the physical quantity being indicated. The quantity we seek, therefore, is evidently the hidden physical quantity whose magnitude is indicated by the height h of the liquid in the manometer tube, measured from a standard datum.

The clue to this quantity is to be found if we direct our attention momentarily to an apparently irrelevant experiment. Suppose we take a simple pendulum, start it swinging with a wide amplitude, and then leave it entirely free from outside disturbance. We record its motion by means of time exposures taken periodically, the time of each exposure being made equal to the period of the pendulum. We shuffle the photographs and ask a second person to arrange them in chronological order. This is illustrated by Figure 2, where A, B, C, D, and E are prints selected at random, and the problem is to determine the chronological order in which the exposures were made.

By inspection we would say that the order was D, B, E, A, and C, because this is the order of decreasing amplitude of swing, and our experience tells us that an isolated pendulum always swings with decreasing amplitude—never the reverse.

We have, therefore, an experimental process which only goes in a single direction, and it is this unidirectional characteristic that we wish to consider. This we may best do by taking into account the energy transformations of the process. To set the pendulum swinging in the first place, we had to give it an initial supply of potential energy. As it swung back and forth, there were periodical transformations of potential energy to kinetic energy and back to potential energy again, the sum of the two comprising the mechanical energy of the system and remaining constant for constant amplitude of swing. But we have noted already that the amplitude continuously diminished; consequently, there must have been a continuous dissipation of the mechanical energy initially supplied to the system. Also, ultimate equilibrium corresponds to a state of rest with the pendulum at its lowest possible position, that is to say, with the

kinetic energy of the system equal to zero, and the potential energy the minimum possible compatible with the constraints of the system.

We know, moreover, that the progressive decrease in the amplitude of swing is due to frictional resistances; and, by the principle of the conservation of energy, we know that the mechanical energy lost by the system reappears as heat at the temperature of the surroundings. Now, if we could transform this thermal energy back to mechanical energy again without other permanent changes, then we could remotivate the pendulum, allowing it to use over and over again the same energy, which would be a form of perpetual motion.

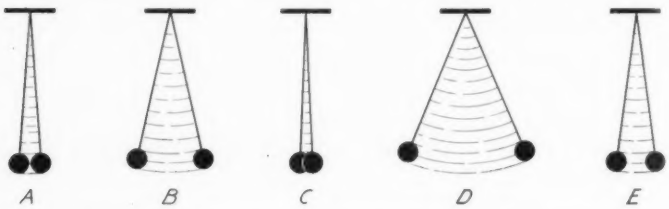

FIG. 2.—Unidirectional and irreversible transformation of isolated mechanical system.

Our purely negative experience in this connection leads to the conclusion that such a process is impossible, and a generalization of this fact so as to apply to all manner of processes gives us the Second Law of Thermodynamics, which states, in essence, that any material transformation which involves friction, or its equivalent, is unidirectional and irreversible in character, meaning that, once the process has taken place, by no method whatsoever can it be undone again. In other words, if we have any initial configuration of matter in an isolated system, and this configuration undergoes spontaneous change accompanied by friction, it is quite impossible ever to restore the matter contained within that system to its initial configuration and at the same time leave the material configuration external to that system undisturbed.

It is this method of reasoning that we now wish to employ with respect to our problem of fluid flow. The flow of a fluid is a mechanical process; and, when the fluid has viscosity and the flow occurs through the small passages of porous rocks, friction is not only

present but is one of the dominant influences in the process. Consequently, if such flow occurs at all, it must be accompanied by an irreversible transformation of mechanical to thermal energy through the mechanism of fluid friction. Furthermore, like the pendulum, final equilibrium must correspond to a configuration in which the kinetic energy is zero; and the potential energy, the minimum possible compatible with the constraints of the system. Hence, to have flow, there must have been supplied an initial store of mechanical energy, and the changes that occur thereafter must always be in the direction of a decrease by dissipation into heat of this mechanical energy.

So far this gives the generalized direction of the process but not the geometrical direction of the flow in space. The latter is obtained, however, when we consider that the mechanical energy of the system is associated with the elements of its mass or volume and that these occupy particular positions in space. The direction of the flow in space must therefore be away from regions in which the mechanical energy per unit of mass is higher and toward regions in which it is lower.

It is not to be inferred that the energy which a system possesses in consequence of the fact that an element of mass occupies a given position resides upon or within the mass element. For example, the potential energy $U = gz$ of a unit mass due to the earth's gravitational field is an energy of the unit mass and the earth considered as a single system; yet we may unambiguously refer this energy to the unit mass at a specified position. This same is true of the fluid system with which we now deal.

The mechanical energy of the fluid per unit of mass is, therefore, evidently the physical quantity we set out to find; and hereafter we shall refer to it as the *potential* of the fluid in question, there being as many distinct potentials as there are distinct fluids to be dealt with.

Our problem now resolves itself into the determination of the fluid potential, or mechanical energy per unit of mass, of the given fluid at any arbitrary point in space. To obtain this we note first that energy is a relative quantity and is measurable by the amount of work required to effect any given transformation from some arbi-

trary initial state to a specified final state. The potential of a fluid at a specified point is, accordingly, the work required to transform a unit of mass of the fluid from an arbitrarily chosen standard state to the state at the point under consideration. For the standard state it is convenient to employ an elevation of zero, a pressure of 1 atmosphere, and a velocity of zero (relative to the earth's surface). Let the fluid in its final state at the point P be characterized by an elevation z, a pressure p, and a velocity v. We may also let V_0 be the volume per unit mass, or specific volume, of the fluid in its standard state, and V be that for the final state. Let the corresponding densities be ρ_0 and ρ. We may also note that the density is the reciprocal of the specific volume: $V = 1/\rho$.

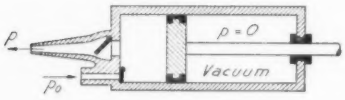

FIG. 3.—Pump for transforming liquid from standard to final state.

We wish to find the work required to transform a unit mass of the fluid from the initial to the final state, and to do this we imagine a pump constructed along the lines indicated by Figure 3. This consists of a cylinder with frictionless piston, on the front of which is the fluid chamber and on the back a perfect vacuum. Inlet and outlet valves are provided. We then imagine the transformation to be effected by the following successive steps:

1. Under standard conditions we slowly withdraw the piston and charge the cylinder with unit mass of the fluid. The work done by the piston on the fluid is then

$$w_1 = -p_0 V_0 . \tag{17}$$

2. Next we lift the pump with its fluid contents to the point P of elevation z. The work expended for this is

$$w_2 = +gz + m_p g z , \tag{18}$$

where gz is the work required to lift the unit mass of the fluid, and $m_p g z$ that required to lift the pump alone.

3. The contents of the cylinder are injected into the system at point P. The work required for this is

$$w_3 = +\int_V^{V_0} p \cdot dV + pV \,. \tag{19}$$

The first term to the right of equation (19) is the work of compression of the fluid in order to raise its pressure from p_0 to p before it can be injected. The pV term is the work of injection against the pressure p.

4. The fluid is accelerated from a velocity of zero to that of v, requiring an amount of work

$$w_4 = +\frac{v^2}{2} \,. \tag{20}$$

5. The cylinder is returned to its initial position at zero elevation, thus completing the cycle. This requires an amount of work

$$w_5 = -m_p g z \,. \tag{21}$$

The sum of these separate amounts of work is the potential Φ of the fluid at the point P. Performing the addition and canceling out terms that repeat with opposite signs gives us

$$\Phi = gz - p_0 V_0 + \int_V^{V_0} p dV + pV + \frac{v^2}{2} \,. \tag{22}$$

In this, the first and last terms on the right-hand side are the gravitational potential energy and the kinetic energy, respectively. The significance of the other three terms is best visualized by means of the "indicator diagram" of Figure 4, in which the pressure in the cylinder is plotted against piston displacement for both compressible and incompressible fluids. If the fluid is incompressible, a condition satisfied approximately by liquids under ordinary pressure ranges,

$$\int p \cdot dV = 0 \qquad \text{and} \qquad V = V_0 \,. \tag{23}$$

In this case the pressure-volume work reduces to $(p - p_0)V$, and equation (22) simplifies to

$$\Phi = gz + (p - p_0)V + \frac{v^2}{2}. \tag{24}$$

By a mathematical transformation we can convert equation (22) into another form whose physical significance may not be im-

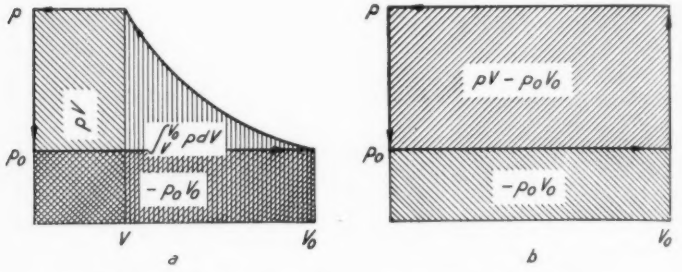

FIG. 4.—Pump indicator diagrams: *a*, for gases; *b*, for liquids

mediately apparent but which will prove to be of great usefulness later. To effect this we make use of the fact that

$$d(pV) = p \cdot dV + V \cdot dp,$$

or

$$\int p \cdot dV = \int d(pV) - \int V \cdot dp. \tag{25}$$

Then, as a definite integral, this becomes

$$\left.\begin{aligned} \int_V^{V_0} p \cdot dV = \int_{pV}^{p_0V_0} d(pV) - \int_p^{p_0} V \cdot dp = p_0V_0 - pV \\ + \int_{p_0}^{p} V \cdot dp. \end{aligned}\right\} \tag{26}$$

Substituting this value for $\int_V^{V_0} p\,dV$ into equation (22) transforms that equation into

$$\Phi = gz + \int_{p_0}^{p} V \cdot dp + \frac{v^2}{2}, \tag{27}$$

which, when we substitute $1/\rho$ for V, becomes

$$\Phi = gz + \int_{p_0}^{p} \frac{dp}{\rho} + \frac{v^2}{2} . \tag{28}$$

A graphical interpretation of equation (26) is readily afforded by noting that the area enclosed by the indicator diagram of Figure 4, *a*, is equal to the work performed by the pump per cycle and that this is given by $\int_{p_0}^{p} V \cdot dp$ or by $\int_{p_0}^{p} \frac{dp}{\rho}$.

Equation (28) is an expression for the fluid potential at a point P in the most general form that we shall require. In order for the value of Φ so defined to be unique, however, it is necessary to stipulate that the density of the fluid must be a function of the pressure only, for otherwise the value of $\int_{p_0}^{p} V dp$ will be indeterminate. For liquids this condition is automatically complied with to the extent that their densities may be regarded as constant. For gases it is satisfied by isothermal conditions, which for many problems is a satisfactory approximation, and also by adiabatic conditions, which are of great importance in meteorology.

If the fluid flows without friction, as is approximately the case for liquids of small viscosity and gases, when moving in large open spaces, then each element of mass retains its mechanical energy undiminished, and along any given path of fluid flow each unit of mass will have the same energy and potential. For that case

$$\Phi = gz + \int_{p_0}^{p} \frac{dp}{\rho} + \frac{v^2}{2} = \text{constant} , \tag{29}$$

which is a generalization of a celebrated theorem announced in 1738 by Daniel Bernoulli relating the elevation, pressure, and velocity along a given flowline of a fluid in frictionless flow.

If the flow is not frictionless, as is pre-eminently the case with ground water and similar fluid flow, then the mechanical energy initially possessed by an element of the fluid must continuously be dissipated as this element traverses its path of flow. Consequently,

the value of Φ in this instance must continuously decrease in the direction of the flow.

Another consequence of friction in ground-water motion is to damp out any large velocities, the flow velocity of ground water being rarely as great as 1 cm/sec and commonly of the order of a few centimeters per day. For our purposes we can accordingly neglect the kinetic energy term $v^2/2$ as being negligible in comparison with the other terms of the equation for the potential. This simplifies the expression for the potential down to

$$\Phi = gz + \int_{p_0}^{p} \frac{dp}{\rho}, \tag{30}$$

which, for liquids, reduces still farther to

$$\Phi = gz + \frac{p - p_0}{\rho}. \tag{31}$$

Now, in order to be able to measure Φ at any point P of elevation z and pressure p in a liquid flow system, suppose we return to our earlier device of terminating at the point P a manometer tube into which the liquid rises to the height h above the standard datum. The pressure p in terms of the manometer reading and the elevation z is then given by equation (10). When this is substituted into equation (31), we obtain the remarkably simple result

$$\Phi = gz + \frac{[\rho g(h - z) + p_0] - p_0}{\rho} = gh. \tag{32}$$

Hence the fluid potential is indeed the hidden physical quantity we originally set out to discover, since its magnitude is indicated by the height h of the manometer and is numerically equal to h multiplied by the acceleration due to gravity.

With this background, let us return now to the results of the Darcy experiment as expressed empirically by equation (8). From equation (32)

$$\frac{dh}{dl} = \frac{1}{g} \cdot \frac{d\Phi}{dl}, \tag{33}$$

which, when employed in conjunction with equation (8), gives the two equivalent alternative expressions of Darcy's law:

$$q = -K \cdot \frac{dh}{dl} = -K \cdot \frac{1}{g} \cdot \frac{d\Phi}{dl}. \tag{34}$$

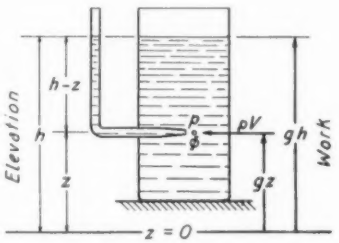

FIG. 5.—Fluid potential at any point inside a body of static liquid

ANALYSIS OF THE PARAMETER K

Our next task is to analyze the parameter K. In the experiment of Figure 1 we investigated certain variables whose effects are stated explicitly in equation (8), but in performing this experiment we arbitrarily kept all other factors constant except the particular ones under investigation. The experiment, however, was incomplete in that a number of possible variables were not taken into consideration. What, for example, would have been the effect of a change of the density or the viscosity of the fluid, of the coarseness of the sand, or of other possible variables of the system?

Manifestly, all these other variables were included in the stipulation "all else remaining constant"; and their combined effects are lumped together into the "constant" of proportionality K, which is accordingly, therefore, not a true constant but a variable parameter whose value depends upon those of the lumped variables. It is important that we find these hidden variables so that we can include them explicitly in our flow equation, enabling us to eliminate K entirely. To do this we must delve somewhat more deeply than heretofore into the mechanics of fluid flow.

In what follows, two different points of view—the microscopic and

the macroscopic—distinguished from one another by the size scale adopted, will prove useful. When we employ the microscopic point of view, we shall be concerned with fluid elements that are large compared with the kinetic irregularities of molecular motion but smaller than the open passages of the medium. When we employ the macroscopic point of view, the fluid elements we speak of shall be large enough that the irregularities of flow due to the medium need not be considered, but only the statistical resultant.

In order to determine what the various factors are that influence the rate of flow, and the part they play, we need to know what the forces are that act upon the fluid elements and upon what these depend. To determine these we shall stipulate that the flow through the sand in the apparatus of Figure 1 be kept *steady*, that is, not changing with time, which will be accomplished if we maintain q constant at any arbitrarily chosen value. Then we adopt the microscopic point of view in order to examine the flow in some detail.

When seen on this scale, the flow will consist of the passage of the fluid through an intricate, branching, three-dimensional network of interstices, analogous to the two-dimensional flow of a river through a complex of small islands. If we choose a particular point, fixed with respect to the framework, then a fluid particle passing through this point will follow a definite path, or *streamline*, and every other particle passing through the same point will transverse the same path and assume the same velocities at corresponding points along the path. Consequently, to every fixed point within the flow system there corresponds a particular fluid velocity, both in magnitude and direction, and through each point there passes a particular streamline. We may accordingly think of the flow as being represented by a family of streamlines, one passing through each point, or by a *field of velocity vectors*, one terminated at each fixed point occupied by the fluid.

In addition to this, around any fixed point we may take a small volume element, also fixed with respect to the framework. While the fluid continuously flows through such an element, at every instant the volume element is occupied by a particular element of the fluid. The forces acting upon this element are of two kinds: those that act upon its surface, or *surface* forces, and those that act upon

the mass within the volume element, or *body* forces. If dV is the volume of the element, then $\rho \cdot dV$ will be its mass, and by Newton's laws of motion the sum of the applied forces is equal to the product of the mass by its acceleration. Then

$$\rho \cdot dV \cdot \mathbf{a} = \mathbf{f}_a + \mathbf{f}_b , \tag{35}$$

where the vector $\mathbf{a}$ is the acceleration and the vectors $\mathbf{f}_a$ and $\mathbf{f}_b$ the surface and body forces, respectively.

Now, by the D'Alembert principle, we can introduce a fictitious force

$$\mathbf{f}_i = -\rho \cdot dV\mathbf{a} , \tag{36}$$

which is the reaction due to inertia of the body to the applied forces $\mathbf{f}_a$ and $\mathbf{f}_b$. Then we have

$$-\mathbf{f}_i = \mathbf{f}_a + \mathbf{f}_b , \qquad \text{or} \qquad \mathbf{f}_i + \mathbf{f}_a + \mathbf{f}_b = 0 , \tag{37}$$

which tells us that the moving element of fluid is in a state of dynamic equilibrium under these three forces in a manner quite analogous to the more familiar static equilibrium.

A more useful classification of the forces acting upon the fluid element is upon the basis of function. On this basis we may speak of a *driving* force $\mathbf{f}_d$, a resistive force arising from frictional resistance due to the fluid viscosity, $\mathbf{f}_r$, and a reactive force due to the inertial reaction to acceleration $\mathbf{f}_i$. We may think of $\mathbf{f}_d$ as being the independently variable force which supplies the energy to the fluid element. Both $\mathbf{f}_r$ and $\mathbf{f}_i$ are dependent variables, depending only upon the state of motion of the fluid and being zero when the fluid motion is zero. The inertial force, $\mathbf{f}_i$, neither contributes energy to nor subtracts it from the system, whereas $\mathbf{f}_r$ is the energy-dissipating force.

From this it is clear that $\mathbf{f}_d$ and $\mathbf{f}_r$ are the principal forces from the point of view of function, while $\mathbf{f}_i$ plays the role of a superimposed modifying influence.

In order to discover the factors which determine $\mathbf{f}_i$ and $\mathbf{f}_r$, the microscopic viewpoint is necessary. The driving force, $\mathbf{f}_d$, can also be deduced from this viewpoint, but to do so is unduly complicated.

We shall accordingly investigate the forces $\mathbf{f}_i$ and $\mathbf{f}_r$ acting upon a microscopic element and shall then extend our results by integration to a macroscopic volume element before deriving $\mathbf{f}_d$. On a microscopic scale, however, when $\mathbf{f}_i$ and $\mathbf{f}_r$ are known, $\mathbf{f}_d$, being the sum of these two, is uniquely determined.

In order to investigate the forces due to inertia and to viscosity, let us erect co-ordinate axes with the x-axis parallel to the direction

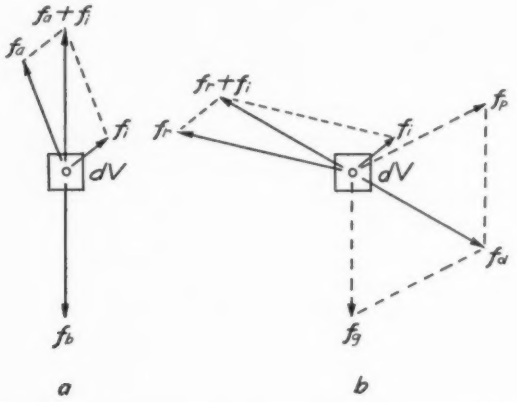

FIG. 6.—The forces which act upon a microscopic fluid element classified *a* as surface force, body force, and inertial force and *b* as driving force, resistive force, and inertial force.

of fluid flow. We let the volume element dV have lengths of side dx, dy, and dz. We let u, v, and w be the components of the velocity parallel to the x-, the y-, and the z-axes, respectively.

Taking first the force due to inertia, we resolve the force and the acceleration upon which it depends into components parallel to the separate axes. Taking the x-component,

$$a_x = \frac{du}{dt} = \frac{\partial u}{\partial t} + \frac{\partial u}{\partial x} \cdot \frac{\partial x}{\partial t} + \frac{\partial u}{\partial y} \cdot \frac{\partial y}{\partial t} + \frac{\partial u}{\partial z} \cdot \frac{\partial z}{\partial t}, \qquad (38)$$

where $\partial u/\partial t$ signifies the change of u with time at a particular point, $\partial u/\partial x$ the change of u with x at a particular time, and $\partial x/\partial t$ the

change of the x-co-ordinate with time, of a particular particle, and so for the other terms. But

$$\left.\begin{aligned} \frac{\partial x}{\partial t} &= u\,, \\ \frac{\partial y}{\partial t} &= v = 0\,, \\ \frac{\partial z}{\partial t} &= w = 0\,, \end{aligned}\right\} \tag{39}$$

and, for steady motion,

$$\frac{\partial u}{\partial t} = 0\,. \tag{40}$$

Then, in this special case equation (38) simplifies to

$$a_x = u \cdot \frac{\partial u}{\partial x}\,, \tag{41}$$

and the force component is

$$f_{ix} = -\rho \cdot dV \cdot u \cdot \frac{\partial u}{\partial x}\,. \tag{42}$$

Similar expressions obtain for the components parallel to each of the other axes; but all that concerns us is the *form* of equation (42), so that we do not need to consider the matter in greater detail.

Now let us consider the force due to viscosity. Upon the y and z faces of the volume-element shear stresses will act. Let τ_{yx} be the shear stress parallel to the x-axis upon the y-face whose outward directed normal is toward the negative end of the y-axis. Upon the opposite face let the corresponding stress be $\tau_{yx} + (\partial\tau_{yx}/\partial y)dy$. Then the net force parallel to the x-axis produced by these two stresses will be

$$f_{\tau yx} = \left(\tau_{yx} + \frac{\partial\tau_{yx}}{\partial y} \cdot dy\right) dxdz - \tau_{yx} \cdot dxdz = +\frac{\partial\tau_{yx}}{\partial y} \cdot dV\,. \tag{43}$$

Complete elaboration would provide additional terms, but again they would all be of the form of the right-hand term of equation (43).

Our next problem is to relate the shear stress acting upon the surface of a fluid element with the state of its flow. By Newton's law of viscosity the rate of shear in a viscous fluid is proportional to the intensity of the shear stress acting upon it. If γ_{yx} is the change of

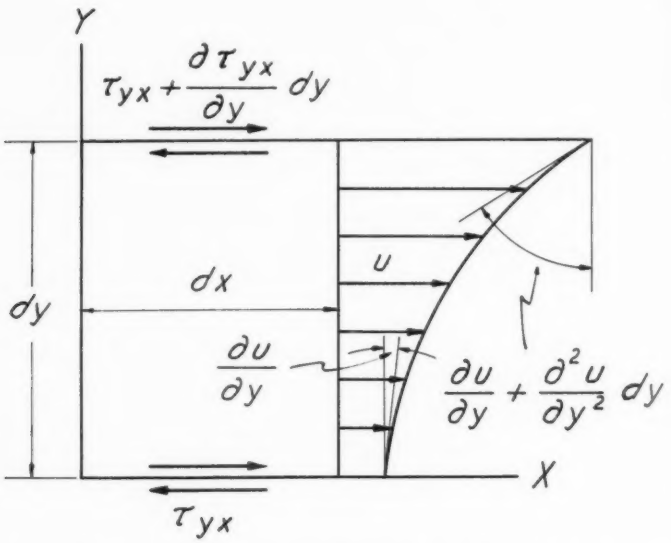

FIG. 7.—Manner of dependence upon the fluid velocity gradients of shearing stresses and unbalanced frictional forces acting upon microscopic fluid element.

an original right angle in the fluid with sides parallel to the x- and y-axes, then $d\gamma_{yx}/dt$ is the time rate of the shear, and

$$\tau_{yx} = \eta \cdot \frac{d\gamma_{yx}}{dt}, \tag{44}$$

where the constant of proportionality η is the viscosity of the fluid. But

$$d\gamma_{yx} = \frac{\left(u + \frac{\partial u}{\partial y} \cdot dy\right) dt - u dt}{dy} = \frac{\partial u}{\partial y} \cdot dt, \tag{45}$$

from which we obtain

$$\frac{d\gamma_{yx}}{dt} = \frac{\partial u}{\partial y}, \tag{46}$$

which, when substituted into equation (44), gives

$$\tau_{yx} = \eta \cdot \frac{\partial u}{\partial y}. \tag{47}$$

Now if we differentiate this with respect to y,

$$\frac{\partial \tau_{yx}}{\partial y} = \eta \cdot \frac{\partial^2 u}{\partial y^2}, \tag{48}$$

which can then be substituted into equation (43), with the result that

$$f_{ryx} = \eta \cdot \frac{\partial^2 u}{\partial y^2} \cdot dV. \tag{49}$$

What we are interested in finding is the manner in which the inertial and resistive forces vary with the specific discharge q and with a change of scale of the medium. For generality, suppose that we have two *geometrically similar* media of different-length scales, and through these we cause two different fluids to undergo *kinematically similar* flow. Geometrical similarity requires that all corresponding lengths of the two systems must have a constant ratio

$$\frac{l_2}{l_1} = \frac{d_2}{d_1}, \tag{50}$$

where d_1 and d_2 are corresponding grain diameters of the two systems, these being taken as characteristic lengths.

Kinematic similarity requires the two flow systems to be exact replicas of one another except for the length and time scales. All streamlines must be geometrically similar, and all corresponding velocities must have identical directions and proportional magnitudes. Since the specific discharge q has the dimensions

$$[q] = \left[\frac{\dfrac{\text{Volume}}{\text{Area}}}{\text{Time}}\right] = [LT^{-1}] = [\text{Velocity}], \tag{51}$$

this represents a generalized velocity. Consequently, in kinematically similar flow all corresponding velocities must bear to each other the ratio

$$\frac{v_2}{v_1} = \frac{q_2}{q_1}. \tag{52}$$

Finally, since forces act at all points upon a fluid in motion, in order for two flows to be kinematically similar, it is necessary for all corresponding forces of the two systems to be similar, that is, to have identical directions and proportional magnitudes:

$$\frac{f_{i2}}{f_{i1}} = \frac{f_{r2}}{f_{r1}} = \frac{f_{d2}}{f_{d1}}. \tag{53}$$

This also necessitates that the corresponding force-equilibrium triangles of the two systems must be similar, so that

$$f_{i1} : f_{r1} : f_{d1} :: f_{i2} : f_{r2} : f_{d2} \tag{54}$$

or

$$\frac{f_{i1}}{f_{r1}} = \frac{f_{i2}}{f_{r2}}. \tag{55}$$

The manner in which the terms of equation (55) depend upon the velocity and the length scales is given by equations (42) and (49). For either of the two flow systems

$$\frac{f_i}{f_r} \propto \frac{f_{ix}}{f_{ryz}} = \frac{\rho u \cdot \dfrac{\partial u}{\partial x} \cdot dV}{\eta \dfrac{\partial^2 u}{\partial y^2} \cdot dV}. \tag{56}$$

In this

$$u \propto q, \qquad \text{and} \qquad \frac{\partial u}{\partial x} \propto \frac{q}{d}. \tag{57}$$

Similarly,

$$\frac{\partial^2 u}{\partial y^2} = \frac{\partial}{\partial y}\left(\frac{\partial u}{\partial y}\right) \propto \frac{q}{d^2}. \tag{58}$$

Substituting these results into equation (56) gives

$$\frac{f_i}{f_r} \propto \frac{\rho \cdot \frac{q^2}{d}}{\eta \cdot \frac{q}{d^2}} = \frac{qd}{\frac{\eta}{\rho}} = R . \tag{59}$$

Since equations (56)–(59) are identical for the two kinematically similar systems, then it follows that the quantity R defined by equation (59) must be the same for each. R is known as the Reynolds' number of the system, so called in honor of Osborne Reynolds,[6] whose pioneer studies first disclosed its significance.

It is important that the generality of equation (59) be appreciated, for, since it applies equally well to either of two kinematically similar systems, then

$$\frac{q_1 d_1}{\frac{\eta_1}{\rho_1}} = \frac{q_2 d_2}{\frac{\eta_2}{\rho_2}} = R , \tag{59a}$$

even though the length scales, the discharges, and the viscosity and density of the fluids may differ widely in the two cases.

Conversely, any two states of flow through geometrically similar frameworks will be kinematically similar when both have the same value of Reynolds' number; but for the same fluid in the same framework, since R is proportional to q, this condition cannot strictly be satisfied for different velocities of flow. Practically, it is satisfied for very small values of R, since, while both f_i and f_r tend to zero as q tends to zero, f_i decreases faster than f_r, and their ratio, which is proportional to R, tends also to zero as q and R tend to zero—the so-called "creeping motion" of flow. When f_i is negligible compared with f_r, then our force equilibrium becomes simply

$$\mathbf{f}_r = -\mathbf{f}_d \tag{60}$$

for every volume element within the flow system.

[6] "An Experimental Investigation of the Circumstances Which Determine Whether the Motion of Water Shall Be Direct or Sinuous and of the Law of Resistance in Parallel Channels," *Phil. Trans. Royal Soc. London*, Vol. 174 (1883), pp. 935–82; also *Papers on Mechanical and Physical Subjects* (Cambridge: University Press, 1901), Vol. II, pp. 51–105.

Now, if we agree to keep the flow velocities small enough so that the forces due to inertia are negligible and so that, therefore, equation (60) is valid, we can integrate f_r over all the microscopic volume elements of a macroscopic volume. The resultant will be $\mathbf{F}_r$, the resistive force acting upon the macroscopic element of volume. To perform this integration we observe that at every point f_r is directed parallel to the streamline, and, at least in the majority of cases, opposite to the direction of motion. Also, at each point f_r is proportional in magnitude to the velocity vector v.

Suppose the macroscopic flow is uniform and rectilinear. Then, if we choose an axis parallel to this macroscopic flow direction, we can resolve the microscopic velocity at every point into an axial component $v \cos \theta$ and a normal component $v \sin \theta$, where θ is the angle the streamline makes with this axis. Since the net fluid motion normal to the axis is zero, then there must be an equal number of normal components in all directions, so that they cancel one another completely.

The axial components, on the contrary, all have the same direction; and their average value, $\bar{v}$, over a macroscopic volume element is to be obtained by integration:

$$\bar{v} = \iiint_{\epsilon \cdot \Delta V} \frac{v \cos \theta \cdot dV}{\epsilon \cdot \Delta V} = \frac{q}{\epsilon}. \tag{61}$$

The product $\epsilon \cdot \Delta V$ is the fraction of a macroscopic volume that is occupied by the fluid, and division by this quantity of the integral of equation (61) is necessary to obtain the average velocity. Otherwise we would have the *sum* of the axial components.

Now, bearing in mind that f_r is proportional to v, it, too, can be resolved into radial and axial components and integrated. For the radial components

$$\iiint_{\epsilon \cdot \Delta V} f_r \sin \theta \cdot dV \propto \iiint_{\epsilon \cdot \Delta V} v \sin \theta \cdot dV = 0. \tag{62}$$

This leaves only the axial components whose algebraic sum or integral over the volume $\epsilon \cdot \Delta V$ is the macroscopic resistive force $\mathbf{F}_r$:

$$\int\int\int_{\epsilon \cdot \Delta V} f_r \cos\theta \cdot dV = \mathbf{F}_r \propto -\eta \cdot \frac{\mathbf{q}}{d^2} \cdot \epsilon \cdot \Delta V . \tag{63}$$

Now, if we let $1/N$ be the constant of proportionality, we may write for the resistive force:

$$\mathbf{F}_r = -\frac{1}{N} \cdot \eta \cdot \frac{\mathbf{q}}{d^2} \cdot \epsilon \cdot \Delta V . \tag{64}$$

If we divide this by $\rho\epsilon \cdot \Delta V$, we shall obtain

$$\frac{\mathbf{F}_r}{\rho\epsilon \cdot \Delta V} = -\frac{1}{N} \cdot \frac{\eta}{\rho} \cdot \frac{\mathbf{q}}{d^2} , \tag{65}$$

which is the resistive force per unit of fluid mass.

On the macroscopic scale the two forces which act upon the fluid contained in a volume element ΔV are the driving force and the resistive force, and these must be equal in magnitude and opposite in direction, so that

$$\mathbf{F}_r = -\mathbf{F}_d . \tag{66}$$

Also, the directions of both of these forces must be parallel to the macroscopic direction of flow, $\mathbf{F}_d$ in the direction of motion and $\mathbf{F}_r$ in the opposite direction.

We have already related $\mathbf{F}_r$ to the macroscopic motion of the fluid; let us now investigate the driving force, $\mathbf{F}_d$. Let us take a macroscopic element of volume consisting of a prism whose length is Δl and whose area of cross section is ΔA, oriented with its axis parallel to the direction of macroscopic flow. The driving force acting upon the fluid within this volume element will be the resultant of the surface forces upon its exterior and the body forces upon the mass within its interior. In this case the surface forces consist of normal stresses only, since the shear stresses are expended against the rigid framework of the medium throughout the interior of the

body and are not transmitted to distances appreciably greater than the mean grain diameter d. Their effect is accordingly, on a macroscopic scale, similar to a body force and gives rise to the resistive force $\mathbf{F}_r$, which has already been evaluated. The normal stress acting upon the surface of the macroscopic volume element is the hydrostatic fluid pressure p. For the body force we have only the attraction due to gravity.

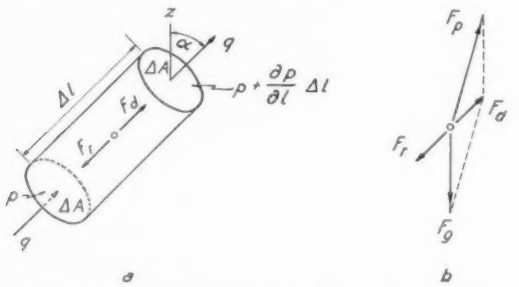

FIG. 8.—*a*, Forces acting upon macroscopic fluid volume element in direction parallel to flow; *b*, relation between forces parallel to flow and the total forces due to pressure gradient and gravity.

The total driving force must be the sum of the net force upon the volume element due to pressure and of the force due to gravitational attraction. Since the fluid is free to flow in any direction, this resultant must be in the direction of the fluid flow, and we need only consider the components of the other two forces in that direction.

For the component of the force due to pressure, let p be the pressure upon the upstream end of the prism, and $p + (\partial p/\partial l)\Delta l$ that upon the downstream end. We define the direction of the flow by the angle α which it makes from the upward directed vertical. Then in the direction of the flow α the component of the driving force due to pressure is

$$F_{p\alpha} = p\epsilon \cdot \Delta A - \left(p + \frac{\partial p}{\partial l} \cdot \Delta l\right) \epsilon \cdot \Delta A = -\frac{\partial p}{\partial l} \cdot \epsilon \cdot \Delta V , \quad (67)$$

where $\epsilon \cdot \Delta A$ is the fraction of ΔA that is occupied by the fluid, and $\epsilon \cdot \Delta V$ the volume of fluid within the prism.

If we divide equation (67) by $\rho\epsilon \cdot \Delta V$, we obtain

$$\frac{F_{p\alpha}}{\rho \cdot \epsilon \cdot \Delta V} = -\frac{1}{\rho} \cdot \frac{\partial p}{\partial l}, \tag{68}$$

which is the component of the force per unit of mass of the fluid in the direction α produced by the change of macroscopic pressure in that direction. It is numerically equal to the rate of increase with distance of the pressure and oppositely directed. That is, the force due to pressure alone is always directed from regions where the pressure is higher toward those where it is lower.

The component in the direction α of the force exerted by gravity acting upon the fluid contained within the volume ΔV is

$$F_{g\alpha} = -g \cos \alpha \cdot \rho\epsilon \cdot \Delta V = -g \cdot \frac{\partial z}{\partial l} \cdot \rho\epsilon \cdot \Delta V. \tag{69}$$

The negative sign here is necessary to allow for the fact that for upward flow $\cos \alpha$ is positive, while for downward flow it is negative. In the expression $\partial z/\partial l$, z is the vertical co-ordinate, or the elevation above the standard datum.

Now, adding equations (67) and (69) gives us the total driving force acting upon the fluid in the volume element ΔV,

$$\mathbf{F}_d = \left(-g \cdot \frac{\partial z}{\partial l} - \frac{1}{\rho} \cdot \frac{\partial p}{\partial l}\right) \rho\epsilon \cdot \Delta V; \tag{70}$$

and, if we divide this by $\rho\epsilon \cdot \Delta V$, we obtain

$$\frac{\mathbf{F}_d}{\rho\epsilon \cdot \Delta V} = -g \cdot \frac{\partial z}{\partial l} - \frac{1}{\rho} \cdot \frac{\partial p}{\partial l}, \tag{71}$$

which is the total driving force acting upon each unit of mass of the fluid.

If we turn now to equations (30) and (31) and differentiate them with respect to l, and then compare the results with equation (71), we shall find that

$$-g \cdot \frac{\partial z}{\partial l} - \frac{1}{\rho} \cdot \frac{\partial p}{\partial l} = -\frac{\partial \Phi}{\partial l}, \tag{72}$$

so that

$$\frac{\mathbf{F}_d}{\rho\epsilon \cdot \Delta V} = -\frac{\partial \Phi}{\partial l} . \tag{73}$$

Hence, the total driving force per unit of mass of the fluid is numerically equal to the rate of increase with distance of the fluid potential and is oppositely directed.

Since the sum of the macroscopic forces per unit of mass must be zero, then, by adding the expressions for these forces as given by equations (65) and (73), we obtain

$$-\frac{1}{N} \cdot \frac{\eta}{\rho} \cdot \frac{q}{d^2} - \frac{\partial \Phi}{\partial l} = 0 ,$$

which, when solved for q, gives

$$q = -Nd^2 \cdot \frac{\rho}{\eta} \cdot \frac{\partial \Phi}{\partial l} = -Nd^2 \cdot \frac{\rho}{\eta} g \cdot \frac{\partial h}{\partial l} . \tag{74}$$

When this is compared with Darcy's law as expressed by equation (34), it is clear that equations (34) and (74) are equivalent and that

$$K = Nd^2\rho \cdot \frac{1}{\eta} \cdot g , \tag{75}$$

so that the five factors to the right of equation (75) are evidently the quantities we originally set out to discover which were lumped together as the parameter K. Of these, all have been defined except the factor N, which we employed as a factor of proportionality when relating the resistive force to the fluid velocity. N is simply a dimensionless numerical coefficient whose value depends upon the geometrical shape of the internal structure of the medium through which the flow occurs. For two geometrically similar media the values of N would be the same; for dissimilar media, such as rounded versus angular grain shapes, the values of N would be different. The dimensions of N are therefore

$$[N] = [\text{angle}] = [LL^{-1}] = [L^0] . \tag{76}$$

Since its effect is determined solely by experiment, no more precise definition of N is required.

That the five quantities to the right in equation (75) are the correct ones, that they occur to their proper powers, and that no other essential quantities have been omitted may be demonstrated by a simple dimensional check. We rearrange equation (74) as follows:

$$\frac{q}{\frac{\partial h}{\partial l}} = -Nd^2\rho \cdot \frac{1}{\eta} \cdot g ,$$

where the terms to be investigated are segregated to the right. If the equation is correct, then the dimensions of the right-hand term must be the same as those of the term to the left.

The dimensions of the separate factors are:

$$\left.\begin{aligned} [q] &= [LT^{-1}] , \\ \left[\frac{1}{\frac{\partial h}{\partial l}}\right] &= [L^0] , \\ [N] &= [L^0] , \\ [d^2] &= [L^2] , \\ [\rho] &= [ML^{-3}] , \\ \left[\frac{1}{\eta}\right] &= M^{-1}L^{+1}T^{+1}] , \\ [g] &= [LT^{-2}] . \end{aligned}\right\} \tag{77}$$

Introducing these values into equation (74) gives the dimensional expression

$$\left[\frac{q}{\frac{\partial h}{\partial l}}\right] = \left[Nd^2\rho \cdot \frac{1}{\eta} \cdot g\right] , \tag{78}$$

or

$$\left.\begin{aligned} [M^0L^{+1}T^{-1}] &= [L^0L^2M^{+1}L^{-3}M^{-1}L^{+1}T^{+1}L^{+1}T^{-2}] \\ &= [M^0L^{+1}T^{-1}] . \end{aligned}\right\} \tag{79}$$

The fact that these dimensions balance is interpreted to mean that all the factors contained in K are given in the right-hand side of equation (78). Of these, only N might be further broken down into additional components, such as porosity and other geometrical parameters. In practice there is no need for such dissection, since N and d^2 are more conveniently lumped together as a single property of the medium. Consequently, we may regard the equations (74):

$$q = -Nd^2 \cdot \frac{\rho}{\eta} \cdot \frac{\partial \Phi}{\partial l} = -Nd^2 \cdot \frac{\rho}{\eta} \cdot g \cdot \frac{\partial h}{\partial l},$$

as equivalent and complete expressions of Darcy's law in the most general form we shall require. This tells us that, in addition to the factors investigated already, q varies directly as a factor N depending upon the internal shape of the medium, as the square of the grain size or other suitable length scale indicating coarseness, as the density of the fluid, and inversely as the viscosity of the fluid.

We come now to the problem of a more precise definition of *permeability* than the qualitative one given earlier. Of the five quantities N, d^2, ρ, $1/\eta$, and g of equation (74), the first two, N and d^2, are properties solely of the medium; the second two, ρ and η, are properties solely of the fluid; the last, g, is a property of the earth's gravitational field and may be taken, for present purposes, as constant. It would be possible to select from these five quantities any combination which includes the properties of the medium, N and d^2, and to make of this a single lumped parameter which could then be called the "coefficient of permeability." As will be discussed later, this is essentially what has been done already, so that numerous dimensionally unlike quantities, all called "permeability," are currently in use.

To avoid this sort of confusion, we ask what it is that we wish a coefficient of permeability to signify. We have already noted that the concept pertains to the facility with which a given rock or material transmits fluids. Persumably, then, permeability is to be taken as a property of the medium alone. If so, then a coefficient of permeability for a given medium should not change value when different fluids are employed. To satisfy this requirement we lump

the factors Nd^2, depending upon the medium only, into the single factor k and then write Darcy's law as

$$q = -k \cdot \frac{\rho}{\eta} \cdot \frac{\partial \Phi}{\partial l}, \tag{80}$$

where k is the coefficient of permeability of the medium. For any given medium its value is obtained by an experiment analogous to that of Figure 1, where all quantities except k are measured by experiment, and then equation (80) is solved for k.

The dimensions of k are

$$[k] = [Nd^2] = [L^2]. \tag{81}$$

For purposes of mathematical analysis we are frequently concerned with the flow rate without regard to the parts played separately by the properties of the fluid and those of the medium. In this case it is more convenient to lump the factors k, ρ, and $1/\eta$ together into a single parameter σ, which then simplifies Darcy's law to

$$q = -\sigma \cdot \frac{\partial \Phi}{\partial l}, \tag{82}$$

a form which is physically, as well as mathematically, analogous to Ohm's law in electricity when applied to extended media. In the flow of electricity the factor analogous to σ is called the *specific electrical conductivity;* here we shall call σ the *specific fluid conductivity.* From its definition it is clear that the specific fluid conductivity is a property both of the medium and of the fluid. For a homogeneous liquid under isothermal conditions the density and viscosity are constant. In this case the specific conductivity will vary proportionately to the permeability of the medium.

RANGE OF VALIDITY OF DARCY'S LAW

We come now to the problem of the range of validity of Darcy's law, which states that the rate of flow increases linearly with the potential gradient. Over what values of q should this be true? This takes us back to our derivation of the value of the resistive force f_r

in terms of q in equation (58) and the equations preceding. It may be recalled that we were obliged to stipulate that the flow was to maintain kinematic similarity for different values of q and that we found we could satisfy this condition only by making the velocities so small that forces due to inertia became negligible. Under these conditions we deduced Darcy's law analytically.

What would happen now if we increased the velocity to where the forces of inertia are not negligible but are comparable in magnitude to the other forces? Since, in general, the inertial forces are not parallel to the streamlines but are randomly oriented, this can only produce distortion in the streamlines, causing crowding where the curvature is sharp. At still higher velocities eddies may also form in the wake of certain of the sand grains where the streamlines pull away from the grain surface. All this is still entirely within the range of strictly laminar flow and does not involve turbulence to any degree.

For uniform rectilinear macroscopic flow of a liquid the integral over a macroscopic volume of the forces due to inertia is zero, so that these can exercise no direct retarding effect upon the fluid motion. What they do, however, is produce distortion which increases the terms of the form $\partial^2 u/\partial y^2$, upon which the resistive forces depend. Since the forces due to inertia increase as the square of the velocity, this effect is nonlinear with respect to q; and for values of q for which the inertial forces are not negligible the resistance to the flow must increase at a progressively greater rate as q is increased. Hence, Darcy's law can only be valid for values of q small enough that the forces of inertia are negligible.

It is more convenient, because of the universality of the relationship, to refer this range of validity to the Reynolds' number R, defined by equation (59), since, in geometrically similar media, kinematically similar flow occurs at the same values of this quantity. In the present problem there are three values of Reynolds' number of particular significance: $R = 0$, corresponding to zero flow; $R = R^*$, the point at which inertial forces become effective; and $R = R_{crit}$, where the flow becomes turbulent. The values of R^* and R_{crit} for any particular geometrical framework can only be determined by experiment. Until now it has been almost the universal custom

among the students of this sort of flow to assume without question that the departure from linearity of q with respect to $d\Phi/dl$, or its equivalent, was evidence of the beginning of turbulence. This error probably arises from the fact that most of the studies of the transition from linear to turbulent flow have been conducted upon flow through uniform straight tubes. In the flow of liquids through rectilinear tubes there exist no accelerations at all until the motion

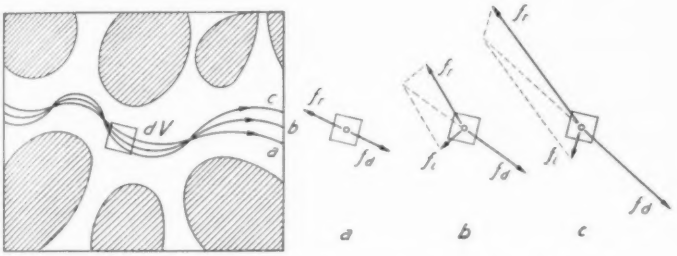

FIG. 9.—Schematic representation of the distortion of flowlines and force equilibria by increase of fluid velocity. *a*, *b*, and *c* represent flowlines and corresponding forces acting upon fixed volume element dV at successively higher velocities. Darcy's law is valid only for case *a*.

becomes unstable and turbulence sets in. Consequently, for this special case, R^* and R_{crit} coincide. In flow with curvilinear motion as well as acceleration parallel to the streamlines, the two values may be remote from one another.

For straight tubes the Reynolds' number is commonly defined in terms of the mean fluid velocity $\bar{v}$ and the radius r. Then the critical value is found experimentally to be

$$R_{\text{crit}} = \frac{\bar{v}r}{\frac{\eta}{\rho}} \cong 1{,}160 .$$

For sediments we have defined the Reynolds' number to be

$$R = \frac{qd}{\frac{\eta}{\rho}} ,$$

where q is the specific discharge and d the mean grain diameter. This obviously gives only an order of magnitude, because different sediments may depart widely from geometrical similarity. Lindquist,[7] employing a medium composed of uniform lead shot with a porosity of 38 per cent, found the value of R^* to be about 4. This was true for different experiments in which shot with diameters ranging from 1 to 5 mm. was employed. For values of R as high as 180 the flow was still laminar, so that for this system R_{crit} must be greater than 180.

For water at 20° C. the kinematic viscosity η/ρ is 0.01 c.g.s., so that through a sand composed of uniform spheres with 38 per cent pore space, the maximum specific discharge for which Darcy's law holds is obtained by solving the following equation for q:

$$\left.\begin{aligned} \frac{q_{max}\, d}{\frac{\eta}{\rho}} &= R^* = 4\,, \\ q_{max} &= \frac{0.04}{d}\ \text{cm/sec}\,. \end{aligned}\right\} \tag{83}$$

For a coarse sand with grain diameter of 0.1 cm. the maximum specific discharge for which Darcy's law would still be valid would be about 0.4 cm/sec. At this rate, from a sand 3 meters thick the flow of water into a well of 10 cm. radius would be at a rate of 7.5 liters (almost a gallon) per second, or about 4,000 barrels per day. For finer sands the limiting value of q would be correspondingly greater. Since, for such flow, the velocity diminishes rapidly with distance from the well, then it is clear that only exceptionally will rates of flow in ground water be encountered that are outside the upper range of validity of Darcy's law.

There is no apparent reason for supposing the existence of any lower limit to the range of validity of Darcy's law short of $R = 0$, corresponding to $q = 0$. Tests made by Fishel[8] of the flow of water

[7] Erik Lindquist, "On the Flow of Water through Porous Soil," *1er Congrès des grands barrages* (Stockholm, 1933), pp. 81–101.

[8] V. C. Fishel, "Further Tests of Permeability with Low Hydraulic Gradients," *Trans. Amer. Geophys. Union, 16th Ann. Meeting* (1935), pp. 499–503.

through sand established the validity of Darcy's law for values of q as small as about 4×10^{-8} cm/sec, corresponding to values of $\partial h/\partial l$ as low as 2 or 3 inch/mile, or about 6×10^{-5}.

DARCY'S LAW FOR GASES

While our investigation of the fluid potential was purposely made general enough to include both liquids and gases, our interest thus far has concerned itself principally with the interpretation of the experiment of Figure 1 in which the fluids employed have been liquids only. Where the permeability of different samples of materials is to be measured, there are many experimental advantages in the use of a gas, such as air, as the experimental fluid. It does not dissolve components of the specimen or react with it chemically. Before a gas can be used, however, we must extend the theory to include compressibility according to the gas laws.

Consider the steady flow of a gas through a tube of uniform section filled with sand or other uniformly permeable material under isothermal conditions. In this case, as the pressure along the tube changes, the specific volume of the gas will also change, so that the volume discharge q will no longer be the same over succeeding cross sections of the tube but will vary inversely as the pressure. Since there is no accumulation of gas in any part of the flow region, then the mass of gas flowing across each cross section must be constant. Then, for any given cross section, if q is the specific volume discharge for that section and ρ the density of the gas as it crosses the section, the mass of gas crossing unit area per unit of time must be

$$j = \rho q = \text{constant}\,, \tag{84}$$

where j is the *specific mass discharge*.

For any infinitesimal distance dl along the axis of the tube in the direction of the flow, the density ρ of the gas may be regarded as constant; and Darcy's law in its differential form,

$$q = -Nd^2 \cdot \frac{\rho}{\eta} \cdot \frac{\partial \Phi}{\partial l}\,,$$

is just as valid for gases as for liquids. Then, if we multiply both sides by ρ, we obtain

$$\rho q = j = -Nd^2 \cdot \frac{\rho^2}{\eta} \cdot \frac{\partial \Phi}{\partial l}, \tag{85}$$

which is also valid for both gases and liquids.

For gases, however, ρ is no longer a constant but varies continuously with distance along the axis of the cylinder, the density and pressure being related by Boyle's law,

$$\frac{p}{\rho} = \frac{p_0}{\rho_0}, \qquad \text{or} \qquad \rho = p \cdot \frac{\rho_0}{p_0}, \tag{86}$$

where ρ_0 and p_0 are the density and pressure at the standard state of 1 atmosphere. Also, for this case we must employ the more general form of the fluid potential

$$\Phi = gz + \int_{p_0}^{p} \frac{dp}{\rho}$$

of equation (30), which, however, has the same derivative,

$$\frac{d\Phi}{dl} = g \cdot \frac{\partial z}{\partial l} + \frac{1}{\rho} \cdot \frac{\partial p}{\partial l}, \tag{87}$$

as the form valid for liquids only.

The viscosity of a gas, however, as predicted by the kinetic theory of gases and confirmed by experiment, is independent of pressure variations over a range of pressures comparable to that for which the gas laws are valid. Hence, η for a single gas at a constant temperature has the same value throughout.

Now, if we introduce equation (87) into (85), this gives us

$$j = -\frac{Nd^2}{\eta} \cdot \rho^2 \left(g \cdot \frac{\partial z}{\partial l} + \frac{1}{\rho} \cdot \frac{\partial p}{\partial l} \right). \tag{88}$$

The first term in the parentheses is the component of the force per unit of mass due to gravity; the second term is the corresponding

force due to pressure. For gases under medium pressures ρ is small compared with unity, and the pressure gradient may be large, so that in all but exceptional cases the second term is so much larger than the first that no significant error will result if we neglect the term $g(\partial z/\partial l)$. With this simplification equation (88) reduces to

$$j = -\frac{Nd^2}{\eta} \cdot \rho \cdot \frac{\partial p}{\partial l}, \tag{89}$$

which then, by introducing the value for ρ given in equation (86), becomes

$$j = -\frac{Nd^2}{\eta} \cdot \frac{\rho_0}{p_0} \cdot p \cdot \frac{\partial p}{\partial l}. \tag{90}$$

Since, however,

$$p \cdot \frac{\partial p}{\partial l} = \frac{1}{2} \cdot \frac{\partial (p^2)}{\partial l}, \tag{91}$$

equation (90) can be written

$$j = -\frac{Nd^2}{\eta} \cdot \frac{\rho_0}{p_0} \cdot \frac{1}{2} \cdot \frac{\partial (p^2)}{\partial l}. \tag{92}$$

Then, since all other terms are constants already,

$$\frac{\partial (p^2)}{\partial l} = \text{constant}, \tag{93}$$

which tells us that the rate of decrease of the *square* of the pressure with distance in the direction of the flow is constant and that the specific mass discharge is proportional to this.

If we insert two pressure gauges into the system at a finite distance l apart (corresponding to the manometer tubes of Fig. 1), then

$$\frac{1}{2} \cdot \frac{\partial (p^2)}{\partial l} = \frac{p_2^2 - p_1^2}{2l} = \frac{p_2 + p_1}{2} \cdot \frac{p_2 - p_1}{l} = \overline{p} \cdot \frac{p_2 - p_1}{l}, \tag{94}$$

where p_1 and p_2 are the two pressures and $\overline{p}$ is their arithmetical average.

Introducing this into equation (92) reduces that equation to the form[9]

$$j = -\frac{Nd^2}{\eta} \cdot \frac{\rho_0}{p_0} \cdot \frac{\bar{p}(p_2 - p_1)}{l}, \qquad (95)$$

for which every term is experimentally determinable except Nd^2. Then solving for Nd^2 gives the permeability k for the medium.

It need hardly be added that the value of the permeability of a given sand obtained in this manner should be in close agreement with the value obtained when a liquid is employed.

FLOW THROUGH EXTENSIVE MEDIA

So far we have considered only the case of uniform, rectilinear flow through a prismatic body of sand which is uniform and isotropic with respect to permeability. It remains now to determine whether the results obtained thus far are applicable to the general case of flow through extensive inhomogeneous media such as are encountered in field problems of ground-water flow. For this purpose we shall employ the macroscopic point of view exclusively. We shall also retain the assumption that the medium is isotropic with respect to permeability, although recognizing that in the case of some sedimentary rocks this assumption is not valid.

Our problem, therefore, is a *field* problem, and we need to introduce a few concepts which have become standard in dealing with such problems. When in any region of space there exists at each point a particular value of some given physical quantity—temperature, for example—that region is said to be a *field* in the quantity considered. If temperature were the quantity, the field would be a thermal field. If the quantity constituting the field is a *scalar*, that is, if it is definable by a single number, like temperature, then the field is a *scalar field*. If the quantity is a vector, like force or velocity, then the field is said to be a *vector field*. A still higher-order field exists for quantities, like stress, which in general are definable by nine independent quantities. This kind of field is a *tensor field*.

[9] This result has been derived earlier, using a different method from that given here, by Wyckoff, Botset, Muskat, and Reed ("Measurement of Permeability of Porous Media," *Bull. Amer. Assoc. Petrol. Geol.*, Vol. XVIII [1934], pp. 161–90).

The variation of most physical quantities in space is continuous with distance, so that the difference of the values of the same quantity at two near-by points decreases continuously as the distance between the points is made smaller and smaller, approaching zero as a limit. Regions in which the variation is continuous may, however, be bounded by surfaces of discontinuity.

In regions free from discontinuities, through each point in a scalar field a surface can be passed upon which all values of the scalar quantity are the same as that at the given point. This surface will then divide the region into two parts, in one of which all the values of the quantity considered will be higher, and in the other lower, than the values upon the surface itself. Such surfaces we may call *field surfaces*, and there will be one field surface passing through each point in the field. An isothermal surface is a field surface for a thermal field.

For vector fields in a region free from discontinuities we have *field lines*. A field line is the locus of a point which moves through a vector field in such a manner that at every point its direction of motion coincides with the direction of the vector at that point.

A *stationary field* is a field throughout which the values of the quantity of which the field consists remain invariant with time.

In a region free from discontinuities in the quantities considered, for every scalar field there exists an associated vector field, the relation between the two being obtained in the following manner:

Let Ω be any scalar quantity whose values are supposed known at every point in its field and whose field is stationary and continuous. At a point O in this field we erect x, y, and z axes. Through the origin let the field surface $\Omega = \Omega_0$ pass. To this we erect the surface normal n in the direction of increasing values of Ω. We let α, β, and γ be the angles that n makes with the positive direction of the x, y, and z axes, respectively. At a distance Δn from the origin the surface $\Omega_0 + \Delta\Omega$, sensibly parallel to the surface Ω_0, intersects the normal n. This same surface intersects the co-ordinate axes at distances Δx, Δy, and Δz from the origin.

Now what we are interested in finding is the rate of change with distance of the quantity Ω in the various directions in space away from the point O. In the direction n the average rate of change over

the distance Δn is $\Delta\Omega/\Delta n$. The corresponding average rates along the three axes are $\Delta\Omega/\Delta x$, $\Delta\Omega/\Delta y$, and $\Delta\Omega/\Delta z$, respectively. But

$$\left.\begin{aligned} \Delta x &= \frac{\Delta n}{\cos \alpha}, \\ \Delta y &= \frac{\Delta n}{\cos \beta}, \\ \Delta z &= \frac{\Delta n}{\cos \gamma}, \end{aligned}\right\} \tag{96}$$

so that

$$\left.\begin{aligned} \frac{\Delta\Omega}{\Delta x} &= \frac{\Delta\Omega}{\Delta n} \cdot \cos \alpha, \\ \frac{\Delta\Omega}{\Delta y} &= \frac{\Delta\Omega}{\Delta n} \cdot \cos \beta, \\ \frac{\Delta\Omega}{\Delta z} &= \frac{\Delta\Omega}{\Delta n} \cdot \cos \gamma. \end{aligned}\right\} \tag{97}$$

Then, if we pass to the limits by letting Δn approach zero, equations (97) become

$$\left.\begin{aligned} \frac{\Delta\Omega}{\Delta x} \rightarrow \frac{\partial\Omega}{\partial x} &= \frac{\partial\Omega}{\partial n} \cdot \cos \alpha, \\ \frac{\Delta\Omega}{\Delta y} \rightarrow \frac{\partial\Omega}{\partial y} &= \frac{\partial\Omega}{\partial n} \cdot \cos \beta, \\ \frac{\Delta\Omega}{\Delta z} \rightarrow \frac{\Delta\Omega}{\partial z} &= \frac{\partial\Omega}{\partial n} \cdot \cos \gamma. \end{aligned}\right\} \tag{98}$$

The direction of the surface-normal n is determined by the field and, hence, fixed in space. The orientation of the x, y, and z axes, on the other hand, is arbitrary, so that, separately, the angles α, β, and γ may vary from 0° to 180°. Consequently, the ranges of the values of their cosines are

$$\left.\begin{aligned} -1 \leqq \cos \alpha \leqq 1, \\ -1 \leqq \cos \beta \leqq 1, \\ -1 \leqq \cos \gamma \leqq 1. \end{aligned}\right\} \tag{99}$$

Now, if we take any line s making an angle θ with the direction of n, we are at liberty to orient the x axis along this line, making α and θ equal. Then

$$\frac{\partial \Omega}{\partial s} = \frac{\partial \Omega}{\partial x} = \frac{\partial \Omega}{\partial n} \cdot \cos \theta \equiv \text{grad } \Omega \cdot \cos \theta \,. \tag{100}$$

Here grad Ω (read "the gradient of Ω") is identical with $\partial\Omega/\partial n$. Since $\cos \theta$ is always equal to or less than unity, it follows that grad Ω, which is the rate of increase of Ω in the direction of the surface-

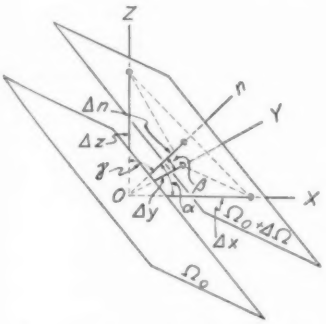

FIG. 10.—Space variation of continuous field of scalar quantity Ω.

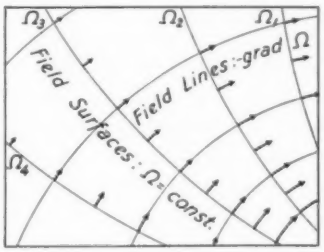

FIG. 11.—Relation between scalar field and derived vector field.

normal, is the maximum rate of increase in any direction. Also, since the rates of change in all other directions are related to grad Ω in the same manner as the components of a vector are related to the vector itself, then grad Ω may be taken to be a vector whose direction is parallel to n and whose magnitude is equal to the maximum rate of change of Ω with distance.

Thus, to every scalar field in any scalar quantity Ω there corresponds a vector field in the vector quantity grad Ω whose field lines are everywhere at right angles to the field surfaces Ω = a constant, and directed from regions where Ω is smaller toward those where it is larger.

The physical dimensions of the vector quantity grad Ω are

$$[\text{grad } \Omega] = \left[\frac{\Omega}{\text{length}}\right], \tag{101}$$

which may represent a force, a velocity, or other vector quantity, depending upon the nature of the scalar Ω. Also, as many different kinds of scalar and vector fields may coexist in the same region of space as there are scalar and vector quantities at each point in that space.

APPLICATION TO FLUID FLOW

With this background, let us now return to consider a field in which ground water or other fluid is our particular concern. We shall suppose that all fields are stationary in order not to be obliged to consider changes of the field with time. Even when such changes are imposed, we shall consider only the steady states that are established before and after the change, and shall avoid the *transient* stage during which the changes take place. In many cases where there are more or less continuous fluctuations governed by irregularities of local precipitation and other climatic factors, we shall be content to consider the average state of the system over a time period of a year or more.

Among the scalar quantities whose fields are of interest in the study of fluid motion are those of the hydrostatic pressure p, the gravity potential U, and the fluid potential Φ. Each of these quantities has its separate family of field surfaces, normal to which is the respective family of field lines corresponding to the vector fields of the quantities grad p, grad U, and grad Φ. In addition to these three derived vector fields we have that of the flow of the fluid itself.

Our problem now is to investigate these several kinds of fields in order to learn the manner in which they influence the flow of a fluid through a permeable medium in an extensive region of space. Taking the most obvious vector field first, let us consider that of the flow itself. By injecting filaments of dye or other visible markers at specific points, we find that the fluid passing through each point follows a definite path, which we shall speak of as a *flowline* or *streamline*. The family of all flowlines is evidently the system of field lines of a vector field. The vector itself is still to be determined.

The flow vector can be determined if we delineate a small plane surface element of area ΔS whose normal makes the angle θ with

the lines of flow. Then the projection ΔS_n of this surface element upon a plane perpendicular to the flowlines is given by

$$\Delta S_n = \Delta S \cdot \cos \theta . \tag{102}$$

Across ΔS_n the volume of fluid discharging per second is

$$q \cdot \Delta S_n = q \cdot \Delta S \cdot \cos \theta = q_n \cdot \Delta S , \tag{103}$$

where

$$q_n = q \cos \theta . \tag{104}$$

Thus the total discharge across a surface ΔS due to the specific discharge q making an angle θ with the surface normal is exactly the same as the discharge across the same surface due to a specific dis-

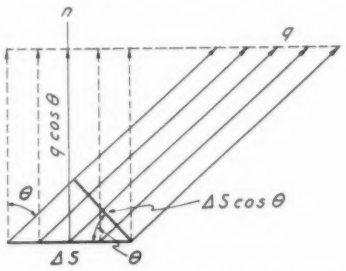

FIG. 12.—Vector properties of the specific volume discharge q

charge q_n parallel to the surface normal, where q_n bears the relation to q of a vector component to the vector itself. Consequently, the specific discharge q, which has a definite magnitude and direction at every point, is a vector, and its components in all other directions are obtainable by the usual methods of vector resolution. The vector $\mathbf{q}$ is everywhere tangential to the flowlines and so is a fundamental vector of the field of flow.

Another equally important flow vector, however, is the specific mass discharge $\mathbf{j}$. In direction this coincides at every point with $\mathbf{q}$, but its magnitude is $\rho\mathbf{q}$ where ρ is constant for liquids but varies along the flowlines for a gas. Thus the vector fields for the quantities $\mathbf{q}$ and $\mathbf{j}$ have identical flowlines but different magnitudes at corresponding points.

A fundamental analytical property of the vector **j** is discovered if we erect co-ordinate axes in the field of flow and choose a small macroscopic volume element whose lengths of sides are Δx, Δy, and Δz. We resolve the vector **j** into components j_x, j_y, and j_z parallel to the axes. We then determine the net mass of fluid flowing *out of*

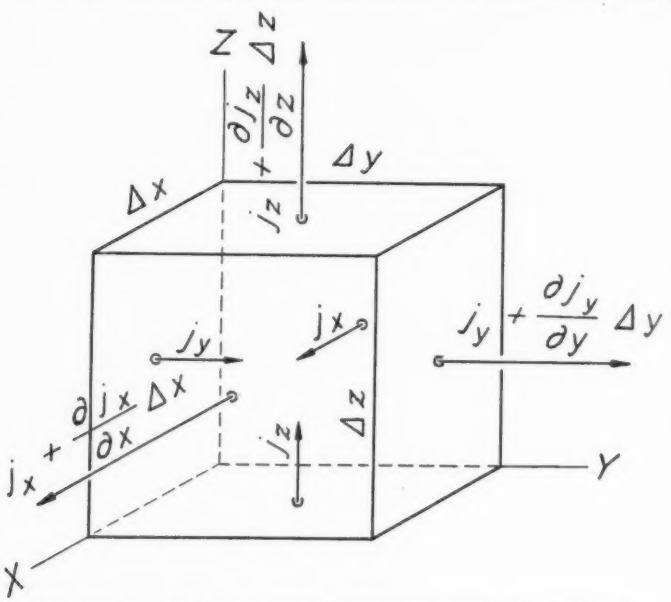

FIG. 13.—Mass discharge across the faces of macroscopic volume element

the volume element ΔV per unit of time. To do this we investigate the outward discharge across each of the six faces of the volume element. If we let J_x, J_y, and J_z be the total outward mass discharge across the x, the y, and the z faces, respectively, we shall have

$$J_x = -j_x \Delta y \cdot \Delta z + \left(j_x + \frac{\partial j_x}{\partial x} \cdot \Delta x\right) \Delta y \cdot \Delta z = \frac{\partial j_x}{\partial x} \cdot \Delta V , \quad (105)$$

$$J_y = -j_y \Delta z \cdot \Delta x + \left(j_y + \frac{\partial j_y}{\partial y} \cdot \Delta y\right) \Delta z \cdot \Delta x = \frac{\partial j_y}{\partial y} \cdot \Delta V , \quad (106)$$

$$J_z = -j_z \Delta x \cdot \Delta y + \left(j_z + \frac{\partial j_z}{\partial z} \cdot \Delta z\right) \Delta x \cdot \Delta y = \frac{\partial j_z}{\partial z} \cdot \Delta V . \quad (107)$$

Then the net outward mass discharge per unit of volume will be

$$\frac{J_x + J_y + J_z}{\Delta V} = \frac{\partial j_x}{\partial x} + \frac{\partial j_y}{\partial y} + \frac{\partial j_z}{\partial z} . \tag{108}$$

Since mass is a conservative property of matter, the net mass outflow per unit of time per unit of volume must equal the loss of mass in that time by the volume. The mass content of unit volume is

$$m = \rho\epsilon , \tag{109}$$

so that the mass lost per unit volume in unit time must be

$$-\frac{dm}{dt} = -\epsilon \cdot \frac{\partial \rho}{\partial t} . \tag{110}$$

Equating (110) with (108) gives

$$\frac{\partial j_x}{\partial x} + \frac{\partial j_y}{\partial y} + \frac{\partial j_z}{\partial z} = -\epsilon \cdot \frac{\partial \rho}{\partial t} , \tag{111}$$

which is known as the *equation of continuity* for fluid motion. It states the conditions that the flow vectors must satisfy at all points if the principle of the conservation of matter is not to be violated.

But for stationary flow $\partial\rho/\partial t = 0$. Then for this condition we have for both liquids and gases

$$\frac{\partial j_x}{\partial x} + \frac{\partial j_y}{\partial y} + \frac{\partial j_z}{\partial z} = \frac{\partial(\rho q_x)}{\partial x} + \frac{\partial(\rho q_y)}{\partial y} + \frac{\partial(\rho q_z)}{\partial z} = 0 . \tag{112}$$

For an incompressible fluid the density is constant and so may be factored out of equation (112), leaving

$$\frac{\partial q_x}{\partial x} + \frac{\partial q_y}{\partial y} + \frac{\partial q_z}{\partial z} = 0 \tag{113}$$

as a special form of the equation of continuity valid for liquids only.

It is customary, when dealing with liquids, to measure the volume rather than the mass; and, since in what follows our concern will be almost exclusively with the flow of liquids, we shall employ the form given in equation (113) using $\mathbf{q}$ as our flow vector, unless cases arise

which require the more general form of equation (112). Equation (113) may be thought of as expressing the constancy of the fluid volume, or better, of defining the properties of the flow if the condition of the constancy of volume is not to be violated. This condition makes it impossible for the flow vector to change capriciously or discontinuously with distance, and so justifies our earlier stipulation of continuity in our vector and scalar fields except across bounding surfaces.

Another consequence of the condition of incompressibility of fundamental importance with regard to the motion of ground water is this: If we take a closed surface S enclosing a finite volume V within the field of flow, then across an element ΔS of the surface the outward directed flow per unit of time will be

$$\Delta Q = q \cos \theta \cdot \Delta S = q_n \cdot \Delta S , \tag{114}$$

where θ is the angle between the flow vector $\mathbf{q}$ and n, the outward directed surface normal. Then the net outward discharge over the whole surface will be

$$Q = \iint_S q_n \cdot dS = 0 . \tag{115}$$

This becomes especially useful when we form the surface S in the following manner: Upon a surface which is normal to the flowlines we draw a closed curve enclosing an area A_1. Through each point of this curve a particular flowline passes, and the *ensemble* of such contiguous flowlines forms a sort of sleeve or *stream tube*. Some distance downstream from the surface A_1, we take another surface orthogonal to the flowlines and upon this the streamlines forming the walls of the stream tube circumscribe an area A_2. These two ends, A_1 and A_2, and the side walls of the tube in the intervening section then, together, form a closed surface, S. Over the area A_1 the angle θ is 180°, and its cosine -1; over A_2, θ is 0 and its cosine $+1$; over the side walls θ is 90° and its cosine 0.

Then for this case the integral (115) over the surface S reduces to

$$Q = \iint_{A_1} -q \cdot dS + \iint_{A_2} q \cdot dS + 0 = 0 . \tag{116}$$

Furthermore, if the tube is made narrow enough, the magnitude of $\mathbf{q}$ over the cross sections A may be considered constant, in which case equation (116) simplifies to

$$-q_1A_1 = +q_2A_2 ,$$

or, in magnitude,

$$q_1A_1 = q_2A_2 = qA = \text{constant} , \tag{117}$$

which tells us that for an incompressible fluid in steady flow the discharge across each cross section of any given stream tube is a constant. Also, there is a reciprocal relationship between specific discharge and area of cross section, the former tending to infinity as the latter tends to zero, and vice versa.

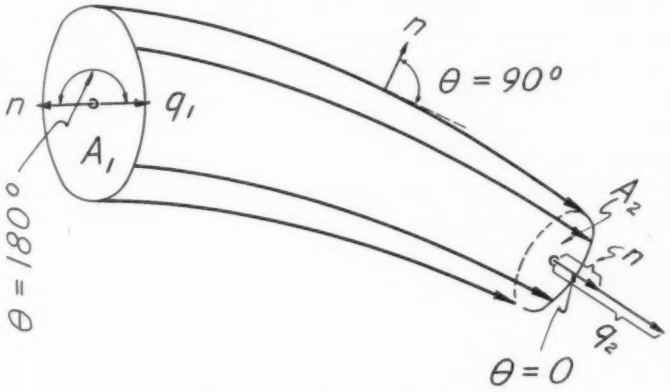

FIG. 14.—Net discharge over the surfaces of a stream tube

Since infinite specific discharge is precluded by the increase of resistance with velocity of flow, then a convergence of a stream tube to zero without violating the condition of incompressibility or the principle of the conservation of matter is impossible. Consequently, except at certain "singular points" characterized by a velocity of zero, no two noncontiguous streamlines can ever intersect or come together, since we can always choose a stream tube in such a manner that these two lines occur diametrically opposite each other, so that in order for them to come together the tube would have to converge to zero area of cross section.

Since the discharge along a stream tube is unidirectional and constant in amount, it follows that no stream tube of finite cross section can terminate except upon boundaries of the flow region, one end of each tube acting as an inlet and the other as an outlet. If the flowlines are radial with respect to an inlet or outlet region, then away from this region the cross section of each tube increases without limit as the distance increases, and the velocity of flow proportionately diminishes, tending to the limit zero. While this limit may not be reached, the motion becomes imperceptibly small, and we may think of the stream tube as having terminated by dispersion.

The intake end of a stream tube we may speak of as its *source*, and the outlet end as its *sink*. This usage is slightly different from that of standard potential theory in which a source is a region where the field is, so to speak, created, and a sink a region where it is annihilated. In that sense, if wheat in its granular form were the flow medium, then a wheat field would constitute an absolute source of this medium, and a flour mill an absolute sink. At those points the amounts entering and leaving would not be the same, whereas between those points the total quantity would be conserved, and the flow said to be *solenoidal*.

By our usage, an example of a sink in ground-water flow would be a well toward which the flowlines converge; an example of a source would be a lake from which water flows into the ground. Between source and sink the quantity of fluid is conserved, and the character of the flow is solenoidal.

Let us now consider the fields of the aforementioned scalar quantities: the pressure p, the gravity potential U, and the fluid potential Φ.

Take the pressure first. To every point within the fluid there will correspond a particular value of the hydrostatic pressure p. Through each point there passes one of a family of field surfaces, p = constant, to be known as "surfaces of equal pressure," or "*isobaric* surfaces." The corresponding vector field is made up of the vectors grad p which generate a family of field lines everywhere normal to the isobaric surfaces.

By reasoning analogous to that which led to equations (70) and (71), if we take a small fluid prism with its axis parallel to the

normal n of the isobaric surface erected in the direction of increasing pressure, then the net force acting upon it in the direction n is

$$\mathbf{f}_p = -\frac{\partial p}{\partial n} \cdot \Delta V = -\text{grad } p \cdot \Delta V . \tag{118}$$

The force per unit of volume of the fluid is

$$\frac{\mathbf{f}_p}{\Delta V} = -\text{grad } p .$$

This is the total pressure force, of which that in any other direction is only a component. Consequently, at every point within the fluid there acts, owing to the pressure gradient, a force per unit of fluid volume which is numerically equal to grad p and oppositely directed. Hence, associated with the scalar field in p there exists an orthogonal family of lines of force per unit of volume, $-\text{grad } p$.

The force due to pressure per unit of mass is

$$\frac{\mathbf{f}_p}{\rho \cdot \Delta V} = -\frac{1}{\rho} \cdot \text{grad } p . \tag{119}$$

Now let us consider the gravity potential U. This quantity we shall define as equal to the gravity potential energy of unit mass with respect to the standard datum. Then, regarding g as constant,

$$U = gz , \tag{120}$$

where g is merely the scalar magnitude of gravity acceleration and z, as previously, is the vertical elevation.

The field surfaces, U = constant, known as *gravity equipotential surfaces*, obviously correspond to z = constant and are level surfaces. The field lines normal to these are parallel to the direction of gravity and are given by

$$\mathbf{g} = -\text{grad } U , \tag{121}$$

where in this case the vector $\mathbf{g}$ signifies the force per unit of mass, or acceleration due to gravity, both in magnitude and direction.

Finally, for the fluid potential Φ we have the family of *fluid equipotential* surfaces and its associated field lines,

$$\frac{\mathbf{f}_d}{m} = -\text{grad } \Phi \,, \tag{122}$$

where $-\text{grad } \Phi$ represents the force per unit of mass acting upon the fluid due to the gradient of the fluid potential Φ. This family of lines of force is normal to the fluid equipotential surfaces and oppositely directed from grad Φ.

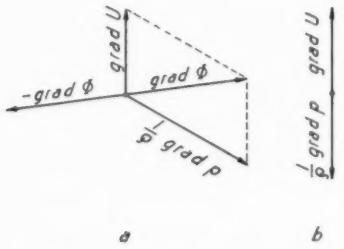

FIG. 15.—*a*, Vector relations between the gradients of the scalar fields of gravity potential, pressure, and fluid potential; *b*, condition for static equilibrium.

As we have seen already, the fluid potential is the sum of the work done against both gravity and pressure and is, in fact, given by

$$\Phi = U + \int_{p_0}^{p} \frac{dp}{\rho} \,, \tag{123}$$

where the gravity potential U is employed in place of gz. Then, since $-\text{grad } \Phi$ is the total force acting per unit of mass, it must be equal to the vector sum of the other two component forces:

$$-\text{grad } \Phi = -\text{grad } U - \frac{1}{\rho} \cdot \text{grad } p \,. \tag{124}$$

The other two fields, being thus combined into the single field $-\text{grad } \Phi$, may therefore be dropped from further consideration except for special purposes which may arise. The surfaces $U =$ constant are horizontal and the direction $-\text{grad } U$ is always down-

ward; the vectors $-\text{grad } p$ and $-\text{grad } \Phi$, however, may have any direction whatever. Only in the special case that

$$-\text{grad } \Phi = 0$$

do we have

$$-\frac{1}{\rho} \cdot \text{grad } p = -(-\text{grad } U), \tag{125}$$

for which hydrostatic equilibrium prevails.

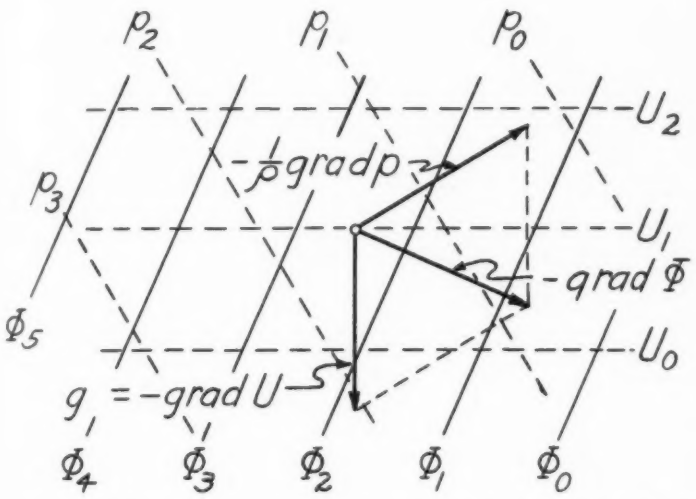

FIG. 16.—Relation between superimposed scalar fields of p, U, and Φ, and their corresponding negative gradients.

We are now in a position to elucidate the properties of the potential Φ in yet another manner. Within a flow field of a general kind, starting from an initial point P_0, let us carry, by a frictionless process (infinitely slow motion), an element of the fluid of unit mass along any arbitrary path A to a final position P. Under these conditions, owing to the field there will act upon the mass at each point a force $\mathbf{f}_d$, and to move the fluid we shall have to exert upon it an equal

and opposite force $-\mathbf{f}_d$. The work required to traverse the distance ds of the path will be

$$dw = f_d \cdot ds \cdot \cos\theta\,, \tag{126}$$

where the quantity to the right is the product of the displacement by the component of force in that direction, and θ is the angle between the direction of the displacement and of the force $-\mathbf{f}_d$. But

$$f_d \cdot ds \cdot \cos\theta = \left(\frac{\partial U}{\partial s} + \frac{1}{\rho} \cdot \frac{\partial p}{\partial s}\right) ds = dw\,. \tag{127}$$

Then the total work required to carry the mass along the path A from P_0 to P is

$$w_A = \int dw = \int_A \left(\frac{\partial U}{\partial s} + \frac{1}{\rho} \cdot \frac{\partial p}{\partial s}\right) ds\,, \tag{128}$$

where $\int_A$ signifies the line-integral along the path A.

Next, suppose we carry a unit mass from P_0 to P along a different path B. The work required to do this will be

$$w_B = \int_B \left(\frac{\partial U}{\partial s} + \frac{1}{\rho} \cdot \frac{\partial p}{\partial s}\right) ds\,. \tag{129}$$

Then, if w_A is equal to w_B for all possible paths A and B, we may characterize the fluid at the point P by its possession of a uniquely determinable amount of mechanical energy Φ per unit of mass defined by

$$\Phi = \Phi_0 + w = \Phi_0 \int \left(\frac{\partial U}{\partial s} + \frac{1}{\rho} \frac{\partial p}{\partial s}\right) ds\,, \tag{130}$$

where Φ_0 is the corresponding quantity at the point P_0. If, on the contrary, the value of the line integral from P_0 to P is different for different paths, then $w_A \neq w_B$, and the quantity Φ defined by equation (130) is not unique. In the first case, where the line integral is unique, we say the field has a potential; in the second case, no potential is possible.

The most rigid criterion for the existence of a potential is obtained

if we traverse a closed path, proceeding from P_o to P by the path A and returning by B. Then the total work along the closed path is

$$w = w_A + w_B = \oint \left(\frac{\partial U}{\partial s} + \frac{1}{\rho} \cdot \frac{\partial p}{\partial s} \right) ds \,. \qquad (131)$$

If this line-integral around all possible closed paths is equal to zero, a potential exists, and to each point in the field there corresponds a uniquely determinable value of the quantity Φ. If this integral around a closed path is not zero, no potential is possible, and there will be a circulatory component of the fluid flow around this path. This does not imply perpetual motion but indicates the presence of a heat engine, where heat is being added at one temperature in one part of the circuit and withdrawn at a lower temperature at another.

Interpreting equation (131) mechanically, we know already that work against gravity is independent of the path, so that

$$\oint \frac{\partial U}{\partial s} \cdot ds = 0 \,. \qquad (132)$$

Then, if we are to have a fluid potential, it is also necessary that

$$\oint \frac{1}{\rho} \cdot \frac{\partial p}{\partial s} \cdot ds = 0 \,, \qquad (133)$$

which is satisfied completely when the density ρ is uniquely determined for each value of the pressure. This condition is satisfied for incompressible fluids for which the density is constant and for isothermal or adiabatic transformations in gases. For liquids under a temperature gradient there actually may be a slight rotational component due to changes of density with temperature, but in ground water this is ordinarily of a negligible magnitude compared with the potential forces acting.

Equation (130) transforms to our earlier definition of fluid potential derived from thermodynamic reasoning when P_o is situated at a point $z = 0$ with a pressure of p_o, and $\Phi_o = 0$. Then at point P

$$\Phi = \int_{U_o}^{U} dU + \int_{p_o}^{p} \frac{dp}{\rho} = gz + \int_{p_o}^{p} \frac{dp}{\rho} \,, \qquad (134)$$

where the right-hand quantity is our original definition of the fluid potential.

Potentials are classified according to the vector quantity to which they are related. Thus, a scalar quantity, the space derivative of whose field is a force, is said to be a *force potential;* if the space derivative is a velocity, the quantity is a *velocity potential.* Since the space derivative of the quantity Φ is a force, Φ must be a force potential.

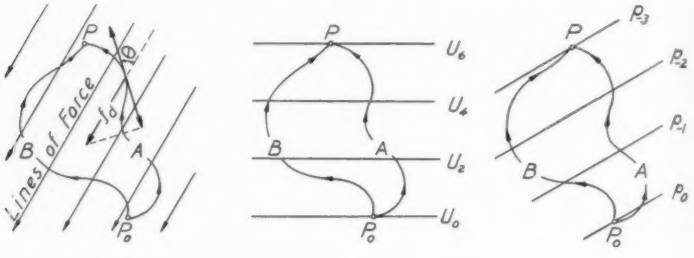

FIG. 17.—*a*, Fluid potential as a line integral in a field of force; *b* and *c*, the corresponding line integrals in the scalar fields of p and U.

RELATION BETWEEN THE POTENTIAL FIELD AND THE FLOW FIELD

So far we have investigated separately the properties of the fields of flow whose vectors are $\mathbf{q}$ and $\mathbf{j}$, respectively, and of the scalar field of the fluid potential and its associated force field $-\text{grad } \Phi$. These fields coexist in the same region of space, and our problem now is to relate them one to the other. This is accomplished directly by means of Darcy's law, of which we may employ either of the equivalent forms

$$\left.\begin{aligned} q_s &= -\sigma \cdot \frac{\partial \Phi}{\partial s}\,, \\ j_s &= -\rho\sigma \cdot \frac{\partial \Phi}{\partial s}\,, \end{aligned}\right\} \tag{135}$$

where q_s and j_s are the components in the direction s of the specific volume discharge and mass discharge, respectively. The total flow vectors, of which these are the components, are likewise given by

$$\left.\begin{aligned} \mathbf{q} &= -\sigma \text{ grad } \Phi\,, \\ \mathbf{j} &= -\rho\sigma \text{ grad } \Phi\,, \end{aligned}\right\} \tag{135a}$$

which may be taken as equivalent general statements of Darcy's law. In these the vectors **q** and **j** are everywhere parallel to each other and to the streamlines, and the magnitude of **j** is equal to that of **q** multiplied by the factor ρ.

The relation of the vectors **q** and **j** to that of $-\text{grad}\,\Phi$ can best be seen by recalling that $\sigma = k\rho/\eta$ and that each of these quantities is a possible variable in the field of flow. If the value of k changes from point to point, the medium is inhomogeneous; and if it varies at the same point for flow in different directions, it is anisotropic.

For isotropic media the directions of both **q** and **j** will be the same as that of $-\text{grad}\,\Phi$; and their magnitudes will be σ and $\rho\sigma$, respectively, times that of $-\text{grad}\,\Phi$, and the flowlines will be normal to the equipotential surfaces. For anisotropic conditions the flowlines will, in general, be somewhat oblique to the direction of $-\text{grad}\,\Phi$.

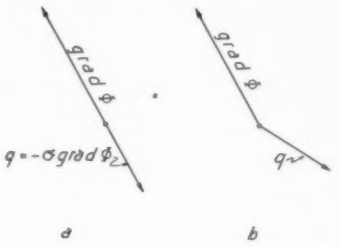

FIG. 18.—Vector representation of Darcy's law: *a*, for isotropic; *b*, for anisotropic media.

For the general fluid, ρ will vary as a function of the pressure, and η as a function of the temperature, and both as a function of distance in the field of flow, though for liquids at constant temperature this variation becomes negligibly small. Since we have agreed to consider only isotropic media, the flowlines with which we deal will be everywhere parallel to $-\text{grad}\,\Phi$ and will form an orthogonal system with the family of equipotential surfaces $\Phi = \text{constant}$. Homogeneity, however, cannot be assumed, for in rocks the value of k varies from zero for impermeable materials to infinity for large open spaces. For a fluid of constant density and viscosity flowing through rocks with similar internal structures, σ varies as k, or as the square of the grain diameter or other characteristic length. Thus, for a range of grain diameters from 10^{-3} to 1 cm., corresponding to the range of sediments from silt to coarse gravel, the increase of permeability and conductivity is of the order of a million-fold. It is highly important, therefore, that we develop our theory so as to take large differences of permeability into account.

Attention may here be directed to an important consequence of the wide variation of σ, which will be discussed in more detail later. There is an extensive employment among authors on this subject of an expression of the form

$$\mathbf{q} = -\text{grad}\,(\sigma\Phi)\,, \tag{136}$$

which is stated to be Darcy's law. Comparison of this with equation (135*a*) shows that, in order for this to be true, grad $(\sigma\Phi)$ must be equal to σ grad Φ. Actually, however, if we expand grad $(\sigma\Phi)$, we obtain

$$\text{grad}\,(\sigma\Phi) = \sigma\ \text{grad}\,\Phi + \Phi\ \text{grad}\,\sigma\,,$$

from which it is clear that equations (135*a*) and (136) can only be equivalent provided Φ grad $\sigma = 0$. This last condition is satisfied only in case $\sigma = k\rho/\eta$ = constant. Hence, for inhomogeneous media or for fluids of variable density or viscosity—that is to say, for general conditions—equation (136) must be ruled out as an expression of Darcy's law, on the grounds of being physically erroneous.

REFRACTION OF FLOWLINES ACROSS BOUNDARIES BETWEEN DIFFERENT MEDIA

With this point clear let us now proceed to investigate the flow of a liquid through inhomogeneous media. Consider first the case of flow across the boundary between regions of markedly different conductivities. Let σ_1 be the conductivity of the first region, and σ_2 that of the second. Let the interface be a plane surface whose normals into the two regions are n_1 and n_2. Let θ_1 and θ_2 be the angles the flowlines make with the normals in the first and second regions, respectively; and $\mathbf{q}_1$ and $\mathbf{q}_2$, the corresponding flow vectors.

At the boundary between these two regions two independent physical requirements must be satisfied simultaneously. The principle of the conservation of matter requires that the fluid leaving one region per unit of time must equal that entering the other. Since this involves only normal components of the flow

$$-(q_n)_1 = +(q_n)_2\,, \tag{137}$$

where $(q_n)_1$ and $(q_n)_2$ signify the normal components of flow *away from* the boundary in the two regions, respectively.

The principle of the conservation of energy requires that the line integral of the potential around a closed path, starting at a point on the boundary, proceeding a distance Δs along the boundary inside

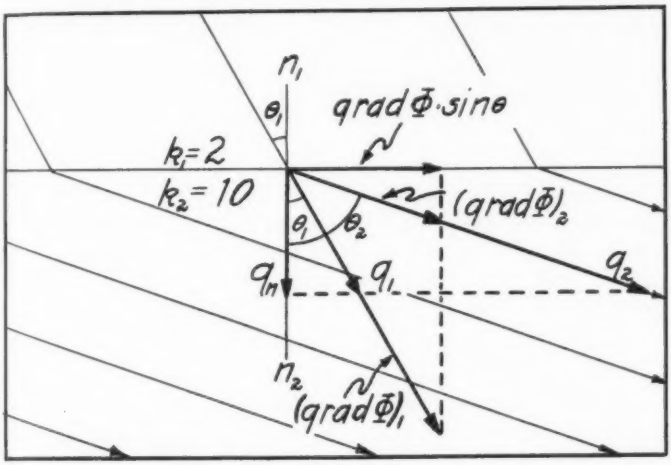

FIG. 19.—The refraction of flowlines at the interface between media of different permeabilities. The value of k_2/k_1 is here taken to be 5. The refraction obeys a tangent law.

region 2 and returning along a parallel path just inside region 1, must be zero. Hence,

$$\left(\frac{\partial \Phi}{\partial s}\right)_1 = \left(\frac{\partial \Phi}{\partial s}\right)_2 . \tag{138}$$

If we carry out these operations in the plane containing the two surface normals n_1 and n_2 and the two flow vectors $\mathbf{q}_1$ and $\mathbf{q}_2$, and express the rates of flow in terms of the potential gradients and the conductivities, we shall have for the normal components of flow

$$\sigma_1(\text{grad } \Phi)_1 \cos \theta_1 = \sigma_2(\text{grad } \Phi)_2 \cos \theta_2 ; \tag{139}$$

and for the tangential components of the potential gradient,

$$(\text{grad } \Phi)_1 \sin \theta_1 = (\text{grad } \Phi)_2 \sin \theta_2 . \tag{140}$$

Dividing equation (140) by (139) then gives us

$$\frac{\sin \theta_1}{\sigma_1 \cos \theta_1} = \frac{\sin \theta_2}{\sigma_2 \cos \theta_2},$$

or

$$\frac{\tan \theta_1}{\tan \theta_2} = \frac{\sigma_1}{\sigma_2} = \frac{\dfrac{k_1 \rho_1}{\eta_1}}{\dfrac{k_2 \rho_2}{\eta_2}} = \frac{k_1}{k_2}, \tag{141}$$

which may be thought of as the law of refraction of the flowlines in fluid flow. At the boundary between media of different permeabilities both the flowlines and the equipotential surfaces change direc-

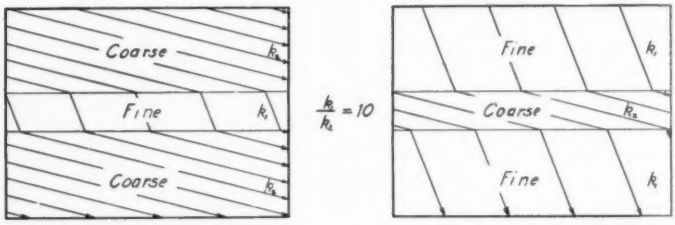

FIG. 20.—Refraction across layers of coarse and fine sand with a permeability ratio of 10.

tion abruptly. This resembles the refraction of light except that the latter obeys a sine law instead of a tangent law of refraction. It should be remarked, however, that this law of refraction is only true provided both media are completely filled with the same fluid.

The two cases of greatest importance are those for which, while one of the conductivities, say σ_1, remains finite, the other approaches either zero or infinity. The consequences of this are best brought out by equations (139) and (140). When $\sigma_2 \to 0$, equation (139), becomes

$$\sigma_1 (\text{grad } \Phi)_1 \cos \theta_1 = 0. \tag{142}$$

When $\sigma_2 \to \infty$, $(\text{grad } \Phi)_2 \to 0$ and equation (140) becomes

$$(\text{grad } \Phi)_1 \sin \theta_1 = 0. \tag{143}$$

Since both σ_1 and $(\text{grad } \Phi)_1$ are finite, then in the first case $\cos \theta_1 = 0$, and in the second, $\sin \theta_1 = 0$, corresponding to $\theta_1 = 90°$ and $\theta_1 = 0$ in the first and second cases, respectively.

Hence, in a region of finite permeability, equipotential surfaces terminate perpendicularly upon all impermeable boundaries; whereas upon permeable boundaries to regions of infinite conductivities (large voids) filled with the same fluid, all flowlines terminate perpendicularly.

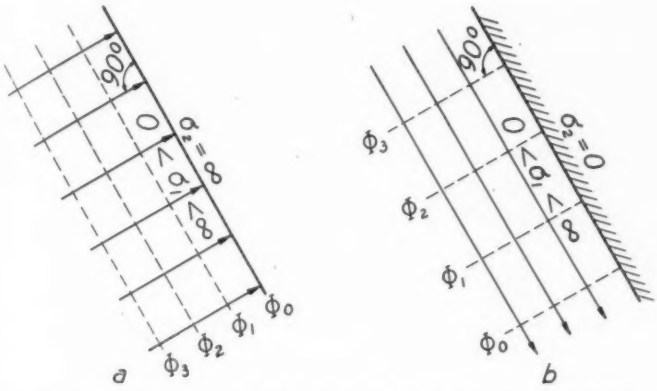

FIG. 21.—*a*, Flow from region of finite into one of infinite permeability; *b*, flowlines and equipotential surfaces along impermeable boundaries.

That this should be so becomes more obvious when we consider that upon impermeable boundaries the normal components of the flow are zero, so that the total flow to which the equipotential surfaces are perpendicular is the tangential component. For the case of flow into a fluid filled void or basin, the rate of flow is finite, but the conductivity is essentially infinite. Then, since $\mathbf{q} = -\sigma \text{ grad } \Phi$, it follows that grad Φ must tend to zero as σ increases without limit. Such a region approaches a condition $\Phi = \text{constant}$, or becomes essentially an equipotential region. Since the tangential components of the potential gradient on both sides of the boundary must be the same, and in this case zero, then the total flow in the region of finite conductivity must be its normal component.

FLOW FROM POINT-SOURCE AND LINE-SOURCE

When dealing with the flow field only and discussing tubes of flow, we established in equation (118) the fact that the total volume-discharge along any given stream tube was constant, so that, as the tube contracted, the velocity of flow, or specific discharge $\mathbf{q}$, must proportionately increase. Now, when we relate the rate of flow with the potential gradient, we obtain

$$\mathbf{q}A = -A\sigma \operatorname{grad} \Phi , \tag{144}$$

which tells us that, as any stream tube in a region of uniform conductivity contracts, the potential gradient correspondingly increases and equidifferent surfaces of constant potential crowd corresponding-

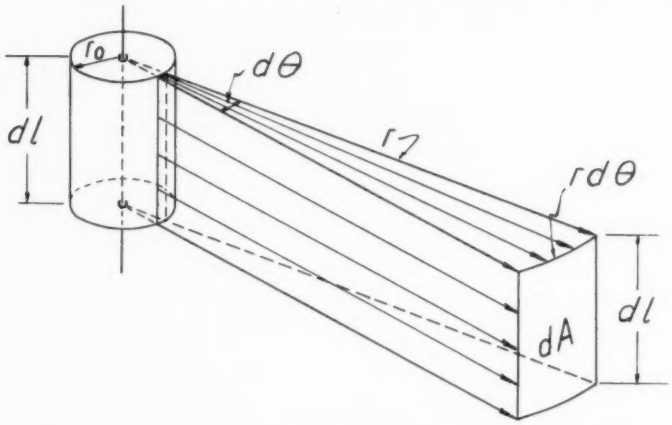

FIG. 22.—Elementary stream tube in flow from line- or cylindrical-source

ly closer together. Thus, in any region where the streamlines converge, the potential gradient will increase in the direction of convergence in proportion to the increase of $\mathbf{q}$.

Two cases of such convergence are of considerable importance because of their ease of calculation and because they are frequently approximated in practice. One of these is flow toward or away from a line-sink or line-source, where the flowlines are all normal to the line and radial with respect to it as a center. Radial flow into a well

that extends from top to bottom of an aquifer with upper and lower impermeable boundaries is an example of this type of flow. Flow from a region of uniform permeability into a drainage ditch is, in some cases, a good approximation to it.

The other case is radial flow away from or toward a point-source or point-sink through media of uniform permeability.

For each of these two types of flow let us now determine both the magnitude of the specific discharge q and the potential Φ at all points in the field. For this we shall regard the discharge as positive when the flow is outward from a source and negative when directed inward toward a sink.

Consider the case when the flow is radially away from a line-source. Let this be represented by a cylinder of indefinite length and of radius r_o. Let the potential on the surface of the cylinder be Φ_o. Consider next the volume discharge dQ through a flow tube subtending upon the cylinder a length dl and a circumferential angle $d\theta$. At the distance r_o the cross-sectional area of this tube will be

$$dA_o = r_o \cdot d\theta \cdot dl \,, \qquad (145)$$

and at distance r this will become

$$dA = r \cdot d\theta \cdot dl \,. \qquad (146)$$

Since the discharge over all cross sections of the tube is constant, then

$$dQ = q_o r_o \cdot d\theta \cdot dl = qr \cdot d\theta \cdot dl \,,$$

or

$$q = q_o \cdot \frac{r_o}{r} \,, \qquad (147)$$

which indicates that the rate of flow decreases inversely as the first power of the distance.

The potential is obtained by introducing Darcy's law into equation (147)

$$q = q_o r_o \cdot \frac{1}{r} = -\sigma \cdot \frac{d\Phi}{dr} \,, \qquad (148)$$

from which

$$d\Phi = -\frac{q_o r_o}{\sigma} \cdot \frac{dr}{r}$$

and

$$\Phi = \Phi_o - \frac{q_o r_o}{\sigma} \int_{r_o}^{r} \frac{dr}{r} = \Phi_o - \frac{q_o r_o}{\sigma} \cdot \log_e \frac{r}{r_o} . \tag{149}$$

In case the flow is inward toward a sink, q_o is negative, so that the last term of equation (149) becomes positive.

Over a finite angle θ and length l the total discharge Q is

$$Q = q_o r_o \theta l ; \tag{150}$$

and when the flow is from all sides, θ is 2π radians, giving

$$Q = 2\pi q_o r_o l , \qquad \text{or} \qquad q_o r_o = \frac{Q}{2\pi l} . \tag{151}$$

Replacing $q_o r_o$ in equation (149) with $Q/2\pi l$ then gives

$$\Phi = \Phi_o - \frac{Q}{2\pi\sigma l} \cdot \log_e \frac{r}{r_o} , \tag{152}$$

showing that for this case the potential decreases or increases, depending upon whether the flow is outward or inward, logarithmically with distance.

Next consider radial flow from a point-source which we will take as the center of an equipotential sphere of radius r_o and potential Φ_o. Let $d\Omega$ be an elementary solid angle whose area of cross section at distance r_o is dA_o, and at distance r is dA. Through this the discharge is

$$dQ = q_o \cdot dA_o = q \cdot dA = q_o r_o^2 \cdot d\Omega = q r^2 \cdot d\Omega . \tag{153}$$

Hence,

$$q = q_o r_o^2 \cdot \frac{1}{r^2} , \tag{154}$$

showing that in this case the intensity of the flow varies with the inverse square of the distance. By Darcy's law

$$q = -\sigma \cdot \frac{d\Phi}{dr} = q_0 r_0^2 \cdot \frac{1}{r^2}, \tag{155}$$

from which

$$d\Phi = -\frac{q_0 r_0^2}{\sigma} \cdot \frac{dr}{r^2}$$

and

$$\Phi = \Phi_0 - \frac{q_0 r_0^2}{\sigma} \int_{r_0}^{r} \frac{dr}{r^2} = \Phi_0 + \frac{q_0 r_0^2}{\sigma} \left(\frac{1}{r} - \frac{1}{r_0} \right). \tag{156}$$

For inward flow the sign of q_0 becomes negative, changing the sign of the last term.

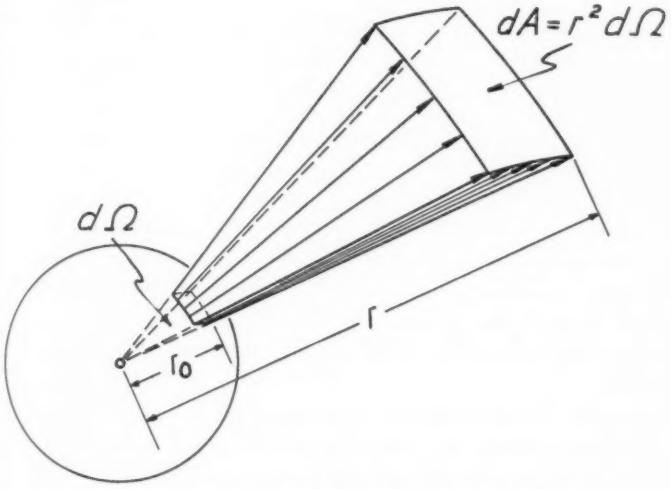

FIG. 23.—Elementary stream tube in flow from point- or spherical-source

For flow of this kind the flow commonly occurs over either half or the whole of the space about the point. For half-space the total discharge is

$$Q = 2\pi r_0^2 q_0, \tag{157}$$

and for whole space

$$Q = 4\pi r_0^2 q_0 , \tag{158}$$

from which

$$q_0 r_0^2 = \frac{Q}{2\pi} \quad \text{or} \quad \frac{Q}{4\pi} , \tag{159}$$

depending upon which of the two cases is dealt with. Taking the first, which corresponds to flow from or toward a point upon an impermeable plane boundary of a medium of uniform permeability and great extent, and introducing this into equation (156), we obtain

$$\Phi = \Phi_0 + \frac{Q}{2\pi\sigma}\left(\frac{1}{r} - \frac{1}{r_0}\right). \tag{160}$$

In either of these two cases, let Φ_1 be the potential at a point P_1 of radial distance r_1, and Φ_2 that of a point P_2 of distance r_2. Then for flow toward a line-sink by equation (152)

$$\left.\begin{aligned} \Phi_1 &= \Phi_0 - \frac{Q}{2\pi\sigma l}\log_e \frac{r_1}{r_0} , \\ \Phi_2 &= \Phi_0 - \frac{Q}{2\pi\sigma l}\log_e \frac{r_2}{r_0} , \end{aligned}\right\} \tag{161}$$

and

$$\Phi_2 - \Phi_1 = \frac{Q}{2\pi\sigma l}\log_e \frac{r_1}{r_2} = g(h_2 - h_1) , \tag{162}$$

where h_2 and h_1 are the manometer heights at points P_2 and P_1.

Solving equation (162) for σ then gives

$$\sigma = \frac{Q}{2\pi l g(h_2 - h_1)}\log_e \frac{r_1}{r_2} = \frac{k\rho}{\eta} , \tag{163}$$

where k is the permeability of the medium. The heights h_2 and h_1 may be the elevations of water in two observation wells, while Q is the steady discharge of a pumping well.

For radial flow through half-space toward a point we have from equation (160)

$$\left.\begin{aligned}\Phi_1 &= \Phi_0 + \frac{Q}{2\pi\sigma}\left(\frac{1}{r_1} - \frac{1}{r_0}\right),\\ \Phi_2 &= \Phi_0 + \frac{Q}{2\pi\sigma}\left(\frac{1}{r_2} - \frac{1}{r_0}\right),\end{aligned}\right\} \tag{164}$$

and

$$\Phi_2 - \Phi_1 = \frac{Q}{2\pi\sigma}\left(\frac{1}{r_2} - \frac{1}{r_1}\right) = g(h_2 - h_1)\,. \tag{165}$$

Solving this for σ gives

$$\sigma = \frac{Q}{2\pi g(h_2 - h_1)}\left(\frac{1}{r_2} - \frac{1}{r_1}\right) = \frac{k\rho}{\eta}\,. \tag{166}$$

Equations (163) and (166) afford a means of determining permeability in the field when flow systems approximating those for which the two equations were developed exist. Thiem[10] appears to have been the first to utilize this principle in measuring permeability, and we may speak of it as the "Thiem method," although the method of analysis here employed differs markedly from the one used by him, and only one of the cases here used, that of flow to a line-sink, was considered by him.

The principle is by no means confined to the cases discussed; it is applicable to any flow system for which it is possible to deduce theoretically the potential field and the flow field from the known boundary conditions. The above cases were only chosen as an illustration.

Wenzel[11] has recently made use of the Thiem method for permeability measurements in the United States.

Another important property of the flow field derives from the principle of superposition. For example, suppose we have two point-sources at points O_1 and O_2 distance a apart inside a medium of uniform permeability whose extent in all directions is large, com-

[10] G. Thiem, *Hydrologische Methoden* (Leipzig, 1906).

[11] Leland K. Wenzel, "The Thiem Method for Determining Permeability of Water-bearing Materials," *U.S.G.S. Water-Supply Paper 697A* (1936).

pared with a. Let the discharge from one of these be Q_1 and from the other Q_2. Let r_1 and r_2 be the bi-polar co-ordinates of any point P in space measured from O_1 and O_2. If only the source Q_1 operates, then all flowlines will extend radially from O_1, and at $P(r_1, r_2)$ the flow vector will have the magnitude

$$q_1 = \frac{Q_1}{4\pi r_1^2} \tag{167}$$

and a direction parallel to r_1.

If only the source Q_2 operates, all flowlines will radiate from O_2 and at $P(r_1, r_2)$ the magnitude of the flow vector will be

$$q_2 = \frac{Q_2}{4\pi r_2^2}, \tag{168}$$

and its direction will be parallel to r_2.

If both Q_1 and Q_2 operate simultaneously, then $\mathbf{q}_1$ and $\mathbf{q}_2$ will be the two components of the flow, and the resultant flow will be the vector sum

$$\mathbf{q} = \mathbf{q}_1 + \mathbf{q}_2 . \tag{169}$$

To obtain the resultant flowlines throughout the field by this method we should have to repeat the operations of equations (167),

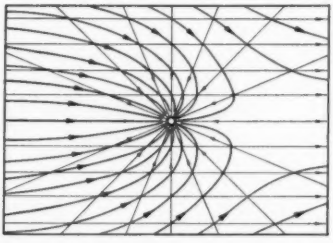

FIG. 24.—Graphical method of compounding two plane flow fields. The component fields are radial flow toward a line sink and rectilinear flow in the same plane. The flow-lines are so spaced that between each pair the same discharge occurs. The method is *not applicable to other than plane fields.*

(168), and (169) for a large number of points in space before we could sketch them in—a very difficult and tedious process.

Suppose, however, we consider the potentials at the point $P(r_1, r_2)$ due to each source operating alone, and then the two together. For Q_1 alone

$$\Phi_1 = \Phi_{10} + \frac{Q_1}{4\pi\sigma}\left(\frac{1}{r_1} - \frac{1}{r_{10}}\right), \tag{170}$$

and for Q_2 alone

$$\Phi_2 = \Phi_{20} + \frac{Q_2}{4\pi\sigma}\left(\frac{1}{r_2} - \frac{1}{r_{20}}\right). \tag{171}$$

Then for both sources operating simultaneously we should have

$$\Phi = \Phi_1 + \Phi_2 . \tag{172}$$

But in this case the potentials are scalar quantities and so add algebraically, giving us

$$\Phi = \Phi_{10} + \Phi_{20} + \frac{Q_1}{4\pi\sigma}\left(\frac{1}{r_1} - \frac{1}{r_{10}}\right) + \frac{Q_2}{4\pi\sigma}\left(\frac{1}{r_2} - \frac{1}{r_{20}}\right), \tag{173}$$

by means of which we obtain the potential for every point $P(r_1, r_2)$ in space. The flowlines are then everywhere normal to the surfaces $\Phi =$ constant.

In the case that Q_1 is a source and Q_2 an equal sink, with $\Phi_{20} = -\Phi_{10}$ and $r_{20} = r_{10}$, equation (182) reduces to

$$\Phi = \frac{Q}{4\pi\sigma}\left(\frac{1}{r_1} - \frac{1}{r_2}\right), \tag{174}$$

the gradient of which defines a flow field identical with the lines of force about an idealized bar magnet or with the lines of flow of an electric current between point electrodes through a space of uniform electrical conductivity.

By a generalization of this process the resultant potential at each point is always the sum of the partial potentials due to separate causes:

$$\Phi = \Phi_1 + \Phi_2 + \Phi_3 + \cdots + \Phi_n , \tag{175}$$

and always

$$\mathbf{q} = -\sigma \operatorname{grad} \Phi . \tag{176}$$

We have already demonstrated that upon all impermeable boundaries of a region of flow equipotential surfaces terminate perpendicularly. It remains to be seen how else such surfaces may terminate. For example, can an equipotential surface close completely upon itself, enclosing a volume of the flow region? Can an equipotential surface terminate inside a flow region away from all boundaries? Can two equipotential surfaces intersect each other or coincide?

In dealing with these problems let us keep in mind that we are assuming the presence of only a single homogeneous fluid of sensibly constant density, so that in the field of flow all voids are occupied by the fluid. The boundaries of the field of flow may be either permeable or impermeable. The flow field thus defined constitutes a closed volume through which the flow must satisfy equation (116), which states that the net outward flow across its boundaries must be zero. Consequently, in such a region all flow tubes must terminate upon the permeable boundaries, one terminus upon a fluid entrance or source, and the other upon a fluid exit or sink. Within the region at all points the flow is solenoidal, that is, devoid of absolute sources or sinks.

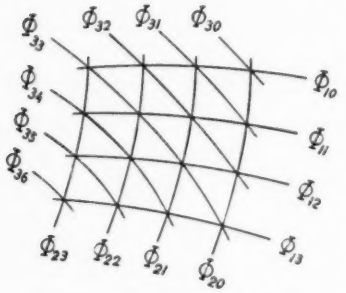

FIG. 25.—Graphical addition to potential fields. Φ_3 is the sum of Φ_1 and Φ_2.

One of the fundamental properties of an equipotential surface is that it separates a region of higher from one of lower potential. Consequently, across any given surface the flow always takes place in the same direction, that is, a single flowline never crosses the same equipotential surface twice. If an equipotential surface were to close completely upon itself, then we should have a volume into or out of which all flowlines converged or diverged. But this could only be possible provided the enclosed volume were a region in which the fluid was annihilated or created—a region containing either absolute sinks or sources. Since the existence of these has already been ruled out, then we may say that in the flow of an incompressible fluid it is

impossible for an equipotential surface to terminate upon itself and completely enclose any given volume of space.

The same is true of the steady flow of a compressible fluid, only in this case the continuity equations apply to the mass discharge vector **j** instead of the volume discharge **q**, so that a completely closed equipotential surface for the steady motion of any kind of a fluid would involve a violation of the principle of the conservation of matter.

What we have here called "sinks" and "sources" inside a region of flow are actually achieved by a suitable arrangement of impermeable boundaries. We get something approaching a point sink inside a flow region by terminating a tube at that point. What we have actually done is to extend the impermeable boundaries in the form of a hollow cylinder to the given point. If the flow is from the medium to the end of the tube, then all near-by equipotential surfaces close completely about this point, except for the area of cross section of the tube. But this is the area of fluid exit, and the potential inside the tube is markedly different from that immediately outside. Consequently, even in this case, the surfaces cannot close but must terminate perpendicularly upon the impermeable boundaries of the tube.

Can equipotential surfaces terminate inside the flow region away from all boundaries? Equipotential surfaces must exist at all points for which there is a potential gradient and, hence, for which the fluid is in motion. If an equipotential surface should terminate away from all boundaries, this would imply that we had gone from a region in which the fluid was in motion into one where the fluid was completely stationary and, hence, at constant potential. If such an equipotential region existed adjacent to a region where the fluid was in motion, then we should have different equipotential surfaces terminating upon this stagnant region. This would enable us to carry a unit mass of fluid from a point upon an equipotential surface Φ_1 along this surface into the stagnant region and thence to a surface of higher potential Φ_2 with zero work. Then, carrying it directly back to its initial point would yield the positive work $\Phi_2 - \Phi_1$. In this manner we should achieve a perpetual-motion mechanism and violate the principle of the conservation of energy. Hence we must

conclude that no equipotential surface can terminate in this manner but must continue to a boundary. A corollary to this is that in a region occupied by a homogeneous fluid it is impossible to have one part of the fluid in motion and another part stagnant, except when the two are separated by impermeable boundaries—a proposition of some significance with regard to certain theories of ore deposition.

Can two equipotential surfaces intersect or coincide? Let one of these have the value Φ and the other $\Phi + \Delta\Phi$. Let the distance between them along the flowline be Δn. Then by Darcy's law

$$\mathbf{q} = \lim_{\Delta n \to 0} \left(-\sigma \frac{\Delta \Phi}{\Delta n} \right). \tag{177}$$

Since $\Delta\Phi$ is the constant difference of potential between the two surfaces, then as they approached each other, Δn would approach zero, and $\Delta\Phi/\Delta n$ would become infinite, corresponding to an infinite value of $\mathbf{q}$. Hence, at all points where the flow vector $\mathbf{q}$ is finite, no two different equipotential surfaces can ever coincide or intersect.

Exceptions to this occur at certain *singular points* in the flow region, one example of which is the flow around a sharp exterior angle of an impermeable boundary. As the corner is approached, the different equipotential surfaces which are normal to each of the two faces approach a point of coincidence. In the immediate neighborhood of such a point the velocity increases markedly, and Darcy's law loses its validity.

THE BOUNDARIES BETWEEN INHOMOGENEOUS FLUIDS

So far we have dealt only with the flow of a single homogeneous fluid through a region all voids of which were supposedly filled completely by that fluid. By our usage a homogeneous fluid is one whose density is a function of pressure only. Continuing this usage, we now wish to investigate the bounding surface between two different homogeneous fluids occupying different parts of a single flow region. Different homogeneous fluids may be immiscible, like water and oil, or miscible in all proportions, like water and alcohol. Where they are immiscible, their interface is a discrete surface of separation; where they are miscible, no such precise surface exists, but its place is taken by a zone of diffusion.

For immiscible fluids with their discrete surfaces of separation there exists an amount of surface energy where the two fluids are in mutual contact, and also other surface energies between each of the fluids separately and the solid medium. These give rise to capillary forces which act as a modifying influence upon an equilibrium that would obtain were such forces nonexistent. In many instances the effect of these modifying influences of capillarity are not of great importance; in other instances, especially in dealing with the oil-water relations of petroleum production, their effect appears to be far from negligible.

In ground-water problems the surface energies are effective along the air-water contacts but are lacking along the fresh-water—salt-water contacts. For simplicity we shall first assume that capillary forces do not exist, and then later introduce their effects as a modifying influence upon the results thus obtained.

While dealing with a single fluid we have had to consider only a single potential. In dealing with several fluids we shall have as many different potentials as there are fluids. These we shall define in such a manner that the definitions will be valid at all points in space not occupied by an impermeable solid. Thus, at each point in space, regardless of which fluid occupies that space, there will be a particular value of each of the several potentials. Also, there will be a complete scalar field in each potential throughout the region of space considered. In addition to this, each fluid will occupy a particular domain of its own with a surface of contact, or interface, between adjoining regions occupied by different fluids.

To deal with this more complex system we must generalize our notation somewhat if we are to avoid ambiguity and confusion. We must be able to distinguish the potentials of the several different fluids and the particular values assigned to each. In addition to this we must distinguish the separate regions occupied by the different fluids. The first two requirements are met by the use of two subscripts, the first identifying the fluid concerned, and the second, the particular value assigned. Thus Φ_{ij}, where i and j are 1, 2, 3, ... , signifies the jth particular value of the potential of the ith fluid. Where no particular value is intended, the second subscript will be omitted. Frequently it will be necessary to show that a given opera-

tion is to be performed in a region occupied by a specified fluid. This will be indicated by $(\ )_k$, where the parentheses enclose the operation and $k = 1, 2, 3, \ldots$ indicates the fluid in whose region it is to be performed. Thus $(\text{grad } \Phi_2)_1$ indicates the gradient of the potential of fluid 2 in the region occupied by fluid 1.

The potential of the ith fluid at any given point will be

$$\Phi_i = U + \int_{p_0}^{p} \frac{dp}{\rho_i}, \tag{178}$$

where ρ_i is its density. For liquids this simplifies to

$$\Phi_i = U + \frac{p - p_0}{\rho_i}. \tag{179}$$

At and near the earth's surface, gravity is sufficiently nearly constant that we may set $U = gz$. Then

$$\Phi_i = gz + \frac{p - p_0}{\rho_i}. \tag{180}$$

Also,

$$\frac{\partial \Phi_i}{\partial s} = g \cdot \frac{\partial z}{\partial s} + \frac{1}{\rho_i} \cdot \frac{\partial p}{\partial s} \tag{181}$$

and

$$-\text{grad } \Phi_i = +\mathbf{g} - \frac{1}{\rho_i} \text{ grad } p \tag{182}$$

This last equation is a vector equation, and each of its terms is a force per unit of mass that would act upon an element of the ith fluid placed at the specified point. It is important to observe that, while at a given point both $\mathbf{g}$ and $-\text{grad } p$ are vectors with fixed magnitudes and directions, the vector $-1/\rho_i \text{ grad } p$ has a fixed direction but a variable magnitude, depending upon the fluid density ρ_i. Consequently, for elements of fluids of different densities placed at the same point, the driving forces per unit of mass, $-\text{grad } \Phi_i$, will always be of different magnitudes and, in general, in different directions. Similarly, for different fluids, the equipotential surfaces $\Phi_i = \text{constant}$, passing through a given point, will in general not be parallel to one another, since for each fluid the equipotential surfaces are normal to grad Φ_i.

The importance of this is that it provides a separation mechanism for fluids of different densities. For instance, if we began initially with an emulsion of two immiscible fluids of different densities, the particles of each would be driven at different rates and, in general, along nonparallel paths. This process would continue until the two fluids were segregated into different regions.

Here, again, we are neglecting surface energies, so that for this to be strictly true it is necessary that the fluid particles be large enough for the driving forces to predominate over forces due to surface tensions and colloidal phenomena.

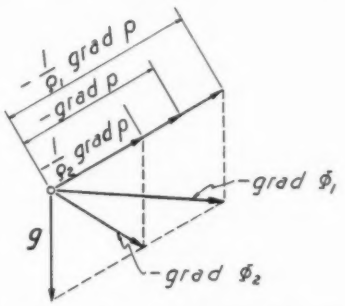

FIG. 26.—Forces acting upon elements of fluids of different densities placed at the same point.

It is not meant to imply that an existing fluid segregation must have arisen in the above manner, but rather to point out that such a mechanism exists. Suppose, for example, that we have two segregated fluids with a common interface. For this arrangement to be a stable one it is necessary for an element of either fluid, if placed in the region occupied by the other, to be repelled and driven back into its own territory. The mechanism for this is that described above.

Now, if we consider a region in different parts of which different fluids are segregated, there will be as many different fluid interfaces as there are pairs of different fluids in contact with one another. It is our purpose to study these interfaces; but since relationships valid for one should be valid for all, we need only consider a single interface between the two fluids of densities ρ_1 and ρ_2, both in steady motion.

For a given steady state of motion a fluid interface will be fixed in space and will exhibit many of the properties of a solid, impermeable boundary. If the segregation of the two fluids is complete, neither fluid can cross the boundary, so that the normal components of the flow of each must be zero and the flowline on each side tangential to

the boundary, although the flowlines of the two fluids on the opposite sides of the boundary may make any angle in that plane with each other.

In case the segregation is not complete, the normal components of flow will not be zero; and in each region where fluid is crossing the boundary, the flowlines will form some angle, $\gamma < 90^\circ$, with the surface normal directed into that region. An important instance of this sort will be considered later.

Considering, for the present, the case of complete fluid segregation, then the interface for each state of flow will act like a rigid impermeable boundary, but for each change in the state of flow of either of the fluids the interface will adjust itself to a new position of equilibrium. It represents, therefore, a configuration of dynamic equilibrium. Let us see how this is related to the potentials of the two fluids.

Let n_1 be the normal of the interface into the region occupied by the fluid of density ρ_1, and n_2 that into the region of the fluid of density ρ_2. Assuming that our fluids are liquids, then at any point in either region

$$\left.\begin{aligned} \Phi_1 &= gz + \frac{p - p_0}{\rho_1}, \\ \Phi_2 &= gz + \frac{p - p_0}{\rho_2}. \end{aligned}\right\} \tag{183}$$

Since stability requires that an element of either fluid in the domain of the other be driven back to its own territory, this implies corresponding repulsive force components along the surface normals in the respective regions. These can only be the result of an increase of the potential of each fluid in the domain of the other in the direction of its surface normal. Thus, for stability,

$$\left.\begin{aligned} \left(\frac{\partial \Phi_2}{\partial n_1}\right)_1 &> 0, \\ \left(\frac{\partial \Phi_1}{\partial n_2}\right)_2 &> 0. \end{aligned}\right\} \tag{184}$$

These are obtained in a convenient form if we eliminate $p - p_0$ from equation (183) and solve for Φ_1 and Φ_2, respectively; we then get

$$\left.\begin{aligned}\Phi_1 &= -\frac{\rho_2 - \rho_1}{\rho_1} \cdot gz + \frac{\rho_2}{\rho_1} \cdot \Phi_2 ,\\ \Phi_2 &= +\frac{\rho_2 - \rho_1}{\rho_2} \cdot gz + \frac{\rho_1}{\rho_2} \cdot \Phi_1 .\end{aligned}\right\} \tag{185}$$

Then

$$\left.\begin{aligned}\left(\frac{\partial \Phi_2}{\partial n_1}\right)_1 &= \frac{\rho_2 - \rho_1}{\rho_2} \cdot g \cdot \frac{\partial z}{\partial n_1} + \frac{\rho_1}{\rho_2}\left(\frac{\partial \Phi_1}{\partial n_1}\right)_1 ,\\ \left(\frac{\partial \Phi_1}{\partial n_2}\right)_2 &= -\frac{\rho_2 - \rho_1}{\rho_1} \cdot g \cdot \frac{\partial z}{\partial n_2} + \frac{\rho_2}{\rho_1}\left(\frac{\partial \Phi_2}{\partial n_2}\right)_2 .\end{aligned}\right\} \tag{186}$$

But since the normal components of flow across the interface are zero,

$$\left(\frac{\partial \Phi_1}{\partial n_1}\right)_1 = \left(\frac{\partial \Phi_2}{\partial n_2}\right)_2 = 0 , \tag{187}$$

so that equations (186) simplify to

$$\left.\begin{aligned}\left(\frac{\partial \Phi_2}{\partial n_1}\right)_1 &= \frac{\rho_2 - \rho_1}{\rho_1} \cdot g \cdot \frac{\partial z}{\partial n_1} ,\\ \left(\frac{\partial \Phi_1}{\partial n_2}\right)_2 &= -\frac{\rho_2 - \rho_1}{\rho_1} \cdot g \cdot \frac{\partial z}{\partial n_2} .\end{aligned}\right\} \tag{188}$$

Stability requires that both the right-hand terms be positive. Bearing in mind that n_2 is oppositely directed from n_1,

$$\frac{\partial z}{\partial n_2} = -\frac{\partial z}{\partial n_1} ,$$

so that if n_1 is upward-directed, $\partial z/\partial n_1$ is positive and $\partial z/\partial n_2$ is negative, and vice versa. Hence if n_1 is the upward-directed normal, stability requires that $\rho_1 < \rho_2$; if n_2 is upward-directed, ρ_2 must be

less than ρ_1. In both cases the less dense liquid must occupy the upper space. When the interface is vertical,

$$\frac{\partial z}{\partial n_1} = \frac{\partial z}{\partial n_2} = 0 ,$$

and neutral equilibrium results.

SLOPE OF THE INTERFACE

Let us now investigate the slope of the interface as a function of the states of flow of the two fluids or of their two potentials in the fields of flow. Eliminating $p - p_0$ from equation (183) and solving for z gives us

$$z = \frac{1}{g}\left(\frac{\rho_2}{\rho_2 - \rho_1} \cdot \Phi_2 - \frac{\rho_1}{\rho_2 - \rho_1} \cdot \Phi_1\right). \tag{189}$$

This is the elevation of any point whatever in either of the two regions, or of any other region for that matter, for which the two potentials Φ_1 and Φ_2 are known. Or, if we like, we may think of every

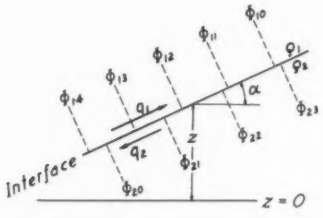

FIG. 27.—Tilt of fluid interface due to flow of both fluids

point in space being characterized by particular values of the three quantities z, Φ_1, and Φ_2, whose relations to each other are given by equation (189), so that if any two of them are known the third is uniquely determined.

Now let us consider the potentials and the components of flow in a vertical plane section through the system. Let s be the trace of the interface along this section. Equation (189) is valid for points on the interface as well as elsewhere; and while in general we do not know

the values of Φ_1 and Φ_2 at given points on the interface, if α is its angle of slope measured positively upward in the direction s,

$$\sin \alpha = \frac{\partial z}{\partial s} = \frac{1}{g}\left(\frac{\rho_2}{\rho_2 - \rho_1} \cdot \frac{\partial \Phi_2}{\partial s} - \frac{\rho_1}{\rho_2 - \rho_1} \cdot \frac{\partial \Phi_1}{\partial s}\right). \qquad (190)$$

Then, since

$$\left.\begin{aligned} \frac{\partial \Phi_2}{\partial s} &= -\frac{q_{2s}}{\sigma}, \\ \frac{\partial \Phi_1}{\partial s} &= -\frac{q_{1s}}{\sigma}, \end{aligned}\right\} \qquad (191)$$

where q_{1s} is the component in the direction s of the flow vector $\mathbf{q}_1$ of the ρ_1-fluid in the section we are considering, and q_{2s} that of the ρ_2-fluid, these can be substituted into equation (190), transforming the latter into

$$\sin \alpha = \frac{\partial z}{\partial s} = \frac{1}{\sigma g}\left(-\frac{\rho_2}{\rho_2 - \rho_1} \cdot q_{2s} + \frac{\rho_1}{\rho_2 - \rho_1} \cdot q_{1s}\right). \qquad (192)$$

If both fluids are static $q_{1s} = q_{2s} = 0$ and $\sin \alpha = 0$, showing that for these conditions the equilibrium configuration for the fluid interface is a horizontal surface. Starting from a static state, let us keep the ρ_2-fluid static and increase q_{1s} by successive steps. Then q_{2s} will be zero, and equation (192) will become

$$\sin \alpha = \frac{\partial z}{\partial s} = \frac{1}{\sigma g} \cdot \frac{\rho_1}{\rho_2 - \rho_1} \cdot q_{1s} = -\frac{1}{g} \cdot \frac{\rho_1}{\rho_2 - \rho_1} \cdot \frac{\partial \Phi_1}{\partial s}. \qquad (193)$$

Hence, if $\rho_1 < \rho_2$, as the rate of flow q_{1s} of the less dense ρ_1-fluid is increased, $\sin \alpha$ will also increase, and the interface will tilt upward in the direction of the flow.

Now, if we repeat this procedure, keeping $q_{1s} = 0$, and gradually increasing q_{2s}, we shall have

$$\sin \alpha = \frac{\partial z}{\partial s} = -\frac{1}{\sigma g} \cdot \frac{\rho_2}{\rho_2 - \rho_1} \cdot q_{2s} = +\frac{1}{g} \cdot \frac{\rho_2}{\rho_2 - \rho_1} \cdot \frac{\partial \Phi_2}{\partial s}, \qquad (194)$$

showing that for flow in the direction s of the denser ρ_2-fluid the interface will tilt downward in the direction of the flow.

If both fluids flow simultaneously, the angle α will be the resultant of the two tilts, as determined by equation (192). If they both flow in the same direction, the two tilts will oppose each other, and α will be intermediate between its values, owing to the two flows occurring separately, becoming zero when

$$\sin \alpha = 0 = \frac{1}{\sigma g}\left(-\frac{\rho_2}{\rho_2 - \rho_1} \cdot q_{2\alpha} + \frac{\rho_1}{\rho_2 - \rho_1} \cdot q_{1\alpha}\right)$$

or when

$$\frac{q_{1\alpha}}{q_{2\alpha}} = \frac{\dfrac{\partial \Phi_1}{\partial s}}{\dfrac{\partial \Phi_2}{\partial s}} = \frac{\rho_2}{\rho_1}. \tag{195}$$

When the two fluids flow in opposite directions, the two component tilts augment one another, and the resultant is greater than that due to either alone.

For simplicity, let us now confine our attention to the equations involving the potentials or their gradients, bearing in mind that we can always switch to the rates of flow by means of the equation of transformation (191) when we wish to do so.

We note, according to the general equation (190) and the particular ones (193) and (194), that sin α increases with the appropriate increase of the components of the potential gradients along the interface in the section considered. Since the maximum value of sin α is unity, it will be interesting to see what happens when this value is reached. Taking the general equation (190), we see that

$$(\sin \alpha)_{\max} = 1 = \frac{1}{g}\left(\frac{\rho_2}{\rho_2 - \rho_1} \cdot \frac{\partial \Phi_2}{\partial s} - \frac{\rho_1}{\rho_2 - \rho_1} \cdot \frac{\partial \Phi_1}{\partial s}\right)_{\max}, \tag{196}$$

which tells us that the maximum value the difference between the two terms in the parentheses can have is g. When only one of the fluids is flowing at a time, the potential gradient of the other will be zero, and

$$\left.\begin{aligned}(\sin \alpha)_{\max} &= +1 = -\frac{1}{g} \cdot \frac{\rho_1}{\rho_2 - \rho_1}\left(\frac{\partial \Phi_1}{\partial s}\right)_{\max},\\ (\sin \alpha)_{\max} &= +1 = +\frac{1}{g} \cdot \frac{\rho_2}{\rho_2 - \rho_1}\left(\frac{\partial \Phi_2}{\partial s}\right)_{\max},\end{aligned}\right\}$$

or

$$\left.\begin{aligned}\left(\frac{\partial \Phi_1}{\partial s}\right)_{\max} &= -g \cdot \frac{\rho_2 - \rho_1}{\rho_1}, \\ \left(\frac{\partial \Phi_2}{\partial s}\right)_{\max} &= +g \cdot \frac{\rho_2 - \rho_1}{\rho_2},\end{aligned}\right\} \tag{197}$$

when the ρ_1- and the ρ_2-fluids, respectively, are flowing.

Equations (196) and (197) are statements that, when each fluid is flowing alone, the component along the interface of its potential gradient cannot exceed a certain critical finite value and that, when both flow simultaneously, the difference of the components of their potential gradients cannot exceed a specified critical finite amount. What is the meaning of this physically? At first thought it seems to imply that these critical potential gradients are the maximum obtainable. That this interpretation is absurd is evident when we consider that the potential gradients are our independent variables and are subject to being given any values we choose over a very wide range.

What it does signify is this: That for values of the gradients greater than those stated, the interfacial surface ceases to exist. When only a single fluid is flowing, this comes about either by lateral migration until the interface coincides with an impermeable boundary or by the confluence of two stream tubes approaching from different directions. In both cases the static fluid is squeezed out from the region where the critical value of the potential gradient is exceeded.

When both fluids are flowing, lateral migration of the vertical interface to an impermeable boundary is impossible, because this would reduce the cross section of the stream tubes of one of the fluids to zero. In this case the interface migrates laterally; and, as it does so, it increases the stream-tube area of one fluid and decreases that of the other, reducing the first potential gradient and increasing the second. This migration will continue until the critical maximum difference of the two potential gradients is again established.

In fact, the same kind of thing happens where only one of the fluids is flowing. If the critical potential gradient is exceeded, the

interface shifts laterally in such a direction as to increase the area of the stream tubes and decrease the potential gradient. This will continue either until the potential gradient is reduced to its critical value or until an impermeable boundary, or another set of stream tubes of the same fluid, is encountered.

THE ELEVATION OF THE FLUID INTERFACE

The elevation of any point at which the potentials of the two fluids is known is given by equation (189). In particular, this is true of a point upon the fluid interface. The difficulty is that, when both

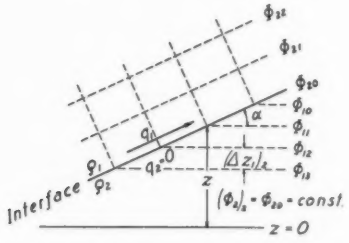

FIG. 28.—Tilt of interface and equipotential surfaces of both fluids when one fluid flows while the other is static.

fluids are flowing simultaneously, we do not know the values of the two potentials at points on the interface; nor is there any convenient method of determining them in most instances. Consequently, to obtain the equation of the interface for this general state of flow we should be obliged to rely upon the integration of slope equations like (190), which in all but the simplest cases is difficult to do.

Fortunately, in practice the most important problems encountered are those in which only one of the two fluids is flowing, while the other remains sensibly static and, hence, at constant potential. The interface then becomes an equipotential surface in terms of this potential, and equation (189) becomes a linear equation between the values of the remaining potential along the interface and the elevation of its points.

For example, let the ρ_1-fluid flow while the ρ_2-fluid remains stationary. Then in the ρ_2-region the potential Φ_2 will be constant, say

of the value Φ_{20}. Then throughout the ρ_2-region and upon the interface the elevation of any given surface $\Phi_1 =$ constant will be

$$z = \frac{1}{g}\left(\frac{\rho_2}{\rho_2 - \rho_1} \cdot \Phi_{20} - \frac{\rho_1}{\rho_2 - \rho_1} \cdot \Phi_1\right). \tag{198}$$

Since, when $\Phi_1 =$ constant, $z =$ constant also, it is clear that in the ρ_2-region the family of surfaces $\Phi_1 =$ constant are horizontal. When they intersect the interface, they then refract into perpendicularity with that surface in the ρ_1-region.

Also from equation (198) the family of equidifferent surfaces $\Phi_1 =$ constant are equidistantly spaced. If $\Delta\Phi_1$ be the potential difference between successive surfaces, their spacing is

$$(\Delta z_1)_2 = -\frac{1}{g} \cdot \frac{\rho_1}{\rho_2 - \rho_1} \cdot \Delta\Phi_1 . \tag{199}$$

In a similar manner, if we let the ρ_1-fluid remain stationary while the ρ_2-fluid flows, and let Φ_{10} be the constant value of the potential (Φ_1), the elevation along the interface and inside the ρ_1-region of a surface $\Phi_2 =$ constant will be

$$z = \frac{1}{g}\left(\frac{\rho_2}{\rho_2 - \rho_1} \cdot \Phi_2 - \frac{\rho_1}{\rho_2 - \rho_1} \cdot \Phi_{10}\right). \tag{200}$$

These surfaces will likewise be horizontal in the ρ_1-region with a spacing for a potential difference $\Delta\Phi_2$ of

$$(\Delta z_2)_1 = \frac{1}{g} \cdot \frac{\rho_2}{\rho_2 - \rho_1} \cdot \Delta\Phi_2 . \tag{201}$$

In these two cases the potential gradients of the moving fluid in the region occupied by the static one will be vertical. In the separate ones of these two cases, by solving equations (198) and (200) for Φ_1 and Φ_2, respectively, we obtain

$$\left.\begin{aligned}(\Phi_1)_2 &= -\frac{\rho_2 - \rho_1}{\rho_1} \cdot gz + \frac{\rho_2}{\rho_1} \cdot \Phi_{20} ,\\ (\Phi_2)_1 &= +\frac{\rho_2 - \rho_1}{\rho_2} \cdot gz + \frac{\rho_1}{\rho_2} \cdot \Phi_{10} ,\end{aligned}\right\} \tag{202}$$

from which

$$\left.\begin{aligned}\left(\frac{\partial \Phi_1}{\partial z}\right)_2 &= -\frac{\rho_2 - \rho_1}{\rho_1} \cdot g\,,\\ \left(\frac{\partial \Phi_2}{\partial z}\right)_1 &= +\frac{\rho_2 - \rho_1}{\rho_2} \cdot g\,.\end{aligned}\right\} \tag{203}$$

Letting $\rho_2 > \rho_1$, then, when the ρ_2-region is at constant potential, the Φ_1 potential decreases upward or increases downward at the rate $[(\rho_2 - \rho_1)/\rho_1]g$. In the ρ_1-region, when this is at constant potential the potential Φ_2 increases upward at the rate $[(\rho_2 - \rho_1)/\rho_2]g$. Stated vectorially,

$$\left.\begin{aligned}(\text{grad } \Phi_1)_2 &= \frac{\rho_2 - \rho_1}{\rho_1} \cdot \mathbf{g}\,,\\ (\text{grad } \Phi_2)_1 &= -\frac{\rho_2 - \rho_1}{\rho_2} \cdot \mathbf{g}\,,\end{aligned}\right\} \tag{204}$$

where **g** is now the downward-directed vector of the acceleration due to gravity.

THREE-FLUID CASE

Now let us consider a special case involving three fluids. Let ρ_1, ρ_2, and ρ_3 be their three densities, and let $\rho_1 < \rho_2 < \rho_3$. Let the ρ_2-fluid flow while the ρ_1 and the ρ_3 fluids remain static. We shall now have the fluids arranged in three layers according to their densities, with the least dense uppermost, with a 1, 2 and a 2, 3 interface.

The three potentials will be

$$\left.\begin{aligned}\Phi_1 &= gz + \frac{p - p_0}{\rho_1}\,,\\ \Phi_2 &= gz + \frac{p - p_0}{\rho_2}\,,\\ \Phi_3 &= gz + \frac{p - p_0}{\rho_3}\,.\end{aligned}\right\} \tag{205}$$

Besides, we shall have

$$\left.\begin{aligned}(\Phi_1)_1 &= \text{constant} = \Phi_{10}\,,\\ (\Phi_2)_2 &\neq \text{constant} = \Phi_2\,,\\ (\Phi_3)_3 &= \text{constant} = \Phi_{30}\,.\end{aligned}\right\} \tag{206}$$

Eliminating $p - p_0$ from contiguous pairs of equations (205) and solving for z, and then substituting the values from equations (206) into the results, gives for the elevations of points on the two interfaces

$$\left.\begin{aligned} z_{12} &= \frac{1}{g}\left(\frac{\rho_2}{\rho_2 - \rho_1} \cdot \Phi_2 - \frac{\rho_1}{\rho_2 - \rho_1} \cdot \Phi_{10}\right), \\ z_{23} &= \frac{1}{g}\left(\frac{\rho_3}{\rho_3 - \rho_2} \cdot \Phi_{30} - \frac{\rho_2}{\rho_3 - \rho_2} \cdot \Phi_2\right). \end{aligned}\right\} \tag{207}$$

The heights z_{12} and z_{23} of these equations are the elevations above the standard datum of the intersection of the two respective interfaces with a surface $\Phi_2 =$ constant. The difference between these two elevations is

$$\left.\begin{aligned} z_{12} - z_{23} = \frac{1}{g}\Bigg[&\left(\frac{\rho_2}{\rho_2 - \rho_1} + \frac{\rho_2}{\rho_3 - \rho_2}\right)\Phi_2 \\ &- \frac{\rho_1}{\rho_2 - \rho_1} \cdot \Phi_{10} - \frac{\rho_3}{\rho_3 - \rho_2} \cdot \Phi_{30}\Bigg]. \end{aligned}\right\} \tag{208}$$

These two elevations are, however, not of points or lines one vertically above the other.

Also, equidifferent surfaces $\Phi_2 =$ constant refract across the two interfaces into the two static regions as equally spaced horizontal surfaces, the scales of the spacing being different in the two cases. For a potential difference $\Delta\Phi_2$ the two spacings are

$$\left.\begin{aligned} (\Delta z_2)_1 &= \frac{1}{g} \cdot \frac{\rho_2}{\rho_2 - \rho_1} \cdot \Delta\Phi_2, \\ (\Delta z_2)_3 &= -\frac{1}{g} \cdot \frac{\rho_2}{\rho_3 - \rho_2} \cdot \Delta\Phi_2, \end{aligned}\right\} \tag{209}$$

and their ratios are given by

$$\frac{(\Delta z_2)_1}{(\Delta z_2)_3} = -\frac{\rho_3 - \rho_2}{\rho_2 - \rho_1}. \tag{210}$$

In the most important three-fluid case in ground-water problems the fluids are the air, fresh water, and salt water. While the forego-

ing equations have been derived for liquids, in this case the air is at sensibly constant potential, and so we can deal with it with no alteration of the above equations. We let ρ_1 be the density of the air, ρ_2 that of fresh water, and ρ_3 that of salt water. Then by choosing our standard datum at sea-level and 1 atmosphere as our standard pressure,

$$\left.\begin{aligned}(\Phi_1)_1 &= gz_1 + \int_{p_0}^{p_1} \frac{dp}{\rho_1} = 0\,,\\ \Phi_2 &= gz_2 + \frac{p_2 - p_0}{\rho_2} = gh\,,\\ (\Phi_3)_3 &= gz_3 + \frac{p_3 - p_0}{\rho_3} = 0\,.\end{aligned}\right\} \tag{211}$$

Also, the density of the air is negligible compared with that of water, and so may be neglected. In this case equations (207) simplify to

$$\left.\begin{aligned}z_{12} &= \frac{1}{g}\cdot\frac{\rho_2}{\rho_2 - \rho_1}\cdot\Phi_2 = h\,,\\ z_{23} &= -\frac{1}{g}\cdot\frac{\rho_2}{\rho_3 - \rho_2}\cdot\Phi_2 = -\frac{\rho_2}{\rho_3 - \rho_2}\cdot h\,.\end{aligned}\right\} \tag{212}$$

The difference between these elevations for a given surface Φ_2 = constant is then

$$z_{12} - z_{23} = \left(1 + \frac{\rho_2}{\rho_3 - \rho_2}\right)h = \frac{\rho_3}{\rho_3 - \rho_2}\cdot h\,. \tag{213}$$

The spacings of the fresh-water equipotential surfaces in regions occupied by air and salt water, respectively, are obtained from equation (209) and are

$$\left.\begin{aligned}(\Delta z_2)_1 &= \frac{1}{g}\cdot\frac{\rho_2}{\rho_2 - \rho_1}\cdot\Delta\Phi_2 = \Delta h\,,\\ (\Delta z_2)_3 &= -\frac{1}{g}\cdot\frac{\rho_2}{\rho_3 - \rho_2}\cdot\Delta\Phi_2 = -\frac{\rho_2}{\rho_3 - \rho_2}\cdot\Delta h\,,\end{aligned}\right\} \tag{214}$$

and their ratio is

$$\frac{(\Delta z_2)_1}{(\Delta z_2)_3} = -\frac{\rho_3 - \rho_2}{\rho_2}\,. \tag{215}$$

It should also be added that, in accordance with an earlier stipulation, we have here neglected the surface tension of the fresh-water–air interface. Strictly speaking, the elevation z_{12} is that of the water table. The actual water-air interface inside a permeable medium will be somewhat higher than this.

In all of these equations h refers to the elevation of the free surface in a manometer tube filled with fresh water and terminated at the point whose potential is to be determined.

Again it should be emphasized that the elevations z_{12} and z_{23} are the elevations above the standard datum of the intersections with the upper and lower interfaces of a particular fresh-water equipotential surface, and only in the case that all three fluids are in static equilibrium do these elevations occur one vertically above the other. In all other cases the surface Φ_2 = constant will be curved and the vertical distance between the upper and lower interfaces will be greater—sometimes but not always by a negligible amount—than the difference $z_{12} - z_{23}$ as given by equation (213).

Where a given surface Φ_2 = constant intersects the upper and lower interfaces, the sines of the angles of slope of these surfaces are

$$\left.\begin{aligned} \sin \alpha_{12} &= \frac{1}{g} \cdot \frac{\rho_2}{\rho_2 - \rho_1} \cdot \frac{\partial \Phi_2}{\partial s_{12}}, \\ \sin \alpha_{23} &= -\frac{1}{g} \cdot \frac{\rho_2}{\rho_3 - \rho_2} \cdot \frac{\partial \Phi_2}{\partial s_{23}}. \end{aligned}\right\} \tag{216}$$

If it be assumed that $\partial \Phi_2 / \partial s_{12} = \partial \Phi_2 / \partial s_{23}$, which in many cases is a good approximation, then the ratios of the sines of these two angles is

$$\frac{\sin \alpha_{12}}{\sin \alpha_{23}} = -\frac{\rho_3 - \rho_2}{\rho_2 - \rho_1} = -\frac{\rho_3 - \rho_2}{\rho_2}, \tag{217}$$

which is the same as the ratio of the equipotential surface spacings given by equation (215). For fresh water and sea water the ratio $(\rho_3 - \rho_2)/\rho_2 \leqq \frac{1}{40}$.

FLOW ACROSS AN INTERFACE

In the foregoing we have assumed that no flow occurred across the fluid interfaces. There are several important instances for which this is not true. If the segregation is not complete, discrete elements

of finite size of either fluid in the territory of the other will be repelled and driven back into their own territory. The fall of raindrops from the atmosphere toward the air-water interface is an important instance of this kind; the rise of gas bubbles through a liquid is another. For processes in the reverse direction we have diffusion and evaporation.

In either case, when a given region is gaining or losing its own fluid across a fluid interface, the flowlines and flow tubes will no longer be parallel to the interface but will terminate upon it. The interface will accordingly act as a source or a sink. Likewise the equipotential surfaces will now approach the interface at some angle different from 90°. The configuration of the interface, however, will still be determined by the two sets of potentials of the contiguous fluids in the same manner as that we have already discussed.

REFRACTION OF A FLUID INTERFACE ACROSS A PLANE BOUNDARY BETWEEN MEDIA OF DIFFERENT PERMEABILITIES

Let us now investigate the behavior of the interface between two fluids when this intersects the plane boundary between media of different permeabilities. These two surfaces will now divide our field of flow into regions a and b of different permeabilities and into regions 1 and 2 occupied by different fluids. We let ρ_1 be the density of one of the fluids and ρ_2 that of the other, with $\rho_1 < \rho_2$, and let k_a and k_b be the two permeabilities.

For simplicity we consider only the components of the flow and the corresponding potential gradients in a single arbitrary vertical plane, and we allow only one of the fluids to flow while the other remains static and at constant potential. The moving fluid is taken to be a liquid, though, if the denser fluid is flowing, the less dense one may be a gas. The moving fluid is made always to cross the a–b plane in the direction from a to b.

We let β be the angle of slope of the a–b plane in the section considered measured upward from the horizontal in the direction of the flow, s_{ab} the length along its trace, and n its normal. Let α_a and α_b be the limiting angles of slope of the fluid interface in the regions a and b

in the vertical section considered as the a–b plane is approached, and s_{12} the length along its trace in the direction of the flow.

Now let the ρ_1-fluid flow while the ρ_2-fluid remains stationary. Then the surfaces Φ_1 = constant will approach the fluid interface perpendicularly in the ρ_1-region and then refract into a family of

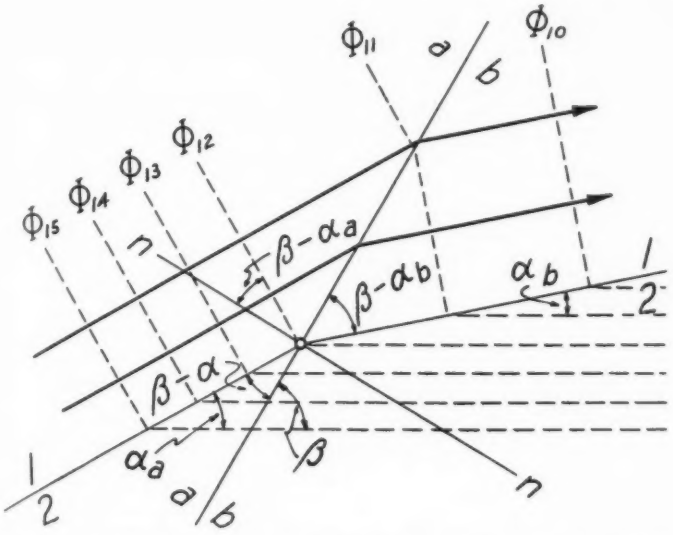

FIG. 29.—Diagram for the identification of quantities employed in discussing intersection of fluid interface with boundary between regions of different permeabilities.

equally spaced horizontal surfaces in the ρ_2-region. Inside the ρ_1-region along the a–b plane as the fluid interface is approached, the boundary conditions which must be satisfied are the following: The normal components of flow across the a–b plane must be the same in both the regions a and b, and the tangential components of the potential Φ_1 must be the same in both these regions:

$$\left(\frac{\partial \Phi_1}{\partial s_{ab}}\right)_{1a} = \left(\frac{\partial \Phi_1}{\partial s_{ab}}\right)_{1b}, \tag{218}$$

$$(q_{1n})_{1a} = (q_{1n})_{1b}. \tag{219}$$

Each of these quantities can now be evaluated separately in terms of the gradient of Φ_1 in region 2, which is fixed, and of the permeabilities k_a and k_b and the angles α_a, α_b, and β. We then get

$$\left.\begin{aligned}\left(\frac{\partial \Phi_1}{\partial s_{ab}}\right)_{1a} &= \left(\frac{\partial \Phi_1}{\partial s_{12}}\right)_{1a} \cos(\beta - \alpha_a) = \left(\frac{\partial \Phi_1}{\partial z}\right)_2 \sin \alpha_a \cdot \cos(\beta - \alpha_a)\,, \\ \left(\frac{\partial \Phi_1}{\partial s_{ab}}\right)_{1b} &= \left(\frac{\partial \Phi_1}{\partial s_{12}}\right)_{1b} \cos(\beta - \alpha_b) = \left(\frac{\partial \Phi_1}{\partial z}\right)_2 \sin \alpha_b \cdot \cos(\beta - \alpha_b)\,.\end{aligned}\right\} \quad (220)$$

Similarly,

$$\left.\begin{aligned}-(q_{1n})_{1a} = \sigma_a \left(\frac{\partial \Phi_1}{\partial n}\right)_{1a} &= \sigma_a \left(\frac{\partial \Phi_1}{\partial s_{12}}\right)_{1a} \sin(\beta - \alpha_a) \\ &= \sigma_a \left(\frac{\partial \Phi_1}{\partial z}\right)_2 \sin \alpha_a \cdot \sin(\beta - \alpha_a)\,, \\ -(q_{1n})_{1b} = \sigma_b \left(\frac{\partial \Phi_1}{\partial n}\right)_{1b} &= \sigma_b \left(\frac{\partial \Phi_1}{\partial s_{12}}\right)_{1b} \sin(\beta - \alpha_b) \\ &= \sigma_b \left(\frac{\partial \Phi_1}{\partial z}\right)_2 \sin \alpha_b \cdot \sin(\beta - \alpha_b)\,.\end{aligned}\right\} \quad (221)$$

Equating the separate equations (220) gives

$$\sin \alpha_a \cdot \cos(\beta - \alpha_a) = \sin \alpha_b \cdot \cos(\beta - \alpha_b)\,. \quad (222)$$

Equations (221) give

$$\sigma_a \sin \alpha_a \cdot \sin(\beta - \alpha_a) = \sigma_b \sin \alpha_b \cdot \sin(\beta - \alpha_b)\,. \quad (223)$$

But, since

$$\sigma_a = \frac{k_a \rho_1}{\eta_1}\,, \qquad \text{and} \qquad \sigma_b = \frac{k_b \rho_1}{\eta_1}\,,$$

equation (223) reduces to

$$k_a \sin \alpha_a \cdot \sin(\beta - \alpha_a) = k_b \sin \alpha_b \cdot \sin(\beta - \alpha_b)\,. \quad (224)$$

Equations (222) and (224) give the relations between α_a, α_b, β, k_a, and k_b, which must simultaneously be satisfied at the intersection of the fluid interface with the a–b plane. Since the fluid crosses this plane from a to b,

$$\alpha_a \gtrless \beta\,, \qquad \alpha_b \gtrless \beta\,.$$

The angles α_a and α_b are the dependent variables whose values are to be determined when the values of the independent variables β, k_a, and k_b are given.

Equation (222) is given a simple geometrical interpretation if we draw a circle whose vertical upward-directed diameter is taken as a unit vector. Then at the lower end of this diameter we draw a horizontal line. Taking the intersection of these two lines as a polar origin, we lay off the angles α_a, α_b, and β measured from the horizontal. The lines through the origin making the angles α_a, α_b, and β, respectively, form chords to the circle. The length of the α_a-chord is numerically to sin α_a, and its projection upon the β-chord is equal to sin $\alpha_a \cdot \cos(\beta - \alpha_a)$; the length of the α_b-chord is equal to sin α_b, and its projection upon the β-chord is sin $\alpha_b \cdot \cos(\beta - \alpha_b)$.

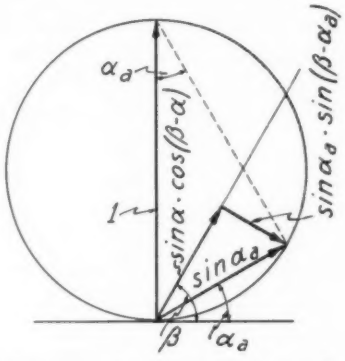

FIG. 30.—Graphical representation of quantities in equations (222) and (224)

When this has been done, it is seen by inspection that equation (222) can only be satisfied by

$$\alpha_a = \alpha_b \,. \tag{225}$$

Introducing this result into equation (224) transforms the latter into

$$k_a \sin \alpha_a \cdot \sin(\beta - \alpha_a) = k_b \sin \alpha_a \cdot \sin(\beta - \alpha_a) \,. \tag{226}$$

Before solving this for α_a, however, another condition needs to be taken into account, namely, that, owing to instability of the inter-

face which would result for values greater than this, the maximum possible value of α_a is 90°. We must therefore make a distinction between the solutions of equation (226) for values of β less than 90° and values greater than 90°. For $\beta < 90°$ the solutions of equation (226) for different values of k_a and k_b are

$$k_a \neq k_b: \quad \sin \alpha_a \cdot \sin (\beta - \alpha_a) = 0, \qquad \alpha_a = 0 \text{ or } \beta. \tag{227}$$

$$k_a = k_b: \quad 0 \lesseqgtr \sin \alpha_a \cdot \sin (\beta - \alpha_a) \lesseqgtr 1, \qquad 0 \lesseqgtr \alpha_a \lesseqgtr 90°. \tag{228}$$

When $\alpha_a = 0$, both fluids are in static equilibrium so that their interface is a horizontal surface upon which the a–b plane exerts no influence. When the ρ_1-fluid flows, however, α_a cannot be zero; and if $k_a \neq k_b$, then the interface must twist around so as to approach and leave the a–b plane tangentially. Physically, this is somewhat similar to an easement curve on railroads, where the centrifugal force is made to increase gradually from zero to a maximum and then decline gradually to zero again. In the fluid case discontinuities are avoided when the interface approaches and leaves the a–b plane tangentially. When $k_a = k_b$ the problem reduces to that of the flow through a homogeneous medium.

When $90° < \beta < 180°$, $0 \lesseqgtr \alpha_a \lesseqgtr 90°$; and, strictly speaking, it is impossible to satisfy equation (226) except for $\alpha_a = 0$, corresponding to zero flow, or for $k_a = k_b$, corresponding to a homogeneous medium.

Evidently in this case, when $k_a \neq k_b$, some discontinuity has to take place, and our problem resolves itself into determining the nature of the discontinuity. When $k_b > k_a$, this is fairly obvious. Imagine the flow to occur from a to b while the angle β is slowly increased from a value less than 90° to one greater than this amount. Until β reaches 90° and the a–b plane is vertical, the angles α will equal β, and the interface will approach the surface tangentially. When it is rotated farther, α will remain at 90°. The discharge q_{1a} will then be at its maximum in region a, but across the a–b plane in region b there will be the same potential gradient as in a but a higher permeability. This will produce a faster velocity of flow than in a; but since the total discharge cannot be different from that in a, the ρ_1-fluid in b will break up and will either mix with the ρ_2-fluid or,

if they are immiscible, drops will form and rise vertically upward through a ρ_2-matrix until the interface in the b region is encountered and crossed.

Upgrade along the a–b plane the flowlines in the a region will gradually swing around toward the surface normal. When the angle θ_a they make with this normal reaches such a value that

$$\tan \theta_a = \frac{k_a}{k_b} \tan \theta_b = \frac{k_a}{k_b} \tan (180° - \beta) , \qquad (229)$$

corresponding to the tangent law of refraction with the flowlines in the b region vertical, continuity of flow will again be established.

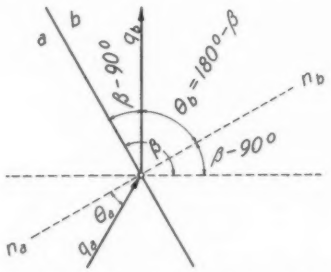

FIG. 31.—The angles referred to in equation (229)

Thus, for $\beta > 90°$ and $k_b > k_a$ there will be a finite displacement of the interface in the b-region upward along the a–b plane from its terminus in the a-region, with both the angles α_a and α_b equal to 90°. Between the termini of these two interfaces the flow across the a–b plane will give rise in the b-region either to a zone of diffusion and mixing or to one in which the ρ_1-fluid will percolate upward through the ρ_2-fluid until it again crosses the interface.

When $90° < \beta < 180°$, and $k_a > k_b$, and $0 < \alpha_a \gtrless 90°$, the problem is indeterminate, for no value of α_a within this range will satisfy equation (226). Neither can there be a fluid discontinuity across the a–b plane, because the higher velocity fluid is now in the a-region; nor is a displacement of the fluid interface in the b-region *down* the a–b plane possible because this would correspond to a flow in the direction of increasing potential. What must happen is that a zone

of distortion exists in the immediate vicinity of the intersection of the two surfaces so that equation (226) does not represent the true state of affairs. Evidently the interface is continuous across the a–b plane; and in the special cases that the flow is zero or that $k_a = k_b$, $\alpha_a = \alpha_b$. More than this one cannot say.

If we keep the ρ_1-fluid stationary and let the ρ_2-fluid flow, equations analogous to those from (218) to (229) may be derived. In this case the angle of tilt α of the interface will be downward in the direction of the flow, and the angle β should be measured in the same direction as α.

The most important case of this in practice occurs when k_a is finite and k_b infinite, corresponding to the flow from an underground region into an open space. In this case, when $0 < \beta < 90°$, $\alpha_a = \beta$ and the interface will approach the a–b plane tangentially. Since, however, discharge across this plane must occur (by hypothesis), the flowlines in the a-region away from the interface must swing around so as to intersect it. Across the boundary in the b-region either this fluid is absorbed by mixing and diffusion or else it forms a thin sheet and flows upward along the a–b plane until it encounters a horizontal interface between static bodies of the two fluids.

When $90° < \beta < 180°$, a similar thing occurs except that $\alpha_a = 90°$, and either the ρ_1-fluid mixes or diffuses into the ρ_2-fluid or else it rises vertically by percolation until it crosses the horizontal interface between static bodies of the two fluids.

In both of these cases the zone along the a–b plane between the terminus upon it of the interface in the a-region and the static fluid interface in the b-region is called a *surface of seepage*. Along the surface of seepage the ρ_1-fluid occupies one side of the a–b plane; and, except for a possible veneer of the ρ_2-fluid on the b-side, the ρ_2-fluid occupies the other. Consequently, along the a–b plane in the zone of seepage the component of the gradient of Φ_1 is

$$\frac{\partial \Phi_1}{\partial s_{ab}} = (\text{grad } \Phi_1)_{1a} \sin \theta = (\text{grad } \Phi_1)_2 \sin \beta ,$$

or

$$(\text{grad } \Phi_1)_{1a} = (\text{grad } \Phi_1)_2 \frac{\sin \beta}{\sin \theta} , \tag{230}$$

where θ is the angle these flowlines make with the normal to the a–b plane.

For constant values of β, $(\text{grad } \Phi_1)_2 \sin \beta$ is constant, indicating that along the surface of seepage the tangential component of the potential gradient is constant, so that, as the values of θ decrease from 90° to 0°, the corresponding value of $(\text{grad } \Phi_1)_{1a}$ increases from zero to infinity.

In the a-region at the fluid interface the flowlines approach the a–b plane either tangentially or vertically, and here the respective

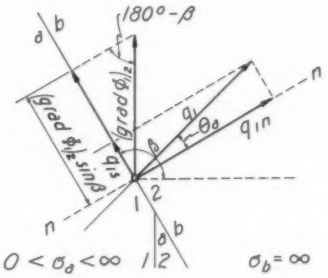

FIG. 32.—Manner of increase of the rate of flow of fluid 1 from region of finite permeability into one of infinite permeability occupied by fluid 2, as θ_a decreases.

values of θ are 90° or 180° − β. Then beyond the interface between the static bodies of ρ_1 and ρ_2 fluids in the b-region, the tangential component of the gradient of Φ_1 abruptly becomes zero, because the ρ_1-body is a region of Φ_1 = constant. Opposite to this the flowlines in the a-region must approach the a–b plane perpendicularly, so that here the angle θ is zero.

Hence, in the a-region, from one edge of the zone of seepage to the other, the direction of the flowlines with respect to the plane-normal must change from $\theta = 0$ to $\theta = 180° - \beta$, or 90°. This change cannot be discontinuous with distance because, if it were, we should have two separate flowlines in the a-region intersecting upon the a–b plane, or a finite stream tube converging to zero cross section. Consequently,

$$\frac{\partial s_{ab}}{\partial \theta} > 0 . \qquad (231)$$

If we let A and B mark the edges of the zone of seepage with A corresponding to $\theta = 0$ and B to $\theta =$ maximum, then the width of the zone of seepage is

$$s_{ab}\Big|_A^B = \int_{\theta_A}^{\theta_B} \frac{\partial s_{ab}}{\partial \theta} \cdot d\theta > 0 . \tag{232}$$

Consequently, so long as $\theta_A \neq \theta_B$, the width of the zone of seepage must always be greater than zero.[12]

The normal component of the flow across the zone of seepage will be

$$\left.\begin{aligned} q_{1n} &= -\sigma_a (\text{grad } \Phi_1)_{1a} \cos\theta = -\sigma_a (\text{grad } \Phi_1)_2 \frac{\sin\beta}{\sin\theta} \cdot \cos\theta \\ &= -\sigma_a (\text{grad } \Phi_1)_2 \sin\beta \cdot \cot\theta . \end{aligned}\right\} \tag{233}$$

For a given case all the quantities in equation (233) are constant except q_{1n} and θ, so that, as θ decreases from its maximum value to zero, along the zone of seepage, q_{1n} simultaneously increases along this zone from a minimum (zero if $\theta_{\max} = 90°$) to a maximum approaching infinity as the static fluid interface is approached. Actually, in this vicinity the velocities exceed those for which Darcy's law is valid, so that all this really means is that q_{1n} reaches a finite maximum value at that point.

APPLICATION TO GROUND WATER

In ground-water problems where our fluids are the air, fresh water, and salt water, we have an interface between the fluids air–fresh-water and air–salt-water and between fresh-water–salt-water. The last is only stable underground, being broken up in open basins by diffusion and mixing due to motions resulting from very small potential gradients. Consequently, in open basins we may have a more or less uniform body of salt water or of fresh water, but not a static layering of both with a discrete fluid interface.

When fresh water flows into a fresh-water basin having an air-water interface, a zone of seepage of finite width will form along the ground surface above the level of the water in the basin. If this

[12] Both Dachler and Muskat have discussed this problem for the air–fresh-water interface and have reached conclusions in conformity with those here.

ground slope is less than vertical, the air-water interface will approach it tangentially; if it overhangs, the air-water interface will approach vertically. In the zone of seepage the water will either flow or drip to the basin of fresh water or else will evaporate into the air.

If the basin of water is salt water with a static air–salt-water interface and the fresh water is flowing, then both the air–fresh-water and the air–salt-water interfaces will be effective. Above the water surface in the open basin there will be a fresh-water–air zone of seepage, and below that level a fresh-water–salt-water zone of seepage. In

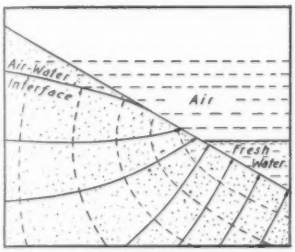

FIG. 33

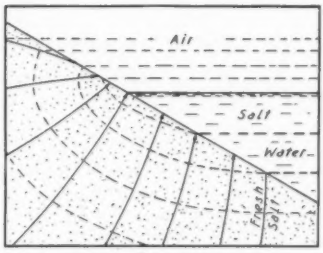

FIG. 34

FIG. 33.—Approximate manner of flow of fresh water into open space containing bodies of air and fresh water.

FIG. 34.—Approximate manner of flow of fresh water into open space containing air and salt water. Note orientation of the flowlines and the two interfaces as boundary to open space is approached.

the first zone the fresh water will either evaporate or will flow on the ground surface to the salt-water basin; in the second it will flow into it directly. In both cases mixing of the fresh and salt water will occur, and the fresh water, as such, will disappear.

For the fresh-water–air zone of seepage the angle β will, in most cases, be less than 90°, while for the fresh-water–salt-water zone it will almost always be greater than 90°. Hence, under a basin of salt water the fresh-water–salt-water interface will approach the basin boundary vertically.

Also, for the flow into a salt-water basin the entire fresh-water discharge must flow across the combined zones of seepage, since the outer boundaries of these are the two fluid interfaces. Consequent-

ly, their combined width cannot be zero but must be finite and great enough to accommodate the discharge.

Since there is no equipotential body of fresh water in the basin, then along the surface of the ground (the a–b plane) the tangential components of the potential gradient will be

$$\left.\begin{aligned}\left(\frac{\partial \Phi_2}{\partial s_{ab}}\right)_1 &= (\text{grad } \Phi_2)_1 \sin \beta\,,\\ \left(\frac{\partial \Phi_2}{\partial s_{ab}}\right)_3 &= (\text{grad } \Phi_2)_3 \sin \beta\,,\end{aligned}\right\} \tag{234}$$

where the subscripts 1, 2, and 3 refer to air, fresh water, and salt water, respectively, and where s_{ab} is the distance along the upward slope of the a–b plane, whose angle of slope in both cases is β. The quantity $(\text{grad } \Phi_2)_1$ is a vector directed vertically upward, and $(\text{grad } \Phi_2)_3$ another directed vertically downward. Consequently, the components of these two gradients along the a–b plane (the surface of the ground) will be oppositely directed, each away from the salt-water–air interface. The intersection of the static salt-water–air surface with the surface of the ground will accordingly be a line across which the tangential component of the potential gradient along the a–b plane suddenly changes direction. The flowlines at the same time will have to make a transition from one side of the surface-normal to the other. In order for the angle θ not to change discontinuously with distance, the potential gradient and the rate of flow q must become very great at the point of this transition. Consequently, the intersection of the static salt-water–air surface with the surface of the ground will be the region in which the flow of the fresh water from the ground will be the most concentrated.

THE EFFECT OF CAPILLARITY

In all our discussions of fluid interfaces we have assumed that capillary forces were nonexistent. In the case of an interface between miscible fluids like fresh water and salt water this assumption is valid; but for water-air, water-oil, and other similar interfaces it is not valid.

When two fluids are in contact with each other and with the plane

face of a solid, there are three surface tensions: T_{12}, T_{23}, and T_{31}, one between each pair of substances indicated by the subscripts 1, 2, and 3. These tensions are forces per unit of length along the surface. Let substance 3 be the solid, and let γ be the angle between the inter-

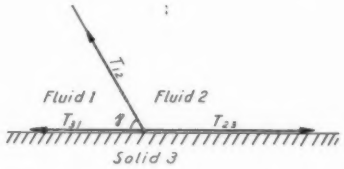

FIG. 35.—Surface tensions between two fluids and a plane solid

faces of fluid 1 with the solid and fluid 2. For equilibrium the components of all tensions parallel to the face of the solid must balance. Hence,

$$T_{31} + T_{12} \cos \gamma = T_{23} ,$$

or

$$T_{12} \cos \gamma = T_{23} - T_{31} . \qquad (235)$$

These tensions are constants for given pairs of materials. When $\gamma < 90°$, the fluid 1 is said to *wet* the solid; when $\gamma > 90°$ (mercury on glass, for example), no wetting occurs. In the first instance, the line of junction of the three substances tends to move away from the region of fluid 1; in the second case, toward it.

When

$$T_{23} - T_{31} > T_{12} ,$$

the angle γ is zero, and fluid 1 is said to wet the solid completely. This is exhibited by a water-air interface on glass, quartz, and other rock-forming minerals.

Parallel to the face of the solid and directed from fluid 1 to fluid 2, there acts upon the interface 1, 2 a net force of $T_{12} \cos \gamma$ per unit of length of contact with the solid. This causes the interface to migrate in the direction of the force until the two fluids build up a difference of pressure, the force due to which counterbalances that due to the surface tension.

When dealing with two fluids occupying the pore spaces of a permeable solid, the interfaces whose surface tensions are to be dealt with are those of the two fluids and the solid framework. The walls of the solid, instead of being plane, are now rounded or angular. If the solid medium is macroscopically isotropic, the surfaces of the solid along the trace of the fluid interface will be randomly oriented. Microscopically, therefore, the fluid interface will be very complicated, having radii of curvature of the order of magnitude of the width of the open spaces in the rock. Macroscopically, however,

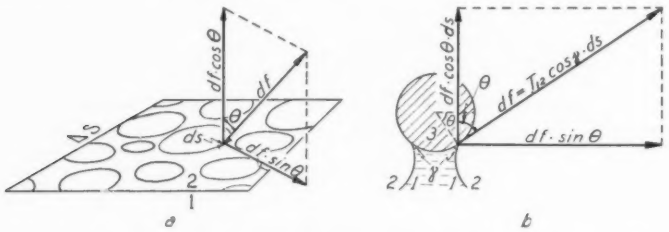

FIG. 36.—Macroscopic surface element of interface in sand between two fluids having surface tensions. *a*, Forces acting upon length *ds* of line of contact; *b*, detail of the same.

these minute irregularities are lost sight of and the fluid interface becomes smooth, with radii of curvature so large that macroscopic surface elements may generally be regarded as plane.

Now, upon the interface let us take a macroscopic surface element ΔS to which we erect a surface-normal in the direction from fluid 1 to fluid 2. Within this surface area we let ds be a microscopic element of length of the line of contact of the 1, 2 interface with the solid surface of the medium, and $d\mathbf{f}$ the element of capillary force normal to ds and parallel to the solid face. Let θ be the angle between the direction of $d\mathbf{f}$ and the surface-normal n. The magnitude of this force will be

$$df = T_{12} \cos \gamma \cdot ds \; ; \tag{236}$$

and, if we resolve it into components tangential and normal to the surface ΔS, these will be

$$df_t = T_{12} \cos \gamma \cdot ds \cdot \sin \theta \tag{237}$$

and

$$df_n = T_{12} \cos \gamma \cdot ds \cdot \cos \theta , \tag{238}$$

respectively. The total force over the area ΔS is then obtained by integration.

When it is considered that the tangential components of force $d\mathbf{f}_t$ are randomly oriented in the surface element ΔS and so have radial symmetry about the normal n, it is clear that these, considered vectorially, must cancel each other, and

$$\int_{\Delta S} d\mathbf{f}_t = 0 . \tag{239}$$

The normal components, on the contrary, must be of the same sign algebraically, since the direction of the force element $d\mathbf{f}$ which makes the angle θ with the normal n is essentially restricted to the half-space occupied by one fluid or the other. Consequently,

$$f_n = \int_{\Delta S} df_n = T_{12} \cos \gamma \int_{\Delta S} ds \cdot \cos \theta . \tag{240}$$

An analytical evaluation of $\int_{\Delta S} ds \cdot \cos \theta$ involves making assumptions regarding the microscopic structure of the medium and fluid interface, which at best can only be fair approximations, so that, like the permeability k, this quantity is more readily and accurately obtainable by experiment. We can, however, transform it into a more convenient form by writing

$$\int_{\Delta S} ds \cdot \cos \theta \equiv s \, \overline{\cos \theta} , \tag{241}$$

where s is the total length in the area ΔS of the contact of the 1, 2 interface with the surfaces of the solid medium, and $\overline{\cos \theta}$ a mean or effective value of $\cos \theta$ for the whole macroscopic area. The quantity $\overline{\cos \theta}$ depends only upon the internal shape of the medium and not upon its size scale, and so it should be constant for geometrically similar media.

Combining equations (241) and (240) then gives us

$$f_n = T_{12} \cos \gamma \cdot s \, \overline{\cos \theta} \, . \tag{242}$$

This force, which is distributed over the fluid interface, causes it to migrate in the direction of f_n until a difference of pressure in the fluid bodies on opposite sides of the interface great enough to counteract it is developed. The amount of this pressure difference, or *capillary* pressure, is given by

$$p_2 - p_1 = p_c = \frac{f_n}{\epsilon \cdot \Delta S} = \frac{T_{12} \cos \gamma \cdot s \, \overline{\cos \theta}}{\epsilon \cdot \Delta S} \, . \tag{243}$$

For interfaces between the same two fluids in two geometrically similar media, a and b, of the same material

$$\frac{(p_c)_b}{(p_c)_a} = \frac{\left(\dfrac{T_{12} \cos \gamma \cdot s \, \overline{\cos \theta}}{\epsilon \cdot \Delta S} \right)_b}{\left(\dfrac{T_{12} \cos \gamma \cdot s \, \overline{\cos \theta}}{\epsilon \cdot \Delta S} \right)_a} = \frac{s_b}{s_a} \cdot \frac{\Delta S_a}{\Delta S_b} \, . \tag{244}$$

But

$$\frac{s_b}{s_a} = \frac{d_b}{d_a} \, , \qquad \text{and} \qquad \frac{\Delta S_a}{\Delta S_b} = \frac{d_a^2}{d_b^2} \, , \tag{245}$$

so that when these are introduced into equation (244) the latter reduces to

$$\frac{(p_c)_b}{(p_c)_a} = \frac{d_a}{d_b} \, , \tag{246}$$

where d_a and d_b are the mean grain diameters or other characteristic lengths of the two media. In general, for the same materials and geometrically similar media,

$$p_c = C \cdot \frac{1}{d} \, , \tag{247}$$

where C is a constant of proportionality.

In ground-water problems, across the fresh-water–air interface in a quartz sand the water wets the sand, and the angle γ is sensibly zero. Consequently, the force f_n on the interface is directed from the region occupied by the water to that occupied by the air.

Equilibrium is established when the pressure against the air exceeds that against the water on opposite sides of the interface by the amount p_c. The order of magnitude of this capillary pressure for different degrees of coarseness of the sand can be obtained by noting that for an unconsolidated mixed quartz sand of mean grain diameter of about 0.02 cm. the vertical increase of the manometer height of otherwise static water is about -15 cm. In this case

$$\rho g h_c = C \cdot \frac{1}{d}, \qquad \text{or} \qquad C = \rho g h_c d, \tag{248}$$

where h_c is the increase in the manometer height of the water (in this case negative) due to the capillary pressure against the water (also negative). Supplying the numerical values above gives

$$p_c \cong -1.5 \times 10^4 \text{ dyne/cm}^2,$$
$$C \cong -300 \text{ dyne/cm}^2.$$

This value for C is not based upon precise sedimentary analysis and so is to be taken only as an order of magnitude. Using it in this capacity, however, we obtain an idea of the pressure difference p_c and the manometer rise h_c for the static water-air interface in similar sediments of increasing fineness, by solving equation (245) for h_c and p_c when the grain diameters are given. A few such values are plotted in Table 1, from which it is clear that for sediments of large permeabilities the drop in manometer height is unlikely to exceed 1 meter, whereas for sediments with manometer drops greater than a meter the permeabilities become vanishingly small.

INFLUENCE OF CAPILLARITY UPON A TWO-FLUID INTERFACE

In our earlier discussion of fluid interfaces we assumed that p_c was zero, so that at one and the same point the pressure against which either of two fluids would have to be injected was the same. Also, it was assumed that the pressures at contiguous points on opposite sides of the fluid interface were the same. We now see that, if the two fluids are immiscible, they will always be separated by a fluid interface on opposite sides of which the pressures will have the

difference p_c, where p_c depends upon the nature of the fluids and the medium in the manner already indicated. This is equally true whether the interface be that between large segregated bodies of the two fluids or whether it be that surrounding a small macroscopic volume of one fluid injected into the region occupied by the other.

TABLE 1

INCREASE OF MANOMETER HEIGHT AND CAPILLARY PRESSURE OF THE WATER-AIR INTERFACE IN SIMILAR SEDIMENTS

Rock Type	Grain Diameter d (Cm.)	Increase of Manometer Height h_c (Cm.)	Capillary Pressure p_c (Dynes/Cm^2)
Gravel	$-$ 1	-3×10^{-1}	-3×10^{2}
	$-$ 10^{-1}	$-$ 3	-3×10^{3}
Sand	$-$ 10^{-2}	$-3\times10^{+1}$	-3×10^{4}
Silt	$-$ 10^{-3}	-3×10^{2}	-3×10^{5}
Clay	$-$ 10^{-4}	-3×10^{3}	-3×10^{6}

To deal with this circumstance it is only necessary to extend our definition of fluid potential so as to include the work against interfacial capillary pressure. The potential of any fluid in any region is then

$$\Phi = gz + \int_{p_0}^{p+p_c} \frac{dp}{\rho}, \tag{249}$$

where ρ is the density of the injected fluid, p the pressure of the fluid occupying the point in question, and p_c the capillary pressure *against* the injected fluid due to the interfacial tensions of the two fluids at the point of injection. For the same fluids and medium, with the medium homogeneous as regards texture and size scale, p_c may be

treated as a constant; otherwise its variation as a function of position must be allowed for.

The potentials of two fluids at the same point are now

$$\left.\begin{aligned}\Phi_1 &= gz + \int_{p_0}^{p+p_{c1}} \frac{dp}{\rho_1},\\ \Phi_2 &= gz + \int_{p_0}^{p+p_{c2}} \frac{dp}{\rho_2},\end{aligned}\right\} \tag{250}$$

which for fluids of constant densities reduces to the simpler form

$$\left.\begin{aligned}\Phi_1 &= gz + \frac{p - p_0}{\rho_1} + \frac{p_{c1}}{\rho_1},\\ \Phi_2 &= gz + \frac{p - p_0}{\rho_2} + \frac{p_{c2}}{\rho_2}.\end{aligned}\right\} \tag{251}$$

These equations are analogous to equation (183), and again we may eliminate $p - p_0$ and solve for z, obtaining

$$z = \frac{1}{g}\left(\frac{\rho_2}{\rho_2 - \rho_1} \cdot \Phi_2 - \frac{\rho_1}{\rho_2 - \rho_1} \cdot \Phi_1 - \frac{p_{c2} - p_{c1}}{\rho_2 - \rho_1}\right). \tag{252}$$

Also, if we like, we may observe that

$$\left.\begin{aligned}\frac{p_{c1}}{\rho_2 - \rho_1} &= \frac{\rho_1}{\rho_2 - \rho_1} \cdot \frac{p_{c1}}{\rho_1} = \frac{\rho_1}{\rho_2 - \rho_1} \cdot \Phi_{c1},\\ \frac{p_{c2}}{\rho_2 - \rho_1} &= \frac{\rho_2}{\rho_2 - \rho_1} \cdot \frac{p_{c2}}{\rho_2} = \frac{\rho_2}{\rho_2 - \rho_1} \cdot \Phi_{c2},\end{aligned}\right\} \tag{253}$$

where Φ_{c1} and Φ_{c2} are the parts of the two potentials due to capillarity. Inserting these expressions into equation (252) then gives

$$z = \frac{1}{g}\left[\frac{\rho_2}{\rho_2 - \rho_1}(\Phi_2 - \Phi_{c2}) - \frac{\rho_1}{\rho_2 - \rho_1}(\Phi_1 - \Phi_{c1})\right]. \tag{254}$$

In setting up equations (249) and (250) it was supposed that both fluids were to be injected at the same point in a region occupied by the same fluid. Now, if z represents the elevation of a point on the 1, 2 interface, then we must think of both fluids being injected on the same side of the existing interface against a pressure either of p_1 or p_2, of one fluid or the other.

If the injection is made on the side of fluid 1 against pressure p_1,

$$\left.\begin{aligned} \frac{p_{c1}}{\rho_1} &= \Phi_{c1} = 0 , \\ \frac{p_{c2}}{\rho_2} &= \Phi_{c2} \neq 0 . \end{aligned}\right\} \tag{255}$$

Or, if the injection is made on the side of the interface occupied by fluid 2 against pressure p_2,

$$\left.\begin{aligned} \frac{p_{c1}}{\rho_1} &= \Phi_{c1} \neq 0 , \\ \frac{p_{c2}}{\rho_2} &= \Phi_{c2} = 0 . \end{aligned}\right\} \tag{256}$$

It makes no difference in the results which of these sets of relations we employ, but we must use one or the other.

With this understanding we obtain from equation (252) or (254) the elevation of any point on a fluid interface at which the corresponding potentials are known. For example, if we consider a water-air interface and define our potentials on the air side of the interface, letting air be the fluid of density ρ_1 and water that of density ρ_2, then both Φ_1 and Φ_{c1} are sensibly equal to zero, and

$$\left.\begin{aligned} z &= \frac{1}{g} \cdot \frac{\rho_2}{\rho_2 - \rho_1} \cdot (\Phi_2 - \Phi_{c2}) \\ &= \frac{1}{g} \cdot \frac{\rho_2}{\rho_2 - \rho_1} (gh_2 - gh_{c2}) \cong h_2 - h_{c2} , \end{aligned}\right\} \tag{257}$$

where h_2 is the customary manometer height of the water at the interface in a tube of large enough diameter that capillary forces are negligible and $-h_{c2}$ is the capillary rise due to the forces of the surface tensions between air, water, and the medium at the given point. Also, $\rho_2/(\rho_2 - \rho_2) \cong 1$.

The angle of slope of this interface is obtainable by differentiation:

$$\sin \alpha = \frac{\partial z}{\partial s} = \frac{1}{g} \cdot \frac{\rho_2}{\rho_2 - \rho_1} \left(\frac{\partial \Phi_2}{\partial s} - \frac{\partial \Phi_{c2}}{\partial s} \right) \cong \frac{\partial h_2}{\partial s} - \frac{\partial h_{c2}}{\partial s} . \tag{258}$$

If the medium is homogeneous and the water static, h_2 = constant, h_{c2} = constant, and the surface will be horizontal. If the medium is heterogeneous and the water static, h_2 = constant, $h_{c2} \neq$ constant, and the surface will be undulatory. In coarse gravel and open spaces $h_{c2} \cong 0$, so that the elevation of the surface becomes equal to h_2. When the water is not static but flows through a homogeneous medium, h_{c2} = constant and

$$\frac{\partial h_{c2}}{\partial s} = 0 \qquad \text{and} \qquad \frac{\partial z}{\partial s} \cong \frac{\partial h_2}{\partial s} .$$

Hence, the slope of the surface when the capillarity is constant is related to the rate of flow in the same manner as when the capillarity is zero.

For the more general case the elevation z of the interface is obtainable from equation (254) when one of the fluids is static. Let the ρ_2-fluid be static and the potentials taken on its side of the interface. Then

$$\Phi_2 = \Phi_{20} = \text{constant} ,$$

$$\Phi_{c2} = 0 ,$$

and

$$\left.\begin{aligned} z &= \frac{1}{g}\left[\frac{\rho_2}{\rho_2 - \rho_1} \cdot \Phi_{20} - \frac{\rho_1}{\rho_2 - \rho_1}(\Phi_1 - \Phi_{c1})\right] \\ &= \frac{\rho_2}{\rho_2 - \rho_1} \cdot h_{20} - \frac{\rho_1}{\rho_2 - \rho_1}(h_1 - h_{c1}) , \end{aligned}\right\} \qquad (259)$$

where h_{20} = constant is the manometer height of the ρ_2-liquid, h_1 is that of the ρ_1-liquid, and h_{c1}, which may be either positive or negative, is the additional manometer rise of the ρ_1-fluid due to capillarity. When both fluids are static and the medium homogeneous, the interface is horizontal; when the medium is heterogeneous, it is undulatory.

For the most general state of stationary flow the angle of slope of the interface is obtainable from equation (254) by differentiation:

$$\sin \alpha = \frac{\partial z}{\partial s} = \frac{1}{g}\left[\frac{\rho_2}{\rho_2 - \rho_1} \cdot \frac{\partial \Phi_2}{\partial s} - \frac{\rho_1}{\rho_2 - \rho_1}\left(\frac{\partial \Phi_1}{\partial s} - \frac{\partial \Phi_{c1}}{\partial s}\right)\right] , \qquad (260)$$

where the potentials are taken on the ρ_2-side of the interface. For a homogeneous medium, $\partial\Phi_{c1}/\partial s = 0$ and equation (260) reduces to equation (190) derived for zero capillarity.

From the foregoing we see that the effect upon a fluid interface produced by capillarity is principally one of a greater or less distortion with respect to the configuration of the same interface for zero capillarity. While the interfacial pressure differences due to capillarity between pairs of liquids is, in most cases, less than that for

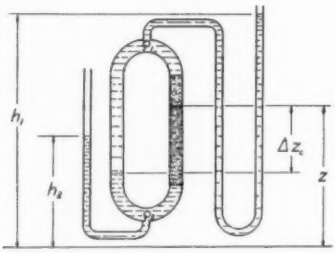

FIG. 37.—Equilibrium levels of the interface between two static liquids of different densities in an open space and in sand.

water-air, the vertical displacements are equal to the manometer rises h_{c1}, or h_{c2}, magnified by the factor $\rho_1/(\rho_2 - \rho_1)$ or $\rho_2/(\rho_2 - \rho_1)$, depending upon which fluid is taken for reference, which commonly is large compared with unity.

Also, in extremely fine-grained rocks whose permeabilities for ordinary purposes may be negligible, the capillary pressures may reach several atmospheres. In the course of geologic time, between otherwise static bodies, this interface will migrate toward a configuration of equilibrium. The vertical distance of such a migration from the corresponding position for $p_c = 0$ would be

$$z_c = +\frac{1}{g} \cdot \frac{\rho_2}{\rho_2 - \rho_1} \cdot \Phi_{c2} = +\frac{\rho_2}{\rho_2 - \rho_1} \cdot h_{c2} = +\frac{1}{g} \cdot \frac{p_{c2}}{\rho_2 - \rho_1}; \quad (261a)$$

or

$$z_c = -\frac{1}{g} \cdot \frac{\rho_1}{\rho_2 - \rho_1} \cdot \Phi_{c1} = -\frac{\rho_1}{\rho_2 - \rho_1} \cdot h_{c1} = -\frac{1}{g} \cdot \frac{p_{c1}}{\rho_2 - \rho_1}, \quad (261b)$$

corresponding to whether the fluid considered is that of density ρ_2 or of density ρ_1, respectively. In either case the capillary pressure is that *against* the fluid considered, so that $p_{c2} = -p_{c1}$.
With $\rho_1/(\rho_2 - \rho_1) = 10$ this would amount to approximately 100 meters per atmosphere. Apparently phenomena of this sort have played a significant role in the accumulation of petroleum and are important in its extraction.

For the dynamic case for which one or both fluids are in steady motion through a homogeneous medium, it is not to be assumed that the interface is simply displaced vertically by the amount $(1/g)$ $p_c/(\rho_2 - \rho_1)$ above or below its position for $p_c = 0$. In this case any shift of the interface causes corresponding changes in the flow patterns and cross-sectional areas of the stream tubes. This results in a shift along the flowlines of the equipotential surfaces, and all of these several changes affect the new position of equilibrium, which, when the potential gradients are large, can only be obtained from equation (254) or its equivalent.

THE WATER TABLE

One additional point should be given attention before leaving the subject of capillarity. If, at any given point in a region underlain by permeable rocks, a vertical, uncased well is dug, it eventually reaches a depth at, and below which, water flows into the hole and stands in static equilibrium. It has become standard usage in ground-water hydrology to refer to such a static air-water interface in an open hole as the "water table" at that point. Hence, the water table represents an elevation below which water flows freely into an uncased hole and above which no such flow occurs.

This fact has led, naturally enough, to the conception, also of wide currency among ground-water hydrologists, that the water table underground forms a bounding surface between a lower region which is completely saturated with water and an upper region in which the saturation is incomplete. The water table is in this manner conceived to be the upper surface (except where this is formed by impermeable rocks) of a "zone of saturation" and the lower surface of a "capillary fringe"—a zone (presumably in which the saturation is incomplete) in which the water is sustained by capillarity.

Of late it has been recognized that flow occurs within this "capillary fringe" zone as well as within the "zone of saturation," and investigations have been suggested to determine the manner of this flow.

Thus, while our facts concerning the water table are limited to observations made within holes or other large voids in the ground, it is clear that the conceptions regarding the water table are not so limited; and, in fact, the water table is conceived to be a continuous surface (except where the rocks are impermeable) whose elevation coincides at every point with the position the air-water interface would assume in an uncased open hole *were one placed at that point.*

Our main interest here centers upon the question of what is the physical significance, if any, of such a surface in an underground region away from holes or other voids larger than the pore spaces of the medium. Does it, in fact, form a boundary between a lower region completely saturated with water and an upper region incompletely saturated? Does it represent the air-water interface? Does it form any kind of a recognizable boundary that one could distinguish visually in a permeable region bounded by a vertical glass plate?

The answers to all of these questions are implicitly contained in the discussion of capillarity that we have just made and are experimentally verifiable by means of very simple apparatus containing sand, water, and air, with one or more vertical glass walls for visual observation and with suitable manometer taps.

The answer is that only one unclosed and continuous air-water interface exists, on either side of which there may or may not occur air bubbles trapped in the region otherwise saturated by water, and water meniscules similarly trapped and held in the region otherwise saturated by air. Furthermore, the isolated air bubbles and water meniscules represent unstable configurations which will disappear spontaneously, the air bubbles by solution and the water meniscules by evaporation, unless renewed by processes foreign to those presently considered.

For simplicity, consider the static example afforded by a large laboratory graduate completely filled with sand and partly filled with water. The air-water interface will be clearly visible (especially if

the water be colored); and the minutest inspection will not indicate the position of the water table, because no boundary between a zone of complete saturation and one of incomplete saturation (other than the air-water interface itself) will be discernible; neither will a surface of any other physical discontinuity appear.

If, on the other hand, we tap manometer tubes into any part of the region below the air-water interface, they will all register the same elevation h corresponding to a region of constant potential, gh. Furthermore, this elevation h will be precisely the same as the elevation of the water table as obtained from a "well" driven inside the graduate, and will be less than the elevation z_{12} of the air-water interface by an amount h_c, which is the decrease of the manometer height owing to the capillary pressure from the value it would assume were the capillary pressure zero.

If we now consider the pressure field in the region below the air-water interface, we shall find, in this static case, that we have an infinite family of horizontal isobaric surfaces with the pressure decreasing upward at the rate $\rho_2 g$ per unit of length, where ρ_2 is the density of the water. Furthermore, the height of the water in the manometer tubes and in the "well" will coincide precisely with the isobaric surface $p = 1$ atmosphere. (In this and the paragraphs immediately following, the term "1 atmosphere" is to be understood to mean prevailing atmospheric pressure, and not "1 standard atmosphere.") Below this surface the pressure will be greater than 1 atmosphere; and above, between it and the air-water interface, the pressure will be less than 1 atmosphere.

From this it is clear that the water table in this static case is nothing other than the isobaric surface, $p = 1$ atmosphere; and the so-called "zone of saturation" comprises the region throughout which $p > 1$ atmosphere. Likewise, the "capillary fringe" is the region between the isobaric surface, $p = 1$ atmosphere, and the air-water interface, characterized by $p < 1$ atmosphere.

While this simpler static case is employed for purpose of illustration, the above results are nowise altered when a potential gradient is impressed upon the system and the water made to flow. The isobaric surface, $p = 1$ atmosphere, still is the water table and represents in underground regions no physical discontinuity of any kind.

The equipotential surfaces cross this isobaric surface without interruption and extend to the air-water interface across which they refract into the horizontal. The fluid flow obeys precisely the same laws in the region where $p < 1$ atmosphere as in that characterized by $p > 1$ atmosphere.

On the other hand, if the upper surface of the "zone of saturation" be regarded to be coincident with the air-water interface—as the term itself suggests that it should be—then it does not coincide with the water table but stands consistently above that surface by a height h_c; and a "capillary fringe" does not exist.

Hence, in either case we are left with no alternative but to discard the conception of the water table as a surface of discontinuity between a "zone of saturation" and a "capillary fringe" having fundamentally different physical characteristics as a misleading fiction.

THE EFFECT OF TEMPERATURE AND PRESSURE UPON THE FLUID PROPERTIES

Aside from surface-tension phenomena, the fluid properties which enter into our equations are the density and viscosity. For a single homogeneous fluid both these properties are single-valued functions of the temperature and pressure. For gases within the range of validity of the gas laws the viscosity and density are determinable from the kinetic theory of gases. For gases outside this range and for liquids these properties must be obtained experimentally.

In the underground regions we are interested in there exists not only a pressure field but a thermal field as well, giving rise to the two families of field surfaces: isobaric surfaces and isothermal surfaces. Each point underground will be located upon one of each of these surfaces, and at that point the values of the density and viscosity of the fluid in question will be those appropriate to the temperature and pressure. This will give rise to two scalar fields—one for viscosity and one for density—each with its appropriate equiscalar surfaces.

Setting

$$\left.\begin{aligned} \eta &= f(T,p)\,, \\ \rho &= F(T,p)\,, \end{aligned}\right\} \tag{262}$$

and considering that T and p are both functions of position underground, then along any path s

$$\left.\begin{aligned} \frac{d\eta}{ds} &= \frac{\partial \eta}{\partial T} \cdot \frac{dT}{ds} + \frac{\partial \eta}{\partial p} \cdot \frac{dp}{ds}, \\ \frac{d\rho}{ds} &= \frac{\partial \rho}{\partial T} \cdot \frac{dT}{ds} + \frac{\partial \rho}{\partial p} \cdot \frac{dp}{ds}. \end{aligned}\right\} \tag{263}$$

Integration of equations (263) along the path s from an initial position s_0 to a final one s gives the corresponding values of η and ρ at the final position. Thus,

$$\left.\begin{aligned} \eta &= \eta_0 + \int_{s_0}^{s} \left(\frac{\partial \eta}{\partial T} \cdot \frac{dT}{ds} + \frac{\partial \eta}{\partial p} \cdot \frac{dp}{ds} \right) ds, \\ \rho &= \rho_0 + \int_{s_0}^{s} \left(\frac{\partial \rho}{\partial T} \cdot \frac{dT}{ds} + \frac{\partial \rho}{\partial p} \cdot \frac{dp}{ds} \right) ds. \end{aligned}\right\} \tag{264}$$

For gases, both of these equations have to be taken into account; but for liquids, which are our principal concern here,

$$\frac{\partial \rho}{\partial T} \cong 0; \qquad \frac{\partial \rho}{\partial p} \cong 0,$$

so that $\rho \cong \rho_0$ or is sufficiently nearly constant that, for most purposes, it may be so regarded. The viscosity for liquids, however, cannot be considered constant within the range of temperatures and pressures encountered by deep wells.

In regions of mild topographic relief and free from thermal anomalies, such as hot springs and volcanic activity, the isothermal surfaces are very nearly horizontal. In similar regions, except locally, where high potential gradients may exist, the isobaric surfaces are nearly horizontal. Under these circumstances, to a very good approximation the pressure and temperature are functions of depth only, and isothermal and isobaric surfaces are substantially parallel. Also, the increase of each of these quantities with depth is approximately linear, and we may set

$$p = -\rho g z + \text{constant} \tag{265}$$

$$T = -\Theta z + \text{constant} \tag{266}$$

where z is the elevation of the point (negative of the depth), ρ the density of water, and Θ the geothermal gradient. In most deep wells it has been found that the fluid pressure is approximately that given by equation (265), though certain anomalous cases where the pressure is much greater than this are known.

We may now consider the path of integration of equation (264) to be vertical and substitute z for s. From equations (265) and (266)

$$\frac{dp}{dz} = -\rho g\,, \tag{267}$$

$$\frac{dT}{dz} = -\Theta\,. \tag{268}$$

Introducing these into the equation (264) for η then gives

$$\eta_z = \eta_0 - \int_{z_0}^{z} \frac{\partial \eta}{\partial T} \cdot \Theta \cdot dz - \int_{z_0}^{z} \frac{\partial \eta}{\partial p} \cdot \rho g \cdot dz\,. \tag{269}$$

By measurements in deep wells Θ is found to vary somewhat widely from one location to another, but for a given well it is approximately constant, an average value being about 3° C. per 100 meters, or 3×10^{-4} °C. cm.$^{-1}$. Also, ρg is approximately constant with the numerical value of about 10^3 gm. cm.$^{-2}$ sec.$^{-2}$.

The values of $\partial\eta/\partial T$ and $\partial\eta/\partial p$ for water are obtainable from Bridgman's[13] experiments, which show that the magnitude of the term under the second integral is less than 10^{-3} of that under the first integral. The second integral may therefore be entirely disregarded for water, leaving

$$\eta_z = \eta_0 - \int_{z_0}^{z} \frac{\partial \eta}{\partial T} \cdot \Theta \cdot dz = \eta_0 + \int_{T_0}^{T} \frac{\partial \eta}{\partial T} \cdot dT\,, \tag{270}$$

where T_0 is the temperature under atmospheric pressure. Computing the approximate temperature as a function of depth, equation (270) gives the viscosity of water as a function of depth. Inserting this into the equation for the specific conductivity then gives the manner in

[13] P. W. Bridgman, "The Effect of Pressure on the Viscosity of Forty-three Pure Liquids," *Proc. Amer. Acad. Arts and Sci.*, Vol. LXI (1926), pp. 57–99.

which that increases with depth for a medium of uniform permeability. These values are computed to depths of 3,000 meters and are given in Table 2, which shows that, when dealing with the flow of water, the decrease of viscosity with depth is equivalent to a corresponding increase of permeability at constant temperature and must be allowed for.

TABLE 2

VARIATION OF VISCOSITY AND SPECIFIC CONDUCTIVITY FOR WATER WITH DEPTH

Depth in Meters	Temperature at °C.	Viscosity of Water Poises	Relative Specific Conductivity
0.....	10	1.308×10^{-2}	1
100.....	13	1.207×10^{-2}	1.08
200.....	16	1.112×10^{-2}	1.18
300.....	19	1.032×10^{-2}	1.27
400.....	22	0.961×10^{-2}	1.36
500.....	25	0.894×10^{-2}	1.46
1,000.....	40	0.656×10^{-2}	2.00
2,000.....	70	0.406×10^{-2}	3.22
3,000.....	100	0.284×10^{-2}	4.61

ROTATIONAL FIELD OF FORCE

In the most general case, where both η and ρ vary appreciably with temperature and pressure and where the isothermal surfaces are not parallel to the isobaric surfaces, the surfaces of equal density—isopycnic surfaces—will intersect the isobaric surfaces, and

$$\oint \frac{dp}{\rho} \neq 0.$$

When this occurs, no potential is possible, strictly speaking. What happens physically in such a case is that the field of force has a rotational component which tends to set up convectional flow in the fluid. This kind of situation arises from unequal heating in different parts of the flow field, causing the fluid at the same pressure and different temperatures to have different densities. Such a state of flow is not a violation of the conservation of energy but an evidence of an interchange between thermal and mechanical energy, producing a heat engine. The rotational force is commonly superposed upon a

potential field of force. In ground-water, while the rotational force field exists in certain cases, owing to the approximate constancy of the density of water, it is so small, compared with the potential force field, as to be negligible.

COMPARISON OF PRESENT THEORY WITH METHODS USED BY OTHERS

This concludes our formal development of theory. We have attempted to establish upon a physically sound basis a theory of the motion of a homogeneous fluid through permeable media, capable of extension to include the flow of fluids of the most general kind but here restricted principally to liquids and the problems of ground water. In so doing, we have intentionally confined ourselves to two important restrictions: that the flow dealt with shall be either continuously or statistically steady during the time interval considered and that the medium be isotropic.

The reasons for the first of these restrictions is to avoid serious mathematical difficulties encountered in attempting to deal with transient phenomena. These involve the treatment of fields whose properties are functions both of position and of time. While these problems can be set up simply by adding time to the variables herein considered, their solution is far more difficult than the corresponding ones with steady motion. Besides, most ground-water problems can be reduced to problems of steady states of flow.

Recently Theis[14] has studied the nonsteady flow around a well with very promising results, using an analogy to heat diffusion. He has assumed, erroneously, however, that pressure is the hydraulic analogue of temperature.

The restriction that the medium be considered isotropic is partly to avoid the mathematical difficulties inherent in the treatment of anisotropic phenomena and partly in consideration of the fact that nearly all permeability data are taken on the basis of the same assumption. The effect of anisotropy is to produce a distortion in the stream-flow pattern with respect to the corresponding pattern for isotropic conditions for the same potential field. For isotropic media

[14] Charles V. Theis, "The Relation between the Lowering of the Piezometric Surface and the Rate and Duration of Discharge of a Well Using Ground Water Storage," *Trans. Amer. Geoph. Union*, 1935, pp. 519–24.

the flowlines are parallel to grad Φ; for anisotropic media they make an angle with this direction, the magnitude of which depends upon the degree of anisotropy and upon the direction of grad Φ with respect to the permeability axes of the media.

It is important now that we compare the present treatment with those of other authors. It is to be expected that the points of agreement will far exceed those of disagreement, but it is the latter which are of greatest importance, because they are the ones which lead to disagreement in the conclusions drawn and must therefore embody some of the errors that have been committed.

VELOCITY POTENTIAL

Since the classical studies of Slichter most of the authors who have studied the motion of ground water analytically have sensed that some sort of a potential function was involved and have attempted to formulate this function. The approach to this problem has usually

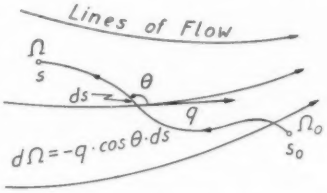

FIG. 38.—The line-integral by means of which a velocity potential Ω is defined

been made by starting with the conceptions of classical hydrodynamics and assuming that the potential function sought was a *velocity potential*.

In this connection it should be explained that a velocity potential is the line-integral of velocity along a path in the flow field, just as a force potential is the line-integral of a force. Hence, if a velocity potential exists in a field of flow, its value at any point is

$$\Omega = \Omega_0 - \int_{s_0}^{s} q \cos \theta \cdot ds \,, \qquad (271)$$

where Ω_0 is the velocity potential of the initial and Ω that of the final point, q the magnitude of the specific discharge, or velocity vector, and θ the angle between direction of flow and the displacement ds.

Slichter stated that the hydrostatic pressure had the property of a velocity potential in ground-water motion and that isobaric surfaces were accordingly normal to the flowlines. Later, however, he violated his own proposition by dealing with a problem in which he showed the isobaric surfaces to be at all angles from normal to tangential to the related flowlines.

Since that time it appears to have been more often the rule than the exception for authors to employ pressure as a potential function and to write what has been represented to be Darcy's law in the form

$$q_s = -K' \cdot \frac{\partial p}{\partial s},$$

which has already been shown to be invalid.

Even when Darcy's law has been correctly stated in the form

$$q_s = -K \cdot \frac{\partial h}{\partial s},$$

one of the most common errors has been to assume that different manometer tubes for which the heights h are the same must be terminated upon the same isobaric surface.

Dachler, who employs the correct form of Darcy's law, states that

$$q_x = -K \cdot \frac{\partial h}{\partial x} = -\frac{\partial (Kh)}{\partial x}, \quad \text{etc.},$$

and concludes that (Kh) has therefore the properties of a velocity potential.

Muskat first sets up Darcy's law in the erroneous form

$$q_s = -\frac{k}{\eta} \cdot \frac{\partial p}{\partial s},$$

but later, for the study of general field problems, employs

$$\Omega = \frac{k}{\eta}(p + \rho g z)$$

as a velocity potential, from which

$$q_x = -\frac{\partial \Omega}{\partial x}, \quad \text{etc.}$$

The same assumption has been stated explicitly by Gardner, Collier, and Farr,[15] who say in their opening sentence: "As was pointed out originally by Slichter, the generalization of Darcy's law is nothing more nor less than the criterion for the existence of a velocity potential for the macroscopic velocity of moisture in the soil." They then state that the quantity

$$\sigma\Phi = \sigma\left(gz + \frac{p}{\rho}\right)$$

is a velocity potential.

The trouble inherent in all approaches to the motion of ground water by means of the employment of a velocity potential arises from the basic assumption that a velocity potential exists. The necessary and sufficient condition for the existence of a velocity potential is that for all closed paths in a singly connected region

$$\oint q \cos\theta \cdot ds = 0. \qquad (272)$$

If this integral is not zero, no velocity potential exists, and any employment of a function supposed to be a velocity potential for such a region is necessarily erroneous.

In this connection it is important to note that in classical hydrodynamics, where the conception of a velocity potential originated, the only fluids to which it is applicable are idealized frictionless fluids. In real fluids for which the friction is not negligible the line integral around a closed curve ceases to be zero, and the motion is not derivable from a velocity potential.

From this fact alone the assumption that ground water possesses a velocity potential might appear to be of doubtful validity, for here friction is a dominant influence. On a microscopic scale there is no question that a velocity potential cannot exist, but whether this is true macroscopically requires further investigation.

One test of the validity of this assumption is provided by the rectilinear flow of water between vessels, through a prism of sand. Let the prism be divided into two sections by a plane parallel to its axis,

[15] Willard Gardner, T. R. Collier, and Doris Farr, "Fundamental Principles Governing the Control of Ground-Water," *Trans. Amer. Geoph. Union*, 1934, pp. 563–66.

one section containing sand of permeability k_2 and the other of k_1, where $k_2 > k_1$. The flowlines will be parallel to the sand interface; but in the sand of permeability k_2, the specific discharge will have the magnitude q_2, and in that of permeability k_1 the magnitude of the discharge will be q_1.

Let A be a point at the end of the sand prism in the downstream vessel, and B a corresponding point in the upstream vessel. Let us assume that a velocity potential exists, and let Ω_A be its value at A. Then at B

$$\Omega_B = \Omega_A - \int_A^B q \cos\theta \cdot ds \,. \tag{273}$$

Now let us evaluate this integral along two separate paths: (1) From A the path follows the normal to the flowlines until a flowline through

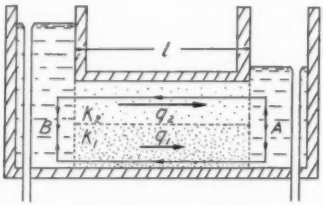

FIG. 39.—The velocity line-integral from A to B by two different paths traversing sands of different permeabilities.

the k_1 region is encountered. It then follows this flowline until the normal passing through B is reached; thence along that normal to B. (2) For the second path we proceed, as before, along a flowline-normal from A, then along a flowline in the k_2 region until the normal through B is reached, and finally along this to the point B. In both cases the distance l along the flowlines is the same. When the flowlines are followed, θ is 180°, the cosine of which is -1; and when the flowline-normals are followed, θ is 90°, whose cosine is zero.

By these separate paths the values of the potential at B are

$$\left.\begin{aligned} \Omega_{B1} &= \Omega_A + q_1 \cdot l \,, \\ \Omega_{B2} &= \Omega_A + q_2 \cdot l \,, \end{aligned}\right\} \tag{274}$$

from which

$$\Omega_{B_2} - \Omega_{B_1} = (q_2 - q_1)l \neq 0 \tag{275}$$

and

$$\oint q \cos\theta \cdot ds \neq 0 .$$

This shows us clearly that in this special case no velocity potential is possible and that the value of the assumed velocity potential at B depends upon the path traversed.

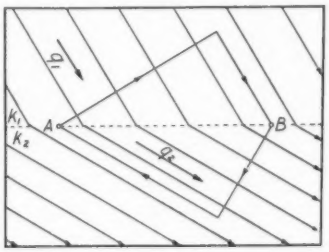

FIG. 40.—Line-integral around a closed path traversing regions of different permeabilities.

A more general case is encountered if we take the points A and B upon the interface between two sands of permeabilities k_1 and k_2 across which the flowlines pass obliquely. Starting from A we traverse the flowline-normal in the k_1 region until the flowline passing through B is reached. We follow this to B and then follow the flowline-normal through B in the k_2 region until the flowline through A is encountered along which the return to A is made.

If we let γ_1 and γ_2 be the angles between the flowlines and the surface-normals in the two regions, then from the tangent law of refraction, when $k_2 > k_1$,

$$\gamma_2 > \gamma_1 , \qquad \text{and} \qquad q_2 > q_1 .$$

The line-integral around the path described is therefore

$$\oint q \cos\theta \cdot ds = \pm \overline{AB}(q_2 \sin\gamma_2 - q_1 \sin\gamma_1) \neq 0 , \tag{276}$$

so that for this case, too, no velocity potential exists.

While it is possible by the extension of the above method of analysis to arrive at a generalization, we can do this better by returning to our fundamental equations. The expressions for a velocity potential employed by Dachler, by Muskat, and by Gardner, Collier, and Farr are all equivalent and are related to the force potential Φ, as herein employed, in the following manner:

$$\Omega = Kh = \frac{k}{\eta}(p + \rho g z) = \sigma\Phi . \tag{277}$$

From the definition of a velocity potential, if one exists,

$$\mathbf{q} = -\text{grad}\,\Omega = -\text{grad}\,(\sigma\Phi) ,$$

which is none other than equation (136) that has already been shown to be invalid as a general expression of Darcy's law.

The same result is obtained if we perform the line-integral around a closed path:

$$\oint q \cos\theta \cdot ds = -\oint \sigma \cdot \frac{\partial\Phi}{\partial s} \cdot ds , \tag{278}$$

which, if a velocity potential exists, must be zero for all possible paths.

But we know already that for all cases for which Φ is determinate, namely, when the density of the fluid is a function of its pressure only so that its isopycnic and isobaric surfaces are mutually parallel,

$$\oint \frac{\partial\Phi}{\partial s} \cdot ds = 0 . \tag{279}$$

This property of Φ is entirely independent of any properties of the medium, whether homogeneous or inhomogeneous, isotropic or anisotropic, or whether the closed path is confined to the region of the fluid concerned or makes excursions into regions occupied by other fluids. Hence, in order for equation (278) to be zero, it is necessary that σ be eliminated from the integrand, which is only allowable provided the value of σ is independent both of position in the field and of the direction of the flow. Since $\sigma = k\rho/\eta$, these conditions are only satisfied provided $k\rho/\eta$ = constant. It is also necessary that the

value of k be independent of the direction of the flow, that is, that the medium be isotropic. Since k, ρ, and η are all independently variable, this requires that all three of them separately must remain constant.

Hence, a velocity potential exists only for fields of flow involving a fluid of constant density and viscosity and a medium which is homogeneous and isotropic throughout. Since these several conditions obtain only in specially set up laboratory problems involving liquids, and are not even approximately realized when fluids of variable density and viscosity are employed, or in ground-water problems involving wide ranges of the permeability, it is clear that the velocity-potential conception of Darcy's law is an inadequate one. Physically, besides possessing an extremely narrow range of validity, the velocity potential conception has only kinematical significance and gives one no insight whatever into the dynamical properties of the flow; mathematically, it has no advantages over the more general dynamical expression here derived since it represents only a special case of the latter. The dynamical expression, on the contrary, is of unlimited validity, being applicable to the flow of fluids of variable density and viscosity through media of space variable permeability. For anisotropic media this validity is still retained, provided the permeability parameter be expressed in the form of a tensor in the place of the scalar k of isotropic media.

THE PIEZOMETRIC SURFACE

Another device that is extensively employed in ground-water practice is the *piezometric surface*. Frequently there exists at depth a stratum of rock such as sandstone or porous limestone of high permeability, overlain by rocks of slight permeability. Wells terminated in these upper rocks yield sparingly, while those reaching the stratum of high permeability, or aquifer, yield more abundantly. This fact focuses attention upon the hydrologic properties of the aquifer, and wells reaching it can be employed as manometer tubes in addition to their function as wells.

In a particular vertical well terminated upon the top of such an aquifer the water will rise to a static elevation h above the standard datum. Now, if we imagine a large number of such wells to be drilled to the top of the aquifer and used as vertical manometer tubes, the

heights h will vary with position, but at any given time they will all lie upon a smooth surface, $h(x,y)$, where x and y are the horizontal co-ordinates of the wells. This surface is what is known as the "piezometric surface."

Now it is clear that at each well the height h gives the potential $\Phi = gh$ at the lower terminus of that well, and a complete knowledge of the piezometric surface of any given stratigraphic horizon over a given area enables one to determine completely the potentials at all points on that horizon over the corresponding area. Lines of equal potential can then be drawn upon the underground horizon; and from these, by means of Darcy's law, if the permeability of the aquifer is known, the component of flow tangential to its upper surface can be determined.

While this is a procedure of great practical importance, it also has serious limitations which must be thoroughly understood if important errors are to be avoided. For one thing, it must be kept clearly in mind that the ground-water potential field and flow field is a three-dimensional field occupying all the space from the air-water interface down to indefinite depths, and all that we have done is to determine the value of this three-dimensional field upon an arbitrary two-dimensional surface through that field. The equipotential lines on this surface are, therefore, but the traces of the equipotential surfaces that have been intersected by it.

In actual practice it is customary to use the piezometric surface, not as a means of obtaining the potential of points on the underground surface, but directly, assuming that the component of the potential gradient on the underground surface is proportional to the slope of the piezometric surface itself, or that

$$\frac{\partial h}{\partial s} = \frac{\partial h}{\partial r}, \tag{280}$$

where s is a length on the underground surface and r its vertical projection upon a horizontal surface. This is strictly true if the bedding surface considered is horizontal, but if s has an angle of slope α, then

$$s = \frac{r}{\cos \alpha}$$

and

$$\frac{\partial h}{\partial s} = \frac{\partial h}{\partial r} \cdot \cos \alpha \,. \tag{281}$$

Hence, such an assumption is not valid for angles of dip greater than about 3°, though in most cases the dips actually dealt with are smaller than this.

A more serious danger lies in the tacit assumptions that are commonly made when computing flow from the geometry of the piezo-

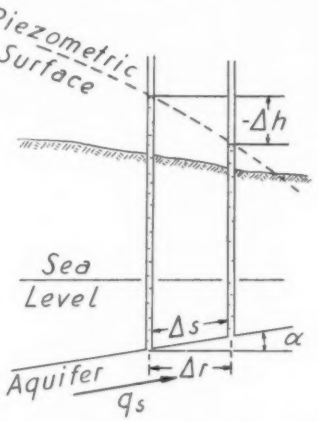

FIG. 41.—Section showing tilted aquifer and piezometric surface

metric surface. These are that the aquifer is bounded above and below by rocks so impermeable that the normal components of the flow across these bounding surfaces are negligible, so that the tangential components are essentially the total flow, and the flowlines from top to bottom of the aquifer are parallel to its bounding faces. The postulated flow is, therefore, parallel to a single plane, and the potentials on one face of the aquifer are the same as those on all other planes parallel to this.

Again, in many instances these assumptions are good approximations; but they must be made knowingly and with caution, because there are many other instances where they are not even approximately correct. If, for example, into a horizontal laminar aquifer

whose upper and lower surfaces are completely impermeable, two separate wells with equal discharges are terminated—one as a point-sink on the upper boundary of the aquifer, and the other as a line-sink extending from top to bottom—the potentials along the upper surface of the aquifer and the corresponding piezometric surfaces will be quite different in the two cases. In the case of the line-sink we shall deal with a problem of plane radial flow with logarithmic potential. For the point sink, in its immediate vicinity the flow will be hemispherically radial and the potential will increase with the inverse first power of the distance. At greater distances this will transform gradually into plane flow with logarithmic potentials. While the potentials are obtainable from the piezometric surface in both cases, the methods of analysis to be used in computing the flow are quite different.

It is not uncommon to encounter on a piezometric surface so-called piezometric "highs"—the large southern high, the Tampa high, and others on the piezometric map based on the top of the Ocala limestone in Florida,[16] for example. These consist of large "mounds" on the piezometric surface or of regions underground where the equipotential lines on the surface of the aquifer enclose areas of higher potential. Since, in such an instance, the component of the flow parallel to the upper surface of the aquifer is radially outward from the high, either of two things must occur: water must be created in the region of the high, or else water must be entering such a region across its upper or lower surfaces, the latter, of course, being the actual situation. Such instances merely show conspicuously that the assumption of impermeable upper or lower boundaries with a zero normal component of flow of an important aquifer is not tenable.

These instances illustrate the caution that must be observed in drawing conclusions from a piezometric surface. It is shown by treatises dealing with the mathematical theory of potential functions that in a region whose geometry and fixed physical properties—in this case permeability—are known completely, it is possible to determine the potential at all points in the field when its value at all

[16] V. T. Stringfield, "The Piezometric Surface of Artesian Water in the Florida Peninsula," *Trans. Amer. Geoph. Union*, 1935, pp. 524–29.

points upon a surface passing through that field is known. This is precisely the problem involved when a piezometric surface is given. In very simple cases, such as the regional flow through an aquifer, simple calculations suffice. When dealing with local anomalies, however, such as the disturbances due to wells, springs, canals, and the like, the method of calculation must be correctly adapted to the geometry of the particular problem considered, otherwise the results obtained will not be reliable.

Among those who employ the piezometric surface as a device for determining regional flow, many of these difficulties are not unrecognized; and on various occasions the statement has been made that for problems involving flow in three dimensions an infinity of piezometric surfaces would be required.

While such a procedure may not be impossible, the difficulties inherent in it are rather formidable. Assuming the permeability throughout the field to be known completely, all that is directly determinable (without recourse to extraneous considerations) from the piezometric surface corresponding to a given plane intersecting the field of flow are the components parallel to that plane of the flow vector at all points in the plane. To obtain the resultant flow vector at any point, three non-coplanar vector components must be known. These necessitate the use of three piezometric surfaces corresponding to three nonparallel planes intersecting at the given point. Then, for all points in the field of flow it would be necessary to have the ensemble of piezometric surfaces corresponding to three infinite families of planes, one family parallel, respectively, to each of the nonparallel planes through the initial point—a triple infinity in all.

But, before we are able to construct these families of piezometric surfaces, we must first know the value of h, and hence of $\Phi = gh$, at every point in the field. If we know this, however, we can solve the problem directly from the known potential gradients by means of Darcy's law, and no piezometric surfaces are required.

THE CONDITION FOR ARTESIAN WATER

At this point it is pertinent to inject a comment regarding the conditions for artesian wells. Since water always flows from regions

of higher to those of lower potential, if we terminate one end of an open tube at a point P_1 in a ground-water field of flow, and the other end at P_2 either inside or outside the field, the water will flow through the tube from P_1 to P_2 provided the potential Φ_1 at P_1 is greater than Φ_2 at the point P_2. The only exception to this occurs when the path traversed by the tube is such that negative fluid pressures are involved, as in the case of too high a syphon.

With this in mind, if we take the point P_2 above the surface of the ground and we wish artesian water at that point, all that is necessary is to find a point P_1 within the ground-water field at which the potential Φ_1 is greater than Φ_2 and connect these two points by an open-ended tube so arranged that no negative pressures exist. Artesian flow will then occur at P_2. If we restrict the location of P_1 to a vertical line through P_2, then it is both necessary and sufficient that a potential greater than Φ_2 exist somewhere along this line beneath the air-water interface if artesian flow is to occur at P_2.

The variety of hydrologic situations that will give rise to potentials below the ground surface larger than those a few feet above is very great. One of these is the familiar textbook illustration of the aquifer that outcrops in the highlands and then passes under the plains beneath an overburden of impermeable strata, a typical example of which is afforded by the Dakota sandstone under the great plains. While this is a sufficient condition for artesian water, it is by no means a necessary one, and its extensive use has obscured a more complete understanding of artesian phenomena.

As a matter of fact, in order to have artesian potentials, an aquifer need not be overlain by impermeable material, and it need not outcrop. Moreover, even if it does outcrop, the outcrop area may just as well be a region of discharge as of intake. All these points, as Paige[17] has pointed out, are illustrated by the Ocala limestone of Florida. Over much of the southern and eastern part of the state the water from this aquifer is under artesian potentials; yet its outcrop area is near sea-level and is a region of discharge. The water enters the formation by downward flow through 500 feet and more of

[17] Sidney Paige, "Effect of Sea-Level Canal in the Gound-Water Level of Florida—A Reply," *Econ. Geol.*, Vol. XXXIII (1938), pp. 647–65.

younger and less permeable formations from regions that are topographically higher than the artesian areas.

If it ever becomes practicable to drill inclined or horizontal wells, artesian water can be obtained at many places where it cannot be obtained from vertical drill holes.

THE PROBLEM OF PERMEABILITY

When Darcy established experimentally by means of the flow of water through filter sands the relationship of equation (8),

$$q = -K \cdot \frac{dh}{dl},$$

he remarked that K was a "coefficient depending upon the permeability of the bed" (of sand). By investigating the flow of all manner of fluids through homogeneous and isotropic media, we were able to show in equation (74) that the complete expression for the flow of any kind of fluid under any condition (subject only to the restriction that the velocity be small enough that forces due to inertia may be neglected) is given by

$$q = -Nd^2\rho \cdot \frac{1}{\eta} \cdot g \cdot \frac{\partial h}{\partial l},$$

which, when compared with equation (8), shows that

$$K \equiv Nd^2\rho \cdot \frac{1}{\eta} \cdot g = k\rho \cdot \frac{1}{\eta} \cdot g,$$

where $k \equiv Nd^2$ and is the only one of the above four quantities that is a property of the medium, the remaining factors being properties of the fluid and of the gravity field at the point of experimentation.

Equation (74), while unknown to Darcy himself, is simply a generalization of the special case which he investigated. In conformity with established usage, it is the general equation, rather than the special case, that constitutes "Darcy's law." Consequently, in what follows, when the term "Darcy's law" is used, it shall be understood to signify the general relationship of equation (74) or its equivalent. Any other expression purporting to be Darcy's law but not equiva-

lent to equation (74) can then be shown to be either physically erroneous or else incomplete, that is, an expression which is physically correct as far as it goes, but which is limited in its validity to a narrower range of phenomena.

The identification of equation (8) with equation (74) is only permissible provided we interpret equation (8) to be a complete expression of Darcy's law. Only under this condition are we permitted to expand the parameter K into the component factors k, ρ, $1/\eta$, and g.

In this expanded form of K we are confronted anew with the problem of what combination of these four factors is to represent the essential element of a coefficient of permeability. Darcy's statement that K is a "coefficient depending upon the permeability" of the sand clearly suggests that K is not itself the coefficient of permeability but is a function of that coefficient. What, then, is the coefficient of permeability of the sand?

Attempts to answer this question have led to more disagreement and confusion than perhaps any other problem in ground-water hydrology. As a result, we have at the present time some four or five physically different—that is, dimensionally unlike—quantities all called by the same name: the "coefficient of permeability." In addition to this, a dozen or more different sets of physical units have been prescribed as the proper ones in terms of which the different coefficients are to be measured.

If this kind of confusion is to be eliminated, it can only be done by reaching an agreement as to what concept we wish the term "permeability" to signify, and then determining a coefficient that varies as a function of the selected permeability and with nothing else. The basis of such a coefficient of permeability must necessarily be some combination of the four factors, k, ρ, $1/\eta$, and g, taken from one to four at a time, because these are the only factors that affect the rate of flow. Conversely, the choice of any combination of these four factors uniquely determines a particular definition of permeability.

We could start out by trying to define the different conceptions that might be called "permeability" and then determine what combination of the above factors varies as a function of each, but it is far simpler to proceed in the inverse manner and let the combinations

of k, ρ, $1/\eta$, and g, taken from one to four at a time, serve to define the different possible conceptions of permeability. Since there are only fifteen such combinations, all dimensionally unlike, then the maximum number of possible different "permeabilities" is fifteen.

Since the time of Darcy there seems to have been general agreement that permeability is, in part at least, a property of the medium. Thus, if two sands, one coarse and the other fine, are used, and ρ, η, and g are kept constant, for the same value of dh/dl the flow will be at a greater rate through the coarser sand, which will therefore be said to be the more permeable of the two. Since, in this case, only the factor k has been varied, it follows that any coefficient of permeability must contain the factor k as an essential element, whatever else it may embrace besides. This then reduces our possible different conceptions of permeability to the number of combinations that can be formed with k of the factors ρ, $1/\eta$, and g taken from zero to three at a time, or eight in all.

The preponderance of contemporary opinion appears to favor the conception that permeability is a function of the medium only; that is, that for a given medium the permeability is a fixed property independent of the intensity of gravity, of the properties of the fluid flowing through it, or of whether any fluid flows at all. Of the eight combinations with k of the factors ρ, $1/\eta$, and g, the only one satisfying this condition is k itself, which depends only upon the geometrical properties of the medium—its internal shape and its size scale—and has the dimensions $[L^2]$.

Thus, if we choose k as our coefficient of permeability, we uniquely determine that permeability is to be a property of the medium and of nothing else. The converse, however, is not true; if we decide that permeability is to be a property of the medium only, a coefficient signifying this fact is not uniquely determined, because, in addition to k itself, any single-valued function, $\Pi = f(k)$, where Π is the coefficient of permeability, can also be made to serve. All that is necessary is that for any given value of k, corresponding to a particular medium, the value of Π must be uniquely determined. This fact enables us to resolve the anomaly that arises when two widely different coefficients of permeability, both capable of being shown to be properties of the medium only, are employed.

Since there are an unlimited number of single-valued functions of k, we are left with an unlimited number of choices for our final coefficient of permeability. For this choice we are concerned only with the dictates of convenience. Out of all possible single-valued functions of k, by all odds the simplest is the identity

$$\Pi \equiv k\,, \tag{282}$$

whose dimensions are $[L^2]$, and this is the coefficient that we shall here recommend.

There remains only the problem of the choice of suitable units of measurement; and again, if simplicity is to be achieved and confusion avoided, the best procedure is to adhere strictly to the fundamental units and the consistent derived units of either the metric or the English system. In the metric system the unit of k is the square centimeter; in the English system it is the square foot. The conversion factor from the English unit to the metric unit is simply the number of square centimeters per square foot, or 929.0.

Stated in this abstract manner, the square centimeter as a unit of permeability is rather meaningless. This obscurity disappears, however, if we substitute $\partial\Phi/\partial l$ for $g(\partial h/\partial l)$ in equation (74) and solve for k:

$$k = -\frac{q\eta}{\rho \cdot \dfrac{\partial\Phi}{\partial l}}\,.$$

Then, if we equate all members in the term to the right to their unit values, we obtain for the unit value of k:

$$1\ [\mathrm{cm}^2] = 1\left[\frac{[(\mathrm{cm}^3/\mathrm{sec})/\mathrm{cm}^2][\mathrm{gm/cm\text{-}sec}]}{(\mathrm{gm/cm}^3)(\mathrm{cm/sec}^2)}\right]. \tag{283}$$

Expressed in words, a medium has a permeability of 1 cm.^{2} when a fluid whose viscosity is 1 poise and whose density is 1 gm/cm^3, flows through it with a specific discharge of 1 (cm^3/sec)/cm^2 under an impelling force of 1 dyne per gram.

Since we do not have available direct measurements of the permeabilities of sediments expressed in square centimeters from which to obtain an idea of the order of magnitude of this unit, let us

postpone further consideration of it until after we have brought up another thread of our discussion.

While it is impracticable to give attention to all the various coefficients of permeability that have been proposed, there are two that merit individual attention; these are that of the Ground Water Division of the United States Geological Survey, which is the one most widely used by ground-water hydrologists, and that proposed originally by Nutting, which is the one most extensively employed by petroleum engineers.

The Ground Water Division unit was suggested by Meinzer[18] and is defined as follows:

> The results of the tests are expressed as a coefficient of permeability, which is based on Darcy's law that the rate of flow varies in direct proportion as the hydraulic gradient. The coefficient of permeability of a material is the rate of flow [of water] in gallons a day, through a square foot of its cross section under a hydraulic gradient of 100 per cent, at a temperature of 60° F. . . . .
>
> The general formula for permeability may be written as follows:

$$P = \frac{qlt}{Tah},$$

in which P is the coefficient of permeability, q the quantity of water, l the length of column of sample, t the correction for temperature, T the time, a the cross-section area of the sample, and h the head.

In later publications of the Ground Water Division it has become customary to employ the equation

$$Q = PIA\,, \tag{284}$$

where Q is the total discharge, P the coefficient of permeability as defined above, I the hydraulic gradient, and A the area of cross section. This is stated to be Darcy's law.

Now if we focus our attention upon equation (284), by converting all of its members except P into the symbols employed here, we bring it into the form

$$q = -P \cdot \frac{dh}{dl}\,. \tag{285}$$

[18] Norah Dowell Stearns, "Laboratory Tests on Physical Properties of Water-bearing Materials," *U.S. Geol. Surv. Water-Supply Paper 596-F* (1928), pp. 121–77.

Since this is stated to be Darcy's law, comparison with equation (74) would lead us to suppose that

$$P \equiv k\rho \cdot \frac{1}{\eta} \cdot g \,, \tag{286}$$

and varies as a function of the properties of the medium, of those of the fluid, and with the intensity of gravity

In this supposition, however, we should be mistaken, for if we restudy the definition of P quoted above, we discover that it applies only to the flow of water at a temperature of 60° F. (and presumably a constant value of g), and to no other fluid. If we wish to know the rate of flow of another fluid—say oil—whose density and viscosity are different from those of water at 60° F., through a medium for which the value of P is known already, not only can we not use equation (284), but we are left without any equation at all.

The equation $Q = PIA$ is therefore an incomplete expression of Darcy's law. To obtain a corresponding equation involving P that is complete, we first translate P into an equivalent expression in terms of k, ρ, η, and g. This we do by noting that for water at 60° F. and a constant value of gravity, ρ, η, and g assume the constant values ρ_0, η_0, and g_0, respectively. In this case equation (284) assumes the form

$$q = -k \cdot \frac{\rho_0 g_0}{\eta_0} \cdot \frac{dh}{dl} \,, \tag{287}$$

which, when compared with the equivalent equation (285), gives

$$P \equiv \frac{k\rho_0 g_0}{\eta_0} \,. \tag{288}$$

Let us now introduce $k(\rho_0 g_0/\eta_0)$ into equation (74) by multiplying the right-hand term of that equation by the quantity

$$\frac{\rho_0}{\rho_0} \cdot \frac{\eta_0}{\eta_0} \cdot \frac{g_0}{g_0}$$

(which is equal to unity). The result obtained is

$$\left.\begin{aligned} q &= -\frac{\rho_0}{\rho_0} \cdot \frac{\eta_0}{\eta_0} \cdot \frac{g_0}{g_0} \cdot \frac{k\rho_0 g_0}{\eta} \cdot \frac{\partial h}{\partial l} = -\frac{\rho}{\rho_0} \cdot \frac{\eta_0}{\eta} \cdot \frac{g}{g_0} \cdot \frac{k\rho_0 g_0}{\eta_0} \cdot \frac{\partial h}{\partial l} \\ &= -\frac{\rho}{\rho_0} \cdot \frac{\eta_0}{\eta} \cdot \frac{g}{g_0} \cdot P \cdot \frac{\partial h}{\partial l} \,, \end{aligned}\right\} \tag{289}$$

which is valid for any intensity of gravity and for the flow of any fluid whatever. Consequently, this represents a complete expression of Darcy's law and should be the expression employed in all cases where Darcy's law is intended. In a case where we are dealing with the flow of water at 60° F. and with the standard intensity of gravity, we have $\rho = \rho_0$, $\eta = \eta_0$, and $g = g_0$, so that equation (289) reduces, as a special case, to the familiar expression: $Q = PIA$.

A complete expression of Darcy's law involving P does not appear in the literature of the Ground Water Division, and the failure to distinguish between a complete and an incomplete expression of the law has been responsible for most of the confusion concerning the significance of the parameter P. The equation $P = QIA$ is customarily stated without qualification to be Darcy's law.

Returning now to equation (288), we see that k is the sole independent variable. Hence, for every value of k, that of P is uniquely determined. Therefore P is a function of the medium only, and so is a valid coefficient of permeability.

The fact that the dimensions of P are $[LT^{-1}]$ while those of k are $[L^2]$ produces an apparent contradiction. It seems strange that a coefficient dependent only upon the unit of length should involve the units of both length and time. This discrepancy is accounted for by the factor of proportionality, which, while constant, is not dimensionless. When these dimensions are taken into account, we obtain

$$[P] = \left[\frac{\rho_0 g_0}{\eta_0}\right][k] = [LT^{-1}], \qquad (290)$$

and the paradox is resolved.

The other coefficient that we wish to consider is that proposed originally by Nutting[19] in 1930 and later adopted by Wyckoff and associates[20] in 1934. In each case an equation of the form

$$q = -\frac{k}{\eta} \cdot \frac{\partial p}{\partial l}$$

was employed, and k was defined to be the coefficient of permeability. Despite the fact that this equation is physically erroneous as an

[19] P. G. Nutting, "Physical Analysis of Oil Sands," *Bull. Amer. Assoc. Petrol. Geol.*, Vol. XIV (1930), pp. 1337–49.

[20] R. D. Wyckoff, H. G. Botset, and D. W. Reed, "Measurement of Permeability of Porous Media," *Bull. Amer. Assoc. Petrol. Geol.*, Vol. XVIII (1934), pp. 161–90.

expression of Darcy's law, owing to the use of pressure as a potential function, the k so defined is identical with that used here.

We return now to the question of the numerical values of k, for the common sediments. These may be obtained directly by solving equation (74) for k when all other quantities of that equation have been determined by measurement. Lacking such data, we may, by means of equation (288), find the value of k indirectly for any sediment for which the value of P is known. Solving equation (288) for k gives

$$k = \frac{\eta_0}{\rho_0 g_0} \cdot P .$$

The measurements of P that are available are expressed in gallons per day per square foot—the units prescribed by Meinzer. To obtain the value of k in square centimeters, we must first convert P into the metric units: cubic centimeters per second per square centimeter. Then, when the values of η_0, ρ_0, and g_0, expressed in c.g.s. units, are supplied, the value of k is obtained directly.

For the conversion of P from Meinzer units to metric units

$$1 \frac{\text{gal/day}}{\text{ft}^2} = 4.716 \times 10^{-5} \frac{\text{cm}^3/\text{sec}}{\text{cm}^2} .$$

We may take the standard values of η_0 and ρ_0 (the viscosity and density of water at 60° F.) to be 0.01125 poise and 0.999 gm/cm^3, respectively; and for a standard value of gravity we may ues 980 cm/sec^2. From these values we obtain

$$\frac{\eta_0}{\rho_0 g_0} = \frac{0.01125}{0.999 \times 980} \text{ cm-sec} = 1.149 \times 10^{-5} \text{ cm-sec} .$$

Then the value of k, expressed in square centimeters, is

$$k[\text{cm}^2] = (1.149 \times 10^{-5} \times 4.716 \times 10^{-5}) P \left[\frac{\text{gal/day}}{\text{ft}^2}\right]$$

$$= (5.419 \times 10^{-10}) P \left[\frac{\text{gal/day}}{\text{ft}^2}\right] .$$

Also, since 1 ft.^{2} = 929.0 cm.^{2}, the value of k expressed in square feet is given by

$$k[\text{ft}^2] = \left(\frac{5.419 \times 10^{-10}}{929.0}\right) P \left[\frac{\text{gal/day}}{\text{ft}^2}\right]$$

$$= (5.833 \times 10^{-13}) P \left[\frac{\text{gal/day}}{\text{ft}^2}\right].$$

Conversely,

$$P \left[\frac{\text{gal/day}}{\text{ft}^2}\right] = (1.845 \times 10^{9}) k[\text{cm}^2] = (1.714 \times 10^{12}) k\,[\text{ft}^2].$$

It is to be emphasized that P and k are two entirely different kinds of quantity and therefore cannot be equated. It is meaningless to ask: "How many units of k are *equal* to 1 unit of P?" The foregoing conversions do not therefore represent a relationship of equality but of function. The common bond between P and k is the permeability of the medium; for a given permeability the values of both P and k are uniquely determined. Consequently, if the value of either, expressed in any arbitrary set of units, is known, the value of the other, expressed in any other arbitrary set of units, can be determined.

The measured values of the permeability of sediments, expressed in Meinzer units, range from the order of 10^{-4} for clayey silt to 10^{+5} for gravel. The corresponding range of the permeability measured in square centimeters would be from the order of 10^{-14} to 10^{-5}, and measured in square feet from 10^{-17} to 10^{-8}. It is obvious, therefore, that a permeability of 1 square centimeter or of 1 square foot is very much larger than the permeabilities encountered in practice.

This, however, presents no serious difficulty. It has become almost the universal practice to express the results of physical measurements in the form of a product of a small decimal number with 10 raised to an integral power, positive values of the exponent corresponding to numbers greater than 1, and negative values to those less than 1.

It is equally easy in this manner to deal with numbers expressed as a product of 10 raised to either a large or a small or to a positive or a negative exponent.

Still, if the need for a smaller "practical" unit be felt, there are two ways of achieving such a unit. One of these is to change the fundamental units employed; instead of the centimeter, the gram, and the second, suitable multiples and submultiples of these might be used. This, however, is likely to be confusing, and it is far simpler to retain the fundamental units and define the "practical" unit to be

$$1\ [\text{practical unit}] = 10^n\ [\text{cm}^2] = 1[10^n\ \text{cm}^2]\ .$$

The choice of n is entirely arbitrary and is dependent upon the properties it is desired to impart to the practical unit. For example, if a practical unit is desired such that all measured values of permeability would be multiples of this unit, then n should have the value of about -15. If a unit is wanted such that the greatest number of measured values would range between 1 and 1,000, then n should be about -10.

THE "LAW" OF BADON GHIJBEN AND HERZBERG

Of late a great deal of emphasis has been placed upon the so-called "law" of Badon Ghijben[21] and Herzberg.[22] Each of these authors independently made the discovery that in wells near the seacoast the salt water was not encountered at sea-level, as they had expected, but at a depth below sea-level of the order of forty times the height of the fresh water above sea-level. For this phenomenon each of them deduced the same explanation, namely, that a static equilibrium existed between the fresh water and the salt water, so that the mass of a unit vertical column of fresh water extending from the water table to the fresh-water–salt-water interface must have the same mass as the displaced salt water—a column extending from the interface to sea-level. Following this reasoning, if we let z'_{12} be the elevation of the water table above sea-level, z'_{23} that of the fresh-water–salt-water interface directly below, ρ_2 the density of fresh water, and ρ_3 that of salt water, we should have

$$\rho_2(z'_{12} - z'_{23}) + \rho_3 z'_{23} = 0\ ,$$

[21] W. Badon Ghijben, "Nota in Verband met de Voorgenomen Put boring Nabij Amsterdam," *Tijdschrift van het Koninkhijk, Institut van Ingenieurs*, 1888–89, p. 21.

[22] Baurat Herzberg, "Die Wasserversorgung einiger Nordseebader," *Journal für Gasbeleuchtung und Wasserversorgung*, Vol. XLIV (1901), pp. 815–19 and 842–44.

from which

$$z'_{23} = -\frac{\rho_2}{\rho_3 - \rho_2} \cdot z'_{12} . \qquad (291)$$

Equation (291) is equivalent to those deduced by both Badon Ghijben and Herzberg. It is a relationship of great usefulness but also one whose use entails considerable danger of error, because it is not correct.

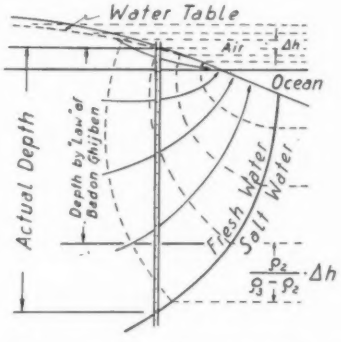

FIG. 42.—Discrepancy between actual depth to salt water and depth as calculated by "law" of Badon Ghijben and Herzberg for flow near outlet.

The assumption upon which the equation is derived is that we are dealing with a case of hydrostatic equilibrium, and to the extent that this assumption is valid the equation is strictly correct. In ground-water problems, however, the assumption is not valid at all, because the fresh water is not at constant potential but in a state of continuous motion. If no additional water were added by precipitation, the flow of the fresh water would continue until it had all been dissipated, and only salt water with a water table at sea-level would remain.

We are therefore dealing with a dynamic equilibrium between flowing fresh water and static salt water, the behavior of which has already been treated in equations (205)–(217). It will be noted that equations (291) and (215) are identical except that in (215) z_{12} is the elevation in air of a particular fresh-water equipotential surface, and z_{23} the elevation in the salt water of the same surface, whereas in

equation (291) z'_{12} is the water-table elevation and z'_{23} the elevation of the fresh-water–salt-water interface in the same vertical line.

For static conditions equation (215) is identical in all respects with (291). For low potential gradients in the fresh water the difference between the two equations is negligible; but for large gradients, such as occur near a pumping well, a canal, or the seacoast, the static relationship of equation (291) may not be even approximately correct, and its use is not warranted under those conditions. In fact, errors can best be avoided by always using the dynamic equations of which a static situation is only a special case.

APPLICATION TO PROBLEMS OF CURRENT INTEREST

Before closing, it will be instructive to examine a few illustrative ground-water problems of current interest in the light of the present theory. The most useful problems for this purpose are those upon which disagreements have arisen or upon which opinions contrary to the present deductions have been held. Since the present theory is based upon the principle of the conservation of matter and the laws of thermodynamics, to which ground-water motion must conform, it is to be expected that a postulated motion of ground water not in conformity with present deductions can be demonstrated to violate one or another of these principles—a violation of either of the laws of thermodynamics being equivalent to a perpetual-motion mechanism.

FLOW NEAR THE WATER TABLE

One such problem is the nature of the flow near the water table. Apparently because of the resemblance between the topography of the water-table surface and that of the surface of the ground, it used to be commonly supposed, and the idea still prevails to some extent, that the ground-water flow is concentrated near the surface of the water table and that the flow down the slope of the water table resembles the corresponding flow down a topographic slope. The intensity of flow was supposed to diminish rapidly with depth, becoming substantially zero in a region of more or less uniform permeability at depths below the level of the lowest parts of the water table. This led to the conception of a large body of stagnant ground water beneath the superficial zone of flow.

This point of view has recently been defended by Swinnerton.[23] Taking a region of mild topographic relief in a humid climate, with rocks of uniform permeability, Swinnerton argues that from a point A (Fig. 43) (shown as a volume element beneath the water table) the water will flow, by all possible paths, to an outlet (shown as a near-by valley). The flow will be distributed among those several paths according to the frictional resistance, the greatest amount of flow following the path of least resistance, and successively lesser amounts the paths of increasing resistance. The path of least resistance is the shortest path, and the resistance increases with increase of length of path. Among the paths 1, 2, and 3 of increasingly greater length, the flow will be greatest along the rectilinear path 1 and successively less along the paths 2 and 3.

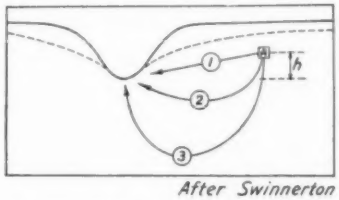

After Swinnerton

FIG. 43.—Flow from region A to outlet according to Swinnerton.

Aside from any question of frictional resistance, this involves directly a violation of the principle of the conservation of matter. If flow occurs from A by all possible paths, of which 1, 2, and 3 are examples, then A will be a volume out of which water flows in all directions and hence a region in which water must be created.

If this postulated flow mechanism were true of an arbitrary point A, then it must also be true of a near-by point A', and the families of flowlines radiating from these two points must form intersecting systems throughout the near-by field. Since two flowlines can only come together at an absolute source or sink (point where water is created or annihilated), which does not exist in ground-water motion, this type of flow would involve the violation of the conservation of matter principle at all points of the field.

Again, no amount of frictional resistance can be assigned to any stream tube because the resistance is a function both of the geometry of the tube and the *rate of flow of the fluid*. We know, for example, that the amount of energy expended per unit of mass by frictional

[23] A. C. Swinnerton, "Origin of Limestone Caverns," *Geol. Soc. Amer. Bull.* 43 (1932), pp. 663–92.

forces is precisely equal to the drop in potential. Therefore, along all streamlines, of whatever shape or length, the amount of work required to drive a unit of mass of the fluid from one equipotential surface to another is precisely the same, although the paths followed by different flowlines may differ widely as to length.

We can get at what actually happens in a case of this sort only by giving due consideration to the distribution of the sources and sinks upon the boundaries of the flow field, and of the corresponding potentials. Here, as explained earlier, a source merely means an area across which water enters the field; and a sink, an area of exit.

In this problem the sources are distributed over the air-water interface, being produced by downward percolating water. The sinks are limited to the bottoms of valleys containing streams. In the field of flow the streamlines and stream tubes originate upon sources and terminate upon sinks. The flow is solenoidal and the velocity finite, so that every stream tube of finite discharge has a finite cross section, and no two flowlines can intersect each other. At a given time one and only one flowline can pass through a given point. All of these are deductions from the principle of the conservation of matter.

Now for the energy relations. The potentials at the sources and sinks are everywhere given by $\Phi = gz$, where z is the elevation of the water table or of the surface of the water in a stream. In air, the surfaces Φ = constant coincide with surfaces z = constant; underground they refract and are everywhere normal to the streamlines. At the sinks the cross section of a stream is sensibly an equipotential region, so that underground the equipotential surfaces about a sink must form a system of more or less concentric surfaces with a radiating system of flowlines in the vertical plane normal to the valley axis.

Since every stream tube has its source on the air-water interface, it is necessary that it intersect this interface at some angle greater than zero, for otherwise its discharge would be zero. We can form some idea of the angle of slope of the stream tube at the air-water interface if we take into account that above this interface there is a vertically downward percolation at a specific discharge of q_i under the gradient of $-g$. The fact that the fluid in this region is discontinu-

ous shows that the discharge is less than that demanded by Darcy's law. Hence,

$$q_1 < -\sigma g \tag{292}$$

and the component normal to the interface is given by

$$q_{n1} < -\sigma g \cos \alpha , \tag{293}$$

where α is the upward slope of the air-water interface.

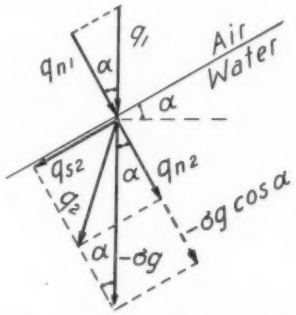

FIG. 44.—Flow vectors at air-water interface when downward infiltration of water occurs.

Along the interface the usual boundary conditions must prevail. The normal component of the flow and the tangential component of the potential gradient must be the same. Thus,

$$q_{n1} = q_{n2} < -\sigma g \cos \alpha , \tag{294}$$

$$\left(\frac{\partial \Phi}{\partial s}\right)_1 = \left(\frac{\partial \Phi}{\partial s}\right)_2 = g \sin \alpha . \tag{295}$$

Consequently the tangential component of flow on the water side of the air-water interface is

$$q_{s2} = -\sigma g \sin \alpha . \tag{296}$$

Equations (294) and (296) give the tangential and normal components of the flow at the air-water interface. The vector sum of

these is $\mathbf{q}_2$. The normal component q_{n2} may vary between the limits zero and $-\sigma g \cos \alpha$, and α between the limits of zero and 90°. As $\mathbf{q}_{n2}$ approaches zero, $\mathbf{q}_2$ approaches $\mathbf{q}_{s2}$ as a limit, and the flowlines become tangential to the interface. As q_{n2} approaches its upper limit, $-\sigma g \cos \alpha$, $\mathbf{q}_2$ approaches the limit $-\sigma \mathbf{g}$, with the flowlines vertical. For a constant value of $\mathbf{q}_{n2} \neq 0$, as α tends to zero q_{s2} tends to zero, and $\mathbf{q}_2$ tends to $\mathbf{q}_{n2}$, which again is vertical.

Hence, in Swinnerton's problem the flowlines at their points of origin on the air-water interface always dip more steeply than the interface itself, becoming vertical at the ground-water divide, where

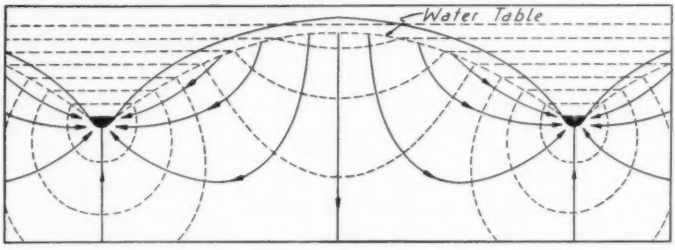

FIG. 45.—Approximate flow pattern in uniformly permeable material between the sources distributed over the air-water interface and the valley sinks.

α is zero and, across the divide, dipping in the opposite direction. Accordingly, at the divide the stream tubes descend vertically; and away from the divide, toward the valleys on either side, the angles of pitch of the flowlines gradually approach the angle of dip of the interface. The stream tubes adjacent to the outlets follow almost rectilinear paths, while each tube originating successively farther away makes a downward loop outside the paths of all stream tubes between it and the outlet, until finally the one at the divide descends to a depth which in uniformly permeable material has no assignable limit.

In such a region there can exist no body of stagnant water unless it be a body of water such as salt water, which is physically different from that flowing. The region of most intense flow is not a zone parallel to the air-water interface but a region where the flowlines converge toward a sink.

THE JOHNSON HYPOTHESIS OF THE ORIGIN OF SUBMARINE CANYONS

For a problem involving energy relationships more directly we turn now to the hypothesis advanced by Johnson[24] of the origin of the submarine canyons off the east coast of North America. All that interests us here is that this hypothesis involves a ground-water

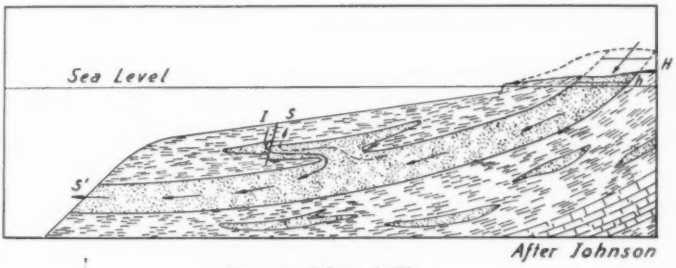

FIG. 46.—Johnson's Fig. 2

mechanism shown in Figure 46, taken from Johnson and described by him (p. 80) as follows:

> One may suppose, for example, that artesian water with a head H (Figure 2) escapes in part (dotted arrows) across adjacent pervious beds and through fissures or other openings to form a shallow submarine spring at S; and in part as deep submarine springs at S'. When erosion reduces the land surface, or subsidence lowers it, or rise of sea level occurs, the lesser head h may be insufficient to cause outflow. Under the new conditions, salt water flowing in through the fissure, now serving as an intake, I, will mix with fresh water in the aquifer, and the mingled waters will find exit at S'. It should be borne in mind that while fresh water descending along a fissure or through pervious beds will not intermingle freely with heavier salt water below, but rather will "float" upon it, salt water penetrating downward in the same manner, tends, because of its higher specific gravity, to enter fresh water below and spread through it, increasing the weight of the mixture.

Without any deeper analysis, the first thing that impresses one about this mechanism is that, if the denser salt water is to penetrate downward and intermingle with the fresh water, and then this mixture, which is still less dense than salt water, is to continue its

[24] Douglas Johnson, *The Origin of Submarine Canyons* (New York: Columbia University Press, 1939).

descent to an outlet at S', we should also expect the denser cold air at the top of a chimney to penetrate downward and intermingle with the warm air in the chimney, and the mixture to continue downward and find an exit through the fireplace.

Now to handle the problem analytically, let ρ_1, ρ_2, and ρ_3 be the densities of the fresh water, the mixture, and the salt water respectively, and Φ_1, Φ_2, and Φ_3, the corresponding potentials. These potentials at all points are

$$\left.\begin{aligned} \Phi_1 &= gz + \frac{p - p_0}{\rho_1}, \\ \Phi_2 &= gz + \frac{p - p_0}{\rho_2}, \\ \Phi_3 &= gz + \frac{p - p_0}{\rho_3}; \end{aligned}\right\} \tag{297}$$

and at the points of contact with the salt water,

$$p = -\rho_3 gz + p_0, \tag{298}$$

which gives as the values of the potentials at those points:

$$\left.\begin{aligned} (\Phi_1)_3 &= -\frac{\rho_3 - \rho_1}{\rho_1} \cdot gz, \\ (\Phi_2)_3 &= -\frac{\rho_3 - \rho_2}{\rho_2} \cdot gz, \\ (\Phi_3)_3 &= \frac{\rho_3 - \rho_3}{\rho_3} \cdot gz = 0. \end{aligned}\right\} \tag{299}$$

From this it is clear that both $(\Phi_1)_3$ and $(\Phi_2)_3$ increase with the depth below sea-level.

Now let P_1 be the point on the main aquifer where the two channels separate, P_2 a point at the zone of mixing, and P_3 the lower outlet (Johnson's S'). By Johnson's hypothesis

$$\Phi_{13} > \Phi_{11} > \Phi_{12}, \tag{300}$$

so that the fresh water of itself is not able to flow out at P_3. At P_2, however, mixing occurs, and the mixture then flows from P_2 to the outlet at P_3.

To determine whether this is possible, we only have to observe that the point P_2, where the mixing occurs, must be somewhere higher than P_3. At these two points the potentials of the mixture are

$$\left.\begin{aligned} \Phi_{22} &= -\frac{\rho_3 - \rho_2}{\rho_2} \cdot gz_2 , \\ \Phi_{23} &= -\frac{\rho_3 - \rho_2}{\rho_2} \cdot gz_3 , \end{aligned}\right\} \tag{301}$$

whose difference is

$$\Phi_{23} - \Phi_{22} = -\frac{\rho_3 - \rho_2}{\rho_2} \cdot g(z_3 - z_2) > 0 . \tag{302}$$

Hence the flow from P_2 to P_3 is from a lower to a higher potential.

We are obliged to conclude, therefore, that the flow mechanism postulated by Johnson, if it could be made to work, would violate the principle of the conservation of energy or the first law of thermodynamics, and hence constitutes a perpetual-motion mechanism of the first kind. In principle it is no different from water flowing slowly uphill in an open channel.

What actually would happen in the situation shown by Johnson's Figure 2 would be this: The fresh-water–salt-water interface would occur at an elevation

$$z_{13} = -\frac{\rho_1}{\rho_3 - \rho_1} \cdot h ,$$

obtained from equation (212), where h is the fresh-water manometer height above sea-level at the point of contact. This h is equal to, or less than, the height of the water table used by Johnson, depending upon whether the water is static or in motion. If

$$z_{13} > z_1 ,$$

the interface will be higher than P_1, and no flow will occur. If

$$z_3 < z_{13} < z_1 ,$$

fresh water will flow out at S and a static interface will exist between P_1 and P_3. If

$$z_{13} < z_3 ,$$

fresh water will flow out at both S and S'.

THE FLORIDA SHIP CANAL

A somewhat more complex problem is afforded by the proposed Florida ship canal, pertaining to which a summary of the essential data has been presented by Paige[25] of the United States Army Corps of Engineers. The proposed canal is to be unlined and at sea-level, and a part of the route chosen extends across the outcrop area of the Ocala limestone. This is a highly permeable limestone and is the principal aquifer of Florida. It outcrops over an area which is roughly a north-south ellipse about 150 miles long and 50 miles wide, and forms the central region of a huge structural dome away from which the Ocala dips and underlies the younger formations of the rest of the state.

About 50 miles to the north of the canal route and 78 miles to the south there occur two large highs in the piezometric surface based upon the Ocala limestone, the one to the north reaching over 90 feet and the one to the south about 135 feet above sea-level. In the outcrop area the piezometric surface merges into the ground-water table. The piezometric highs coincide with topographic highs and are only slightly lower than the water-table surface. In the outcrop area the canal route extends across the saddle of the ground-water table between these two highs. In this region the elevation of the water table is about 40 feet above sea-level.

The principal ground-water problem involved, and the only one we shall consider here, is: What effect will the canal have upon the ground-water table in its vicinity where it traverses the outcrop of the Ocala limestone, and how wide will the belt on both sides of the canal be in which the effect is perceptible in wells? Paige concluded that a new ground-water table with a surface steepest near the canal and approaching the original water table asymptotically with distance would result. The distance from the canal to where this new water table would coincide with the older one Paige estimated to be about 10 or 15 miles.

In this conclusion he has been severely criticized by Brown[26] and

[25] Sidney Paige, "Effect of a Sea-Level Canal on the Gound-Water of Florida," *Econ. Geol.*, Vol. XXXI (1936), pp. 537–70.

[26] John S. Brown, "The Florida Ship Canal," *Econ. Geol.*, Vol. XXXII (1937), pp. 589–99.

by Thompson, Meinzer, and Stringfield,[27] to whom Paige[28] later replied.

Since this is a problem upon which there appears to be substantial agreement with regard to the principal field data, the disagreements evidently arise from a difference in the theory employed in making the predictions. It will therefore be instructive to examine it in the light of the theory developed here.

The only problem we shall consider is that of the new profile of the water table where the canal traverses the Ocala limestone, and the maximum distance to which the lowering of the water table will be appreciable. Only an approximate solution is possible with available data, but one of the correct order of magnitude should be obtainable.

For our approximation we will idealize the problem somewhat by considering a case where the topography and water table are the same as those of Florida but where the rocks are all of Ocala limestone and of uniform specific conductivity σ. We let h' be the original elevation of the water table and h that of the new water table after the canal is dug. The value of h' at the canal route in the saddle is about 40 feet and at the southern high, 78 miles to the south, slightly more than 135 feet, giving an average water-table slope of about 1.2 feet per mile.

Since this is the smallest slope and the highest water table to be encountered, the effect of the canal both in terms of the amount the water table is lowered and the width of the zone affected should here be a maximum. Since we are interested chiefly in this maximum value, we need not consider other cases.

The canal, after it is dug, will act as a horizontal prismatic sink containing water at constant potential with a free surface only slightly above sea-level. The fresh-water flowlines will converge toward this prism perpendicularly to its surface. They will therefore be parallel to a plane normal to the prismatic axis and will approach the canal more or less radially in this plane.

[27] D. G. Thompson, E. O. Meinzer, and V. T. Stringfield, "Effect of a Sea-Level Canal on the Gound-Water Level of Florida," *Econ. Geol.*, Vol. XXXIII (1938), pp. 87–107.

[28] Sidney Paige, "Effect of Sea-Level Canal on the Gound-Water Level of Florida—A Reply," *Econ. Geol.*, Vol. XXXIII (1938), pp. 647–65.

The air–fresh-water interface will slope toward the canal and approach the south bank tangentially (presumably at about 30°). There will be a surface of seepage between this and the water-level in the canal of a finite but unknown width. The fresh-water–salt-water interface will slope upward toward the canal; and, since the flow will be almost bilaterally symmetrical on opposite sides of the canal, the salt water will form a sharp wedge, with its crest parallel to the axis of the canal and reaching to within a few tens of feet of its bottom.

The magnitude of the slopes of both the upper and lower interfaces will decrease rapidly with distance away from the canal; and at some unknown distance, which we shall seek to estimate, the new water table will approach coincidence with that which existed before.

To determine the properties of this new profile analytically, we choose the origin of co-ordinates at sea-level on the axis of the canal and let the x-axis extend southward normal to the canal and the z-axis upward. We take as our flow region a laminar section parallel to the x–z plane and of unit thickness. At some distance, x_1, which we shall seek to determine, the new water-table profile will come into coincidence with the old one. Between this distance and the canal we assume that there are no sources or sinks, so that over this interval the total discharge, Q, is constant. We let h be the elevation of the new water table and A the cross-sectional area of a stream tube of unit thickness normal to the flowlines at any distance x. Equating the discharge at x and x_1 then gives

$$Q = qA = -\sigma g \cdot \frac{dh}{dx} \cdot A = -\sigma g \left(\frac{dh}{dx}\right)_1 A_1 . \tag{303}$$

Eliminating $-\sigma g$ and solving for dh/dx gives

$$\frac{dh}{dx} = \left(\frac{dh}{dx}\right)_1 A_1 \cdot \frac{1}{A} . \tag{304}$$

Setting $(dh/dx)_1 A_1 \equiv a$ and integrating,

$$h = h_0 + a \int \frac{1}{A} \cdot dx . \tag{305}$$

In order to perform this integration and determine h we must find how the area A varies with distance along the profile. In the immediate vicinity of the canal this is not easy to do though we know that the smallest value of A is equal to one-half the wetted perimeter of the canal. But for the part of the profile where the ground-water slope is not more than 100 feet per mile, we may assume, as an approximation, that the area A is equal to the difference of the elevations in air and salt water of the fresh-water equipotential surface occurring at distance x. This is obtained from equation (213) and

$$A \cong (z_{12} - z_{23}) = \frac{\rho_3}{\rho_3 - \rho_2} \cdot h = bh \,, \tag{306}$$

where $b \equiv \rho_3/(\rho_3 - \rho_2)$.

Let x_0 be the distance at which this approximation becomes allowable, and h_0 the height of the water table at that distance. Then, if we introduce the value for A from equation (306) into equation (304), the elevation of the profile between x_0 and x_1 is obtainable by integration. The differential equation of the profile is

$$\frac{dh}{dx} = \frac{a}{b} \cdot \frac{1}{h} \,,$$

and separating the variables and integrating,

$$\int_{h_0}^{h} h \cdot dh = \frac{a}{b} \int_{x_0}^{x} dx = \frac{h^2 - h_0^2}{2} = \frac{a}{b} (x - x_0) \,,$$

from which

$$h^2 = \frac{2a}{b} (x - x_0) + h_0^2 \,. \tag{307}$$

Since all factors of this equation except h^2 and x are constants, this represents a straight line with the slope $2a/b$, passing through the point (x_0, h_0^2), when plotted as a graph using the values of h^2 as ordinates and x as abscissas.

If on the same graph we plot the values of h'^2 of the old water-table profile, the line represented by equation (307) must be a tangent line to this, the abscissa of the point of tangency being x_1. Through

any given point (x_0, h_0^2) only one tangent line to the old profile can be drawn, and by means of this x_1 and a are uniquely determined. The value of b is given by the densities of fresh and salt water and is about 40.

We can only approximate x_0 and h_0. Since the area A decreases continuously as the canal is approached, the slope of the water table, as given by equation (304), must continuously increase, that is, at the canal the slope has its maximum value (30° or so) and decreases continuously with distance. Hence, the average slope from the canal to any distance x is always greater than that at x. Also, at any distance x,

$$0 < h < h' ;$$

and at x_0,

$$0 < h_0 < h_0' .$$

We chose x_0 as the distance at which the water-table slope becomes 100 feet per mile. Between $x = 0$ and $x = x_0$ the average slope must be greater than 100 feet per mile. At the same time h_0 must be less than the elevation of the old water table, or less than 40 feet. Therefore x_0 must be less than $\frac{1}{2}$ mile from the south bank of the canal.

To be conservative, let x_0 be taken to be 1 mile. At this distance h_0 will be greater than zero by an unknown amount, possibly by 10 or 20 feet; but again, in order to be conservative, let us set it equal to zero. Then the squared profile of the new water table is the straight line passing through the point (1, 0) and tangent to the h'^2 profile of the old water table.

These operations have been performed and the results plotted graphically in Figure 47. Coincidence between these profiles occurs at about 23 miles south of the canal at an elevation of about 60 feet. At 20 miles the lowering of the water table is negligible; at 15 miles the drawdown is 2 feet (from 52 to 50 feet); at 10 miles, 5 feet (from 45 to 40 feet); and at 5 miles, 15.5 feet (from 42 to 26.5 feet).

Now is the time to examine our assumptions. We assumed that the Ocala limestone was of uniform permeability and unlimited thickness. Locally, of course, owing to solution channels or other

inhomogeneities, the permeability is not uniform; yet the smoothness of the hydrologic contours on the Ocala shows that regionally it does have an effective permeability uninfluenced by such local irregularities. It is the effective regional permeability that we have employed here, and we have so arranged our equations that it cancels out and saves us the necessity of knowing its value.

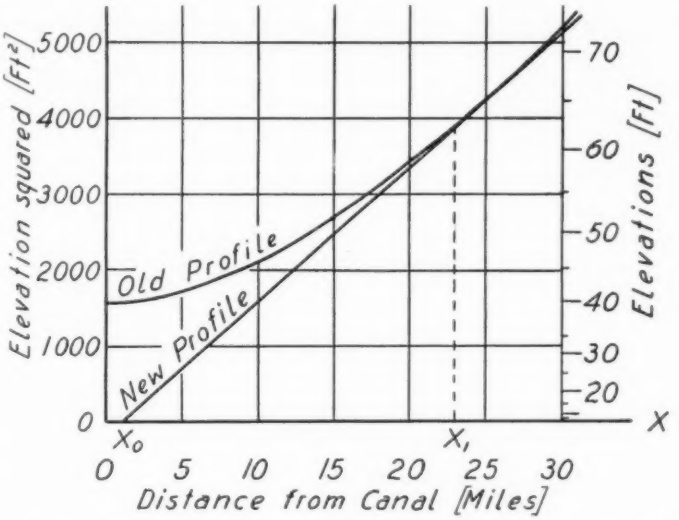

FIG. 47.—Comparison of the original ground-water profile south of the Florida ship canal with the limiting value of the new one as calculated here.

With the assumption that the Ocala limestone is of unlimited thickness, the area A continuously increases with distance from the canal because of the lowering of the salt-water interface. At 23 miles this represents a depth of about 2,400 feet. If the Ocala is less than this thickness and is underlain by impermeable rocks, then x_1 will very nearly coincide with the distance at which the salt-water interface reaches the lower surface of the limestone, and the width of the affected zone will then be narrower than that calculated here.

We assumed that no sources and sinks existed from the canal to the distance x_1 and that Q was constant over this length. This as-

sumption is false, but again the error is on the conservative side. Owing to precipitation, there will be distributed sources all along the profile. There will also be sinks where the water discharges locally into springs and streams. These, however, will diminish as the canal is approached and the water table is lowered, so that, on the whole, the difference between sources and sinks, or the net sources, will increase toward the canal. The effect of this will be to cause Q to increase toward the canal, making the water-table

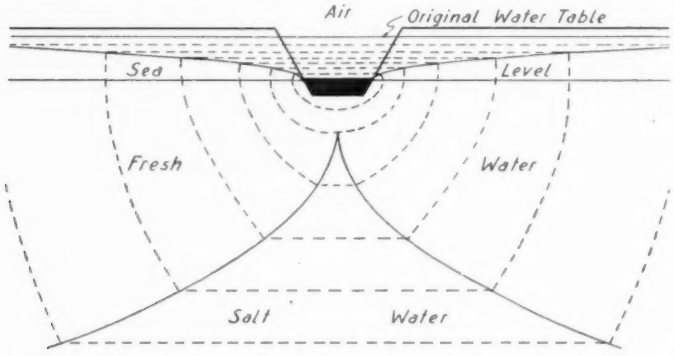

FIG. 48.—Schematic diagram showing approximately the type of relationship between the bodies of air, fresh water, and salt water to be expected near a sea-level canal in uniformly permeable material. The scales are greatly distorted. The depths to salt water should be four times those shown here.

profile higher at all points than that which we have computed. This will correspondingly reduce the amount of drawdown at each distance. Also, the curve of h^2 plotted as a function of x will no longer be a straight line but will be an arc convex upward. The point of tangency with the old profile will therefore also be nearer to the canal than that which we have computed.

We assumed that at a distance of 1 mile from the axis of the canal the elevation of the new water-table profile was zero. Since, at the south bank of the canal, the profile has an initial elevation equal to that of the upper edge of the zone of seepage and an initial slope equal to that of the south bank (30° or more), and since the slope remains positive, decreasing at an unknown rate with the dis-

tance, then its elevation at a mile from the axis of the canal must be greater than zero by some unknown amount—possibly 10 or 20 feet. It is clear, therefore, that the assumption that at this distance the elevation of the profile is zero is in error, and perhaps widely so. Again, however, the error is on the conservative side, and all points on the actual profile must be higher than those given on the basis of this assumption, and the true distance of approximate coincidence correspondingly nearer.

Our assumptions have therefore all been made on the conservative side, so that the elevations of the profile shown in Figure 47 are lower and the distance x_1 is greater than would be the case for the actual profile. The present values are, therefore, extreme ones and are intended to establish a limit to the effects to be expected.

A drawdown less than 5 feet at 10 miles and 2 feet at 15 miles is of negligible importance in its effect upon local wells and water supply, because at these distances the depth to salt water would still be 1,600–2,000 feet below sea-level.

Hence, the estimate made by Paige and his colleagues that the zone of appreciable lowering of the water table would not extend farther than about 10 or 15 miles from the canal is entirely confirmed by the present analysis and appears to be a conservative estimate. The misgivings of Paige's critics, one of whom (Brown) predicted that water-table slopes of 1–2 feet per mile with a water table only slightly above sea-level over a zone 20–40 miles wide would result, appear, so far as this problem is concerned, to be entirely unfounded.

CONCLUSION

While the analytical theory of ground-water motion has made great progress during the last fifty years toward becoming a branch of exact physical science, we have found that progress has been continuously impeded by certain persistent fundamental misconceptions regarding the potential function governing ground-water motion. It has been our attempt here to re-examine the fundamentals of this subject from first principles and to establish it upon a basis more in conformity with the physical principles governing the motion of terrestrial matter—the principle of the conservation of

matter and the laws of thermodynamics—than has been the case with the earlier treatments.

In the present paper the effort has been directed primarily at deriving fundamental relationships of interest and importance when dealing with problems of ground-water hydrology. In doing this, advantage has been taken of the close analogy between many aspects of ground-water theory and electrical theory, so that the relationships established are, as nearly as possible, expressed in a form already familiar to students of electricity. Thus Darcy's law, as here established, is strictly analogous to Ohm's law in electricity. Fluid potential is analogous to electrical potential; the flow vector $\mathbf{q}$ is analogous to the electrical current vector $\mathbf{i}$; the specific fluid conductivity is analogous to specific electrical conductivity; and the tangent law of refraction is common to both fluid and electrical flow. By means of these analogies treatises of electricity become among our most authoritative texts upon ground-water motion and are commended as such to students of this subject. On the other hand, multifluid problems have no counterpart in electricity and so have been given special attention here.

In the development of the present theory every effort has been made to satisfy a twofold objective: to so express the results obtained that they may easily be employed for the attainment of quick, graphical, approximate solutions of ground-water problems; and at the same time to formulate the basic equations in such a manner as to make them readily adaptable to the more precise analytical treatments of two- and three-dimensional scaler and vector fields.

For most ground-water problems rapid graphical solutions are possible which will give results of the desired accuracy. These involve the drawing of the flow fields in one or more principal vertical cross sections in conformity with the geometry and permeability of the medium, and the known boundary conditions. For this purpose, rigid observance of a small number of fundamental rules will prevent the making of serious blunders. Among the more important restrictions to be observed are these:

1. At points where the velocity is not zero, one and only one flowline can pass through the same point at the same time.

2. Ground-water flow is solenoidal, and the discharge along any stream tube is constant.

3. A stream tube cannot converge to zero and can only terminate upon permeable boundaries of a field of flow or else within the field by having the velocity approach zero as the cross-sectional area of the tube becomes unlimitedly large.

4. The normal component of the flow vector $\mathbf{q}$ on both sides of all surfaces is the same.

5. The flow vector $\mathbf{q}$ at every point in an isotropic permeable medium is given in both direction and magnitude by

$$\mathbf{q} = -\sigma \, grad \, \Phi .$$

The flowlines are everywhere normal to the equipotential surfaces, and the intensity of the flow increases as the distance between equidifferent equipotential surfaces decreases.

6. No two equipotential surfaces of different potentials can intersect.

7. No equipotential surface can close completely upon itself.

8. No equipotential surface can terminate except upon a boundary of the field of flow.

9. The tangential components of the potential gradient on opposite sides of any permeable surface are the same.

10. When ground water flows across a plane interface between rocks of different permeabilities, the flowlines and equipotential surfaces refract by the tangent law.

11. A static or slowly moving body of water occupying a void or basin is at constant potential.

12. The flowlines terminate perpendicularly upon the permeable surfaces of all equipotential regions.

13. Equipotential surfaces terminate perpendicularly upon all impermeable boundaries of a field of flow.

14. When two fields of flow are superposed, the resultant flow vector at each point is the vector sum of the vectors of the component fields, and the resultant potential field is the algebraic sum of the component potentials.

15. When fresh water coexists with bodies of static air and salt

water, if the fresh water is static the interfaces are horizontal, and the sequence of the fluids in the upward direction is in the order of decreasing density.

16. If the fresh water flows, the interfaces will both tilt toward the fresh-water layer in such a manner as to decrease its area of cross section in the direction of the flow.

17. Equidifferent fresh-water equipotential surfaces refract at the interfaces with static bodies of air and salt water into equally spaced horizontal surfaces, the spacing in salt water being $\rho_2/(\rho_3 - \rho_2)$ times the spacing in air, where ρ_3 and ρ_2 are the densities of salt and fresh water, respectively.

ACKNOWLEDGMENTS.—The present study is, in many respects, a co-operative enterprise, and the author is deeply grateful to all of those who in one way or another over a period of years have contributed to it. The principal indebtedness, however, is to those who have assisted directly in its production. Among these should be mentioned particularly: Carl Eckart, of the Department of Physics of the University of Chicago, who made a useful criticism of an earlier treatment of two-fluid potentials and who later read the finished manuscript and suggested an important revision; C. H. Dix, mathematical physicist of the Socony Oil Company, who read critically the first quarter of the manuscript; Bernard D. Holbrook, mathematical physicist of the Bell Telephone Laboratories, who painstakingly edited the entire theoretical development contained in the paper; Fritz A. Weitzel, architect, who made the drawings for the figures; Sidney Paige, of the United States Army Corps of Engineers, who kindly provided data pertaining to the Florida ship canal; Oscar E. Meinzer and C. E. Jacob of the Ground Water Division of the United States Geological Survey, who provided useful information pertaining to the coefficient of permeability used by the Ground Water Division; and volunteer editorial and stenographic assistants, who modestly insist upon remaining anonymous.

VOLUME XLVIII NUMBER 8, PART II

THE
JOURNAL OF GEOLOGY

November-December 1940

MAX MEADOWS FAULT BRECCIA[1]

BYRON N. COOPER
University of Wichita

JOHN C. HAFF[2]
Colorado School of Mines

ABSTRACT

The fault breccia along the Max Meadows overthrust in the Draper Mountain area, Virginia, consists of three cataclastic zones: an upper autoclastic breccia composed of large, angular blocks and smaller tabular fragments of quartz sericite phyllite; a lower autoclastic zone consisting of angular blocks and fractured masses of Elbrook limestone and dolomite; and an intervening zone of crush conglomerate composed chiefly of rounded fragments of limestone, dolomite, and phyllite. Contacts of the upper and lower breccias with contiguous wall rocks are gradational. Crush conglomerate, which grades into the autoclastic breccias above and below, was formed by mingling, crushing, and rolling out of parts of the autoclastic breccias.

The crush-conglomerate zone contains fragments of several types of rocks which are not found in the adjacent autoclastic breccias. These must have been acquired down the original dip of the Max Meadows fault surface where it cuts Lower Cambrian and pre-Cambrian rocks. Parts of the Max Meadows fault breccia have been squeezed into fractures of the rocks on both sides of the fault zone and occur in the form of dikes of crush conglomerate.

Of the several modes of origin discussed, only strictly tectonic processes could have produced the breccias and crush conglomerate occurring along or near the Max Meadows fault in this area.

INTRODUCTION

LOCATION OF AREA

The Draper Mountain area, a polygonal tract of approximately 100 square miles, is situated in west-central Pulaski County and

[1] Published with the permission of the state geologist of Virginia.

[2] Author of the petrographic descriptions.

adjacent portions of Wythe County, Virginia. It lies in the southern Appalachian Valley and Ridge province, approximately 10 miles northwest of the Blue Ridge plateau and midway between Roanoke, Virginia, and Bristol, Virginia-Tennessee.

FIG. 1.—Index map showing location of Draper Mountain area

STRATIGRAPHY

The formations of this area have a total thickness of about 13,000 feet, and they represent a rather full record of sedimentation from Middle Cambrian to Middle Mississippian time. Part of the Rome formation was dynamically metamorphosed during the Appalachian revolution, and the phyllite produced is considered to be of late Paleozoic age. It and the Max Meadows fault breccia, which was produced about the same time, are not shown in Figure 2.

STRUCTURE

The Rome and Elbrook formations have been thrust over the other, younger formations along two closely spaced low-angle overthrusts which are nearly parallel. The lower and older of these faults is the Pulaski overthrust[3] and the upper one is the Max Mead-

[3] M. R. Campbell, "The Valley Coal Fields of Virginia," *Va. Geol. Surv. Bull. 25* (1925), pp. 76–96; B. N. Cooper, "Geology of the Draper Mountain Area, Virginia," *Va. Geol. Surv. Bull. 55* (1939), pp. 56–63.

FIG. 2.—Bedrock formations exposed in the area shown in Plate I

ows overthrust.[4] The strata overridden by the Pulaski and Max Meadows overthrust sheets seem to have remained essentially undeformed during overthrusting. Later, however, they were folded and faulted, as were the thrust sheets above them. During this later deformation, the Pulaski and Max Meadows fault surfaces were folded and overturned as though they were bedding planes.

Where erosion has penetrated the thrust sheets windows have resulted. At one time the central portion of the Draper Mountain area was a true window, but since then erosion has breached the surrounding fringe of overthrust rocks northwest of Draper Mountain and Caseknife Ridge (see Pl. I).

The interval between the Max Meadows and Pulaski faults is not more than 1,000 feet in this area. Hence, relatively slight irregularities of their fault surfaces cause the overthrusts to intersect in places. Where the faults intersect, the Max Meadows overthrust sheet rests upon strata which elsewhere compose the mass overridden by the Pulaski thrust sheet.

ROCKS OF THE PULASKI THRUST SHEET

The Pulaski overthrust mass, which lies directly upon the overridden strata of this area, is composed of crumpled and faulted beds of the Elbrook formation of Middle and late Cambrian age. It is not known whether the Elbrook beds comprising the Pulaski thrust sheet represent the full thickness of the formation as elsewhere seen in the Appalachian Valley, because in the Draper Mountain area the Elbrook is bordered above and below respectively by the Max Meadows and Pulaski faults. At least 1,700–1,800 feet of the formation are present. A sequence of about 500 feet of beds consists almost wholly of dark bluish-gray limestone containing discontinuous clay partings which produce a ribbon effect on weathered surfaces. These beds are succeeded by 1,200–1,300 feet of thin-bedded ash-gray dolomitic limestones and platy calcareous shales.

ROCKS OF THE MAX MEADOWS THRUST SHEET

The Max Meadows thrust sheet, which in most places lies upon the Pulaski thrust sheet, contains only rocks of the Lower and Middle Cambrian Rome formation. The Rome is a very hetero-

[4] Cooper, *op. cit.*, pp. 58–63.

geneous formation composed primarily of maroon-drab noncalcareous shale, sericitic green shale, and black ferruginous dolomite. Smaller amounts of ocherous-yellow shale, brown micaceous siltstone, and salmon-pink limestone are also present.

At the base of the Max Meadows overthrust sheet the Rome has been dynamically metamorphosed to phyllite. This metamorphic zone appears to have been formed by overthrusting, for it is developed wholly with respect to the Max Meadows fault which it parallels.

DISTRIBUTION OF FAULT BRECCIA

In the Draper Mountain area, fault breccia,[5] part of which has been modified into crush conglomerate, occurs along or near the Max Meadows fault. Locations of a number of representative occurrences are shown on Plate I. In addition to detailed studies of the breccia in the Draper Mountain area, it has been traced continuously for 25 miles from $1\frac{1}{4}$ miles east of Wytheville, Wythe County, to Snowville in eastern Pulaski County (see Fig. 1). Similar breccia occurs also at several places somewhat distant from the Wytheville–Max Meadows–Snowville belt of outcrop. That in the east bluff of the New River gorge near Peppers Ferry, in Montgomery County, has been described by Campbell.[6] The full geographic extent of the breccia has not yet been ascertained. So far as known, no similar breccia occurs along the Pulaski overthrust.

LITHOLOGY

The fault breccia separating the sole and tread[7] of the Max Meadows overthrust consists of three cataclastic zones, each of which possesses distinctive textures and structures and different assemblages of rock fragments. These zones are designated phyllite breccia, limestone breccia, and crush conglomerate.

[5] *Fault breccia* is herein used in a broad sense. Some of the tectonic material so designated is not strictly breccia.

[6] *Op. cit.*, pp. 17–19; Pl. VIII-A.

[7] Use of the terms *hanging wall* and *foot wall*, respectively, for these surfaces is inadvisable, because the Max Meadows fault surface has been so folded and overturned that its hanging wall is locally made by the top of the overridden block. *Sole* refers to the lower surface of the overthrust block and *tread* to the opposing upper face of the overridden block.

PLATE I

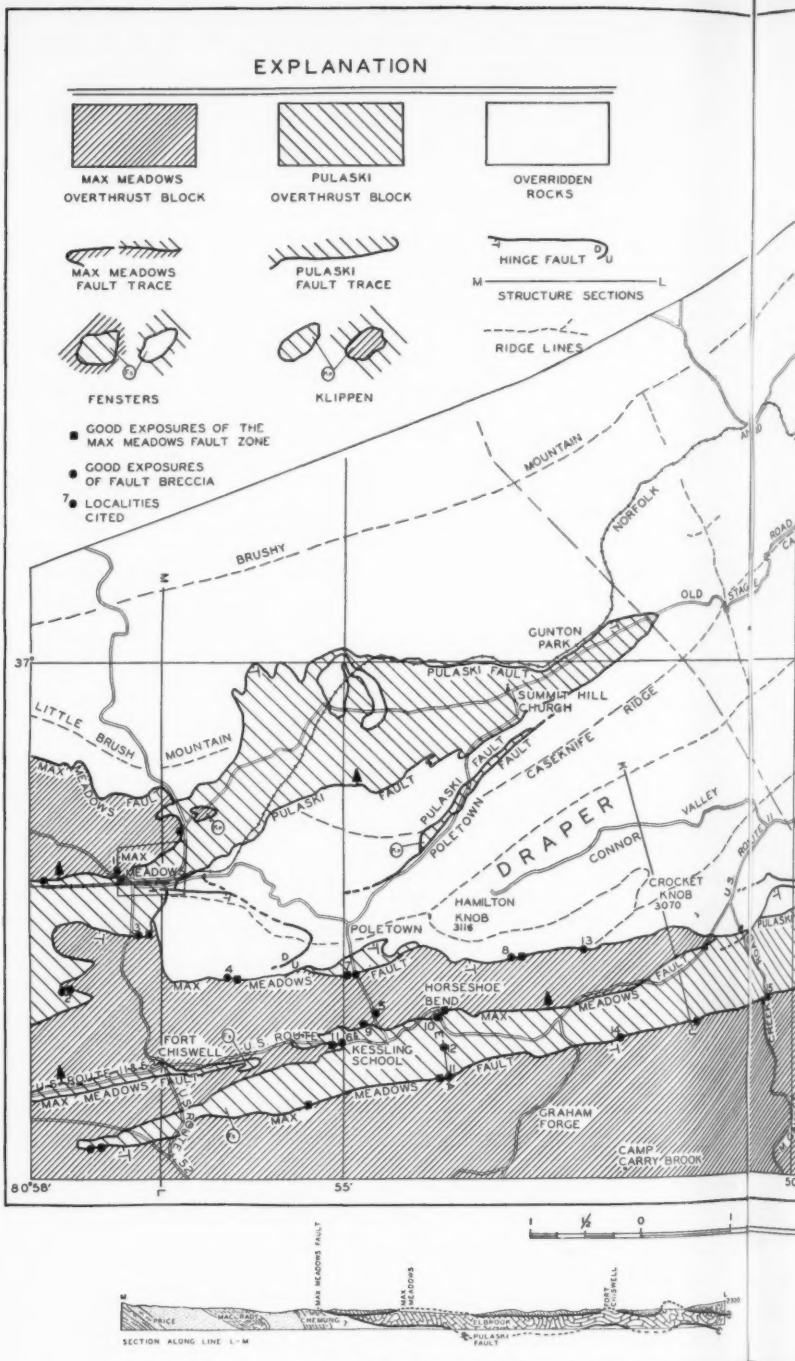

AREAL RELATIONS OF THRUST SHEETS AND ASSOCIATED TECTONI

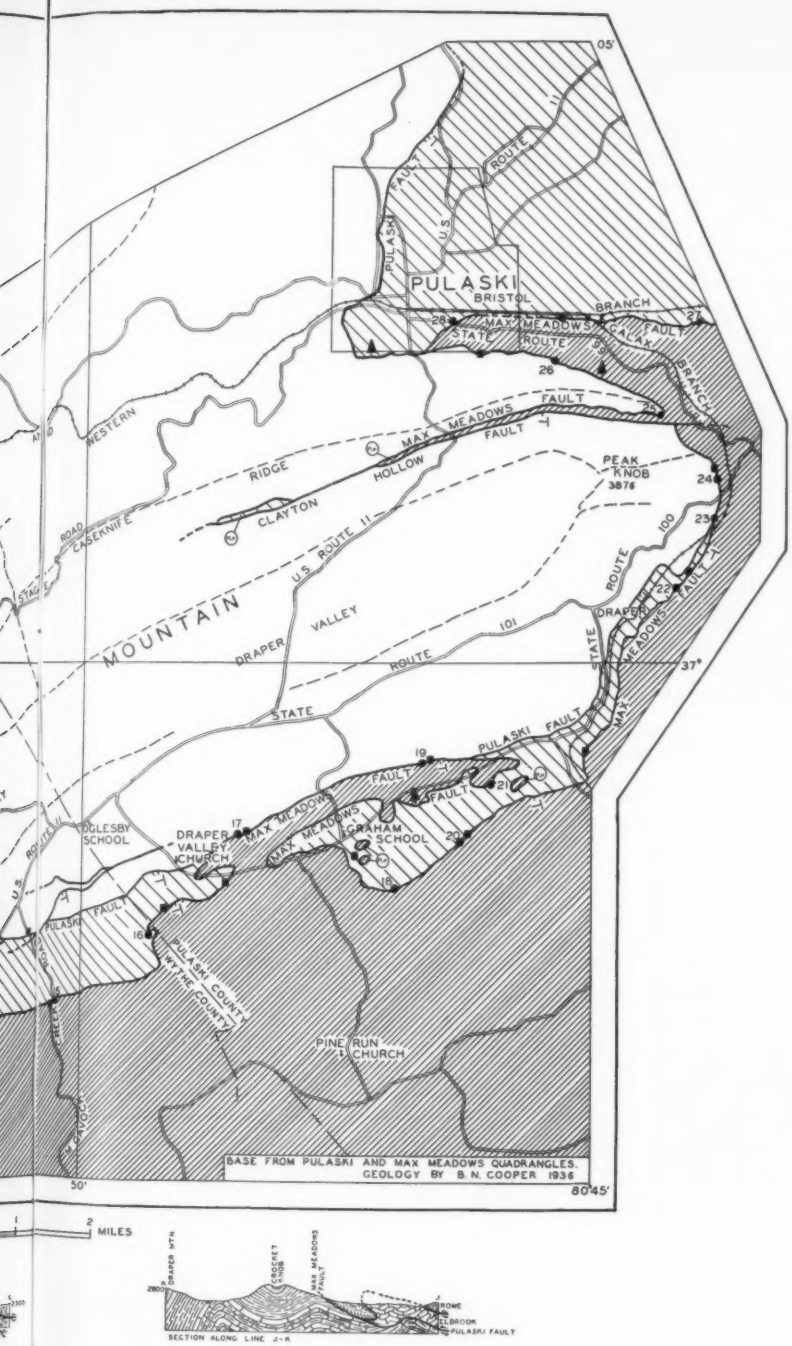

...IATED TECTONIC ROCKS OF THE DRAPER MOUNTAIN AREA, VIRGINIA

PHYLLITE BRECCIA

The uppermost zone of the fault breccia immediately underlies the Rome phyllite which forms the base of the Max Meadows overthrust mass. It is an autoclastic breccia composed of large, angular blocks and smaller slivery fragments of Rome phyllite. Foliation in many of the fragments has been intricately contorted and macerated, and all of the pieces have slickensided, wavy surfaces. Foliation of the Rome phyllite appears to have controlled the development of the characteristically tabular shapes of the slivers. The sutures between the smaller fragments are outlined by films of yellowish clay, granular carbonates, and drusy quartz. Powdery gouge composed of sericite, calcite, chlorite, dolomite, and quartz fills the interstices between the larger blocks of phyllite. Although pieces up to 3 feet in diameter are common near the sole of the fault, most of the fragments are less than 1 inch in greatest diameter. Their size decreases progressively downward from the sole of the overthrust mass. Phyllite breccia is difficult to identify except in fresh exposures. Where weathered, its rusty-brown color masks the texture and structure. Moreover, blocks of the breccia disintegrate rapidly into a rubble similar to that formed from Rome phyllite in the contiguous overthrust sheet.

LIMESTONE BRECCIA

The lowermost zone of fault breccia, which lies directly upon the tread of the Max Meadows fault, is an autoclastic aggregate consisting of large, irregular masses of thin-bedded limestone, angular blocks of dolomitic limestone, and small chips of ash-gray calcareous shale. All of the limestone fragments are either dark bluish-gray or ash gray. Both the irregular frayed masses of limestone and the dolomitic limestone blocks appear to have been displaced only slightly from their original positions in the tread of the overridden Elbrook. Upward from the base of this zone the size of the rock fragments decreases and they become less angular. The smaller, tabular pieces have been formed by the fracturing and partial dismemberment of larger masses of Elbrook limestone and their shortest diameters represent the thickness of the beds from which they were derived. The interstices between the disarranged blocks of this brec-

cia are partly filled with mealy calcareous gouge. That this breccia was derived from the underlying beds is shown by its transitional contacts with the Elbrook and by the lithologic identity of the fragments to beds of that formation. This breccia was nowhere found in an indurated condition. It weathers to a rubble which cannot be easily distinguished from that of the underlying Elbrook tread rocks.

FIG. 3.—Lower limestone breccia along state highway 100, 6 miles east of Pulaski and 1.8 miles beyond the eastern edge of the area shown in Plate I.

CRUSH CONGLOMERATE

The middle zone of the fault breccia is the thickest. It is composed chiefly of nearly equidimensional, rounded fragments of limestone, dolomite, and phyllite, most of which are less than 3 inches in diameter. Phyllite fragments are relatively small and pale green, but their abundance accounts for the characteristic greenish-gray color of this zone. Shapes of the larger fragments are distinctly different from those of water-worn pebbles. All show sharp corners and rounded sides. Most of the limestone fragments were derived from the Elbrook, but those composed of coarse-grained saccharoidal dolomite and limestone probably came from the Lower Cambrian Shady for-

mation which normally underlies the Rome but which does not crop out in the area shown on Plate I. The material surrounding the larger fragments consists of minute rounded particles of limestone, dolomite, and phyllite. These particles are knit together by interlocking euhedral dolomite and quartz. Numerous vugs are partially filled with calcite, dolomite, and quartz. Secondary pyrite locally com-

FIG. 4.—Crush conglomerate along Reed Creek near Horseshoe Bend. (Photograph by Arthur Bevan.)

prises as much as 10 per cent of the crush conglomerate, and traces of galena, straw-yellow fluorite, sphalerite, and barite are rarely present. The middle part of the crush-conglomerate zone is generally finer grained than the marginal portions. Although the distinctly conglomeratic aspect of the crush conglomerate is a sharp contrast to the autoclastic breccias above and below, margins of the pebbly zone are texturally gradational with the contiguous breccias.

Cavities in leached portions of the crush conglomerate are partially filled with the insoluble residues of calcareous fragments. Weathered surfaces are deeply pitted and stained rusty brown.

THICKNESS

Thicknesses of the Max Meadows fault breccia are difficult to measure because of the lithologic identity of fragments of the lower and upper zones to the respectively contiguous Elbrook and Rome and because of the transitional contacts of the fault breccia with these formations. In the few places where the three zones are rather fully exposed their combined thicknesses exceed 75 feet. Thicknesses of fault breccia in a number of representative localities are shown in Table 1.

FIELD RELATIONS

FAULT-ZONE OCCURRENCES

Fault breccia occurring along the Max Meadows overthrust is overlain by the Rome formation. The lower portion of the overthrust Rome was metamorphosed to phyllite by frictional forces active during overthrusting. These phyllitic sole rocks grade downward into the uppermost zone of breccia, which is composed wholly of phyllite fragments. From the top of this zone downward, toward the middle zone of crush conglomerate, there is a progressive decrease in size of fragments and a corresponding increase in amount of their rotation and dismemberment. These relationships show that the phyllite breccia was formed by the incipient dismemberment of masses of phyllite dislodged from the sole of the Max Meadows overthrust sheet.

In most places in the Draper Mountain area, the fault breccia is underlain by folded, fractured Elbrook beds which comprise the thin Pulaski overthrust sheet. The lowermost zone of fault breccia grades into the underlying Elbrook, and near their contact large masses of limestone appear to have been displaced but slightly from their original positions in the underlying Pulaski thrust sheet. Upward from the tread of the Max Meadows fault, toward the zone of crush conglomerate, both the size and the angularity of fragments comprising the limestone breccia decrease. This indicates that fragments near the crush-conglomerate zone have been subjected to more rotation and cataclastic abrasion than those just above the base of the limestone breccia.

Locally, where the Pulaski and Max Meadows faults inter-

sect, the tread of the latter fault is made by formations other than the Elbrook—formations which both thrust sheets overrode. In these places the lower limestone breccia is absent and crush conglomerate, which usually occurs in the middle of the fault breccia, lies directly upon the underlying rocks. Such contacts are sharply defined, in contrast to gradational contacts of limestone breccia with the Elbrook. These relationships are well shown in exposures

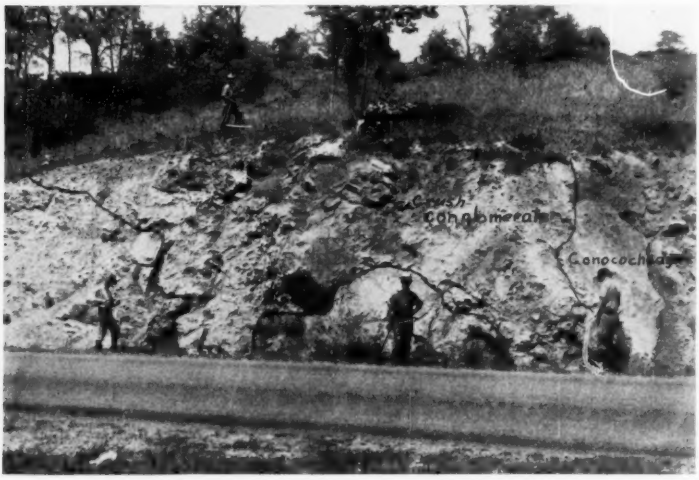

FIG. 5.—Crush conglomerate resting on Conococheague limestone, 4 miles west of Fort Chiswell, along U.S. Route 11. (Photograph by Arthur Bevan.)

along U.S. Route 11, 4 miles west of Fort Chiswell, where crush conglomerate lies in contact with the Conococheague formation.[8] Since the lower limestone breccia is present only where the Elbrook forms the tread rocks of the Max Meadows fault, relatively few fragments in the limestone breccia could have come from any other formation.

Textural and structural transitions between the middle zone and bordering autoclastic breccias suggest that the fragments in the crush conglomerate came from the breccia zones above and below. Shapes of the fragments in crush conglomerate are indicative of cata-

[8] This place is about 3 miles beyond the western border of the Draper Mountain area.

clastic abrasion rather than stream abrasion. These relationships suggest that the crush conglomerate was formed by continued action of the tectonic processes which made the bordering autoclastic zones.

CONGLOMERATE DIKES

Crush conglomerate, identical to that in the middle of the Max Meadows fault zone, occurs locally in the form of dikelike masses within the Rome and Elbrook formations. These masses have sharply defined contacts and show cross-cutting "intrusive" relations to the enclosing beds. Several of these peculiar masses are exposed

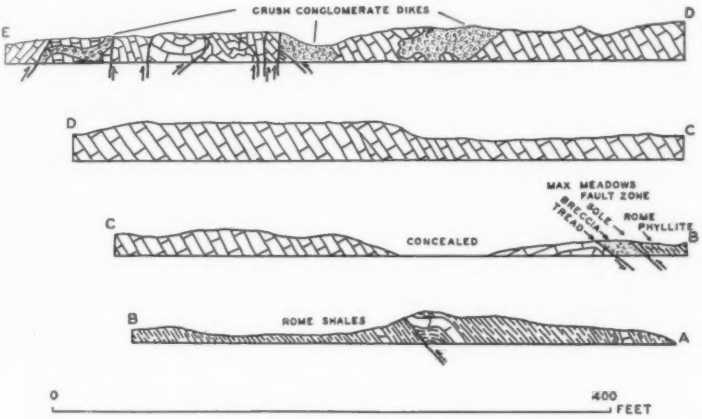

FIG. 6.—Cross section showing breccia along Max Meadows fault and conglomerate dikes in Elbrook, south of the Horseshoe Bend of Reed Creek.

along the Poletown road (Pl. I, locality 5). Marginal autoclastic zones, such as flank the crush conglomerate in the Max Meadows fault zone, are absent. Numerous apophyses of the conglomerate dikes are wedged between shale laminae, and some of the limestone pebbles have been deeply impressed into the shale wall rocks.

South of the Horseshoe Bend of Reed Creek (Pl. I, locality 12), three conglomerate dikes cut across folded and faulted Elbrook beds. An S-shaped mass, partly shown in Figure 7, is bounded on the north and south by minor faults. The wall rocks bordering the horizontal part of the dike are deeply grooved and slickensided, but the beds

above and below the crush conglomerate have not been displaced laterally. Markings on the wall rocks trend east and west, whereas direction of movement along major thrusts of this area has been to the north-northwest. The trend of the markings probably indicates direction of emplacement of crush conglomerate. Another dike of crush conglomerate, exposed 100 feet farther south, has tapered lateral extensions which are wedged between limestone layers. The

FIG. 7.—S-shaped conglomerate dike in Elbrook, south of the Horseshoe Bend of Reed Creek. (Photograph by Arthur Bevan.)

wall rocks of a third dike exposed still farther south are marked by a meshwork of intersecting grooves and striae, but this dike is not bordered by faults.

Only a small amount of the material in the conglomerate dikes appears to have been derived from the wall rocks. Moreover, these masses contain phyllite fragments and pieces of Shady dolomite which could not have come from the wall rocks. The intrusive relations of the crush-conglomerate dikes to the enclosing Elbrook and Rome, striations and slickensides of the wall rocks, and the extremely granulated margins of parts of the dikes indicate that the crush

conglomerate was forcibly injected into these formations. The lithologic identity of crush conglomerate in the dikes to that in the Max Meadows fault zone strongly suggests direct connections between fault-zone occurrences of crush conglomerate and the conglomerate dikes. Exposures in the northeast turn of the Horseshoe Bend of Reed Creek confirm this suggestion, for a dike of crush conglomerate

FIG. 8.—Lateral extension of crush-conglomerate dike wedged in a bedding joint in the Elbrook, south of Horseshoe Bend. Margins of the wedge are very fine grained and show schistose partings parallel to the sides of the wedge. (Photograph by Arthur Bevan.)

in the Elbrook merges with fault breccia occurring along the Max Meadows overthrust-fault surface.[9] It is believed that the material in the dikes came from the fault zone and that fault breccia was squeezed into pre-existing fractures in the Rome and Elbrook. The roundness of the larger fragments and the fine texture of margins of the dikes are results of the mutual abrasion of fragments and of their attrition with wall rocks during transposition of the material from the fault zone.

[9] In this locality the Elbrook overlies the Rome along the Max Meadows fault, because the fault surface has been overturned by folding.

TYPICAL OCCURRENCES

All of the fundamental relations of the Max Meadows fault breccia are rarely seen in a single exposure. All three zones are exposed along the east bank of Cove Creek about 3 miles west of Max Meadows (Table 1, locality A). The best exposure of phyllite breccia and one of the best of the crush-conglomerate zone is along the McGavock Creek road, 1 mile south of U.S. Route 11 (Pl. I, locality 15). Probably the best exposure of crush conglomerate is along U.S.

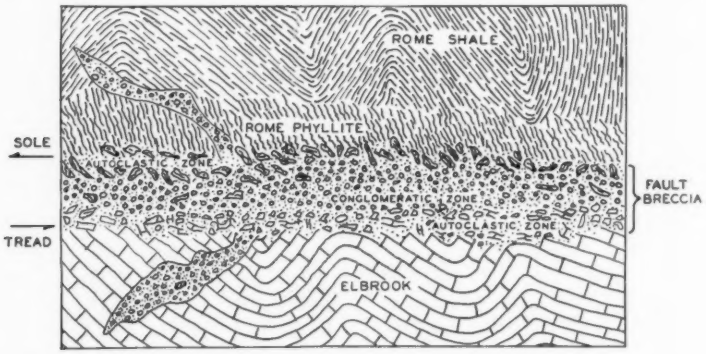

FIG. 9.—Structural relations of breccias, crush conglomerate, and conglomerate dikes along the Max Meadows fault.

Route 11, 4 miles west of Fort Chiswell (Table 1, locality B). The lower limestone breccia is well exposed along State Highway 100, 6 miles east of Pulaski and 1.8 miles beyond the eastern edge of the Draper Mountain area (Table 1, locality C).

PETROGRAPHIC DESCRIPTIONS

ROME PHYLLITE

Microscopic study indicates that the essential minerals of this finely phyllitic rock are quartz, acid plagioclase, sericite, muscovite, chlorite, and biotite. Shreds of chlorite, minute anhedra of apatite and green tourmaline, magnetite, rutile needles, epidote, and iron oxides which contribute the characteristic red color of the rock are also present. The quartz grains are uniformly small (0.05 mm. in

TABLE 1

LIST OF TYPICAL OCCURRENCES* OF THE MAX MEADOWS FAULT BRECCIA

Locality	Type of Occurrence		Thickness (Feet)	Autoclastic Zones		Conglomerate Zone	Contiguous Formations
	Fault Zone	Dike		Lower	Upper		
A	x		100	x	x	x	Lower Elbrook Rome phyllite
B	x		5–15			x	Conococheague Rome phyllite
C	x		75	x			Upper Elbrook Rome phyllite
1	x		10		x	x	Lower Elbrook Rome phyllite
2	x		5–20		x	x	Upper Elbrook Rome phyllite
3	x		60	x	x	x	Lower Elbrook Rome dolomite
4	x		8			x	Chambersburg Rome phyllite
5		x	5–12			x	Rome shale
6	x		5–15	x		x	Lower Elbrook Rome dolomite
7	x		5–25	x		x	Upper Elbrook Rome dolomite
8	x		15		x		Clinch ss. Rome phyllite
9	x		5–15	x		x	Lower Elbrook Rome phyllite
10	x	x	5–25		x	x	Upper Elbrook Rome phyllite
11	x		20		x	x	Lower Elbrook Rome phyllite
12		x	2–20			x	Lower Elbrook
13	x		30	x		x	Martinsburg sh. Rome phyllite
14	x		10–15	x	x		Lower Elbrook Rome phyllite
15	x		125	x	x	x	Lower Elbrook Rome phyllite
16	x		30		x	x	Lower Elbrook Rome phyllite
17	x		25			x	Conococheague Rome phyllite
18	x		5–10		x		Lower Elbrook Rome phyllite
19	x		5–25			x	Conococheague Rome phyllite
20	x		5–10			x	Lower Elbrook Rome phyllite

* Location of numbered occurrences shown on Plate I.

TABLE 1—*Continued*

Locality	Type of Occurrence		Thickness (Feet)	Autoclastic Zones		Conglomerate Zone	Contiguous Formations
	Fault Zone	Dike		Lower	Upper		
21.....	x	.....	3–12	.....	x	x	Lower Elbrook Rome phyllite
22.....	x	.....	10	.....	x	x	Lower Elbrook Rome phyllite
23.....	x	.....	15	.....	x	.....	Elbrook ls. Rome phyllite
24.....	x	.....	20	.....	x	x	Clinch ss. Rome phyllite
25.....	x	.....	40	.....	.....	x	Millboro sh. Rome phyllite
26.....	x	.....	10	.....	x	.....	Price ss. Rome phyllite
27.....	x	.....	30	x	.....	x	Upper Elbrook Rome phyllite
28.....	x	.....	15	.....	x	.....	Upper Elbrook Rome phyllite

diameter) and have sharply angular outlines. Cataclastic granulation of originally larger grains is not evident. Feldspar grains are anhedral and but slightly altered. Some of the larger feldspar grains show anomalous pseudo-microcline grid structure, but most of the feldspar is albite ($Ab_{90}An_{10}$). Most of the quartz and possibly some of the feldspar are of clastic origin, but the major part of the albite appears to have been introduced. The latter occurs chiefly in coarse-grained equigranular aggregates of irregular outline but some of it is finely disseminated in the rock. Veinlets and blebs of albite cut the foliation, but most of the feldspar has been introduced lit-par-lit. Fine-grained micaceous foliae alternate with thicker, more abundant foliae composed of equigranular quartz and feldspar. Bent mica flakes, undulose extinction of the quartz, and the contorted condition of the foliae show that the rock is definitely metamorphosed as compared with Rome shale occurring higher in the Max Meadows overthrust sheet. Fracture-cleavage planes cut the foliage nearly at right angles and produce minute corrugations of the foliation. Locally small hornblende veinlets line the fracture-cleavage surfaces.

PHYLLITE BRECCIA

In thin section the matrix of this breccia consists of equigranular carbonate and quartz (0.25 mm. in diameter). The only rock fragments present are shreds and slivers of quartz-sericite phyllite which is identical to that described above. Crushing appears to have been incipient, and only slight disarrangement and partial replacement of the phyllite slivers by carbonates is apparent. Flaser-like augen

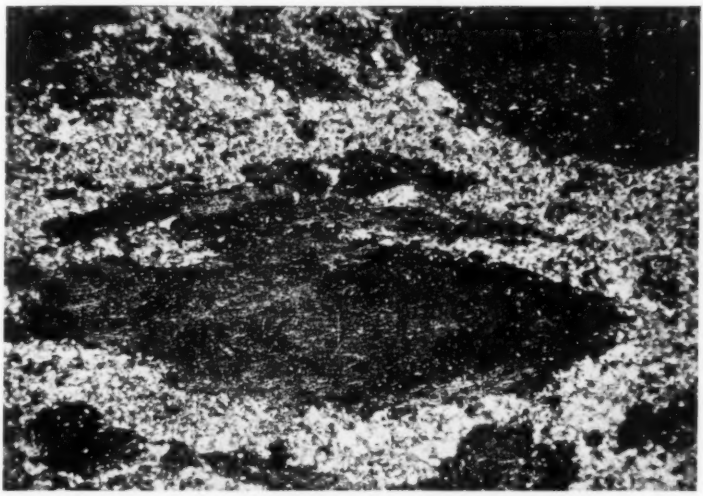

FIG. 10.—Photomicrograph of phyllite breccia. Shreds of phyllite are partially replaced by calcite and dolomite, but some continuity of structure persists from one sliver to another. Crossed nicols, ×16. (Photomicrograph by George A. Rev.)

and elongate shreds of phyllite are uniformly aligned within the limits of the thin sections. Such alignment suggests that a moderate degree of structural continuity has persisted despite obvious brecciation and partial replacement. Specimens from lower portions of the phyllite breccia show more effects of crushing. Those collected near the base of the upper zone and close to crush conglomerate show an admixture of phyllite, dolomite, and limestone fragments, and all vestiges of continuity between phyllite slivers have been obliterated.

CRUSH CONGLOMERATE

The most abundant minerals of this zone are dolomite, calcite, and quartz. Rather coarsely crystalline dolomite and subordinate quartz constitute the matrix, and both calcite and quartz occur as the essential minerals of individual fragments. Minute cubes and anhedra of limonitized pyrite are disseminated throughout the thin sections examined. Albitic plagioclase, sericitized orthoclase, chlorite, biotite, sericite, apatite, magnetite, limonite, rutile, and prisms of green tourmaline also occur but are restricted to phyllite and schist fragments.

The structure of the specimens examined in thin section is cataclastic. Most of the fragments are conspicuously rounded, regardless of their original structure. Pieces of limestone and dolomite are most abundant. Those of quartzite, phyllite, and schist, though common, are collectively subordinate.

The matrix consists predominantly of coarse-grained (0.5 mm.) dolomite rhombs of strong euhedral tendency. The dolomite crystals generally show several well-developed crystal faces and have strong cleavage and coarse twinning lamellae. Disseminated in the dolomite are small (0.1–0.2 mm.) rounded quartz grains. These grains contain rhomb-shaped dolomite inclusions and flakes of green chlorite.

Fragments detached from sedimentary and metamorphic rocks are present in the crush conglomerate. The lithologic identities of most of the fragments are still preserved, and hence their source can be determined. Fragments of the Rome, Elbrook, Shady, and Erwin (Lower Cambrian quartzite) have been detected. In the following description, the rock types represented are discussed in the order of their relative abundance.

Fragments of sedimentary rocks are of either limestone or dolomite and vary from exceedingly fine-grained to coarse-grained types. All are uniformly dense, unfossiliferous, and consist almost wholly of equigranular carbonates and a few crystals of pyrite. Traces of original stratification are rare and confined to coarse-grained pieces. In plane-polarized light the calcareous fragments are turbid. For this reason and because of their fine texture, they stand out in bold relief in the coarser-grained matrix. Crenulated outlines of some fragments

are suggestive of replacement, whereas those of other fragments are the result of cataclastic abrasion.

Metamorphic rocks are represented by pieces of several varieties, but those of fine-grained, highly foliated sericite phyllite are the most abundant. In addition to sericite, these fragments also contain epidote, magnetite, leucoxene, specular hematite, rutile needles, dolomite and calcite, and shreds of chlorite. The pronounced lepidoblastic structure of these phyllite fragments is remarkably uniform.

Quartzite fragments are fine grained (0.1 mm.) and have a finely granoblastic structure. In addition to quartz, minute shreds of sericite and chlorite, granules of epidote, magnetite, and a few grains of acid plagioclase are usually present. Many such fragments are partially carbonated and some of the feldspar and mica probably destroyed. Where carbonatization is more advanced, quartzite fragments are difficult to distinguish from calcareous ones containing siliceous impurities.

Fragments of pre-Cambrian(?) biotite schist consist of quartz, altered feldspar, and biotite with subordinate sericite, epidote, magnetite, pyrite, rutile, and carbonate. The highly altered feldspar is sensibly isotropic, apparently untwinned, but still shows traces of pinacoidal cleavage. Accurate determination of its composition is impossible, although low refringence suggests potash feldspar or an acid plagioclase. The biotite flakes are pale brown with bleached margins and strongly pleochroic centers. Schist fragments are blotched, due to the abundance of fine-grained secondary epidote and magnetite granules.

In one variety of schist fragment the micaceous foliae have been replaced by carbonates, whereas more quartzose foliae have not been changed. In fragments which have been greatly carbonated the present structure is more massive than schistose. However, even these fragments retain a streaked appearance which reflects the original foliation. In fragments which have been largely replaced by carbonates, small grains (0.04 mm.) of feldspar and quartz are disseminated in the carbonates. The finer-grained micas are generally destroyed by carbonatization, but occasional blades of biotite indicate original schistose structure.

The dolomite and quartz of the matrix have slightly replaced a

number of the calcareous fragments. Some pieces have veinlets of relatively coarse-grained dolomite in continuity with the matrix. These veinlets are anastomosing, are commonly enlarged at intersections, and ramify so irregularly that their patterns cannot be ascribed to simple fracture filling. Many of the larger fragments have suffered further encroachment and are virtually dismembered. The adjacent margins of the residuals are crenulate, although original bedding can sometimes be traced across intervening veinlets. Sharply idiomorphic dolomite crystals locally penetrate calcareous fragments as wedge-shaped indentations. In places, drusy quartz deeply embays an otherwise smoothly oval phyllite fragment. These structures indicate appreciable, though slight, replacement. The smoothly rounded outlines and sharp contacts of most fragments definitely indicate that wholesale replacement has not taken place.

Continued action of the processes by which the crush conglomerate was formed has resulted in the dismemberment of almost all of the fragments and in mass recrystallization of the cataclastically comminuted grains. Such material is found in the middle of the crush-conglomerate zone. Specimens collected from the middle of the crush conglomerate at locality 11 (Pl. I) show the following characteristics. The structure is uniformly granoblastic, but traces of a pre-existing cataclastic structure of coarser fabric are present. Interlocking turbid grains of carbonates and subordinate quartz are the chief constituents. The quartz grains, which are disseminated throughout the groundmass, contain peripherally arranged chloritic inclusions like those of the matrix of less deformed crush conglomerate. The turbidity of the carbonates in these intimately crushed zones is due to minute rhomb-shaped dolomite inclusions identical in aspect to those of crush conglomerate. Blebs of limonite, usually concentrated at grain contacts, also contribute to the turbidity.

In such rocks only a few fragments have survived crushing. Attenuated remains of identifiable limestone fragments merge with the groundmass. These remnants still possess an equigranular texture but are coarser than fragments which occur in typical crush conglomerate. Although many limestone fragments have been al-

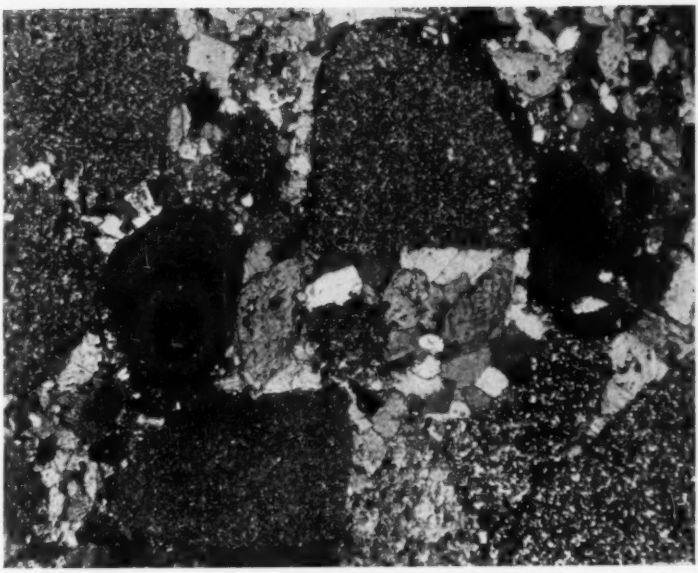

a

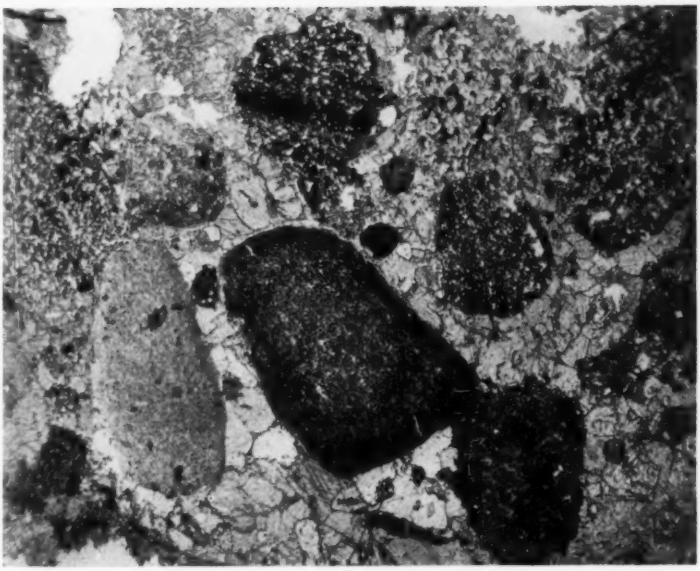

b

FIG. 11.—(*a*) Photomicrograph of crush conglomerate. The lighter, rounded fragments are fine-grained limestones. The two dark, rounded fragments are sericite phyllites. Matrix minerals are coarse-grained dolomite and quartz. Crossed nicols, ×22. (Photomicrograph by George A. Rev.) (*b*) Photomicrograph of crush conglomerate containing several rounded phyllite fragments. Some of the fragments are more quartzose than others, and they show variations in the texture of individual foliae. The matrix is coarsely crystalline dolomite. Crossed nicols, ×22. (Photomicrograph by George A. Rev.)

most completely obliterated, schist and phyllite fragments still retain their sharp contacts with the matrix.

Specimens collected from about the middle of the fault breccia exposed along the McGavock Creek road (Pl. I, locality 15) show even more advanced effects of granulation of fragments and mass recrystallization. Their matrix consists of fine-grained equigranular carbonates (largely dolomite) and coarse-grained patches of clear calcite rhombs. The only distinguishable fragments are those of sericite-quartz phyllite and modified, originally calcareous rocks.

The more micaceous foliae of the phyllite fragments have undergone most replacement by carbonates and only the quartzose foliae remain unchanged. A few of the larger phyllite relicts exhibit fracture cleavage, along which planes dolomite has been introduced. The fragmentary remnants of phyllite are frayed and ragged in outline and are conspicuously elongate. In less granulated portions of the middle zone, fragments of phyllite are nearly equidimensional.

Remains of fragments of rather pure calcareous rocks are as abundant as those of phyllite but are not nearly so conspicuous. Their texture, which is largely the result of recrystallization, is nearly the same as that of the matrix. Original structures are absent, but the recrystallized carbonates enclose minute particles of sericite, quartz, and euhedral dolomite which contributed to the turbidity of the original carbonate of the fragments.

Granulation of crush conglomerate is most advanced along margins of the crush-conglomerate dikes. Thin sections of specimens from the margin of the wedge shown in Figure 8 show the following characteristics. The rocks are granoblastic and consist of calcite and dolomite, a little quartz, and a few cubes of secondary pyrite. Quartz grains are equidimensional, have markedly crenulate margins, and are tightly knit together by dolomite. The uniformly granoblastic structure is broken by rudely lenticular wisps of finely foliated sericite-chlorite phyllite. Though these wisps are distributed throughout the carbonate-quartz mesostasis, they are similarly aligned, at least within the limits of the thin sections examined. Their distribution and alignment produce a rude foliation which is conspicuous at low magnifications. The structure and texture of the carbonate-quartz mesostasis are similar to those of recrystallized portions of crush

conglomerate. Microscopic studies support the view that the margins of the conglomerate dikes have been subjected to extreme crushing and have undergone almost complete recrystallization. The subparallel alignment of the phyllite shreds is interpreted to be a result of friction of the injected material with the adjacent wall rocks.[10]

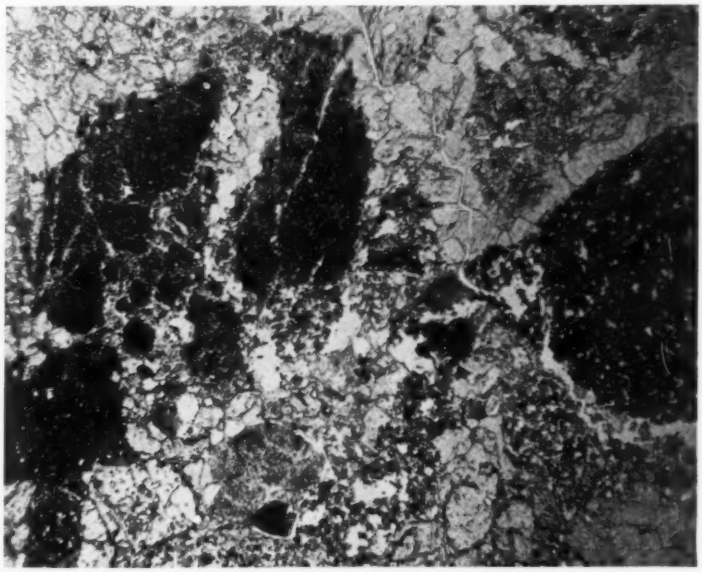

FIG. 12—Photomicrograph of crush conglomerate showing evidences of recrystallization and replacement. The limestone fragment on the left is cut by calcite veins which are co-extensive with the matrix. A corner of the limestone grain on the right has been partly obliterated by recrystallization. Crossed nicols, ×43. (Photomicrograph by George A. Rev.)

ORIGIN

CONSIDERATION OF PREVIOUS INTERPRETATIONS

Although the fault breccia in the Draper Mountain area apparently was not recognized by previous field workers, lithologically simi-

[10] Thin-section studies of the lower autoclastic zone of the Max Meadows fault breccia were not undertaken. The sizes of its fragments are so large that the texture and structure of the breccia are megascopically apparent.

lar material and material of analogous geological occurrence have been studied in other parts of the southern Appalachian Valley of Virginia.

Campbell[11] mentioned the occurrence of limestone breccia in nearby areas. He interpreted the breccia and conglomerate exposed in the east bluff of the New River gorge, near Peppers Ferry in Montgomery County, as an alluvial deposit made by tributaries of that river. The close lithologic similarity of the material exposed there to fault breccia in the Draper Mountain area makes it advisable to reconsider his interpretation. He states:

> Although the writer made no attempt to determine accurately the geographic distribution of the limestone breccia, the data at hand seem to show that, if not limited to the basin of New River, it certainly is more common there than in other parts of the district. This apparent limitation not only to the drainage basin of New River but largely to the vicinity of the river itself may have a physiographic significance, as the breccia seems to have been largely formed at the time when New River began to cut into the Blacksburg peneplain . . . . that marks the upland level about 400 feet above the river. It seems probable that in a basin which was reduced to a very perfect peneplain, the streams, both those flowing in caverns and narrow underground channels, would be more heavily charged with carbonate of lime than streams in a more rugged region, that flow swiftly into the trunk streams. Much of the water in such a basin would flow toward the trunk streams in underground channels and would enter the main streams as springs, either at water level or higher up on the river banks. As the river deepened its channel the spring would tend to discharge at lower and lower levels, but with the final result that the breccia would be deposited from top to bottom of the cliffs, as it appears today in places along New River.[12]

Campbell's explanation is not applicable to the breccia occurring in the Draper Mountain area. The Max Meadows fault breccia lacks the essential characteristics of a stream deposit. Two of its zones are obviously autoclastic. Even the conglomeratic zone is unsorted and unstratified, and the shapes of its fragments are the result of cataclastic rather than fluvial processes. The outcrop of the Max Meadows fault breccia bears no relation to the course of New River or to any of its tributaries. Gradational contacts of the fault breccia with the Rome and Elbrook could not be accounted for by fluvial processes. The rather restricted range in variety of rock fragments

[11] *Op. cit.*, pp. 17–19. [12] *Ibid.*, p. 19.

composing the breccia would be hard to explain as the result of stream erosion and deposition.

Currier[13] described breccias occurring along low-angle overthrusts of the Austinville lead and zinc district, located 20 miles south of Pulaski. He postulated a lithologic-stratigraphic control of brecciation. According to his theory, dolomite zones in the Shady formation yielded to shearing stresses by intimate fracturing and autobrecciation, whereas intervening zones of limestone yielded by plastic distortion accompanied by relatively little brecciation. Where thrust faults cut across brecciated zones some of the breccias were rolled out along the fault and modified into a rubbly fault breccia. The Max Meadows fault breccia evidently had a different origin, because there are no selectively brecciated zones of dolomite in either the Rome or the Elbrook, which formations furnished the majority of rock fragments in the fault breccia. The preponderance of limestone pieces over those of dolomite and the abundance of phyllite fragments could not be accounted for by Currier's theory.

It has been suggested that the Max Meadows fault breccia is a cavern filling made by subsurface streams. Neither the transitional contacts of the breccia with the Rome and Elbrook nor the presence of cataclastic zones is explained by such an interpretation. The material in the conglomerate dikes could not have been forced into the Rome and Elbrook by stream action, neither could the markings on the wall rocks be the result of corrasion by stream-borne rocks. One of the strongest refutations to the cavern-filling hypothesis is the occurrence of some of the conglomerate dikes in Rome shales, in which solution caverns are not produced.

From an inspection of only a few localities where the breccia occurs along the Max Meadows fault, it might appear that the breccia was a sedimentary deposit intercalated between the Rome and Elbrook. The commonly observed association of the breccia with these formations is not without numerous exceptions. Within the Draper Mountain area the breccia lies in contact with twenty-two different formations. In no place does it mark a depositional contact between formations. The cataclastic structures of the breccia and the transi-

[13] L. W. Currier, "Zinc and Lead Region of Southwestern Virginia," *Va. Geol. Surv. Bull. 43* (1935), pp. 68–70.

tional nature of its contacts with the Rome and Elbrook indicate that it could not have been formed by sedimentary processes.

SUGGESTED ORIGIN

During the Appalachian revolution the Max Meadows overthrust block advanced northwestward at least 8 miles (see Pl. I). As is suggested by the stratigraphic throw of the fault,[14] this overthrust mass may have been 10,000–12,000 feet thick. The extensive movement of such a heavy block could have produced enough friction to metamorphose the base of the advancing block to phyllite and to dislodge blocks from the sole and tread of the fault. As additional blocks were torn from the overthrust and overridden rocks, previously dislodged fragments were gradually forced in toward the middle of the fault zone and were crushed and rolled out along the fault. The ultimate product of the cataclastic reduction of the sole and tread rocks is an even-grained, granoblastic, recrystallized calcareous rock of rudely schistose structure analogous to a mylonite. Schist slivers, feldspathic aggregates, quartzite fragments, and fragments of the Shady formation were dislodged far down the original dip of the Max Meadows fault, where it cut Lower Cambrian and pre-Cambrian rocks.

Parts of the fault breccia were forced into fractures of the rocks above and below the fault zone. Although the principal avenues of emplacement appear to have been pre-existing fractures in the Rome and Elbrook, these openings were probably widened by the injection of material from the fault zone. The conglomerate dikes are, therefore, cataclastic intrusions of breccia originally formed in the Max Meadows fault zone and modified into crush conglomerate by the mutual abrasion of fragments and by attrition with the wall rocks during their transposition from the immediate fault zone. The downward force exerted upon the fault breccia by the weight of the Max Meadows overthrust block may have caused the intrusion of the conglomerate dikes. But, since the fault breccia was formed prior to folding of the Max Meadows overthrust, the dikes may have been formed by the deformation of the fault surface.

Overthrusting alone did not produce the Max Meadows fault breccia, because there are other faults of comparable displacement,

[14] In places the Rome lies upon the Mississippian Price formation.

such as the Pulaski fault, along which no fault breccia occurs. That occurring along the Max Meadows fault owes its origin, in part, to the lithology and structure of the Elbrook and of the phyllitized zone of Rome, which evidently made them particularly susceptible to brecciation.

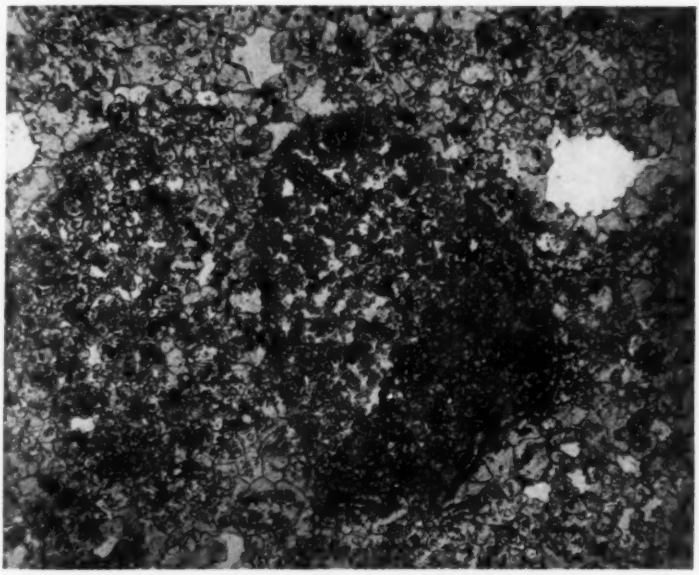

FIG. 13.—Photomicrograph of deformed crush conglomerate. The large limestone fragment, though not greatly distorted, has been largely replaced by fine-textured carbonates and quartz. On the left vestiges of another rock fragment which has suffered even more replacement are still evident. Crossed nicols, ×43. (Photomicrograph by George A. Rev.)

Evidences favoring the proposed interpretation of the Max Meadows fault breccia are:

1. The areal distribution of the fault breccia is essentially coextensive with the trace of the Max Meadows overthrust in the Draper Mountain area.

2. All three zones of the breccia are confined to the fault zone, with the exception of crush-conglomerate dikes, which extend into the rocks above and below the fault.

3. The lithologic identity of the preponderant limestone, dolomite, and phyllite fragments to the Rome phyllite and Elbrook formation strongly suggests the derivation of the fragments from these rocks. The Rome phyllite forms the sole of the Max Meadows overthrust mass and the Elbrook, in most places, the tread of the overridden block.

4. A subordinate number of fragments of Erwin quartzite, Shady dolomite, and pre-Cambrian biotite schist form a selective group of rock fragments which scarcely could have been segregated by any agent of erosion without including fragments of the many other formations exposed in this and near-by regions. The particular assemblages of fragments in the zones of the Max Meadows fault breccia can be explained by the proposed origin.

5. The cataclastic structures of each zone of the fault breccia limit the possible formative agents to diastrophism alone.

6. From the middle of the breccia zone the size, angularity, and abundance of phyllite fragments increase toward the sole of the Max Meadows overthrust sheet. In addition, the amount of rotation which these fragments have undergone increases from the top of the phyllite breccia toward the middle zone.

7. Since the phyllite zone at the base of the Max Meadows overthrust sheet seems to have been produced by overthrusting, the phyllite breccia which is structurally transitional with this metamorphosed zone must have had a similar origin.

8. Downward from the middle of the fault breccia the size, angularity, and abundance of Elbrook fragments increase, and the amount of rotation which the dislodged fragments have undergone decreases in the same direction.

9. The absence of the lower breccia zone in all places where the tread of the fault is made by formations other than the Elbrook is evidence that little material was derived from any other underlying formation.

10. Transitional contacts of the autoclastic breccias with their contiguous bedrocks and the structural and textural gradations of these breccias with crush conglomerate definitely imply a tectonic origin.

11. This interpretation explains the conglomerate dikes in the Rome and Elbrook, which are apparently continuous with breccia occurring along the Max Meadows fault.

INTRUSIVE ROCKS OF THE LEEWARD SLOPE OF THE KOOLAU RANGE, OAHU

CHESTER K. WENTWORTH
Board of Water Supply, Honolulu, T.H.

AND

AUSTIN E. JONES
U.S. Coast and Geodetic Survey, Los Angeles, California

ABSTRACT

The Koolau dome, forming the east half of the island of Oahu, is notably elongate, built about a linear rift zone in which numerous feeder dikes occur in a dike complex over 30 miles long. Scattered dikes and sills occur in the leeward parts of the dome, the concentration being progressively reduced with the distance away from the dike complex. There are secondary rift zones and subcomplexes with increased concentrations of dikes and sills, which trend at right angles to the main rift zone. The dikes and sills show three stages and patterns of columnar jointing which are related to the cooling history. Shallow intrusives are vesicular and banded but not columnar jointed. Dikes with a thickness of about 2 feet are preponderant to such an extent as to suggest that this is an optimum determined by the amount of lateral crowding-together of contracted lava formations which can be achieved by the pressures of invading lava.

INTRODUCTION

PURPOSE AND METHOD

In the course of a very detailed study of the geology of the Honolulu watershed with areal mapping at a scale of 500 feet to the inch, special attention has been given to the dikes, sills, and other intrusive bodies which cut the rather monotonous lava-flow structure of the Koolau Range. In the principal valleys there are late basaltic lava flows, late pyroclastic formations, and alluvial and talus formations to diversify the areal and structural map, but within the mass of the Koolau series itself the intrusive rocks and a few tuff lenses, probably from local phreatic explosions, furnish the chief variety.

Most of the area is difficult of access, heavily wooded, and not intimately known by anyone. Such parts of the Honolulu leeward slope as have been studied reveal important details about the distribution and character of the intrusive bodies. These findings are described for comparison with results of detailed studies elsewhere.

HISTORY OF GEOLOGIC STUDIES

The general lava-flow structure of the Koolau Range has been recognized since the visit of J. D. Dana with the Wilkes Expedition in October, 1840. While the presence of dikes cutting the lava flows was undoubtedly known to Dana and Dutton and has been noted in print by C. H. Hitchcock,[1] not even a rudimentary statement of their distribution or characteristics published prior to 1900 is known. There can be little doubt that some engineers and laymen were aware of the greater concentration of dikes in the upper valleys of streams of the windward slope of the Koolau Range, and the distribution of artifacts indicates that the Hawaiians were familiar with the occurrence of intrusive rock in the upper courses of both leeward streams and windward streams and also in the dike-riddled mass of the Mokulua Islands. Use of such rock by the Hawaiians in the making of adzes and other artifacts has led to the vernacular designation of "kanaka rock," current among older residents at present.[2]

Attention was first focused on dikes and sills as water-restraining members in the course of driving the Waiahole Tunnel; and the marked concentration of dikes in the belt parallel to the crest of the Koolau Range has become well known largely in connection with developing the system of catchment basins, tunnels, and ditches which augments the supply of the main tunnel in this project.[3] First systematic reference to the dikes and sills of the mountainous parts of the Honolulu district was made by H. S. Palmer in his report on high-level water. He mentioned a number of dikes and sills in various valleys and noted the greater abundance of dikes in the vicinity of Kaau Crater. He recognized the dikes and sills as offshoots from the feeder conduit by which the Koolau flows reached the surface.[4] The first systematic areal geologic survey of the

[1] "Geology of Oahu," *Bull. Geol. Soc. Amer.*, Vol. XI (1900), pp. 34–35.

[2] It appears that on islands composed of the normal basalt flows, which are vesicular, the natives used the denser intrusive dike rock. On Hawaii, however, the rock of thicker, less basic lava flows, such as that near the summit of Mauna Kea, was used for artifacts.

[3] H. T. Stearns, "Geology and Ground Water Resources of the Island of Oahu, Territory of Hawaii," *Div. Hydrography Bull. 1* (1935), pp. 399–409.

[4] "Possible Occurrence of High Level Ground Water in the Honolulu Region" (manuscript rept., U.S. Geol. Surv. [1921]).

island of Oahu was made by Stearns, in the course of which he recognized the zone of more numerous dikes, paralleling the axis of the Koolau Range, which he referred to as a "dike complex."[5] The term "dike complex," as used by Stearns, refers to the entire mass—both country rock and dikes—and thus differs somewhat from the term "dike swarm" as used elsewhere, which refers to the dikes only.[6] The Koolau dike complex is interpreted as the main rift zone of the range and the dikes as the filled, feeding channels through which all the flows of the range probably rose to the surface. A few of the stray dikes outside the dike complex were mapped by Stearns, but the greater detail of the present survey has revealed many more, and in some areas has made possible a statistical evaluation of frequency.

THE KOOLAU RANGE

PHYSIOGRAPHY

The Koolau Range forms the northeastern and larger part of the island of Oahu (Fig. 1). It is 40 miles long, and its rugged parts range from 4 to 10 miles in width. The northwestern half is less markedly eroded on the windward or northeastern side, whereas the southeastern half shows the effects of profound marine and subaerial erosion, probably aided by downfaulting of a considerable area. As a result, this portion is marked by a nearly continuous, but by no means straight or uniform, cliff or "pali" on the windward side, facing northeast. The leeward slope of the range is generally dissected by upward of fifty streams to form consequent valleys, between which are narrow ridges, many of the crests of which still rise nearly to the original surface of the elongate dome. It is clear that the original Koolau dome was several times as long as it was wide and that it was built by effusive eruptions from an elongate rift zone, now marked by the dike complex.

STRUCTURE AND PETROGRAPHY

The Koolau Range is composed of a vast number of thin lava flows mostly not over 5–15 feet thick, with individual flows ranging

[5] *Op. cit.*, pp. 95–97.

[6] R. A. Daly, *Igneous Rocks and the Depths of the Earth* (New York: McGraw-Hill Book Co., 1933), pp. 94–95.

exceptionally to 50 feet thick (Fig. 2). The flows mostly exhibit dense interior parts with broken, clinkery upper, and sometimes lower, surfaces. Consequently, when seen in section, the structure shows a marked stratification with the resistant ledges of dense basalt in contrast to the intercalated clinkery layers in which grass and other plants more readily root.

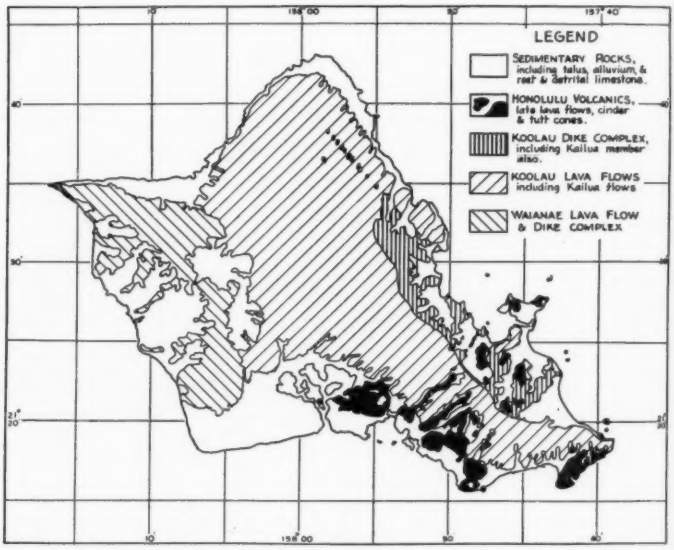
LEGEND
SEDIMENTARY ROCKS, including talus, alluvium & reef & detrital limestone.
HONOLULU VOLCANICS, late lava flows, cinder & tuff cones.
KOOLAU DIKE COMPLEX, including Kailua member also.
KOOLAU LAVA FLOWS including Kailua flows
WAIANAE LAVA FLOW & DIKE COMPLEX

FIG. 1.—Sketch map of the island of Oahu, showing chief groups of formations. Boundaries generalized from *Geologic Map of Oahu* by H. T. Stearns (U.S. Geol. Surv., 1935).

The lava flows of the Koolau series consist wholly of normal basalt with olivine present usually as phenocrysts in a more or less porphyritic texture. Variations in texture are not rare, but despite these common variations from flow to flow there is no evidence yet known indicating a general petrographic or chemical difference between the earlier basalts of the series, deep in the gulches, and the later basalts, near the top of the dome. An almost monotonous general similarity marks the basalts from all parts of the range.

The feldspar basalt of the Koolau series is readily distinguished

FIG. 2.—View of windward cliff of Koolau Range showing thin lava flows and alternation of dense and clinkery layers. From near Makapuu Head, photograph by H. Winchell.

in thin section from the nepheline or nepheline-melilite basalt of the more recent Honolulu series, exemplified by the several secondary valley-filling flows such as those of Nuuanu, Moiliili, and the like or the cones like Diamond Head, the Koko series, or Ulupau Head.

INTRUSIVE ROCKS

DISTRIBUTION AND ARRANGEMENT

General features.—The intrusive rocks of the Koolau Range consist chiefly of dikes and sills, with associated irregular stringers. In addition, there are chunky masses at the upper edges of a few dikes which are here called "buds" and also the intrusive fillings that occur in some lava tubes. No truly plutonic rocks are known, though a few dike and sill masses are of sufficient size to have a moderately coarse crystallinity. The dikes and sills of the Koolau Range may be considered in two groups: those of the dike complex and those in the scattered systems outside the complex.

The dike complex is briefly described by Stearns,[7] who interprets it as the main rift zone through which the magma of Koolau flows reached the surface. Some earlier writers regarded the range as the curved, southwestern slope of a dome built around some large central crater, and others sought to locate a center of eruption in the vicinity of the Nuuanu Pali gap. Any such interpretation stems from a very imperfect concept of the configuration and structure of the leeward slope of the range and is quite inadequate. Palmer recognized the probability that lavas of the Koolau Range came from a "series of vents" so as to form a dome of "pear-shaped" ground plan.[8] A more complete concept of the continuity and linearity of the rift zone as marked by the existing dike complex was made possible by the survey of the island of Oahu recently completed by the United States Geological Survey.

The present paper confines itself to the leeward slope of the southeastern part of the Koolau Range. The comparatively few buds and lava-flow fillings are described in appropriate sections, but the larger part of the text and the descriptions of texture and structure, except as otherwise indicated, refer to the dikes and sills.

[7] *Op. cit.*, pp. 95–97.

[8] "The Geology of the Honolulu Artesian System," *Rept. Honolulu Sewer and Water Comm., Suppl.* (1927), p. 26.

Location.—Mapping of the leeward slope of the Koolau Range at the scale of 500 feet to the mile has been completed between Wailupe and Nuuanu valleys. The distribution of dikes in the remainder of the leeward slope is known chiefly by the work of Stearns.[9] Experience in the Honolulu area indicates that the major features of distribution are indicated in the earlier mapping but that a consider-

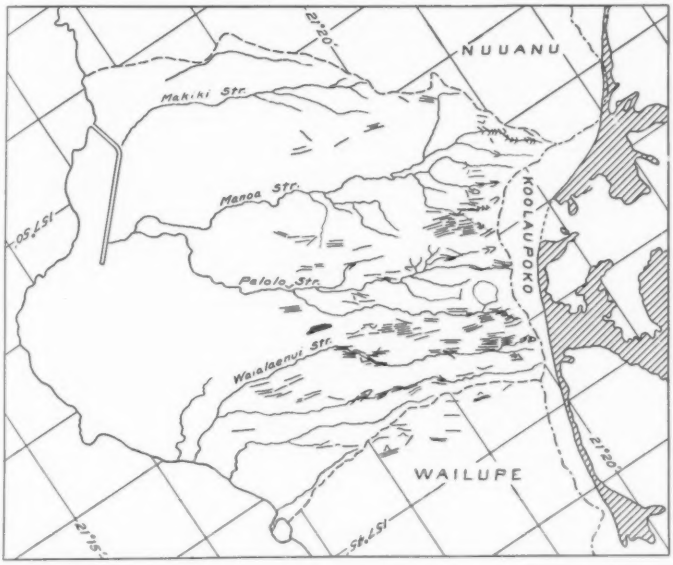

FIG. 3.—Map of Palolo-Waialae and Manoa-Makiki areas of the Honolulu portion of the leeward slope of the Koolau Range showing distribution of intrusive bodies. The cross-hatched area is the dike complex.

able number of details remains to be filled in, especially the determination of areas which are essentially dike free. This product of the more detailed survey has become particularly apparent in the course of mapping the head of Manoa Valley, where a considerable sector is almost without dikes or other intrusive rocks. The location and concentration of dikes and sills is indicated in the accompanying map (Fig. 3). This is essentially an outcrop map, the mapping from any given outcrop being extended 100 or 200 feet on either side of

[9] *Op. cit.*

the outcrop, according to thickness and apparent continuity with dikes of adjacent traverses. The heavily forested country and the cover of mantle rock nearly everywhere defeats direct tracing of dikes.

Attitude.—With few exceptions the dikes cut the lava flows practically at right angles (Fig. 4). The general dip of the lava flows is 3°–6° or 7° in most of the area. In the case of those dikes which strike parallel to the strike of the flows the dikes would be expected to dip at high angles toward the crest of the dome. However, since the greater number of dikes are in the subcomplexes—transverse to the trend of the range and nearly parallel to the dip of the flows—the dikes in general are both vertical and normal to the flows. Measurements of dip in sufficient number to determine statistically whether the dikes tend most strongly toward the vertical or toward being normal to the flows have not been made; and it is somewhat doubtful whether such a determination would be feasible, despite the theoretical interest involved.

The impression gained by extensive field observations is that the dikes are surprisingly straight and direct in cutting across the lava flows, particularly in view of the thinness of the flows, the structural discontinuity represented by the alternation of dense and clinkery portions, and the presumptively available alternate avenues of intrusion offered by the margins between flows and the clinkery layers. There are only a few dikes which follow irregular courses in such clinkery layers or which have invaded the rock in irregular fashion. It is believed that the joints have been structurally determined and then subsequently invaded by the molten rock.

Akin to this question is the relative number and character of sills. In view of the steepness of most of the channels traversed, 30°–60°, the probability of crossing sills is essentially equal to that of crossing dikes, so that there may be only a slight systematic error in the observation of dikes as compared to sills, much less than would be true in many regions.

Sills are much less numerous than dikes;[10] this seems to be in accord with the relatively small number of dikes of irregular atti-

[10] A tabulation made by Jones in 1937 showed that mapped sills were slightly more than half as numerous as dikes.

FIG. 4.—Dike in rock wall on pali road, windward slope, near Honolulu. Photograph by H. S. Palmer.

tude. It seems valid to conclude that dikes have been broadly determined by fracture systems in the rock, developed in relation to the mass and areal extent of the dome and mostly vertical. Possibly the alternation of dense and clinkery layers has defeated the general development of horizontal fractures (such as the sheet jointing of granite) and at the same time has failed to offer avenues of intrusion as generally favorable as the nearly vertical fractures.

The sills occur parallel to the lava flows in clinkery layers between dense portions of adjacent flows and also intruded definitely into

TABLE 1

DISTRIBUTION OF DIKE AND SILL THICKNESSES

Thickness (Inches)*	Number Field Books 5 and 7	Number Field Books 6, 9, and 21	Total
0–9	9	10	19
9–18	12	12	24
18–36	25	28	53
36–72	21	15	36
72–144	3	4	7
144–288	1	1	2
288–575	1	0	1
Total	72	70	142

* These limits are in geometric series selected to avoid as far as possible those figures appearing most commonly in the records. Dike thicknesses falling on the limits are thrown half into the class above and half into the class below the limit.

dense parts of flows. There is no indication that intrusion into clinkery layers is more readily accomplished than intrusion into the dense parts of flows, and the evidence suggests the reverse.

Size and extent.—The thickness of dikes of the leeward slope ranges commonly from 1 foot to 3 or 4 feet. A few thicker dikes up to 10 feet across are known, and there are a few still thicker intrusive masses such as the Palolo dike mass and the buds mentioned earlier. An effort was made to determine the prevailing thicknesses by compilation of all those recorded in several notebooks representing chronologically consecutive field work, chiefly in the Palolo-Waialae area and the Waiakeakua branch of Manoa Valley. The results are shown in Table 1.

The average width of dikes in this series is about 35 inches, owing to the several exceptionally wide dikes. However, the prevailing width, or mode, is very close to 24 inches, which was the estimate of width most commonly made. Nearly two-thirds of all the dikes in this random sample range in thickness from 1 to 3 feet, inclusive, and this distribution is representative of dikes of the leeward slope.

It is pertinent to seek the cause which fixed the thicknesses of most of the dikes in this range at about 2 feet. Since there is no evidence of stoping or assimilation of country rock by the dikes, it appears that the space occupied by the dikes has been developed by cooling shrinkage at the time of forming of individual lava flows by the ordinary process of joint formation through temperature and moisture changes and by the lateral, hydrostatic thrust of the dike-forming magma itself, which results either in crowding together of the jointed rock on the two sides or in developing space by a pivoted uplift or tumescence of the whole overlying mass. The effect of the latter may be important locally, but it is most plausible to assume that the horizontal thrusting is primary and that the thickness of dikes is chiefly determined by the lateral distance to which the thrust can extend and the amount of horizontal compaction which can take place from a given vertical plane under the usual conditions in this area.

No exact measurements are available; a plausible value for the original contraction of the blocks of a lava flow is a $\frac{1}{4}$-inch opening surrounding successive 2-foot blocks, amounting to about 1 per cent. On this basis, space for a 2-foot dike would be developed if the openings were closed up for 100 feet each way from the position of the dike. Following this, reasoning would also suggest that the spacing of dikes would be influenced by the lesser tendency of magma to invade a zone previously somewhat compacted, the combination of the total number of dikes and the average thickness tending approximately to equal the amount of contraction. While this tendency may exist, it cannot be of prime importance, since dikes have invaded dike-complex zones to a degree out of proportion to any possible contraction; and other causes must be sought.

In general, the total lateral hydrostatic pressure of a liquid column is capable of thrusting against friction a column of rock of com-

parable height, of width proportional to the square of the height and proportional to the coefficient of friction. If friction be assumed at 20 per cent, the pressure of a column 500 feet high would suffice to move laterally against friction a column 50 feet wide, assuming rock and liquid at the same density. With a 1,000-foot column the width would be 200 feet. If movement and closing up take place on both sides and the openings amount to 1 per cent of the total, the space provided on the 500-foot basis would be 1 foot; on the 1,000-foot basis, 4 feet. We do not have data to show if width of dike is related to depth below the surface, nor can we prove each of the other assumptions. The general depth below the surface of the dome at which the visible dikes have been intruded is 200–1,500 feet; the mechanism and magnitudes suggested in the above discussion seem at least plausible.

From observations in places where outcrops are somewhat extended, it appears that individual dikes often have an outcrop length of 200–300 feet, thicker dikes probably more. The longest series of outcrops, readily traceable and indicative of the continuity of a single dike, is in the west branch of Waiakeakua Valley, where a string of outcrops occurs in the channel for about 1,200 feet.

It is the impression of the writers and other participants in the field work that sills are in general somewhat thicker than dikes. However, it should also be conceded that there is a greater chance of failing to see and record a thin sill than a thin dike, which may distort the results somewhat. Lengths of sill outcrops and extent of sills in the two large dimensions are probably similar to dikes; most sills observed have a proved and reasonably presumptive extent of 100–300 feet, but a few thick sills are known to extend over areas of at least 1,000 feet in one direction.

Larger intrusive masses.—The intrusive mass in which Palolo quarry is located, known as Palolo dike, trends about north 28° east, is exposed for a total distance of about 1,000 feet, and ranges from 50–200 feet in width. At the south it terminates abruptly in a rounded end separated from the main wall of Palolo Valley by a depression 25–100 feet deep. Across this depression in the plainly exposed wall, at the same level and lower, there is no sign of continuation of the intrusive rock. Along the western limits of the mass

and forming the more continuous lower part, the intrusive rock has well-marked columnar jointing, with columns up to 1 foot in diameter and 5–10 feet long. The jointing occurs in several parallel components which aggregate a total thickness of 50 feet or more. Increasingly on the east side and in the higher parts on this uphill side, the rock is more irregularly joined in systems of platy structure or irregular, polyhedrally broken masses. In several places on the east side the intrusive rock overlies the gently dipping lava flows

FIG. 5.—Jointed intrusive rock in Palolo quarry, Palolo Valley

on the country rock, in abrupt offsets which indicate that the intrusion expanded upward (Fig. 5).

Much of the interior portion of the Palolo dike is holocrystalline, with grain sizes approaching 1 millimeter; near the margins and in various stringers which invade the mass there are exceedingly fine-grained phases. A few veins and cavities show development of both primary and secondary minerals. It appears that the intrusion first took the form of a thick, compound dike, intruded in successive vertical members. Later the intrusion expanded with placement of irregular masses above and to the east of the main dike. This interpretation is suggested by the relationships of columnar and platy

jointing and by the contrasts in texture of the various component masses. The Palolo dike has been described by Stearns as a "boss," which is defined as "a relatively small upright intrusive body having a roughly cylindrical form."[11] In the writers' view the dominance of the linear-dike portion of the Palolo mass weakens the concept of an upright or cylindrical form.

Several similar thickened masses of intrusive rock, much smaller than the Palolo example and most of them visibly connected with

FIG. 6.—View of bud near top of west wall of Kapakahi Valley. Much of the original lateral surface has been removed near the top. Lower, at the left, part of the selvage is preserved, and part of the deeper selvage can be seen in profile on the right. The block jointing is clearly shown, and the upper blocks have been somewhat displaced by creep.

dikes, have been found in the Honolulu area. These probably represent the thickening of the intrusion as the magma closely approached the existing surface of the dome. Most conspicuous of these is a series on the eastern edge of the Waialaenui flow-slope facet at elevations 900–1,000 feet. Here somewhat discontinuous masses of dense rock with a banded, vesicular selvage in contact with country rock extend for several hundred feet. The line strikes about south 20° west and also passes near to several similar masses

[11] *Op. cit.*, p. 21.

a half-mile inland. In the most ideal form these thickened intrusions are rounded in ground plan and have a bulbous vertical section, the lower parts of the sides of several definitely suggesting a narrowing of section downward. Their form and relations suggest the appellation of "bud."

Three of these very typical buds occur at this Waialaenui locality, and remnants of other such masses have been seen in several other places in the Honolulu area. Southernmost of the Waialaenui buds

FIG. 7.—Detail of margin and selvage of bud. The lower part is slightly weathered selvage; above it is the less resistant and deeply pitted and grooved interior part of the bud.

is one of elliptical ground plan about 30 by 20 feet, and standing about 15 feet above the surrounding ground on the uphill side (Fig. 6). Its top is about 200 feet east of the edge of the tabular flow slope, and it stands not over 10 or 20 feet below the plane of the flow slope. The next and largest of the buds is 50 by 30 feet, about 20 feet high, slightly farther from the edge of the facet, and perhaps 30 feet below its present plane. The third bud is smaller and less distinct from the semicontinuous dike.

The two larger buds are broken into large, irregularly polyhedral blocks with curved faces and are deeply pitted by weathering on the

upper surface, which also shows a few flat-bottomed, water-level pans. The mass of the buds consists of medium-grained, crystalline basalt. Completely around the margin is a selvage of banded vesicular structure from 6 to 15 inches thick (Fig. 7). The outer $\frac{1}{4}$ inch is somewhat finer in grain, possibly in places approaching a glass. However, in general it appears that a glassy selvage was not formed, probably because the surrounding rock was so heated that sharp marginal chilling did not take place as the mass cooled. The vesicular banded selvage is brought out strikingly by differential pitting around the upper edge of the margin, the finer-grained outer layer forming a somewhat resistant shell.

The third bud is visibly connected to a continuous dike; the larger first and second buds, by their areal relations, seem to be so connected but show no contact at the surface, the selvage and presumptive contact with country rock passing completely around the narrow ends of the elliptical margins. Relations of the buds may be summarized as follows: they have everywhere been found near the constructional surface of flow-slope facets, they show the vesicular-banded selvages typical of shallow dikes, many show a definite connection with dikes, and they grade into more irregular and rudely linear thickenings of dikes.

STRUCTURE AND PETROGRAPHY

Texture.—The dike and sill rock is chiefly dense and nonvesicular. In the earlier stages of this study the dikes and sills were chiefly recognized by the conspicuous columnar jointing produced by an orderly thermal history and apparently dependent on cooling at a considerable depth. At such depth, vesicles do not develop, and most of the columnar-jointed dikes are of dense rock. Later, we came gradually to recognize that there were banded, vesicular dikes, of less conspicuous jointed structure or with no evidence of jointing, which were found only at slight depths, near the constructional surface of the dome. It appears, therefore, that dikes and sills consist of dense rock with few vesicles at depths of 300 feet or more below the surface of the dome with some probable variation in relation to the type of the surrounding rock and that in situations within 200 feet of the surface the rock is more likely to be vesicular and banded (Fig. 8). It should be pointed out that probably not all dikes

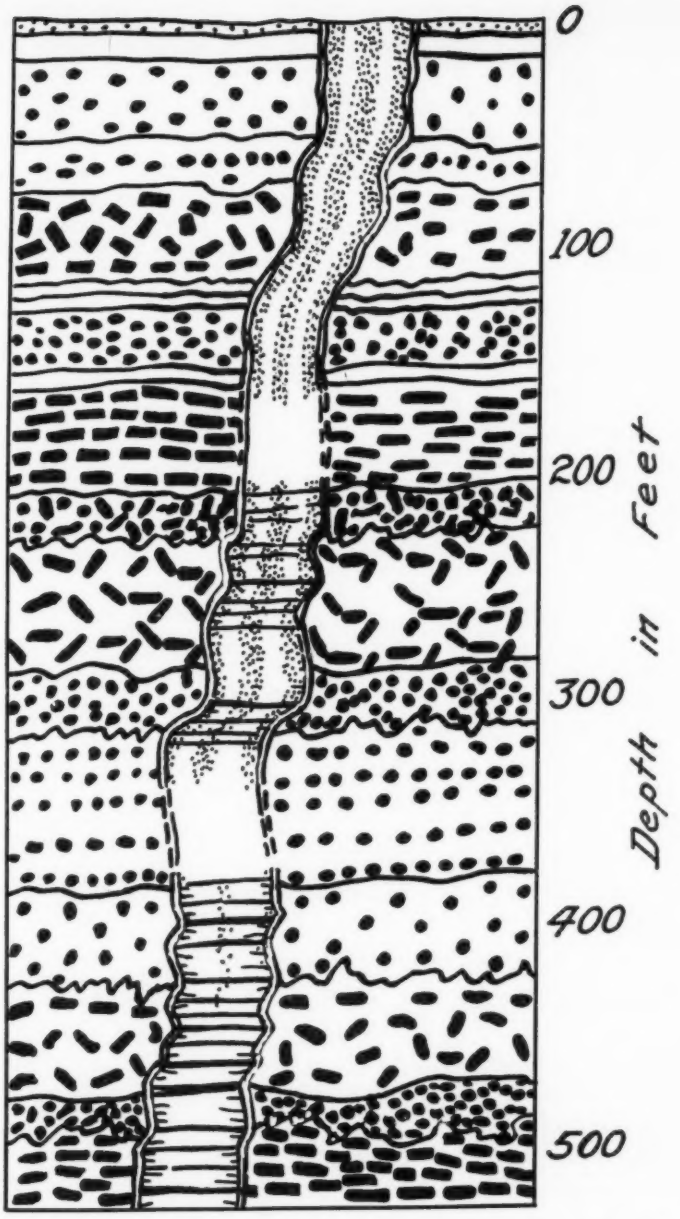

FIG. 8.—Schematic diagram showing changing character of dikes with increase of depth. The entire diagram represents approximately 600 feet of depth, with dikes dominantly of the vesicular, banded type above 200 feet, of the columnar-jointed type below 400 feet, and mixed types in the intermediate zone. The thickness of dikes is exaggerated, and the structure patterns are diagrammatic. Redrawn from a sketch by A. E. Jones in 1937.

represent intrusions which reached the surface of the dome, hence the actual pressure of intrusion may not have been that corresponding to a full column. This fact would account for variations in the vesicularity and columnar jointing of dikes in similar situations. It is true that in the latter situations there is more general weathering, and the full occurrence of such shallow-type, vesicular, and banded

TABLE 2*

RELATION BETWEEN STRUCTURE AND VESICULARITY

Structure	Number of Dikes				
	Dense	Very Fine Vesicles	Fine Vesicles	Medium Vesicles	Large Vesicles
Columnar jointing	20	9	3	2	1
Banded and jointed structure	0	3	0	4	1
Banded structure	0	0	4	7	6

* Based on a compilation made by the junior author in 1937.

TABLE 3*

RELATION BETWEEN DEPTH AND VESICULARITY

Approximate Depth in Feet	Number of Dikes		
	Dense (No Vesicles)	Very Fine and Fine Vesicles	Moderate and Large Vesicles
0–500	1	4	13
500–1,000	2	6	7
1,000–1,500	16	8	9
Below 1,500	4	6	1

* Rearranged from a tabulation made by the junior author in 1937.

dikes is not so well mapped as that of the more conspicuous, jointed types (Fig. 3). After a considerable experience in the field one becomes qualitatively aware of the systematic relationship between the vesicularity and vesicularity-banding and the columnar jointing. An attempt was made in the course of studies in the Palolo-Waialae area to indicate such relationships by compilation of notes on the character of dikes, as shown in Tables 2 and 3.

While these data are by no means precise, they are sufficient to indicate the general reciprocal relation between vesicularity and columnar jointing, as also the decrease of vesicularity and increase of columnar jointing with depth.

Banding.—The banding of the shallow-type dikes (few or no sills of this type have been observed) is expressed in the size and pattern of vesicles. It is fairly regular and parallel to the margins of the dike within any distance of 10–20 feet. Vesicles range up to 5 or 10 millimeters in length and may be somewhat elongated in the direction of flow.

The columnar-jointed dikes and sills also show a banding of a more systematic and structurally important sort. Three zones can be identified in most well-developed dikes: a central zone of finely crystalline rock, comprising most of the thickness of the medium and thicker dikes; a glassy selvage which is usually $\frac{1}{8}$–$\frac{1}{4}$ inch thick on each of the margins; and a subselvage inside the glassy selvage on each side, which consists of rock clearly finer in grain and less completely crystallized than the center zone. This subselvage is commonly 2–4 inches thick and is the least constant of the zones. In some dikes, especially thinner ones, it may not be present. These zones appear to be wholly due to the history of cooling and crystallization; in the usual case there is no evidence that they represent successive intrusion, though multiple dikes are known. The probable significance of these zones will be discussed in the section on jointing.

Excentric vesicularity banding is prominently displayed by some lava-tube fillings which must in some degree be considered as intrusive. Not only are lava tubes progressively sealed off in the course of the eruption by which they were formed, but such openings are unquestionably susceptible of later filling by molten rock from cross-cutting dikes. The resulting fillings are in either case often more dense than the surrounding rock[12] (Fig. 9).

Jointing.—The most typical feature of the intrusive masses—dominantly dikes and sills—is the columnar jointing of the kind common in basaltic dikes elsewhere and in some basaltic flows. In Hawaii, though some flows show a moderate amount of ill-developed

[12] H. S. Palmer, "A Fossil Lava Tube," *Jour. Geol.*, Vol. XXXVII (1929), pp. 272–74.

FIG. 9.—Banded, filled lava tube exposed near the base of the cliff of Makapuu Head. The vertical diameter is about 14 feet.

columnar jointing, they are mostly too irregular, too vesicular, and too irregularly jointed to display the characteristic appearance of the Giant's Causeway and other famous examples.

Only in the dikes and sills is such jointing well marked in Hawaii. The main jointing of thicker dikes consists of joints transverse to the greater dimensions, arranged in trifold fashion about tension points and merged to form a polygonal pattern similar to other contraction cracks like those on drying mud flats.[13] The ideal form of the intervening columns is that of regular hexagonal prisms; only a few of the actual columns are of this sort, and many are five sided or are quite irregular in the angles and lengths of sides. The sections often change somewhat from end to end of the columns. Nevertheless, the general effect is that of polygonal columns, the diameter of which is commonly from one-third to one-sixth the length. Thus, a dike 1 foot thick is likely to be divided into columns 2–4 inches across; a dike or sill 10 feet thick is commonly composed of columns 2–4 feet across. It is not unusual for a long column to break squarely across in the outcrop in a way to suggest that there is an incipient system of cracks parallel to margins of the dike.

The jointing of the subselvage is similar to that of the center zone, except that it is a closer pattern, roughly of the same ratio between diameter and length of resulting columns as in the former case. Since this subselvage is often 2–4 inches thick, the component columns are commonly from 1 to 2 inches across. The jointing of the subselvage grades into the jointing of the center section; the boundary or zone of separation, while fairly restricted to 1 or 2 inches, is not sharp like that between the subselvage and the outer glassy selvage (Fig. 10).

The jointing of the glassy selvage is of still closer mesh than that of the subselvage, apparently related to the thickness of the glassy zone. A common relationship for a $\frac{1}{4}$-inch glassy layer would be division into joint units of perhaps $\frac{1}{4}$ inch across. The joint-bounded units in the glass are more like blocks than columns, the pattern being a checking rather than a hexagonal development. The glassy selvage often shows dominance of the lines of the polygonal jointing

[13] T. C. Chamberlin and R. D. Salisbury, *Geology* (1909), Vol. I, p. 499.

of the main part of the dike or of the subselvage or both, in addition to its own pattern (Fig. 11).

Observations on several hundreds of dikes furnish a basis for discussion of the origin of contraction joints. In a homogeneous material subject to contraction by drying or cooling with the effect penetrating progressively from the outside toward the center, the initial result is the development of three-pointed tension stars by the radiating of cracks in three directions, ideally at 120° separation.

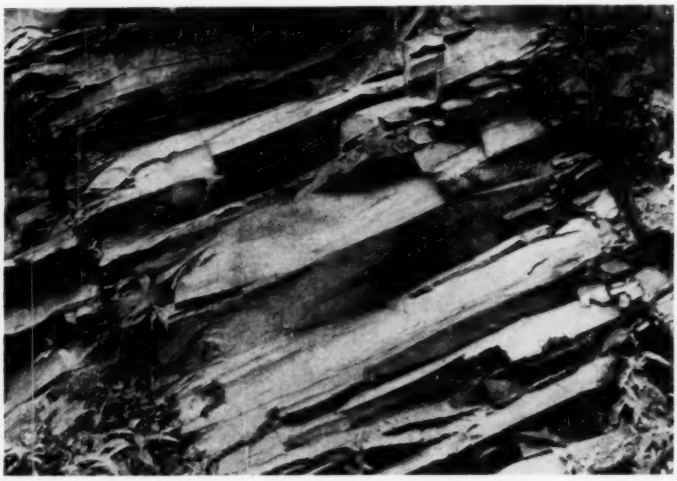

FIG. 10.—Detail of dike in road bank, Waikane Valley, showing interior jointing and splinter jointing in the subselvage.

Under highly uniform conditions the points will be rather regularly spaced; on a mud flat where grass stems or other foreign fragments furnish a discontinuity these are likely to initiate the cracking. If the material is quite homogeneous in section, the cracks may extend inward as the process goes on, and they will be controlled by the rates and progress of the drying or cooling as transmitted inward and as affected by the opening of the initial cracks. The spacing of the original cracks depends essentially on the area over which contraction can be accommodated by a single crack. Movement corresponding to the opening of the crack requires either shear along a

surface parallel to the outer surface or a deformation which is progressively less from the outside inward, by which the volume reduction takes place without reaching a shearing failure at any zone. The rates of contraction, the distribution of heat or moisture changes, and the elastic properties of the material are controlling factors.

Without undertaking detailed treatment of these factors, it is evident that any plane of physical discontinuity parallel to the outer

FIG. 11.—View of dike selvage in Waiomao Valley showing three types of jointing. The ends of four or five major columns are shown, with the bounding joints somewhat frayed. Each of these ends is crossed by several joints corresponding to the splinter jointing of the subselvage, and the space between these is broken by the close, check jointing of the glassy selvage. The pencil shows scale.

surface is likely to become a surface of separation under the stress conditions developed. If an outer layer of definite thickness contracts so as to separate structurally from the material below it, its thickness at once becomes a factor in determining the size of the polygons into which it is divided by the contraction joints. The polygons in such cases are as large as, and no larger than, the unit of competence for tension stresses. Since in any given section the stress is proportional to the distance from a tension crack and the

capacity for tensional stress is proportional to the thickness of the layer, in any given material the joint spacing is large for thick layers and small for thin layers. This can readily be seen on any multi-layered mud deposit where close-jointed, thin top layers commonly ride the tops of the larger polygonal columns. This general law of spacing of joints so as to separate masses which are just competent from the standpoint of push and pull, internal stress, crushing support at the base, and the like is commonly recognized by engineers in the design of joints in masses of concrete of various sizes and shapes.

In the case of the dikes and sills it appears that the physical differences between the inner and the outer parts of the mass as developed by crystallization or the lack of it are the controlling factors in the development of the polygonal jointing. First, cooling has taken place in the outer few millimeters adjacent to the country rock, producing a glassy texture with a few crystallites only. This layer has a rather sharp inner boundary and has developed a fine-meshed pattern of joints consistent with its thinness. It seems likely that the actual, open tension cracks have developed later and at a lower temperature than the initial freezing, since the joint pattern has apparently been influenced by the adjacent coarser pattern of the main dike.

At any rate, solidification of the interior of the dike has probably been discontinuous in that the glass solidified quickly and to a sharp limit, followed by a crystallization proceeding inward to form the subselvage, and finally a fairly general freezing of the interior part. It is apparent, at any rate, that the pattern of the glassy selvage has been adapted to the thickness of the glassy layer and that of the subselvage to its own thickness, each at a time when the adjacent layers were either insufficiently solid or cool or otherwise of different properties not physically continuous with the layer in question. On the other hand, even with complete solidification of any thinner outer layer, it is evident that a thicker inner layer would probably project the main lines of its larger pattern on the thinner layer. It is also most likely that the cooling and cracking of the several layers overlapped sufficiently so that the lines of the coarser inner pattern controlled some of the detail of the finer outside pattern. Thermal conditions and thermal behaviors may have differed in different dikes, and there is a possibility that in some instances the glassy layer may not have become jointed until after the formation of the

joints of the main dike, the thin glass, however, still retaining its physical identity in controlling the mesh of the pattern.

While not directly applicable to dike masses, it is worthy of remark that it is not uncommon, especially in large polyhedral blocks of Honolulu basalt which have become somewhat separated by contraction jointing, to see a secondary system of imperfect polygonal joints developed on the surfaces of the block. In such a case we must conceive a development of the primary joints and a certain degree of separation of the blocks while still very hot so that the joints themselves become avenues of cooling. Thus, the adjacent surfaces are contracted by cooling while the interiors of the blocks still remain hot.

Mineralogy.[14]—The minerals of the dikes and the general petrography are substantially identical with that of the Koolau lavas. Some of the thicker dikes are coarsely crystalline; most of those of 2 or 3 feet in thickness are slightly finer in grain than the lava flows and tend to be imperfectly crystalline, with interstitial glassy areas (Fig. 12). Some thin dike stringers up to 1 or 2 inches thick are wholly glassy, like the usual selvage of thicker dikes.

Olivine forms prominent phenocrysts, comprising 0–15 per cent of the rock of Koolau dikes. Some olivine phenocrysts are very small, but the usual size is of the order of 1–4 millimeters. The optic angle of the material is nearly 90°; therefore, its composition is near 15 per cent fayalite and 85 per cent forsterite. Alteration rims of iddingsite are common in the dike olivines, as in the lava-flow olivines, and commonly invade deeply the boundaries of the grains or even completely replace the grains themselves.

Phenocrysts of feldspar—a basic labradorite usually—are found more or less developed in the majority of the dike rocks. In some cases they appear well developed to moderate sizes (1–4 millimeters long) in dikes in which the glassy selvage is poor or lacking in corresponding phenocrysts or has labradorite of much smaller size, showing that the phenocrysts continued growth after emplacement of the dike.

Augite phenocrysts are occasionally observed. Optically, they correspond to the augite from Haleakala described by H. S. Wash-

[14] The large part of this section has been contributed by Horace Winchell, assistant geologist, Honolulu Board of Water Supply.

ington[15] but rarely show any appreciable zoning. In thin section they are usually of very fresh appearance and sometimes control the precipitation of thin rims of olivine and magnetite around them, though this is not common. The groundmass minerals are pyroxene (probably augite of very nearly the same composition as the phenocrysts), feldspar (labradorite), and magnetite (possibly some ilmenite) with occasional small grains of olivine and frequent patches of

FIG. 12.—Exposure of dike in stream channel, Waiomao Valley

glassy material containing considerable amounts of magnitite in the form of very fine dust sprinkled throughout the glass and making it relatively dark or even opaque. Magnetite microlites, margarites, and other skeletal aggregations are common, especially in the portions containing glassy basis. The accompanying photomicrograph shows the general aspect of typical dike rock, with the olivine phenocrysts, labradorite laths, and fine-granular pyroxene, sprinkled almost throughout the whole by magnetite grains of varying sizes (Fig. 12).

[15] "Augite of Haleakala, Maui, Hawaiian Islands," *Amer. Jour. Sci.*, Vol. CCIII (1922), pp. 117–22.

Texturally, the Koolau dikes must be described as nearly always porphyritic, usually intergranular, in the central best-crystallized portions; and intersertal to hyalophitic in the commoner, more poorly crystallized portions. The selvages are usually glassy, with microlites of magnetite and feldspars and phenocrysts of olivine. The glassy selvage is commonly hyalophitic. These terms are used in the sense employed by A. Johannsen.[16]

Weathering and exposure.—First response of a dike or sill to weathering is the opening of thermal contraction cracks consequent to the relief of pressure near the surface. This probably takes place sooner than any expansion due to chemical weathering can operate. Broadly, the dikes are slightly more resistant to chemical weathering than the lava flows, probably because of the greater difficulty of access of water. The chemical composition is the same. However, the broken and jointed character of the dike rock, combined in some places with the very lack of chemical weathering which rams and indurates the mass, often leads to a physical separation such that dikes in weathered banks may ravel down and form a depression. Regionally, the difference in weathering between the dike rock and flow rock is rather slight; either in particular situations may be the protruding or the depressed rock. In stream channels dikes may stand 1 or 2 feet above surrounding rock or may form the face of low falls, with the country rock stripped away on the low side (Fig. 13). Similarly, on the sides of valleys or cliffs the dike often forms a parting, with the country rock stripped away, leaving the dike adherent to the wall, or in places the dike may also be stripped away. Sills and irregular intrusive masses commonly form a somewhat irregular channel pavement, showing higher resistance to abrasion but little or no capacity to overhang. Sills are often exposed in the faces of cliffs but usually are flush or protrude by less than half the diameter of a joint column.

It is common for the glassy selvage of a dike to be oxidized and rusty in appearance, possibly in part owing to palagonitization. Interstitial oxidation often develops along the surfaces between joint columns, and there is occasionally evidence that the surface of the

[16] *Petrography* (Chicago, 1931), Vol. I, p. 47.

dike itself serves as an avenue for movement of ground water or for small amounts of mineralization to take place.

In the deeper parts of the lava domes of Hawaii, prior to the release of pressure, the dikes are relatively impermeable, forming barriers to movement of water which are known in places to maintain head differences in the ground water of 100 or more feet.

FIG. 13.—Dike in channel of Wailupe stream. Contrast between dense texture of dike and vesicular texture of lava flows is well shown at the right, and the splinter jointing of the subselvage is shown on both margins.

In valleys where dikes are fairly numerous the hard and slightly abraded dike columns of various sizes are conspicuous components of the stream gravel and often give the first intimation of the existence of dikes or sills.

SUMMARY

AREAL ARRANGEMENT

This paper is restricted to the leeward slope of the range. The full pattern of arrangement of dikes and sills consists of the following: (*a*) dikes and sills of the dike complex, windward side of range crest, Waimanalo to Laie; (*b*) various subcomplexes of dikes and sills chiefly known in the Wailupe to Nuuanu sector, trending trans-

versely to the main range crest and dike complex; and (*c*) scattered dikes and sills, progressively less numerous away from the range crest and away from subcomplexes. The main dike complex is the feeder system through which the lava to build the elongate dome was erupted; the subcomplexes are on cross-fissures which appear to be accommodation joint lines cutting the longest dimension of the range. They are very close in some instances to the lines of vents of the Honolulu series of southeast Oahu. The leeward slope of the range northwest of the Honolulu area is not yet sufficiently well known to say definitely whether or not subcomplexes exist there. They were not determined in the course of mapping by Stearns; it is possible that the development of subcomplexes is coextensive with the subsequent eruption of lavas and tuffs from the vents of southeastern Oahu alone.

VERTICAL ARRANGEMENT

It is an inviting speculation to consider whether dikes and sills are not more numerous at depths of 500, 1,000, or 2,000 feet below the surface of the dome or, in general, at the lower absolute elevations in any one part of the dome. Unfortunately, available and comparable sections through a range of 500 or 1,000 feet are not accessible. Perfection and completeness of exposure increase at lower elevations, within the upper, rugged area; any increase in numbers of dikes at greater depths below the dome surface can as well be attributed to this factor as to absolute increase. Most of the subcomplexes are exposed in the sides of valleys, where continuous observation is favored; however, it is doubtful whether important or equally widespread swarms of dikes have been passed over, either in the bottoms of valleys or on the narrow but somewhat residuum-covered ridge tops.

Most significant fact in this connection is the indicated change in textural and structural character between the deep-seated, more typical, dense, polygonal-jointed dikes and sills and the shallow, vesicular, banded, and nonjointed dikes. It is generally assumed that the dike concentration increases downward; direct field evidence indicates that dense dikes with well-marked jointing are more numerous a few hundred feet down but does not, in the leeward area, give clear proof of progressive increase downward to greater depths.

TYPES: PHYSICAL AND PETROGRAPHIC CHARACTER

Most conspicuous are the columnar-jointed dikes and sills, with glassy selvage and more or less development of a subselvage zone. A few irregular, rounded, whaleback shapes of intrusive masses are seen, and some irregular, tapering, or ramifying stringers are offshoots from main dikes or sills. A few examples of buds—expanded elliptical sections at the upper edges of dikes—are known. They are all located where they appear to have expanded at or very near to the constructional surface of the dome and show similar selvage to the shallower dikes and an irregular jointing comparable to that of thick masses of lava generally in Hawaii.

MECHANICS OF INTRUSION

Facts presented in this paper and observed in the field have a bearing on the question of mechanics of intrusion. It is believed that the dikes (primary form of intrusion) have been intruded chiefly along lines already determined by primary crustal rifting or secondary rock jointing and that they have not in any large measure followed lines determined by stoping. The regularity of horizontal pattern, the prevalence of clean, nearly vertical cross-cutting of lava flows even where clinkery layers might seem to offer mechanical or thermally easier courses, and the nearly uniform thickness of many of the dikes and the sharpness of their edges strongly support this interpretation, which interpretation does not necessarily assert whether the intrusion was active or passive. In the writer's opinion this problem has taken an undue prominence because of failure to recognize the dimensional aspect of the matter. In the case of movement by faulting of masses of rock 500 feet or more thick transverse to the plane of movement, it is not very material whether the rock is or is not attached across the plane of movement to the main mass. The frictional and inertia resistances for such masses preponderate over coherence resistances, thus approaching liquid behavior. Similarly, if liquid lava has the hydrostatic pressure to rise in an open column to the surface of a dome at an elevation of, say, 3,000 feet above sea-level, it will nowhere en route encounter pressures of rock on rock greater than its own hydrostatic pressure; and anywhere lower than about 500 feet below the surface the tensile strength of

any rock section is less than the hydrostatic pressure due to superincumbent load. Moreover, this figure holds only for sound, small sections of rock. It is doubtful if any large section of basalt flows with its natural joints and openings would show a tensile strength greater than about 1 or 2 tons to the square foot. On this basis it is doubtful if a 50-foot section of rock of the ordinary continuity of lava flows would resist the separating tendency of a hydrostatic pressure of more than 70 or 75 feet of liquid lava by the combined effect of its own cubic pressure and such cohesion as it possesses. Moreover, with a hydrostatic pressure in excess of the load of rock, there is added to tensile failure the fact that the superincumbent layers would literally be blown or floated off with addition of bending or shearing failure. The contention of the writers is that in large masses the domes of Hawaii have little, if any, greater material integrity or adherence than would a pile of 1- or 2-ton, somewhat interlocking blocks piled fairly closely together, with cushioning layers of cinders, the latter only lightly cemented. Such a mass would offer to the movement of liquid rock only such resistance as comported with its cubic pressure.

One of the queries likely to arise is why there are not more sills. It is the writers' belief that this is due to the natural development of roughly vertical joints and the nondevelopment of horizontal joints. Any extensive mass under the effect of gravity tends to develop vertical joints; horizontal joints are somewhat less likely to develop. Apparently, few such have developed in the Hawaiian domes, owing perhaps to the cushioning tendency of the clinkery layers. In the intrusion of the lava the effects of progressive hydrostatic wedging would be most effective in opening vertical joints because of the riding of upper layers on lower. Wedging along horizontal planes would be much less effective and less progressive. This is believed to be the reason for greater development of dikes, though sills occur in moderate numbers. Moreover, if the notion of pressure-opening of joints by invasion of magma from below as developed here is correct, any dike so formed would tend to be practically vertical rather than normal to the flows. Even if the joints cross-cutting individual flows be normal to the inclined flows, this conception of intrusion would involve progressive offsetting of the line of dike so

as to keep its course approximately vertical, since any systematic departure from verticality would imply a hanging wall and cantilevered condition inconsistent with the basic notion.

ACKNOWLEDGMENTS.—The present paper is based on about six years' work by the senior author and about two years' work by the junior author, with additional work by other geologic assistants, aggregating some six to seven hundred days of field work. Parts of the present paper are based on tabulations and conclusions by the junior author, prepared in 1937. Thanks are due especially to our several assistants for their indispensable aid in the cutting of trails and handling of rope in traversing this precipitous and difficultly accessible mountain country. The data here presented, in which general geologic relations are emphasized, constitute an essential part of the results of geologic and hydrologic studies carried on by the Honolulu Board of Water Supply and are published with the approval of Frederick Ohrt, chief engineer.

STUDIES FOR STUDENTS

FOLDING, ROCK FLOWAGE, AND FOLIATE STRUCTURES

W. J. MEAD
Massachusetts Institute of Technology

ABSTRACT

Variations in opinions as to the usefulness of cleavage in the interpretation of folded structures is due in part to lack of discrimination among the several varieties of foliate structures and the assumption by some observers that all cleavage is flow cleavage. Five varieties of foliate structures—bedding fissility, bedding foliation, fracture cleavage, flow cleavage, and shear cleavage—are described and discussed from the standpoint of physical characteristics and genesis. It is emphasized that compressional folding necessarily involves plastic deformation. Such plastic response is of two kinds, intergranular and interatomic. The folding of an incompletely cemented sedimentary series may occasion only intergranular plastic deformation and grain-crushing, without development of cleavage, until the limits of this type of plastic response are reached by consolidation. If folding continues beyond the limits of intergranular plasticity, interatomic plasticity functions, with development of flow cleavage. Dynamic metamorphism reduces interatomic plasticity, and continued deformation may develop shear failures in the form of thrust faults or shear cleavage.

INTRODUCTION

In a region of folded rocks the problem of the structural geologist is frequently the building of a reasonable three-dimensional picture of folded structures from the fragmental evidence afforded by scattered outcrops, drill holes, test pits, and mine workings. Dip, strike, and lithology of beds alone are inadequate because they do not afford unique solutions. Determinations of "top or bottom" of beds are of great value because they make possible unique solutions of many situations, and it is now generally recognized by structural geologists that every reasonable effort should be made to ascertain the stratigraphic sequence of beds. Unfortunately, sedimentation features useful as indicators, such as cross bedding, ripple marks, and grain-size gradation, are not always available and have a perverse way of being absent when most vitally needed.

Irving, Van Hise, Leith, and other students of folded pre-Cambrian rocks have made the important contribution that the me-

chanics of folding may develop certain secondary structures—fracture cleavage, flow cleavage, and drag folds—which enable the observer to infer correctly the stratigraphic sequence of the beds and the inclination and pitch of the folds. The application of these principles has been of inestimable value to structural geologists and has made possible the correct solution of countless structural problems not otherwise soluble.

In more recent years, under the leadership of Sander, Schmidt, and their students, much attention has been directed to the study of the orientation of the nonplaty minerals as a means of inferring the mechanical history of deformed rocks. The application of the principles and techniques of petrotectonics requires the use of a microscope and the universal stage. Foliation, or cleavage, and its relation to stratification are available for immediate study and interpretation in the field.

It is the observation of the writer that much confusion exists among geologists as to the usefulness of cleavage in the interpretation of the structures of folded rocks. Unfortunately, it is frequently a matter of belief or disbelief, faith or doubt, instead of judgment based on discriminating observation and an understanding of the factors and principles involved. Much of the confusion is occasioned by failure to realize that there are several types of cleavage or foliation, developed in a variety of manners. Flow cleavage and fracture cleavage may develop incidental to, and as a consequence of, folding and may, therefore, be of reliable usefulness in the interpretation of the structures of folded rocks. However, fracture cleavage or flow cleavage also may be developed in zones of shear deformation quite unrelated to folding. Other types of foliation to be described later—types which are neither flow cleavage nor fracture cleavage and which may occur or be developed in folded rocks but not as a consequence of folding—serve further to confuse the structural geologist and call for most careful discrimination in the field.

In this paper it is proposed to review in as simple and elementary a manner as possible the several varieties of cleavage or foliate structures and their causes and the relationships of folding and cleavage, in the hope that such a review may to some extent clarify the situation and may stimulate further discussion and investigation.

VARIETIES OF FOLIATE STRUCTURES

In the following discussion the term "foliate structures" is used in a broad sense to include the textural or structural properties of certain rocks which permit them to be cleaved or parted along approximately parallel surfaces or lines. This property has a wide range of appearances and may be developed in the rocks in various manners. In the following paragraphs an attempt is made to describe and differentiate the principal varieties.

Bedding fissility.—This is the capacity to part parallel to the stratification in many of the finer-grained sedimentary rocks. This property is attributed to compositional and grain-size variation between layers but may be and probably is in many cases due to the low-angle attitudes of platy and elongate rains. It seems reasonable to presume that bedding fissility is accentuated during consolidation by the rotation of platy and elongate particles toward horizontal positions.

Bedding foliation.—In deeply buried, thin-bedded sediments possessing an initial bedding fissility, it seems reasonable that metamorphism induced by heat, pressure, and the permeation of mineralizing solutions, possibly from magmatic sources, would accentuate the bedding by growth and enlargement of the primary platy and elongate constituents, developing a gneissic or a schistlike rock without the operation of plastic deformation or shear usually assumed to be necessary in the development of schists. It is not intended to imply that all flat-lying schists are developed in this manner or that they have not undergone shear or flow. It is unreasonable to assume that all bedding foliation has escaped subsequent deformation. In some instances the development of this type of foliation may well be an accompaniment of flow or creep due to load, described by R. A. Daly[1] as load cleavage.

Fracture cleavage.[2]—This type of foliate structure is a phenomenon of rock fracture and consists of closely spaced, parallel, shear joints or ruptures usually confined to a weaker layer between stronger layers. It is frequently observed in the limbs of moderate folds where

[1] "Metamorphism and Its Phases," *Bull. Geol. Soc. Amer.*, Vol. XXVIII (1917), p. 375.

[2] C. K. Leith, "Rock Cleavage," *U.S. Geol. Surv. Bull. 239* (1905), pp. 119 ff.

it has developed as a consequence of interlayer shear incidental to folding. Fracture cleavage is in no way dependent on the orientation of constituent minerals, and the plates between the shear ruptures are themselves not cleavable. This type of cleavage is commonly but not necessarily an accompaniment of folding. It is also found in fault gouges and shear zones and serves as an admirable indicator of the direction of shear displacement.

Flow cleavage.—This type of cleavage has been variously described as "flow cleavage,"[3] "slaty cleavage,"[4] and "axial-plane cleavage."[5] It is due to the parallel orientation of platy and elongate minerals and is the result of plastic deformation by interatomic rearrangement of constituents. It is a consequence of dynamic metamorphism. It is homogeneously or evenly developed in the rock and not spaced into parallel surfaces as is the case of shear cleavage. Its orientation is perpendicular to the short axis of strain, which is equivalent to saying that it is perpendicular to the direction of the resultant of compressional stresses. It may likewise be described as developing in the directions of greater elongations of the plastically deformed mass. Its relationship to strain places it approximately parallel to the axial plane of folds. The simple relationship between flow cleavage and strain makes it reliably useful in the interpretation of folds. It is generally but not exclusively a consequence of folding.

Flow cleavage may be accentuated and rendered coarser grained by subsequent static metamorphism in a manner similar to the development of bedding foliation described in the foregoing section.

Shear cleavage.—This type of cleavage consists of roughly parallel, closely spaced surfaces of shear displacement on which platy minerals may have developed and into which they may have been dragged. The spacing of shear surfaces varies from a millimeter or less to such wide spacing that the term "cleavage" becomes no longer applicable, and the rock is best described as having undergone minor parallel faulting. When the spacing is unusually close, shear cleavage may simulate and be easily confused with flow cleavage.

[3] *Ibid.*, pp. 23 ff. [4] *Ibid.*, p. 15.

[5] H. W. Fairbairn, "Notes on Mechanics of Rock Foliation," *Jour. Geol.*, Vol. XLIII (1935), p. 591.

Shear cleavage may be developed in rocks having earlier flow cleavage or bedding foliation. It may have any angular relationship to these earlier foliate structures but is most likely either to parallel earlier foliation or to cross it at relatively large angles. Small angular differences between shear cleavage and an earlier foliation are not to be expected, because the earlier foliation affords planes of weakness which prevent the formation of shear failures at angles close to them. Closely spaced shear cleavage, when it crosses earlier flow cleavage, may nearly or completely obliterate the latter. When it is parallel to an earlier flow cleavage, it may be difficult or impossible to recognize its presence.

Shear cleavage is a phenomenon of rock flowage rather than of fracture, but it is not a consequence of homogeneous plastic yielding of the rock. Deformation is accomplished by shear along more or less closely spaced surfaces, but the mineral rearrangement along these surfaces is largely by interatomic adjustments without the development of fracture ruptures in the rock. Brittle layers and brittle minerals may be locally fractured.

This type of cleavage is oriented approximately 45° from the axis of the compressive resultant of force. Each shear surface may be considered as a minute thrust fault. Since two directions of shear approximately perpendicular to each other are always possible, and since one may develop to the exclusion of the other, the inferring of the direction of the causal stresses is not a simple problem. Shear cleavage, although commonly found in folded rocks, is not a consequence of folding. This statement will be amplified in a later section of this paper.

FOLDING

Definitions are difficult, dangerous, but necessary. For the purposes of this discussion folds are defined as undulations formed by the flexing of layered rocks.[6]

There is a wide range in the degree or intensity of folding, from very gentle undulations which may or may not be original or depositional to extremes of folding in which the degree of deformation

[6] It is not intended to imply that other types of folds such as shear folds, contorted masses of marble, rock salt, or ice, or the folded structures formed by differential loading or squeezing of muds or clay, are not properly called "folds."

and structural disturbance is intense. The present discussion is not concerned with the more gentle or moderate phases of folding and is intended to apply to deformation which might be described as more-than-moderate folding.

Very gentle flexing of layered rocks may conceivably occur, with negligible plastic deformation, by minute fracturing, crushing, and opening of joints. In folding that is more-than-moderate, plastic deformation of at least some of the layers is imperative. It may be stated as a fundamentally important principle that folding requires the plastic behavior of part or all of the layers involved—that plasticity is demanded in proportion to the degree of folding.

PLASTIC DEFORMATION (ROCK FLOW)

The term "plastic deformation" is here used broadly to include homogeneous change in shape, regardless of the internal mechanism by which it is accomplished. Plastic deformation involves the differential, positional shifting of constituent materials.

In fine-grained soft rocks (clays, muds, compaction shales, marls, etc.), positional shifting is largely intergranular, and these materials may be said to possess intergranular plasticity. This type of plasticity may involve a certain amount of grain-crushing. It does not develop cleavage. It may develop crenulations and minor distortions, including drag folds, in thinly bedded sediments. In special cases, not believed to be common or important, the mica plates in extremely micaceous muds may be oriented along flow directions, producing some degree of foliation.

In compact, dense, well-cemented rocks, intergranular plasticity is minimized and positional shifting of constituents is largely by interatomic rearrangement by physical or chemical means. This type of plasticity functions by recrystallization, neo-crystallization, and gliding, with a minor amount of granular rotation and shifting, and may be designated as interatomic plasticity. The results of this type of plastic deformation are generally described as dynamic metamorphism.

Depending on the composition of the rock, interatomic plastic deformation may or may not develop cleavage. The cleavage of dynamically metamorphosed rock is dependent on the parallel orientation of elongate or platy minerals, largely the latter. Rocks

such as limestone, marble, quartzite, and rock salt may be deformed plastically without the development of cleavage. These rocks are not compositionally capable of producing mineral types essential to cleavage.

The shales and related rock types—arkose, graywacke, impure limestones, and impure quartzites are compositionally capable of developing micas, chlorite, and other platy and elongate minerals under conditions of dynamic metamorphism. Leith[7] developed the now generally recognized principle that in flow cleavage the orientation of the platy and elongate minerals is determined and controlled by the orientation of strain in the plastically deformed rock, and that the cleavage due to the parallel arrangement of the platy and elongate minerals developed by dynamic metamorphism is perpendicular to the shortest axis of strain. This cleavage may be variously described, therefore, as being perpendicular to the axis of compression or being parallel to the elongations of the rock mass.

Intergranular plasticity is obviously dependent on freedom of intergranular movement and is limited by intergranular friction. Adsorbed water films and interstitial moisture contribute to the intergranular plasticity of clays and other fine-grained rocks, and this type of plasticity is diminished by consolidation. In so far as plastic deformation squeezes out water, reduces voids, and consolidates the rock, the material becomes less intergranularly plastic.

Interatomic plasticity also has its modifications and limitations. Pure marble, pure quartzite, and rock salt, when plastically deformed, respond by intracrystal gliding and recrystallization. In rocks of the shale group interatomic plasticity functions largely by the development of the platy and elongate minerals. In such rocks interatomic plasticity is to a degree determined by the compositional ability to produce these new minerals. As dynamic metamorphism proceeds, this ability of the rock is reduced and its interatomic plasticity is correspondingly diminished, except in rocks having a sufficient content of carbonates to dominate the situation.

RELATION OF PLASTICITY AND CLEAVAGE TO DEFORMATION

With the foregoing summary of the various types of foliate structures and with emphasis on the fact that plastic deformation, which

[7] *Op. cit.*, p. 112.

may be accomplished either by intergranular rearrangement or by interatomic reorganization, is an essential accompaniment of folding, we may turn to a consideration of the series of events involved in the compressional deformation of a thick accumulation of sediments.

Fine-grained, argillaceous rocks, which may be called "shale" under a broad usage of the term, may be presumed to predominate in any great series of sediments. It has been estimated by F. W. Clarke[8] and others that sediments of the shale type account for approximately 80 per cent of all sediments. The behavior of a great accumulation of sediments during the earlier stages of compressional deformation may therefore be assumed to be largely controlled by the behavior of shale. The mechanically stronger and stiffer layers of sandstone and carbonate rocks commonly referred to as the more competent layers, of course, play an important part in determining the type and characteristics of the folds developed.

Under load of superimposed sediments the consolidation of clays and muds into shale proceeds with astonishing slowness. This is due to the fact that consolidation can be accomplished only by the squeezing-out of interstitial water, and this loss of water is inhibited by the low permeability of the material itself and by the fact that in these fine-grained materials, containing much matter of colloidal size, a large proportion of the water is rather firmly held on the grain surfaces by adsorption. The retention of water in shales is illustrated in the following specific cases.

A large number of moisture determinations on core-boring samples of Fort Union shale of Tertiary age in North Dakota showed an average moisture content equivalent to 40 per cent of the volume of the shale. An average of a great number of moisture determinations on core-boring samples from the Bear Paw shale of Cretaceous age at the Fort Peck Dam site in eastern Montana showed an average content equivalent to 30 per cent of the volume of the shale. Similar moisture determinations on a large number of core samples of shale of Pennsylvanian age from the Possum Kingdom Dam site on the Brazos River in Texas gave an average moisture content equivalent to 18 per cent of the volume of the shale. Some years ago the writer had occasion to examine in detail a 500-foot section

[8] "Data of Geochemistry," *U.S. Geol. Surv. Bull. 770* (1924), p. 34.

of Pennsylvanian shales underlying the La Salle limestone in Illinois. No moisture determinations were made, but slaking tests showed that the entire shale section was compaction shale[9] which had undergone very little, if any, intergranular cementation and presumably possessed intergranular plasticity.

The conclusion seems inescapable that folding, developed in the earlier stages of compressional deformation of a thick mass of sediments, is accomplished by intergranular plasticity and consequently without the development of cleavage. Fine-grained sediments may be folded to an extreme degree without the development of secondary cleavage where conditions have not produced sufficient consolidation to prevent intergranular plasticity. Closely folded shales devoid of flow cleavage are not uncommon. Folded shales of this type are excellently exposed in the Claremont formation along the "Tunnel Road" east of Oakland, California.

Pressure and deformation involved in the folding of a mass of shale are very effective in promoting consolidation. As folding proceeds, with reduction of intergranular plasticity by consolidation, a condition is eventually reached where further plastic deformation requires the functioning of interatomic plasticity, and this stage marks the initiation of the development of flow cleavage.

The amount of folding that is possible before the limits of intergranular plasticity are reached depends on a variety of factors, among which are fineness of grain, which influences permeability and, consequently, degree of consolidation under load, and thickness of shale formations, because thick formations consolidate by compaction less readily, owing to the longer travel distance for the escaping water through the impervious material. Thin layers of shale between sandstone beds consolidate more easily because of the opportunity for escape of water.

After the limit of intergranular plasticity is reached, continued deformation demands interatomic plasticity, and folding proceeds with the development of flow cleavage essentially parallel to the axial planes of the folds. It is not unreasonable to expect to find flow cleavage developed in thin shale layers between layers of sandstone and absent in thicker shale layers of the same series, because the

[9] W. J. Mead, "Geology of Dam Sites," *Civil Engineering* (1937), p. 392.

limits of intergranular plasticity may be reached earlier in the more easily consolidated thin layers, as explained above.

It should be emphasized that the development of flow cleavage does not necessarily begin in the early stages of folding of a thick sedimentary series. Flow cleavage is not initiated until the limits of intergranular plasticity are approached, which means that it may not make its appearance until the later stages of folding and thus escapes the distortion and change in orientation that would have been necessary had it developed in the early stages of folding.

It is not inconceivable that a series of sedimentary beds may be thoroughly lithified by consolidation and cementation prior to deformation. Such rocks would have little intergranular plasticity, and folding would call upon interatomic plasticity from the start, resulting in the initiation of flow cleavage in the early stages of folding.

As folding proceeds by interatomic plasticity and the development of flow cleavage, interatomic plasticity is progressively diminished. Dynamic metamorphism of shales involves changes in composition, both chemical and mineralogical, and develops a slate or a schist less interatomically plastic than the parent-rock. Just as a limit of intergranular plasticity is reached by consolidation, a limit of interatomic plasticity is approached by metamorphism.

When compressional stresses continue after a thorough dynamic metamorphism of the shale has been accomplished, the rock, less willing to deform homogeneously in the manner of a plastic material, may respond by yielding along surfaces of shear failure. This may result in the development of thrust faults or, depending on conditions of restraint and manner of easiest relief from stress, deformation may be accomplished on multiple surfaces of shear dislocation. If conditions are those of rock flowage, these are tight shears accomplished by interatomic rearrangement and are not shear fractures. The phenomenon is one of rock flowage rather than of rock fracture but differs from flow cleavage by being confined to separate surfaces or thin zones of shear dislocation.

If the rate of deformation exceeds the time requirements for interatomic rearrangement, shear fractures necessarily result, and fracture cleavage as distinguished from shear cleavage is developed.

In a mass of rock which has been deformed in this manner, it is to be expected that certain lithological types will undergo tight-shear foliation (shear cleavage), while other types, less amenable to flowage phenomena, exhibit shear-fracture foliation (fracture cleavage). There is little importance in distinguishing between these two varieties of cleavage, because they have the same relationship to causal stresses and accomplish the same deformational results.

This type of deformational response which is a consequence of the reduction of interatomic plasticity is not a continuation of folding. The folded mass of rock has lost to a considerable extent its layered nature necessary to folding, and the continuance of deformation by multiple shearing cannot be regarded as a continuation of flexing. The folds themselves are deformed, not accentuated.

Masses of layered sediments which have been folded to a degree to develop thorough dynamic metamorphism and flow cleavage may later be subjected to deformative stresses operating in directions different from those which caused the original folding. If this deformation occurs at relatively shallow depth or too rapidly to permit flow phenomena, faults and fracture patterns are developed. If the deformation occurs under sufficient load and at a rate slow enough to permit flowage phenomena, it appears probable that such deformation would be accomplished by shear rather than by folding. Thrust faults might result, but, depending on load and restraint, shear cleavage might well develop as a means of accomplishing the required deformation of the mass. Folding does not seem probable because the mass has lost its layered condition and because interatomic plasticity has been so greatly reduced by the earlier dynamic metamorphism.

INTERPRETATION OF FOLIATE STRUCTURES

Intelligent utilization of cleavage in the interpretation of the structures of folded rocks requires correct classification of the type or types of foliate structures observed. Much of the existing confusion in the utilization of cleavage as a guide to structural interpretation has been due to the incorrect assumption that all cleavage is flow cleavage. The statement that flow cleavage develops essentially parallel to the axial planes of folds has been doubted and

discredited by geologists who have observed cleavage following around the crests and troughs of folds. The writer has heard many discussions, in which one observer insists that all cleavage is axial-plane cleavage and does not follow the bedding around the convolutions of folds, another insisting that the first man is wrong because cleavage follows the beds in folded rocks. One has seen flow cleavage (axial-plane cleavage); the other had observed bedding foliation which had been folded or developed subsequent to folding.

No hard and fast specifications can be written for the identification of foliate structures. The problem perhaps falls more into the category of an art than a science. Experience and familiarity with a wide variety of occurrences is of value. A geologist whose experience has been confined to the folded rocks of the Lake Superior region, where flow cleavage uncomplicated by bedding foliation or shear cleavage is so successfully applicable to the structural problems, may well experience some astonishment in other regions where bedding foliation and shear cleavage complicate the structural picture. A student of structural geology, initially confronted with the foliation complexities of the folded rocks of New England, may doubt the practical usefulness of cleavage and the statements in the literature that "cleavage develops parallel to the axial planes of folds."

The outstanding characteristic of flow cleavage is that it develops homogeneously through a given bed. Since it is a product of plastic deformation, the entire bed has been uniformly affected. Every cubic millimeter has taken part, and a homogeneous development of cleavage has resulted. This is particularly true in the fine-grained rocks. Flow cleavage may easily be confused with bedding foliation, and the best means of identification is to find flow cleavage in angular relationship to stratification.

Shear cleavage, in contrast to flow cleavage, is not homogeneously distributed through the mass but is spaced into parallel surfaces, each one of which is a surface of shear failure with some degree of shear displacement, however minute. When shear cleavage consists of extremely closely spaced surfaces, it may simulate flow cleavage, and identification may be difficult or impossible in the hand specimen. In the field, however, the true nature of the shear cleavage

is usually discernible in neighboring beds or on tracing it into areas in the vicinity where it is less closely spaced.

The angular relationship between shear cleavage and the effective resultant of causal compressional stress is not a simple one in contrast to the simple perpendicular relationship of flow cleavage to the least axis of strain. Shear cleavage is a manifestation of shear failure and presumably develops at angles somewhat less than 45° to the direction of compression.

There seems to be a reasonable analogy between the orientation of thrust faults and shear cleavage in their angular relationship to causal stresses. When the direction of easiest relief is upward, thrust faults strike at right angles to the direction of compression and dip either way, depending on whether we consider them as overthrusts or underthrusts. Similarly, where easiest relief is upward, shear cleavage strikes at right angles to the direction of compression and may dip either way from that strike. Wherever two sets of shear failures are possible, one set generally develops to the exclusion of the other, as either set is capable of providing the necessary deformational response. Shear cleavage, dipping in opposite directions in separate portions of a single region of deformation, may therefore have been developed by the same deformation.

Where the direction of easiest relief is lateral (horizontal), steep-angle thrust faults are developed with horizontal displacement striking somewhat less than 45° either to the right or to the left of the direction of compressive force. Continuing the analogy between shear cleavage and compressional faults, we may infer that where the direction of easiest relief is lateral, shear cleavage with vertical dip may develop, striking somewhat less than 45° either to the right or to the left of the direction of compression and that locally within the deformed mass either of these two directions of strike may develop to the exclusion of the other.

It should not be inferred from the two preceding paragraphs that the direction of easiest relief is necessarily either vertical or laterally horizontal. Where the direction of easiest relief is inclined, the dip of shear cleavage should be correspondingly intermediate between 45° and 90°, with a shift in the strike directions called for by the geometry of the situation.

Since each surface in shear cleavage is actually a minute thrust fault, it is frequently possible to observe the direction of displacement, which aids materially in determining the approximate direction of the axis of compression. Drag-lineation, minute slickenslides, or scoring are also useful in indicating the line of displacement.

Shear cleavage developed by rotational deformation in a weaker layer between two or more competent layers should have the same relationship to causal stresses as does fracture cleavage. The writer has seen instances of fracture cleavage in the field with development of platy minerals between the cleavage plates, strongly suggesting that the cleavage should have been interpreted as shear cleavage rather than fracture cleavage.

In regions which have had a complex history of deep-seated deformation, it is reasonable to expect a discouraging complexity of shear cleavages, usually superimposed with varying angular relationships on an earlier flow cleavage.

Bedding foliation is an accentuation of primary stratification by metamorphic mineralizing processes involving grain enlargement, recrystallization, and replacement, with implied compositional changes both mineralogical and chemical. There seems to be no reason why it should not develop prior to folding, during folding, or subsequent to folding. Its development depends upon temperature, pressure, and the availability of mineralizing solutions. The development of bedding foliation may reasonably be looked upon as an early stage of granitization. Mineralogically, it may differ from flow cleavage and shear cleavage in that albitization, the development of garnets, staurolite, etc., may be an accompaniment. However, since similar mineralization may be superimposed on flow cleavage or shear cleavage, its presence may not be considered as diagnostic.

In fine-grained, homogeneously thin-bedded rocks, bedding foliation may simulate flow cleavage in appearance. In general, the spaced or layered nature of the foliation and its faithful parallelism with stratification are the best criteria for distinguishing it from flow cleavage.

Folding may occur subsequent to the development of bedding foliation and produce a folded schist in which the schistosity follows faithfully around the crests and troughs of the flexures. Such folded

schists have been incorrectly pointed out as a refutation of the usefulness and reliability of cleavage as an aid to the interpretation of folded structures. Most folded schists possess only bedding foliation that follows the original stratification. The writer has seen no instances in which flow cleavage developed in the folding of schists, but such cases may, and probably do, exist.

It is of interest to note that the Z or Gothic type of folding is frequently found in folded schists. An explanation of this type of folding may lie in the fact that the metamorphism which developed the foliation reduced the interatomic plasticity of the rock, and a type of folding calling for a minimum of rock flowage is the one to develop. The mechanical requirements for folds formed with a minimum of plastic deformation in laminated materials having abundant interlayer shear facilities are sharply angular crests and troughs with a minimum of curvature in the limbs.

REVIEWS

German-English Science Dictionary for Students in the Agricultural, Biological and Physical Sciences. By LOUIS DE VRIES, with the collaboration of members of the Graduate Faculty of Iowa State College. New York and London: McGraw-Hill Book Co., 1939. Pp. 473. $3.00.

As no branch of science is sufficient unto itself but draws more and more upon the various other branches, the need of a comprehensive German-English science dictionary has become strongly felt. Confronted with this need, members of the science faculty at Iowa State College prevailed upon Professor De Vries to compile for them and their students a suitable dictionary to facilitate reading scientific German. Each department began by submitting a list of outstanding German texts, reference books, journals, dictionaries, encyclopedias, and glossaries from which information and specific word lists could be derived. The result is the present volume of 48,000 entries.

While the practical value of this volume can properly be appraised only after some experience in its use, it would seem to the reviewer that this dictionary, strong in scientific terms and concentrating on the words most frequently encountered in scientific literature, is likely to prove a boon to scientists reading German publications.

R. T. C.

The Geology of the Kaitangata-Green Island Subdivision, Eastern and Central Otago Divisions, by M. ONGLEY. (New Zealand Geological Survey [new ser.] Bull. 38.) Wellington, N.Z., 1939. Pp. 90; Pls. 5; figs. 7; maps 9.

The Geology of the Naseby Subdivision, Central Otago, by J. H. WILLIAMSON. (New Zealand Geological Survey [new ser.] Bull. 39.) Wellington, N.Z., 1939. Pp. 141; pls. 33; figs. 28; maps 10.

The report on the geology of the Kaitangata-Green Island subdivision describes an area of 1,100 square miles in the southeastern part of Otago, one of the earliest districts settled in New Zealand. The proximity of this region to important commercial and industrial centers has insured utilization of the extensive seams of low-grade coal found in the Cretaceous.

Naseby Subdivision in Central Otago includes about 960 square miles. The report describes the general and economic geology of the Maniototo

depression, where in the last half of the nineteenth century several extensive alluvial diggings supported a considerable population. Some sluicing is still carried on, quartz lodes yield gold and scheelite, and lignite is mined for local use.

Both of these bulletins have complete bibliographies and are well illustrated with good photographs, sketches, and maps. They present important contributions to the study of the geology of New Zealand.

LOUISE BARTON FREEMAN

The Physiography of Victoria. By E. SHERBORN HILLS. Melbourne: Whitcombe & Tombs, Ltd., 1940. Pp. xx+292; figs. 351. 8*s.* 6*d.*

This book is subtitled "An Introduction to Geomorphology," and as such presents the principles of this science illustrated as far as possible from the state of Victoria. An introductory chapter on geological principles is included for the guidance of readers who have had no such training; then the various agents and their effects are discussed. The last quarter of the book is devoted to the physiographic divisions of the region.

The title is unfortunate, for it might well lead one to believe the volume has only a limited application whereas it really is general in character. It is ably written, extremely easy to read, and the illustrations are, in the main, excellent, although a few were ill chosen for the method of reproduction employed and so are murky. The Subject Index is full, and an Index of Places is a feature of especial value to persons who are not familiar with this region.

C. W. STERNBERG

The Physiographic Provinces of North America. By WALLACE W. ATWOOD. Boston: Ginn & Co., 1940. Pp. 536; figs. 281; color plates 4; 1 folded map. $4.80.

Professor Atwood has prepared this book to accompany a college course in regional physiography of the North American continent. The principles of physiography which must be used in the interpretation of the present physical features in the landscape are reviewed in the text.

The first chapter, giving "The Regional Idea of Geography," discusses climatic, agricultural, political, vegetation, industrial, soil, and physiographic regions, and cites the Black Hills as an illustration of the interrelation of regional studies. For each province the author describes the physical features of the area involved, structure and materials, geologic history, and the evolution of present land forms. At the end of each

chapter there is a list of references for additional reading and a list of topographic maps to illustrate the particular provinces covered in that chapter.

The book is written in an interesting compact style, and the illustrations are unusually fine. They include many excellent photographs of scenic features discussed in the text, relief maps and block diagrams, several colored plates, and a series of sections by Erwin Raisz. A large map by Dr. Raisz, showing with fine definition the land forms of the United States, is folded in the book.

LOUISE BARTON FREEMAN

"Characteristics of Minable Coal of West Virginia." By A. J. W. HEADLEE and JOHN P. NOLTING, JR. (*West Virginia Geological Survey*, Vol. XIII.) Morgantown, W.Va., 1940. Pp. viii+272; figs. 130. $1.53.

This report compiles and summarizes present knowledge of the physical and chemical characteristics of all minable coals of West Virginia. Prepared in order to answer inquiries from producers and consumers relative to these coals, it will undoubtedly be of value to such individuals.

The sixty-two minable seams range in age from the Pocahontas group to the lower part of the Dunkard series and underlie approximately 55 per cent of the area of the state. The second part of the report is a statistical and correlational study of the coal analyses. Individual analyses are gathered to give a cumulative distribution curve of each seam, such a curve readily lending itself to the classification of coal. The Appendix gives nomenclature of minable seams and tables of coal reserves.

C. W. STERNBERG

Geology of the Draper Mountain Area, Virginia. By BYRON N. COOPER. (Virginia Geological Survey Bull. 55.) University, Va., 1939. Pp. 98; pls. 23; figs. 4.

The Draper Mountain area, which lies in the southwestern part of the Appalachian Valley and Ridge province, is a maturely dissected tract within the New River drainage basin. The stratigraphic succession ranges from Lower Cambrian to Middle Mississippian with about 16,000 feet of beds exposed. The rocks are broken by several low-angle overthrust faults of great horizontal displacement. A geological map of the area, several cross sections, and numerous photographs add to the value of this report.

LOUISE BARTON FREEMAN

INDEX TO VOLUME XLVIII

Absaroka Range, Wyoming (R. T. Chamberlin), 679

Absaroka Range, Wyoming, geology along the southern margin of the: discussion (C. M. Bauer), 324

Absaroka Range, Yellowstone Valley, Montana (L. Horberg), 296

Accumulation of peat, rate of, in Bermuda (A. S. Knox), 778

Age of Absaroka Range, Wyoming (C. M. Bauer), 324
- of dikes in Pacific Northwest (G. E. Goodspeed), 175
- of dune systems in southern High Plains (F. A. Melton), 137
- of faulting, southern California (W. J. Miller), 408
- of isolated transverse dune ridges in southern High Plains (F. A. Melton), 137
- of loess and lake silts in Indiana (W. D. Thornbury), 460
- of Mistassini series, Quebec (G. W. H. Norman), 520
- of sand dunes in southern High Plains (F. A. Melton), 143
- of transverse dune series, southern High Plains (F. A. Melton), 137

Akermanite, formation of (N. L. Bowen), 248

Albanel Lake, Quebec (G. W. H. Norman), 520

Alden, William C. Cited on geology of Yellowstone Valley, Montana (L. Horberg), 288, 290, 291, 295

Alluvial fan deposits, Santa Fe formation, New Mexico (C. S. Denny), 86

Analysis of regional fault pattern in Pryor uplift, Montana (D. L. Blackstone, Jr.), 616

Anchored dune forms (complex) in southern High Plains (F. A. Melton), 135

Anderson, Alfred L., and Veral Hammerand. *Contact and endomorphic phenomena associated with a part of the Idaho batholith*, 561

Anderson, G. H. Cited on pseudoclastic process of replacement (A. L. Anderson and V. Hammerand), 576

Antevs, Ernst. Cited on age of Lake Estancia (F. A. Melton), 143
Cited on length of postglacial time (A. S. Knox), 779

Aplitic dikes of Pacific Northwest (G. E. Goodspeed), 176

Apparatus for forming artificial helictites (L. C. Huff), 644, 645

Aragonite helictites (L. C. Huff), 659

Armored mud balls (H. S. Bell), 1

Artesian water, condition for (M. K. Hubbert), 913

Artificial gypsum flowers (L. C. Huff), 652

Artificial helictites and gypsum flowers (L. C. Huff), 641

Artiodactyla in Herculaneum, Missouri, region (E. C. Olson), 54

Ash formations of the island, Hawaii. By Chester K.Wentworth. Review by Raymond E. Janssen, 111

Asymmetric anticlines, Pryor Mountains, Montana (D. L. Blackstone, Jr.), 604

Asymmetric folds passing into faults, Pryor Mountains, Montana (D. L. Blackstone, Jr.), 604

Atwood, Wallace W. The physiographic provinces of North America. Review by Louise Barton Freeman, 1023

Augen gneiss of Idaho batholith (A. L. Anderson and V. Hammerand), 575
- origin of (A. L. Anderson and V. Hammerand), 584

Axelrod, Daniel I. *A record of* Lyonothamnus *in Death Valley, California*, 526

Baker, A. A. Cited on geology of southeastern Utah (D. L. Blackstone, Jr.), 614

Bald Ridge Butte, Washington (A. L. Anderson and V. Hammerand), 562

Balk, Robert, and Rudolf Ruedemann (eds.). Geology of North America. Review by Louise Barton Freeman, 221

Ball, the low and, of the eastern shore of Lake Michigan (O. F. Evans), 476

Balls, armored mud (H. S. Bell), 1

Bancroft, Dennison, and Francis Birch. *New measurements of the rigidity of rocks at high pressure*, 752

Banding of shallow-type dikes, Koolau Range, Oahu (C. K. Wentworth and A. E. Jones), 993

Barcan dunes (complex) in southern High Plains (F. A. Melton), 131
age of (F. A. Melton), 140

Barcan dunes (simple) in southern High Plains (F. A. Melton), 115
age of, 137

Basalt dikes in Pacific Northwest (G. E. Goodspeed), 175

Basin, Bighorn, diastrophic behavior around the (R. T. Chamberlin), 673

Basins and ranges, development of, in Beartooth-Bighorn region (R. T. Chamberlin), 701

Bastin, Edson S. *Discussion: A note on pressure stylolites*, 214
Review of Principles of economic geology. By Wm. H. Emmons, 446
Cited on hydrothermal origin of aplites in Ontario (G. E. Goodspeed), 192

Bateman, J. D. *Stratigraphy and correlations in the Birch–Slate Lakes district, Northwestern Ontario*, 619

Batholith, Idaho, contact and endomorphic phenomena associated with a part of the (A. L. Anderson and V. Hammerand), 561

Bauer, C. Max. *Discussion: Geology along the southern margin of the Absaroka Range, Wyoming*, 324

Bays, elliptical, in South Carolina and the shape of eddies (C. W. Cooke), 205
hypotheses of origin of, 205

Bays, South Carolina, comparison of with shape of eddy (C. W. Cooke), 210

Beartooth Range, Montana (L. Horberg), 275

Bedding fissility, physical characteristics and genesis of (W. J. Mead), 1009

Bedding foliation, physical characteristics and genesis of (W. J. Mead), 1009

Behavior, diastrophic, around the Bighorn Basin (R. T. Chamberlin), 673

Behre, C. H., Jr. Review of The volcano-seismic crisis at Montserrat, 1933–37. By Frank A. Perrett, 449

Bell, Hugh Stevens. *Armored mud balls*, 1

Bennett, Hugh Hammond. Soil conservation. Review by Louise Barton Freeman, 560

Bermuda, the peat deposits of, and evidences of postglacial changes in sea-level (A. S. Knox), 767

Berry, Edward W. Contributions to the paleobotany of Middle and South America. Review by Louise Barton Freeman, 112

Betula in Bermuda (A. S. Knox), 774

Bevan, Arthur. Cited on "summit peneplain," Beartooth Range, Montana (L. Horberg), 287

Bighorn Basin, diastrophic behavior around the (R. T. Chamberlin), 673
Montana (D. L. Blackstone, Jr.), 590
Wyoming (C. M. Bauer), 327

Bighorn-Beartooth development, Wyoming (R. T. Chamberlin), 678

Bighorn River, Montana (D. L. Blackstone, Jr.), 591

Billings, M. P. Cited on diabase dike, Medford, Massachusetts (F. A. Melton), 178

Biotite-quartz diorite of Idaho batholith (A. L. Anderson and V. Hammerand), 570
origin of, 583

Birch, Francis, and Dennison Bancroft. *New measurements of the rigidity of rocks at high pressure*, 752

Birch–Slate Lakes district, northwestern Ontario, stratigraphy and correlations in the (J. D. Bateman), 619

Bison in Herculaneum, Missouri (E. C. Olson), 39, 56

Blackstone, D. L., Jr. *Structure of the Pryor Mountains, Montana*, 590
Cited on structure of Pryor block, Montana (R. T. Chamberlin), 704

Blackwelder, Eliot. Cited on fluting and faceting of rock fragments (J. H. Maxson), 748

Blake, W. P. Cited on forms produced by wind in southern California (W. H. Maxson), 724

Blatchley, W. S. Cited on formation of helictites (L. C. Huff), 648

Block behavior, types of (R. T. Chamberlin), 688

Blocks, limestone, in Joliet limestone, northeastern Illinois (J H. Bretz), 361

Bloomer, Robert O., and Joseph K. Roberts. Catalogue of topographic and geologic maps of Virginia. Review by L. C. Glenn, 219

"Blowout" or "parabolic" dune (simple) in southern High Plains (F. A. Melton), 126
age of, 137

Blowouts and windrifts (complex) in southern High Plains (F. A. Melton), 134
age of, 137

Blue Ridge Range, Virginia (E. C. H. Lammers), 305

The Bogotá fault, Colombia, South America (T. Clements), 660

Boone, Lee. Marine *algae, coelenterata, annelida, echinodermata, crustacea,* and *mollusca.* Review by Raymond E. Janssen, 220

Boundary structure of Yellowstone Valley, Montana (L. Horberg), 279

Bovidae in Herculaneum, Missouri, region (E. C. Olson), 56

Bowen, Norman L. *Progressive metamorphism of siliceous limestone and dolomite,* 225
Waldemar Christopher Brøgger, 1851–1940, 444
Review of A descriptive petrography of the igneous rocks, Vol. I. By Albert Johanssen, 219

Breakers, origin and behavior of, in Lake Michigan (O. F. Evans), 505

Breccia, Max Meadows fault (B. N. Cooper and J. C. Haff), 945

Breccias, early basic, of Yellowstone Park, Montana (L. Horberg), 283

Bretz, J Harlen. *Solution cavities in the Joliet limestone of northeastern Illinois,* 337

Brøgger, Waldemar Christopher, 1851–1940 (N. L. Bowen), 444

Broun, G. Cited on lows and balls on shores of Baltic Sea (O. F. Evans), 479

Bruce, E. L. Cited on geologic sequence east of Slate Lake, Ontario (J. D. Bateman), 634
Cited on geologic sequence west of Slate Lake, Ontario (J. D. Bateman), 635

Brunhes, J. Cited on eolian potholes in rocks of Nubian Desert (J. H. Maxson), 725

Bryan, Kirk. Cited on wind-faceting (J. H. Maxson), 734
Cited on solution-faceting (J. H. Maxson), 739

Bucher, W. H., *et al.* Cited on alternating symmetry of Bighorn Range (R. T. Chamberlin), 680

Buried cedar trees and peat bogs as evidence of submergence of Bermuda (A. S. Knox), 770

Buried Eocene sediments near Ventura, California, metamorphism of, and of sediments of the deep well near Wasco, California (J. B. Lyons), 436

Illinoian soils and weathered zones, Indiana (W. D. Thornbury), 455

Burlington (Mississippian) limestone in central Missouri (W. A. Tarr and W. D. Keller), 199

Burwash, E. M. Cited on classification of sediments, Birch–Slate Lakes district, Ontario (J. D. Bateman), 627, 630

Butts, Charles. Cited on structure of Little North Mountain, Virginia (R. S. Edmundson), 534

Buwalda, J. P. Cited on faulting in southern California (W. J. Miller), 399

Calcareous shales, cleavage in (E. C. H. Lammers), 304

California, Crestmore, merwinite from (N. L. Bowen), 252
Mammoth embayment, tectonics of the rhyolite in the (J. R. Chelikowsky), 421
a record of Lyonothamnus *in Death Valley,* (D. I. Axelrod), 526
southern, some features of faulting in (W. J. Miller), 385
Ventura, metamorphism of the deeply buried Eocene sediments near, and of the sediments of the deep well near Wasco, California (J. B. Lyons), 436
Wasco, metamorphism of sediments of the deep well near, and of the deeply buried Eocene sediments near Ventura, California (J. B. Lyons), 436

Cambrian quartzite pebbles, Fincastle, Virginia (E. C. H. Lammers), 305

Camelidae in Herculaneum, Missouri (E. C. Olson), 54

Campbell, M. R. Cited on occurrence of limestone breccia near Draper Mountain area, Virginia (B. N. Cooper and J. C. Haff), 970

Canadian River Valley, Texas (F. A. Melton), 139
Canis dirus in Herculaneum, Missouri, region (E. C. Olson), 38
Canis dirus Leidy in Herculaneum, Missouri, region (E. C. Olson), 42
Canis latrans Say in Herculaneum, Missouri, region (E. C. Olson), 42
Capillarity, effect of (M. K. Hubbert), 884
influence of, upon a two-fluid interface (M. K. Hubbert), 889
Carnivora in Herculaneum, Missouri, region (E. C. Olson), 42
Catalogue of topographic and geologic maps of Virginia. By Joseph K. Roberts and Robert O. Bloomer. Review by L. C. Glenn, 219
Cause of current in elliptical bays, South Carolina (C. W. Cooke), 210
Cavities in Joliet limestone, northeastern Illinois (J H. Bretz), 379
solution, in the Joliet limestone of northeastern Illinois (J H. Bretz), 337
Cavity fillings, composition of, Joliet limestone, northeastern Illinois (J H. Bretz), 365
Cayugan group in Little North Mountain, Virginia (R. S. Edmundson), 541
Cenozoic periods of deformation in San Acacia area, New Mexico (C. S. Denny), 101
time of faulting in southern California (W. J. Miller), 408
Cervidae in Herculaneum, Missouri, region (E. C. Olson), 55
Chamberlin, Rollin T. *Diastrophic behavior around the Bighorn Basin*, 673
Review of German-English science dictionary for students in the agricultural, biological, and physical sciences. By Louis de Vries, *et al.* 1022
Review of Notice sur les travaux scientifiques de M. Emm. de Margerie, 558
Cited on influence of pre-Cambrian rocks and structures upon deformation around Bighorn Basin (D. L. Blackstone, Jr.), 617
Changes, climatic, in southern High Plains (F. A. Melton), 136
evidences of postglacial, in sea-level, the peat deposits of Bermuda and (A. S. Knox), 767
Characteristics of minable coal of West Virginia. By A. J. W. Headlee and John P. Nolting, Jr. Review by C. W. Sternberg, 1024
Chelikowsky, J. R. *Tectonics of the rhyolite in the Mammoth embayment, California*, 421
Chelonia in Herculaneum, Missouri, region (E. C. Olson), 41
Chert in the Grenville marble, Ross township, Renfrew County, Ontario (W. A. Tarr and W. D. Keller), 196, 199
Chibougamau series older than Mistassini series, Quebec (G. W. H. Norman), 515
Chronology, glacial, weathered zones and, in southern Indiana (W. D. Thornbury), 449
Clapp, F. G. Cited on classification of silts of southwestern Indiana (W. D. Thornbury), 459
Clark, B. L. Cited on age of faulting in southern California (W. J. Miller), 410
Classification, tentative, of sand dunes and its application to dune history in southern High Plains (F. A. Melton), 112
Cleavage in calcareous shales (E. C. H. Lammers), 304
and composition of calcareous shales, relationship between (E. C. H. Lammers), 305
Clements, Thomas. *The Bogotá fault, Colombia, South America*, 660
Climatic changes in southern High Plains (F. A. Melton), 136
succession during Tertiary time of western Mohave area (D. I. Axelrod), 528
Clinton formation, Little North Mountain, Virginia (R. S. Edmundson), 541
Cloos, Ernst and Hans. Cited on pre-Cambrian structure of Bighorn uplift (R. T. Chamberlin), 703
Cited on structure of Pryor Mountains, Montana (D. L. Blackstone, Jr.), 617
Coconino Plateau, Grand Canyon district (J. H. Maxson), 740
Co-existence in equilibrium of calcite, dolomite, and quartz (N. L. Bowen), 236
of larnite and spurrite (N. L. Bowen), 234

Colombia, South America, The Bogotá fault (T. Clements), 660

Colubridae in Herculaneum, Missouri, region (E. C. Olson), 41

Columnar jointing in dikes and sills, Hawaii (C. K. Wentworth and A. E. Jones), 993

"Common loess" in Indiana (W. D. Thornbury), 459

Comparison of Indiana glacial stratigraphy with that of Illinois (W. D. Thornbury), 467

Complex dune forms in southern High Plains (F. A. Melton), 130

Composition of cavity fillings, Joilet limestone, northeastern Illinois (J H. Bretz), 365
and cleavage of calcareous shales, relationship between (E. C. H. Lammers), 305
of gravels below basalt, Yellowstone Valley, Montana (L. Horberg), 286
of metamorphosed, siliceous, dolomitic limestone (N. L. Bowen), 235

Conditions favorable for development of elliptical lakes in South Carolina (C. W. Cooke), 210

Conglomerate dikes, Draper Mountain area in Virginia (B. N. Cooper and J. C. Haff), 957

Connections and shapes of solution cavities in Joliet limestone, northeastern Illinois (J H. Bretz), 340

Contact and endomorphic phenomena associated with a part of the Idaho batholith (A. L. Anderson and V. Hammerand), 561

Contributions to the paleobotany of Middle and South America. By Edward W. Berry. Review by Louise Barton Freeman, 112

Cooke, C. Wythe. *Elliptical bays in South Carolina and the shape of eddies*, 205

Cooper, Byron N. Geology of the Draper Mountain area, Virginia. Review by Louise Barton Freeman, 1024
and John C. Haff. *Max Meadows fault breccia*, 945

Cornish, V. Cited on formation of sand dunes (F. A. Melton), 122
Cited on dune topography (F. A. Melton), 132
Cited on relation between low and ball (O. F. Evans), 491
Cited on subaqueous ridges along British coast (O. F. Evans), 476, 480

Cornucopia, Oregon, dilation and replacement dikes of (G. E. Goodspeed), 176

Correlations and stratigraphy in the Birch–Slate Lakes district, northwestern Ontario (J. D. Bateman), 619
within Birch–Slate Lakes area, Ontario (J. D. Bateman), 632

Corylus in Bermuda (A. S. Knox), 774

Courses, summer field, in geology (R. P. Sharp), 310

Crazy Mountain Basin, Wyoming (R. T. Chamberlin), 682

Crestmore, California, merwinite from (N. L. Bowen), 252

Cricetidae in Herculaneum, Missouri, region (E. C. Olson), 46

Crocodilia in Herculaneum, Missouri, region (E. C. Olson), 42

Crocodilidae in Herculaneum, Missouri, region (E. C. Olson), 42

Croneis, Carey. Review of Foraminifera, their classification and economic use. By Joseph A. Cushman, 552
Review of Geological expedition to the Lesser Sunda Islands under the leadership of H. A. Brouwer, Vol. I, 553
Review of Index of paleozoic coral genera. By W. D. Lang, Stanley Smith, and H. D. Thomas, 781
Review of Manuel de paléontologie animale. By Léon Moret, 670

Crooked Creek fault, Montana (D. L. Blackstone, Jr.), 603

Cross section showing breccia along Max Meadows fault, Virginia (B. N. Cooper and J. C. Haff), 957

Cross sections demonstrating relation of subsurface fracturing to surface folding (D. L. Blackstone, Jr.), 609
geologic, Big Pryor Mountain, Montana (D. L. Blackstone, Jr.), 608
geologic, Dryhead fault area, Montana (D. L. Blackstone, Jr.), 607
geologic, of Little North Mountain, Virginia (R. S. Edmundson), 546
geologic, of Sykes Spring area, Wyoming (D. L. Blackstone, Jr.), 608

Cross winds in windrifts (complex) in southern High Plains (F. A. Melton), 134

Crotolidae in Herculaneum, Missouri, region (E. C. Olson), 41

Crush conglomerate, description of, Draper Mountain area, Virginia (B. N. Cooper and J. C. Haff), 964
distribution of, Draper Mountain area, Virginia (B. N. Cooper and J. C. Haff), 953

Crystalline, pre-Cambrian, rocks of north-central Utah (A. J. Eardley and R. A. Hatch), 58

Currents, rotating, figure assumed by (C. W. Cooke), 208

Currier, L. W. Cited on breccias near Draper Mountain area, Virginia (B. N. Cooper and J. C. Haff), 971

Curry, H. Donald. Cited on Furnace Creek formation, California (D. I. Axelrod), 527

Cushman, Joseph A. Foraminifera. Their classification and economic use. Review by Carey Croneis, 552

Dalloni, M. Géologie appliquée de l'Algérie. Review by Louise Barton Freeman, 558

Daly, R. A. Cited on depth of eolian limestone (A. S. Knox), 769

Dana, E. S. Cited on formation of helictites (L. C. Huff), 651

Darcy, Henry. Cited on method involved in ground-water motion experiment (M. K. Hubbert), 791
experiments on flow of ground water (M. K. Hubbert), 787

Darcy's law for gases (M. K. Hubbert), 823

Date of discovery of metamorphic minerals (N. L. Bowen), 264

Death Valley, California, a record of Lyonothamnus *in* (D. I. Axelrod), 526
wind-fluting in (J. H. Maxson), 726

De Beaumont, Elie. Cited on origin of lows and balls (O. F. Evans), 503

Decarbonation, progressive, as progressive metamorphism (N. L. Bowen), 232

Deep Creek Ridge fault, Montana (L. Horberg), 280

Deep well near Wasco, California, metamorphism of sediments of the, and of the deeply buried Eocene sediments near Ventura, California (J. B. Lyons), 436

Deeply buried Eocene sediments near Ventura, California, metamorphism of sediments of the deep well near Wasco, California, and of the (J. B. Lyons), 436

Deformation in cavity walls, Joliet limestone, northeastern Illinois (J H. Bretz), 357
of fault blocks, southern California (W. J. Miller), 404
of fillings, Joliet limestone, northeastern Illinois (J H. Bretz), 367
relation of plasticity and cleavage to (W. J. Mead), 1013

Denny, Charles S. *Tertiary geology of the San Acacia area, New Mexico*, 73

Depositional basins, Santa Fe formation, New Mexico (C. S. Denny), 94

Deposits, the peat, of Bermuda and evidences of postglacial changes in sea-level (A. S. Knox), 767

Depth of peat and postglacial time, Bermuda (A. S. Knox), 776

Descriptive petrography of the igneous rocks, a. By Albert Johanssen. Review by N. L. Bowen, 219

Detailed structure, Pryor Mountains, Montana (D. L. Blackstone, Jr.) 603

Development of lesser folds around Bighorn Basin, Wyoming (R. T. Chamberlin), 710
of ranges and basins in Beartooth-Bighorn region (R. T. Chamberlin), 701

Devonian of Pennsylvania, the. By Bradford Willis. Review by Louise Barton Freeman, 784

Devonshire marsh, Bermuda (A. S. Knox), 771

De Vries, Louis, *et al.* German English science dictionary for students in the agricultural, biological, and physical sciences. Review by R. T. Chamberlin, 1022

Diabase dikes in Pacific Northwest (G. E. Goodspeed), 175

Diastrophic behavior around the Bighorn Basin (R. T. Chamberlin), 673

Differentiation of substages of Wisconsin till in Indiana (W. D. Thornbury), 452

Digest of summer field courses in geology (R. P. Sharp), 310

Dike and sill thicknesses, distribution of (C. K. Wentworth and A. E. Jones), 984

Dikes, dilation and replacement (G. E. Goodspeed), 175
and sills of Koolau Range, Hawaii (C. K. Wentworth and A. E. Jones), 980
Dilation and replacement dikes (G. E. Goodspeed), 175
Diopside, formation of (N. L. Bowen), 243
Discovery of metamorphic minerals, date of (N. L. Bowen), 264
Discussion: Geology along the southern margin of the Absaroka Range, Wyoming (C. M. Bauer), 324
A note on pressure stylolites (E. S. Bastin), 214
Displacement markings in and on cavity walls, Joliet limestone, northeastern Illinois (J H. Bretz), 352
Displacements, horizontal, of faults, magnitude of, in southern California (W. J. Miller), 397
Distribution of fault breccia in Draper Mountain area, Virginia (B. N. Cooper and J. C. Haff), 949
of intrusive rocks, Oahu (C. K. Wentworth and A. E. Jones), 980
District, Birch–Slate Lakes, northwestern Ontario, stratigraphy and correlations in the (J. D. Bateman), 619
Dolomite formation, Quebec (G. W. H. Norman), 517
progressive metamorphism of siliceous limestone and (N. L. Bowen), 225
Draper Mountain, Virginia (B. N. Cooper and J. C. Haff), 945
Drill hole, world's deepest, at Wasco, California (J. B. Lyons), 436
Dryhead fault, Montana (D. L. Blackstone, Jr.), 603
Dune forms, simple, in southern High Plains (F. A. Melton), 115
history in the southern High Plains, a tentative classification of sand dunes and its application to (F. A. Melton), 113
systems of different age in southern High Plains (F. A. Melton), 137
Dunes, sand, a tentative classification of, and its application to dune history in the southern High Plains (F. A. Melton), 113
Dyer, W. S. Cited on geologic sequence east of Slate Lake, Ontario (J. D. Bateman), 635
Eardley, A. J., and R. A. Hatch. *Pre-Cambrian crystalline rocks of north-central Utah*, 58
Early basic breccias of Yellowstone Park, Montana (L. Horberg), 283
Pleistocene age of Mammoth embayment, California (J. R. Chelikowsky), 431
Wisconsin (Bull Lake) substage of glaciation, Yellowstone Valley, Montana (L. Horberg), 296
Eastern shore of Lake Michigan, the low and ball of the (O. F. Evans), 476
Eaton, J. E. Cited on faulting in southern California (W. J. Miller), 398, 400, 409, 413, 414
Echelon faulting in Bighorn Basin (R. T. Chamberlin), 693
Eddies, the shape of, and elliptical bays in South Carolina (C. W. Cooke), 205
Edmundson, Raymond S. *Origin of Little North Mountain in northern Virginia*, 532
Effect of temperature and pressure upon fluid properties (M. K. Hubbert), 898
of temperature on velocity of shear waves at high pressure (F. Birch and D. Bancroft), 760
Effects of weather and exposure on dikes and sills, Hawaii (C. K. Wentworth and A. E. Jones), 1001
Eitel, W. Cited on dolomite-dissociation curve (N. L. Bowen), 268, 271
Elasticity at 1 atmosphere (F. Birch and D. Bancroft), 761
Elbrook formation, Draper Mountain area, Virginia (B. N. Cooper and J. C. Haff), 946
Elevation of the fluid interface (M. K. Hubbert), 868
Elliptical bays in South Carolina and the shape of eddies (C. W. Cooke), 205
Ells, R. W. Cited on geology of Ross township and adjacent areas, Ontario (W. A. Tarr and W. D. Keller), 197
"Elongate-blowout" dunes (simple) in southern High Plains (F. A. Melton), 127
Elsinore fault, southern California (W. J. Miller), 388
Embayment, Mammoth, California, tectonics of the rhyolite in the (J. R. Chelikowsky), 421

Emigrant Creek, Montana (L. Horberg), 280

Emmons, William H. Principles of economic geology. Review by E. S. Bastin, 446

Endomorphic phenomena, contact and, associated with a part of the Idaho batholith (A. L. Anderson and V. Hammerand), 561

English, W. A. Cited on faulting in southern California (W. J. Miller), 394, 408

Enstatite, formation of (N. L. Bowen), 240

The Eo-Cambrian series of the Tana district, northern Norway. By Sven Føyn. Review by Raymond E. Janssen, 108

Eocene (?) rocks, New Mexico (C. S. Denny), 75
sand, Wilcox, Shreveport, Louisiana (L. B. Roberts), 212
sediments, deeply buried, near Ventura, California, metamorphism of the, and of sediments of the deep well near Wasco, California (J. B. Lyons), 436
time of central Wyoming (C. M. Bauer), 325

Equidae in Herculaneum, Missouri, region (E. C. Olson), 48

Equus in Herculaneum, Missouri, region (E. C. Olson), 38

Erosion, the role of mud balls in (H. S. Bell), 28
surfaces, Yellowstone Valley, Montana (L. Horberg), 286

Eskola, Pentti. Cited on metamorphism of siliceous magnesian limestone (N. L. Bowen), 226, 274

Evans, O. F. *The low and ball of the eastern shore of Lake Michigan*, 476

Evidences of postglacial changes in sea-level, the peat deposits of Bermuda and (A. S. Knox), 767

Extent of Mistassini fault zone, Quebec (G. W. H. Norman), 525
regional, and direction of present-day active sand movement in southern High Plains (F. A. Melton), 141

Eyles, V. A., and Joan M. On the different issues of the first geologic map of England and Wales. Review by A. O. Woodford, 220

Faceting, fluting and, of rock fragments (J. H. Maxson), 717
rate of (J. H. Maxson), 723

Facies of metamorphic minerals (N. L. Bowen), 272

Farmington Canyon complex (A. J. Eardley and R. A. Hatch), 61

Fault, the Bogotá, Colombia, South America (T. Clements), 660
blocks, deformation of, in southern California (W. J. Miller), 404
breccia, Max Meadows (B. N. Cooper and J. C. Haff), 945
trends, southern California (W. J. Miller), 391
-zone occurrences in Draper Mountain area, Virginia (B. N. Cooper and J. C. Haff), 955

Faulting in southern California, some features of (W. J. Miller), 385
thrust, of Grenville gneisses northwestward against the Mistassini series of Mistassini Lake, Quebec (G. W. H. Norman), 512

Faults, major, in southern California (W. J. Miller), 386
minor, in southern California (W. J. Miller), 389

Fauna, a late Pleistocene, from Herculaneum, Missouri (E. C. Olson), 32

Features, field and petrographic, of dikes in Pacific Northwest (G. E. Goodspeed), 194
some, of faulting in southern California (W. J. Miller), 385

Felidae in Herculaneum, Missouri, region (E. C. Olson), 45

Ferguson, R. N. Cited on faulting in southern California (W. J. Miller), 399, 413

Field courses, summer, in geology (R. P. Sharp), 310
and petrographic features of dikes in Pacific Northwest (G. E. Goodspeed), 194

Flaxville Plain, Yellowstone Valley, Montana (L. Horberg), 288

Fleury, Ernest. Cited on arabesque limestones in Portugal (J. H. Maxson), 745
Cited on wind erosional forms in Portugal (J. H. Maxson), 725

Florida Ship Canal (M. K. Hubbert), 934

Floristic succession during Tertiary time of western Mohave area (D. I Axelrod), 528

Flow across an interface (M. K. Hubbert), 873
cleavage (W. J. Mead), 1010
from point-source and line-source (M. K. Hubbert), 848
structure of rhyolite protrusions, Mammoth embayment, California (J. R. Chelikowsky), 422
Flowage, rock, folding and foliate structures: studies for students (W. J. Mead), 1007
Flowers, gypsum, artificial helictites and (L. C. Huff), 641
Flute formation, mechanics of (J. H. Maxson), 728
Fluting and faceting of rock fragments (J. H. Maxson), 717
Folding, narrow zones of, in Bighorn Basin (R. T. Chamberlin), 693
rock flowage, and foliate structures: studies for students (W. J. Mead), 1007
Foliate structures, folding, rock flowage and: studies for students (W. J. Mead), 1007
structures, interpretation of (W. J. Mead), 1017
Foraminifera, their classification and economic use. By Joseph A. Cushman. Review by Carey Croneis, 552
"Foredunes," Lake Michigan (F. A. Melton), 123
Foreland behavior around Bighorn Basin (R. T. Chamberlin), 697
Formation of gumbotil, rate of, Indiana (W. D. Thornbury), 473
Formations outcropping in Pryor Mountains, Montana (D. L. Blackstone, Jr.), 593
Forsterite, formation of (N. L. Bowen), 240
Foshag, W., and E. S. Larsen. Cited on wollastonite and merwinite (N. L. Bowen), 252
Føyn, Sven. The Eo-Cambrian series of the Tana district, northern Norway. Review by Raymond E. Janssen, 108
Fracture cleavage (W. J. Mead), 1009
Fragments, rock, fluting and faceting of (J. H. Maxson), 717
Freeman, B. C. Cited on replacement shells around batholiths, Quebec (A. L. Anderson and V. Hammerand), 586, 589
Freeman, Louise Barton. Review of Conservation in the United States. By A. F. Gustafson *et al.*, 559
Review of Contributions to the paleobotany of Middle and South America. By Edward W. Berry, 112
Review of The Devonian of Pennsylvania. By Bradford Willard, 784
Review of Geologic map and guide of Oahu, Hawaii. By H. T. Stearns, 672
Review of Géologie appliquée de l'Algérie. By M. Dalloni, 558
Review of Geology and allied sciences: a thesaurus, Part I: German-English. By Walther Huebner, 219
Review of Geology of the Draper Mountain area, Virginia. By Byron N. Cooper, 1024
Review of The geology of the Kaitangata–Green Island subdivision, eastern and central Otago divisions. By M. Ongley, 1022
Review of The geology of the Naseby subdivision, central Otago. By J. H. Williamson, 1022
Review of Geology of North America, Vol. I. Rudolf Ruedemann and Robert Balk (eds.), 221
Review of Highway geology, Philadelphia to Pittsburgh. By Bradford Willard, 335
Review of Leaves and stems from fossil forests. By Raymond E. Janssen, 112
Review of Limestones of West Virginia. By John B. McCue, John B. Lucke, and Herbert P. Woodward, 333
Review of On the geology and tectonics of the Outakumpu ore field and region. By Heikki Väyrynen, 333
Review of Petrography and correlation of deep-well sections in West Virginia and adjacent states. By James H. C. Martens, 336
Review of The physiographic provinces of North America. By Wallace W. Atwood, 1023
Review of The pre-Cambrian–Cambrian succession: the general and economic geology of these systems in portions of South Australia. By Ralph W. Segnit, 672
Review of Soil conservation. By Hugh Hammon Bennett, 560
Review of A source book in geology. By Kirtley F. Mather and Shirley L. Mason, 107

Review of Studies on the Ice Age in India and associated human cultures. By H. de Terra and T. T. Patterson, 110

Fuller, M. L. Cited on classification of silts of southwestern Indiana (W. D. Thornbury), 459

Furnace Creek, California (D. I. Axelrod), 526

Furse, G. D. Cited on correlations within Birch–Slate Lakes area, Ontario (J. D. Bateman), 633

Gallatin Range, Montana (L. Horberg), 276

Gardner, James H. Cited on origin of mud balls (H. S. Bell), 3

Garlock fault, southern California (W. J. Miller), 386

Geologic cross sections of Little North Mountain, Virginia (R. S. Edmundson), 546
features of Idaho batholith (A. L. Anderson and V. Hammerand), 564
history of Little North Mountain, Virginia (R. S. Edmundson), 542
map and guide of Oahu, Hawaii. By H. T. Stearns. Review by Louise Barton Freeman, 672
sequence east of Slate Lake, Ontario (J. D. Bateman), 634
sequence west of Slate Lake district, Ontario (J. D. Bateman), 636
studies of Koolau Range, Oahu (C. K. Wentworth and A. E. Jones), 976
work, early, in the Birch–Slate Lakes district, Ontario (J. D. Bateman), 627

Geological expedition to the lesser Sunda Islands under the leadership of H. A. Brouwer, Vol. I. Review by Carey Croneis, 553

Géologie appliquée de l'Algérie. By M. Dalloni. Review by Louise Barton Freeman, 558

Geology and allied sciences: A thesaurus, Part I: German-English. By Walther Huebner. Review by Louise Barton Freeman, 219
along the southern margin of the Absaroka Range, Wyoming: discussion (C. M. Bauer), 324
of Bogotá, South America (T. Clements), 662
of the Draper Mountain area, Virginia. By Byron N. Cooper. Review by Louise Barton Freeman, 1024
and engineering. By Robert F. Legget. Review by W. C. Krumbein, 218
glacial, and geomorphic problems of the Yellowstone Valley, Park County, Montana (L. Horberg), 275
of Herculaneum, Missouri, region (E. C. Olson), 32
of the Kaitangata–Green Island subdivision, eastern and central Otago divisions. By M. Ongley. Review by Louise Barton Freeman, 1022
of the Naseby subdivision, central Otago. By J. H. Williamson. Review by Louise Barton Freeman, 1022
of North America, Vol. I. Rudolf Ruedemann and Robert Balk (eds.) Review by Louise Barton Freeman, 221
of Renfrew County, Ontario (W. A. Tarr and W. D. Keller), 197
summer field courses in (R. P. Sharp), 310
Tertiary, of the San Acacia area, New Mexico (C. S. Denny), 73
of the Uchi–Slate Lakes area, Ontario (J. D. Bateman), 630

Geomorphic problems and glacial geology of the Yellowstone Valley, Park County, Montana (L. Horberg), 275

Geosynclinal behavior around Bighorn Basin (R. T. Chamberlin), 695

German-English science dictionary for students in the agricultural, biological, and physical sciences. By Louis de Vries *et al.* Review by R. T. Chamberlin, 1022

Ghijben, Badon. Cited on ground-water motion (M. K. Hubbert), 924

Gilbert, G. Cited on geologic sequence west of Slate Lake, Ontario (J. D. Bateman), 636

Gilbert, G. K. Cited on origin of lows and balls, Lake Michigan (O. F. Evans), 501
Cited on stream-fluting in Grand Canyon (J. H. Maxson), 718
Cited on wind erosion in Colorado (J. H. Maxson), 724

Giles, A. W. Cited on structure of Little North Mountain, Virginia (R. S. Edmundson), 534, 548

Glacial chronology, weathered zones and, in southern Indiana (W. D. Thornbury), 449
geology and geomorphic problems of the Yellowstone Valley, Park County, Montana (L. Horberg), 275

Glenn, L. C. Review of Catalogue of topographic and geologic maps of Virginia. By Joseph K. Roberts and Robert O. Bloomer, 219

"Gliding" breakers, Lake Michigan (O. F. Evans), 505

Gneisses, metamorphosed injection in north-central Utah (A. J. Eardley and R. A. Hatch), 67

thrust faulting of Grenville, northwestward against the Mistassini series of Mistassini Lake, Quebec (G. W. H. Norman), 512

Goldschmidt, V. M. Cited on rock metamorphism (N. L. Bowen), 226, 229, 268

Goodspeed, G. E. *Dilation and replacement dikes*, 175

Graben structure, and horst in San Acacia area, New Mexico (C. S. Denny), 101

Granitic dikes in Pacific Northwest (G. E. Goodspeed), 184

Granodiorite of Idaho batholith (A. L. Anderson and V. Hammerand), 578

origin of (A. L. Anderson and V. Hammerand), 584

Gravels and overlying basalt, Yellowstone Valley, Montana (L. Horberg), 285

Greig, J. W. Cited on geology of Birch–Slate Lakes district, Ontario (J. D. Bateman), 630

Grenville gneisses, thrust faulting of, northwestward against the Mistassini series of Mistassini Lake, Quebec (G. W. H. Norman), 512

marble, chert in the, Ross township, Renfrew County, Ontario (W. A. Tarr and W. D. Keller), 198

subprovince, Quebec (G. W. H. Norman), 521

Gresswell, R. Ray. Cited on subaqueous ridges along British coast (O. F. Evans), 476

Ground-water flow near the water table (M. K. Hubbert), 926

motion, the theory of (M. K. Hubbert), 785

Grout, F. F. Kemp's handbook of rocks. Review by F. J. Pettijohn, 557

Guadalupe formation, South America (T. Clements), 663

Guaduas formation, South America (T. Clements), 664

Guise, C. H., *et al.* Conservation in the United States. Review by Louise Barton Freeman, 559

Gumbotil, rate of formation of, Indiana (W. D. Thornbury), 473

Gustafson, A. F., *et al.* Conservation in the United States. Review by Louise Barton Freeman, 559

Gutenberg, B. Internal constitution of the earth. Review by H. W. Straley, III, 108

Gypsum flowers, artificial helictites and (L. C. Huff), 641

Haff, John C., and Byron N. Cooper. *Max Meadows fault breccia*, 945

Hamilton, W. J., Jr., *et al.* Conservation in the United States. Review by Louise Barton Freeman, 559

Hammerand, Veral, and Alfred L. Anderson. *Contact and endomorphic phenomena associated with a part of the Idaho batholith*, 561

Harding, W. D. Cited on correlations within Birch–Slate Lakes area, Ontario (J. D. Bateman), 633

Harris, T. F. Cited on faulting in South Carolina (W. J. Miller), 394, 417

Hartnack, Wilhelm. Cited on lows and balls on shores of Baltic Sea (O. F. Evans), 479, 492

Hatch, R. A. and A. J. Eardley. *Pre-Cambrian crystalline rocks of north-central Utah*, 58

Hayford, J. F. Cited on changes in water-level on Great Lakes (O. F. Evans), 500

Headlee, A. J. W., and John P. Nolting, Jr. Characteristics of minable coal of West Virginia. Review by C. W. Sternberg, 1024

Helderberg limestone in Little North Mountain, Virginia (R. S. Edmundson), 542

Helictites, artificial, and gypsum flowers (L. C. Huff), 641

Henderson, L. H. Cited on faulting in southern California (W. J. Miller), 390

Herculaneum, Missouri, a late Pleistocene fauna from (E. C. Olson), 32

Herzberg, Baurat. Cited on ground-water motion (M. K. Hubbert), 924

Hess, H. H. Cited on analysis of anorthosite (F. Birch and D. Bancroft), 754

High pressure, new measurements of the rigidity of rocks at (F. Birch and D. Bancroft), 752

Highway geology, Philadelphia to Pittsburgh. By Bradford Willard. Review by Louise Barton Freeman, 335

Hills, E. Sherborn. The physiography of Victoria. Review by C. W. Sternberg, 1023

Hoffman, M. G. Cited on geology of Paradise Ridge, Idaho (A. L. Anderson and V. Hammerand), 562, 564, 566

Hollister, J. S. Cited on faulting in southern California (W. J. Miller), 394

Hoots, H. W. Cited on faulting in southern California (W. J. Miller), 401, 409

Horberg, Leland. *Geomorphic problems and glacial geology of the Yellowstone Valley, Park County, Montana*, 275

Horizontal displacements of faults, magnitude of, in southern California (W. J. Miller), 397

Hornblende-biotite diorite of Idaho batholith (A. L. Anderson and V. Hammerand), 569
  origin of (A. L. Anderson and V. Hammerand), 582

Horry County, South Carolina, elliptical bays in (C. W. Cooke), 205

Horsethief Cave, Illinois (J H. Bretz), 346, 353

Horst and graben structure, San Acacia area, New Mexico (C. S. Denny), 101

Hovey, H. C. Cited on formation of artificial helictites and gypsum flowers (L. C. Huff), 647, 656

Hubbert, M. King. *The theory of groundwater motion*, 785

Huebner, Walther. Geology and allied sciences: a thesaurus, Part I: German-English. Review by Louise Barton Freeman, 49

Huff, Lyman C. *Artificial helictites and gypsum flowers*, 641

Hunt, A. R. Cited on action of waves on sea-beaches and sea-bottoms (O. F. Evans), 501, 504

Hydrothermal replacement in Idaho batholith, role of (A. L. Anderson and V. Hammerand), 585
  in exomorphism and endomorphism, Idaho batholith (A. L. Anderson and V. Hammerand), 586

Ice-margin channels, Yellowstone Valley, Montana (L. Horberg), 298

Idaho batholith, contact and endomorphic phenomena associated with a part of the (A. L. Anderson and V. Hammerand), 561

Igneous rocks, metamorphosed silicic in north-central Utah (A. J. Eardley and R. A. Hatch), 65

Illinoian soils, buried, and weathered zones, Indiana (W. D. Thornbury), 455

Illinois, northeastern, solution cavities in the Joliet limestone of (J H. Bretz), 337

Index of Paleozoic coral genera. By W. D. Lang, Stanley Smith, and H. D. Thomas. Review by Carey Croneis, 781

Indiana glacial stratigraphy compared with that of Illinois (W. D. Thornbury), 467
  southern, weathered zones and glacial chronology in (W. D. Thornbury), 449

Inhomogeneous fluids, boundaries between (M. K. Hubbert), 858

Inshore sand masses as subaqueous dunes, Lake Michigan (O. E. Fvans), 497
  zone, studies of, Lake Michigan (O. F. Evans), 496

Internal constitution of the earth. B. Gutenberg (ed.). Review by H. W. Straley, III, 108

Interpretation of pattern of regional trends, Mammoth embayment, California (J. R. Chelikowsky), 432

Intersecting transverse dune series (complex) in southern High Plains (F. A. Melton), 131

Intrusion, mechanics of (C. K. Wentworth and A. E. Jones), 1004

Intrusive rocks of the leeward slope of the Koolau Range, Oahu (C. K. Wentworth and A. E. Jones), 975
  petrography of (C. K. Wentworth and A. E. Jones), 977
  structure of (C. K. Wentworth and A. E. Jones), 977

Ireland, Scawt Hill, metamorphic minerals at (N. L. Bowen), 226, 265

Iron formation, Temiscamie River, Quebec (G. W. H. Norman), 520
oxide, petrified wood composed of (L. B. Roberts), 212

Isofaciality of rocks (N. L. Bowen), 273

Isolated transverse dune ridges (simple) in southern High Plains (F. A. Melton), 119
age of (F. A. Melton), 137

Janssen, Raymond E. Leaves and stems from fossil forests. Review by Louise Barton Freeman, 112
Review of Ash formations of the Island, Hawaii. By Chester K. Wentworth, 111
Review of The Eo-Cambrian series of the Tana District, northern Norway. By Sven Føyn, 108
Review of Marine *algae, coelenterata, annelida, echinodermata, crustacea,* and *mollusca*. By Lee Boone, 220
Review of Moskenesøy: a study in high latitude Cirque Lakes. By Kaare Münster Strøm, 107.
Review of On a second collection of fossils and rocks from Kenya made by Miss M. McKinnon Wood. Monographs of the Geology Department of the Hunterian Museum, Glasgow University, 334
Review of Stratigraphy and paleontology of the lower Mississippian of Missouri, Part II. By various authors, 332

Johannsen, Albert. A descriptive petrography of the igneous rocks, Vol. I. Review by N. L. Bowen, 219

Johnson, Douglas. Cited on origin of lake basins, South Carolina (C. W. Cooke), 207
Cited on origin of submarine canyons (M. K. Hubbert), 931

Johnson, D. W. Cited on shore processes and shoreline development (O. F. Evans), 480, 503, 504, 505

Johnson, G. Duncan. Cited on structure of Pryor Mountains, Montana (D. L. Blackstone, Jr.), 597, 612, 613

Joliet limestone of northeastern Illinois, solution cavities of (J H. Bretz), 337

Jones, Austin E., and Chester K. Wentworth. *Intrusive rocks of the leeward slope of the Koolau Range, Oahu,* 975

Juniata formation, Little North Mountain, Virginia (R. S. Edmundson), 541

Jurassic period of Sierra batholith, California (J. R. Chelikowsky), 430

Kay, G. F. Cited on formation of gumbotil, Indiana (W. D. Thornbury), 473
Cited on leaching during Sangamon time (W. D. Thornbury), 471

Keewatin age of Birch–Slate Lakes district, Ontario (J. D. Bateman), 619

Keith, Arthur. Cited on "Potomac marble" (E. S. Bastin), 215

Keller, W. D., and W. A. Tarr. *Chert in the Grenville marble, Ross township, Renfrew County, Ontario,* 196

Kellogg, James R. Cited on subaqueous ridges off coast of Louisiana (O. F. Evans), 478, 492

Kemp's handbook of rocks. By F. F. Grout. Review by F. J. Pettijohn, 557

Kendall, P. F. Cited on glacial geology of Yellowstone Valley, Montana (L. Horberg), 299

Kerr, P. F. Cited on sediments from Ventura Basin, California (J. B. Lyons), 437, 438, 442

Kew, W. S. W. Cited on faulting in southern California (W. J. Miller), 394, 396, 408

Kindle, E. M. Cited on ridges of Chesapeake Bay (O. F. Evans), 477, 492

Knox, Arthur S. *The peat deposits of Bermuda and evidences of postglacial changes in sea-level,* 767

Koch, T. W. Cited on Buena Vista thrust fault, California (W. J. Miller), 412

Koolau Range, Oahu, the intrusive rocks of the leeward slope of the (C. K. Wentworth and A. E. Jones), 975

Krumbein, W. C. Review of Geology and engineering. By Robert F. Leggett, 217

Lagomorpha in Herculaneum, Missouri, region (E. C. Olson), 47

"Lake beds," Tertiary, in western Montana (L. Horberg), 283

Lake Cynthiana, Indiana (W. D. Thornbury), 466
Michigan, the low and ball of the eastern shore of (O. F. Evans), 476

Mistassini, Quebec, thrust faulting of Grenville gneisses northwestward against the Mistassini series of (G. W. H. Norman), 512
silts and loess of southern Indiana (W. D. Thornbury), 459
Lakes, Birch–Slate, district, northwestern Ontario, stratigraphy and correlations in the (J. D. Bateman), 619
elliptical, in South Carolina (C. W. Cooke), 210
Lammers, Edward C. H. *Cleavage in calcareous shales*, 304
Cited on pre-Cambrian control of Laramide structures in Beartooth Range (R. T. Chamberlin), 704
Land sculpture of Little North Mountain, Virginia (R. S. Edmundson), 549
Lang, W. D., *et al.* Index of Paleozoic Coral Genera. Review by Carey Croneis, 781
Larnite, formation of (N. L. Bowen), 233
Larsen, E. S., and W. Foshag. Cited on wollastonite and merwinite (N. L. Bowen), 252
Latah County, Idaho (A. L. Anderson and V. Hammerand), 562
Late Pleistocene fauna from Herculaneum, Missouri, a (E. C. Olson), 32
Wisconsin (Pinedale) substage of glaciation, Yellowstone Valley, Montana (L. Horberg), 301
Laudermilk, J. D. Cited on fluting and faceting of rock fragments (J. H. Maxson), 746
"Law" of Badon Ghijben and Herzberg (M. K. Hubbert), 924
Leaching during Sangamon and post-Wisconsin time, Indiana (W. D. Thornbury), 470
during Sangamon time, Indiana (W. D. Thornbury), 459
Leaves and stems from fossil forests. By Raymond E. Janssen. Review by Louise Barton Freeman, 112
Lee dunes (simple) in southern High Plains (F. A. Melton), 120
Leeward slope of the Koolau Range, Oahu, the intrusive rocks of the (C. K. Wentworth and A. E. Jones), 975
Lehigh quarry, Joliet limestone, northeastern Illinois (J H. Bretz), 338
Legget, Robert F. Geology and engineering. Review by W. C. Krumbein, 217
Lehmann, F. W. P. Cited on lows and balls on shores of Baltic Sea (O. F. Evans), 479
Leighton, M. M. Cited on glacial stratigraphy in Illinois (W. D. Thornbury), 468
Cited on soil profiles, southern Illinois (W. D. Thornbury), 449
Leporidae in Herculaneum, Missouri, region (E. C. Olson), 47
Leucocratic dike of Pacific Northwest (G. E. Goodspeed), 182
Limestone breccia, distribution of, Draper Mountain area in Virginia (B. N. Cooper and J. C. Haff), 952
caverns as evidence of submergence of Bermuda (A. S. Knox), 770
Joliet, of northeastern Illinois, solution cavities in the (J H. Bretz), 337
siliceous, and dolomite, progressive metamorphism of (N. L. Bowen), 225
Limestones of West Virginia. By John B. McCue, John B. Lucke, and Herbert P. Woodward. Review by Louise Barton Freeman, 333
Little North Mountain in northern Virginia, origin of (R. S. Edmundson), 532
Livingston, William. Cited on evidence of submergence of Bermuda (A. S. Knox), 771
Lobeck, A. K. Cited on formation of helictites (L. C. Huff), 648, 649
Local peculiarities of lows and balls, Lake Michigan (O. F. Evans), 482
Location of marble, Renfrew County, Ontario (W. A. Tarr and W. D. Keller), 197
Loess and lake silts of southern Indiana (W. D. Thornbury), 459
or lake silt upon leached Illinoian drift, Indiana (W. D. Thornbury), 463
Longitudinal dunes (simple) in southern Plains (F. A. Melton), 121
Love, John David. Cited on geology along the southern margin of the Absaroka Range, Wyoming (C. M. Bauer), 324
Low and ball of the eastern shore of Lake Michigan, the (O. F. Evans), 476
Lower Devonian formations of Little North Mountain, Virginia (R. S. Edmundson), 542

Lucke, John B., John B. McCue, and Herbert P. Woodward. Limestones of West Virginia. Review by Louise Barton Freeman, 333

Lyonothamnus, *a record of, in Death Valley, California* (D. I. Axelrod), 526

Lyons, John B. *Metamorphism of sediments of the deep well near Wasco, California, and of the deeply buried Eocene sediments near Ventura, California*, 436

MacClintock, Paul. Cited on breaking of waves (O. F. Evans), 505
Cited on pre-Illinoian drift (W. D. Thornbury), 454
Cited on soil profiles, southern Illinois (W. D. Thornbury), 449

McCue, John B., John B. Lucke, and Herbert P. Woodward. Limestones of West Virginia. Review by Louise Barton Freeman, 333

Mafic rocks, metamorphosed in north-central Utah (A. J. Eardley and R. A. Hatch), 69

Major faults, southern California (W. J. Miller), 386

Mammoth embayment, California, tectonics of the rhyolite in the (J. R. Chelikowsky), 421

Manoa Valley, Oahu (C. K. Wentworth and A. E. Jones), 984

Manuel de paléontologie animale. By Léon Moret. Review by Carey Croneis, 670

Map, area in vicinity of Herculaneum, Missouri (E. C. Olson), 90
areal geology of Pryor Mountains, Montana, Wyoming (D. L. Blackstone, Jr.), 598, 599, 600, 601
areal relations of thrust sheets and associated tectonic rocks, Draper Mountain area, Virginia (B. N. Cooper and J. C. Haff), 950, 951
of central Indiana showing depth of carbonates (W. D. Thornbury), 453
of fissure eruptions, Mammoth embayment, California (J. R. Chelikowsky), 424
of flow structure of rhyolite protrusions, Mammoth embayment, California (J. R. Chelikowsky), 422
geologic, of Dryhead fault area, Carbon County, Montana (D. L. Blackstone, Jr.), 602
geologic, of north-central Utah (A. J. Eardley and R. A. Hatch), 59
geologic, of parts of Park and Gallatin counties, Montana (L. Horberg), 277
geologic, of Rice Lake–Lake St. Joseph schist belt, Ontario (J. D. Bateman), 621
geologic, of San Acacia area, New Mexico (C. S. Denny), 78
geologic, of Paradise Ridge, Latah County, Idaho (A. L. Anderson and V. Hammerand), 563
geologic sketch, of Uchi–Slate Lakes area, Ontario (J. D. Bateman), 622
of glacial deposits and generalized areal geology, Yellowstone Valley, Montana (L. Horberg), 281
index, of Mistassini Lake, Quebec (G. W. H. Norman), 513
index, showing location of Draper Mountain area, Virginia (B. N. Cooper and J. C. Haff), 946
isopach, showing thickness of Paleozoic and Mesozoic strata in western Wyoming (R. T. Chamberlin), 675
of lithological characteristics of Santa Fe and surrounding formations, New Mexico (C. S. Denny), 88
paleogeographic of San Acacia area, New Mexico (C. S. Denny), 97
of Palolo-Waialae and Manoa-Makiki areas of Honolulu portion of leeward slope of Koolau Range, Oahu (C. K. Wentworth & A. E. Jones), 981
of past and present distribution of *Lyonothamnus* in California and Nevada (D. I. Axelrod), 527
of principal areas of active or modern sand dunes in southern High Plains (F. A. Melton), 171
of prominent thrust faults in western Wyoming (R. T. Chamberlin), 677
of Rio Grande depression, New Mexico (C. S.Denny), 85
showing extent of Little North Mountain, Virginia (R. S. Edmundson), 533
showing geology of Mistassini Lake region, Quebec((G. W. H. Norman), 516
showing location of principal areas of anchored sand dunes in southern High Plains (F. A. Melton), 172
showing locations of cross sections in Frederick and northern Shenandoah counties, Virginia (R. S. Edmundson), 533
sketch, of the Island of Oahu (C. K. Wentworth and A. E. Jones), 978

of southern California showing most important faults (W. J. Miller), 387
of terraces along Yellowstone Valley, Montana (L. Horberg), 289
tectonic sketch of Bighorn-Beartooth–Wind River area showing strips of reversed asymmetry (R. T. Chamberlin), 681
tectonic sketch, of Pryor Mountains, Montana, and adjacent areas (D. L. Blackstone, Jr.), 591

Marble, Grenville, chert in the, Ross township, Renfrew County, Ontario (W. A. Tarr and W. D. Keller), 196

Margin, the southern, of the Absaroka Range, Wyoming, geology along: discussion (C. M. Bauer), 324

Marine *algae, coelenterata, annelida, echinodermata, crustacea,* and *mollusca.* By Lee Boone. Review by R. E. Janssen, 220

Markings, displacement, in and on cavity walls in Joliet limestone, northeastern Illinois (J H. Bretz), 352

"Marl-loess" in Indiana (W. D. Thornbury), 459

Marshes, existing, as evidence of submergence of Bermuda (A. S. Knox), 771

Martens, James H. C. Petrography and correlation of deep-well sections in West Virginia and adjacent states. Review by Louise Barton Freeman, 336

de Martonne, Emmanuel. Cited on transverse sand ridges (F. A. Melton), 119

Mason, Shirley L., and Kirtley F. Mather. A source book in geology. Review by Louise Barton Freeman, 107

Mather, Kirtley F., and Shirley L. Mason. A source book in geology. Review by Louise Barton Freeman, 107

Max Meadows fault breccia (B. N. Cooper and J. C. Haff), 945
thickness of (B. N. Cooper and J. C. Haff), 955
thrust sheet, rocks of (B. N. Cooper and J. C. Haff), 948

Maxson, John H. *Fluting and faceting of rock fragments,* 717

Mead, W. J. *Studies for students: Folding, rock flowage, and foliate structures,* 1007
Cited on formation of folds (R. T. Chamberlin), 698

Meadows, Max, fault breccia (B. N. Cooper and J. C. Haff), 945

Measurements of lows and balls, Lake Michigan (O. F. Evans), 484
new, of the rigidity of rocks at high pressure (F. Birch and D. Bancroft), 752

Mechanics of flute formation (J. H. Maxson), 728
of intrusion (C. K. Wentworth and A. E. Jones), 1004

Mechanism of replacement dikes in Pacific Northwest (G. E. Goodspeed), 185

Megalonychidae in Herculaneum, Missouri, region (E. C. Olson), 45

Megalonyx in Herculaneum, Missouri, region (E. C. Olson), 38

Melton, Frank A. *A tentative classification of sand dunes: its application to dune history in the southern High Plains,* 113
and William Schriever. Cited on hypothesis of origin of sand ridges and bays, South Carolina (C. W. Cooke), 205

Merrill, G. P. Cited on formation of gypsum flowers (L. C. Huff), 656
Cited on formation of helictites (L. C. Huff), 647, 650

Merwinite, formation of (N. L. Bowen), 252

Mesozoic beds, Yellowstone Valley, Montana (L. Horberg), 279

Metamorphic minerals (N. L. Bowen), 259

Metamorphism, progressive, of siliceous limestone and dolomite (N. L. Bowen), 225

Michigan, Lake, the low and ball of the eastern shore of (O. F. Evans), 476

Middle Cambrian time of Draper Mountain area, Virginia (B. N. Cooper and J. C. Haff), 946
Mississippian time of Draper Mountain area, Virginia (B. N. Cooper and J. C. Haff), 946

Migration of subaqueous ridges, Lake Michigan (O. F. Evans), 500

Miller, William J. *Some features of faulting in southern California,* 385

Mineral relations, significance of, in Idaho batholith (A. L. Anderson and V. Hammerand), 582

Minerals, metamorphic (N. L. Bowen) 259

Minor faults, southern California (W. J. Miller), 389
folds in Rocky Mountain foreland area (R. T. Chamberlin), 695
Miocene lavas of Columbia River in Pacific Northwest (G. E. Goodspeed), 176
(?) rocks, New Mexico (C. S. Denny), 76
time of faulting in southern California (W. J. Miller), 408
Missouri, Herculaneum, a late Pleistocene fauna from (E. C. Olson), 32
Mistassini fault zone, extent of, Quebec (G. W. H. Norman), 525
Lake, Quebec, thrust faulting of Grenville gneisses northwestward against the Mistassini series of (G. W. H. Norman), 512
Modern dune movements in southern High Plains (F. A. Melton), 137
Moencopi Plateau, Arizona (F. A. Melton), 121
Mohave Desert wedge, southern California (W. J. Miller), 405
Montana, structure of the Pryor Mountains (D. L. Blackstone, Jr.), 590
geomorphic problems and glacial geology of the Yellowstone Valley, Park County (L. Horberg), 275
Monticellite, formation of (N. L. Bowen), 249
Moret, Léon. Manuel de paléontologie animale. Review by Carey Croneis, 670
Morphology of rhyolite field, Mammoth embayment, California (J. R. Chelikowsky), 423
Moskenesøy: a study in high latitude Cirque Lakes. By Kaare Münster Strøm. Review by Louise Barton Freeman, 107
Motion, the theory of ground-water (M. K. Hubbert), 785
Mountain, Little North, in northern Virginia, origin of (R. S. Edmundson), 532
Mountains, Pryor, Montana, structure of the (D. L. Blackstone, Jr.), 590
Mud balls, armored (H. S. Bell), 1
origin of (H. S. Bell), 1, 3
shells of (H. S. Bell), 26
size of (H. S. Bell), 10
sphericity of (H. S. Bell), 14
Mustelidae in Herculaneum, Missouri, region (E. C. Olson), 45
Mylohyus in Herculaneum, Missouri, region (E. C. Olson), 38
Myrica in Bermuda (A. S. Knox), 773
Natural helictites composed of calcite (L. C. Huff), 659
"Nested elongate-blowout" dune series in southern High Plains (F. A. Melton), 128
age of (F. A. Melton), 137
New measurements of the rigidity of rocks at high pressure (F. Birch and D. Bancroft), 752
Niagaran limestone of Illinois (J H. Bretz), 337
Niggli, P. Cited on equilibrium in carbonate melts (N. L. Bowen), 270
Noble, L. F. Cited on faults in southern California (W. J. Miller), 386, 393, 397
Nolting, John P., Jr. and A. J. W. Hendlee. Characteristics of minable coal of West Virginia. Review by C. W. Sternberg, 1024
Normal and thrust faulting, importance of, in southern California (W. J. Miller), 392
Norman, G. W. H. *Thrust faulting of Grenville gneisses northwestward against the Mistassini series of Mistassini Lake, Quebec*, 512
North-central Utah, pre-Cambrian crystalline rocks of (A. J. Eardley and R. A. Hatch), 58
North Mountain, Little, in northern Virginia, origin of (R. S. Edmundson), 532
Pryor fault, Montana (D. L. Blackstone, Jr.), 597
Northeastern Illinois, solution cavities in the Joliet limestone of (J H. Bretz), 337
Northern Virginia, origin of Little North Mountain in (R. S. Edmundson), 532
Northwestern Ontario, stratigraphy and correlations in the Birch–Slate Lakes district (J. D. Bateman), 619
Northwestward against the Mistassini series of Mistassini Lake, Quebec, thrust faulting of Grenville gneisses (G. W. H. Norman), 512
Note on pressure stylolites, a: discussion (E. S. Bastin), 214
Notice sur les travaux scientifiques de M. Emm. de Margerie. Reivew by R. T. Chamberlin, 558

Oahu, intrusive rocks of the leeward slope of the Koolau Range (C. K. Wentworth and A. E. Jones), 975
Oblique longitudinal dunes (complex) in southern High Plains (F. A. Melton), 134
windrift dune (complex) in southern High Plains (F. A. Melton), 135
Offshore-bar, low and ball the forerunner of, Lake Michigan (O. F. Evans), 503
movement of sediment as cause for low and ball, Lake Michigan (O F. Evans), 509
Oligocene—early Pliocene age of Tertiary basins, southwestern Montana (L. Horberg), 279
time of Absaroka Range, Wyoming (C. M. Bauer), 326
Olson, Everett Claire. *A late Pleistocene fauna from Herculaneum, Missouri*, 32
On a second collection of fossils and rocks from Kenya made by Miss M. McKinnon Wood. Monographs of the Geology Department of the Hunterian Museum, Glasgow University. Review by Raymond E. Janssen, 334
One-direction asymmetry in Bighorn-Beartooth–Wind River area, Wyoming (R. T. Chamberlin), 681
Ongley, M. The geology of the Kaitangata–Green Island subdivision, eastern and central Otago divisions. Review by Louise Barton Freeman, 1022
Ontario, chert in the Grenville marble, Ross township, Renfrew County (W. A. Tarr and W. D. Keller), 196
northwestern, stratigraphy and correlations in the Birch–Slate Lakes district (J. D. Bateman), 619
On the different issues of the first geological map of England and Wales. By V. A. Eyles and Joan M. Eyles. Review by A. O. Woodford, 220
the geology and tectonics of the Outokumpu ore field and region. By Heikki Väyrynen. Review by Louise Barton Freeman, 333
Ordovician age of calcareous shales, Valley of Virginia (E. C. H. Lammers), 304
Origin and behavior of breakers, Lake Michigan (O. F. Evans), 505
of elliptical bays, South Carolina (C. W. Cooke), 205
of fault breccia, Draper Mountain area, Virginia (B. N. Cooper and J. C. Haff), 969
of Little North Mountain in northern Virginia (R. S. Edmundson), 532
of lows and balls, Lake Michigan (O. F. Evans), 501
of rock types, Idaho batholith (A. L. Anderson and V. Hammerand), 582
of solution cavities in Joliet limestone, northeastern Illinois (J H. Bretz), 379
Oriskany sandstone in Little North Mountain, Virginia (R. S. Edmundson), 542
Oswego sandstone, Little North Mountain, Virginia (R. S. Edmundson), 540
Otto, Theodor. Cited on lows and balls on shores of Baltic Sea (O. F. Evans), 479, 491
Owl Creek. Bridger Range, Wyoming (R. T. Chamberlin), 680
Oxide, iron, petrified wood composed of (L. B. Roberts), 212

Paige, Sidney. Cited on effect of sea-level canal on ground water of Florida (M. K. Hubbert), 935
Paleography, Santa Fe formation, New Mexico (C. S. Denny), 96
Paleozoic sediments, Yellowstone Valley, Montana (L. Horberg), 275
Palmer, H. S. Cited on dikes and sills of Honolulu district (C. K. Wentworth and A. E. Jones), 976, 993
Palolo dike, Oahu (C. K. Wentworth and A. E. Jones), 986
Valley (C. K. Wentworth and A. E. Jones), 987
"Parabolic" or "blowout" dune (simple) in southern High Plains (F. A. Melton), 126
Paradise Ridge, Idaho (A. L. Anderson and V. Hammerand), 561
Park County, Montana, the Yellowstone Valley, geomorphic problems and glacial geology of (L. Horberg), 275
Part of the Idaho batholith, contact and endomorphic phenomena associated with a (A. L. Anderson and V. Hammerand), 561

Passarge, Siegfred. Cited on lows and balls on shores of Baltic Sea (O. F. Evans), 479

Patterson, T. T., and H. de Terra. Studies on the Ice Age in India and associated human cultures. Review by Louise Barton Freeman, 110

Patton, L. T. Cited on philosophical aspects of summer field courses in geology (R. P. Sharp), 310, 311

"Peak and fulje" topography of sand dunes, southern High Plains (F. A. Melton), 131

Peat of Bermuda, physical character of (A. S. Knox), 773
bogs and buried cedar trees as evidence of submergence of Bermuda (A. S. Knox), 770
deposits of Bermuda and evidences of postglacial changes in sea-level, the (A. S. Knox), 767

Peculiarities, local, of lows and balls, Lake Michigan (O. F. Evans), 482

Pegmatites of Idaho batholith (A. L. Anderson and V. Hammerand), 579
origin of (A. L. Anderson and V. Hammerand), 584

Pegmatitic dikes of Pacific Northwest (G. E. Goodspeed), 176

Pembroke marsh, Bermuda (A. S. Knox), 771

Pennsylvanian time of northeastern Illinois (J H. Bretz), 382

Peorian loess, Iowa (W. D. Thornbury), 461

Periclase, formation of (N. L. Bowen), 247

Permeabilities and porosities of sediments near Wasco, California (J. B. Lyons), 440

Permeability in ground-water motion (M. K. Hubbert), 915

Perrett, Frank A. The volcano-seismic crisis at Montserrat, 1933–37. Review by C. H. Behre, Jr., 449

Petrified wood composed of iron oxide (L. B. Roberts), 212

Petrographic description of Max Meadows fault breccias in Draper Mountain area, Virginia (B. N. Cooper and J. C. Haff), 960
and field features of dikes in Pacific Northwest (G. E. Goodspeed), 194

Petrography and correlation of deep-well sections in West Virginia and adjacent states. By James H. C. Martens. Review by Louise Barton Freeman, 336
of Grenville marble in Ontario (W. A. Tarr and W. D. Keller), 201
of Idaho batholith (A. L. Anderson and V. Hammerand), 566
of Koolau Range, Oahu (C. K. Wentworth and A. E. Jones), 977

Petrology of Idaho batholith (A. L. Anderson and V. Hammerand), 582

Pettijohn, F. J. Review of Kemp's handbook of rocks. By F. F. Grout, 557
Cited on stratigraphy of Lake Superior region (J. D. Bateman), 619, 637

Phenomena, endomorphic, contact and, associated with a part of the Idaho batholith (A. L. Anderson and V. Hammerand), 561

Phyllite breccia, description of, Draper Mountain area, Virginia (B. N. Cooper and J. C. Haff), 963
breccia, distribution of, Draper Mountain area, Virginia (B. N. Cooper and J. C. Haff), 952

Physiographic provinces of North America, the. By Wallace W. Atwood. Review by Louise Barton Freeman, 1023

Physiography of Koolau Range, Oahu (C. K. Wentworth and A. E. Jones), 977
of Victoria, the. By E. Sherborn Hills. Review by C. W. Sternberg, 1023

Piezometric surface in ground-water practice (M. K. Hubbert), 909

Pirsson, L. V. Cited on geology of Bermuda Islands (A. S. Knox), 768

Plains, southern High, a tentative classification of sand dunes and its application to dune history in (F. A. Melton), 112

Plastic deformation (rock flow) (W. J. Mead), 1012

Plasticity and cleavage, relation of, to deformation (W. J. Mead), 1013

Pleistocene age of river crossings, northeastern Illinois (J H. Bretz), 382
changes of sea-level in Bermuda (A. S. Knox), 767
a late, fauna from Herculaneum, Missouri (E. C. Olson), 32
terrace material, Bogotá, South America (T. Clements), 666

"Plunging" breakers, Lake Michigan (O. F. Evans), 505
Poisson's ratio computed for certain rocks (F. Birch and D. Bancroft), 761
Popotosa formation, New Mexico (C. S. Denny), 77
age and correlation of (C. S. Denny), 81
origin of (C. S. Denny), 81
Porosities and permeabilities of sediments near Wasco, California (J. B. Lyons), 440
Porphyry dikes in Pacific Northwest (G. E. Goodspeed), 178
Postglacial changes in sea-level, evidences of, the peat deposits of Bermuda and (A. S. Knox), 767
time in Bermuda, estimate of (A. S. Knox), 778
Post-Oligocene deformation in Absaroka Range, Wyoming (C. M. Bauer), 326
Post-Wisconsin and Sangamon leaching in Indiana (W. D. Thornbury), 470
"Potomac marble" (E. S. Bastin), 214, 215
Powder River Basin, Wyoming (R. T. Chamberlin), 680
Pre-Cambrian age of Mistassini strata, Quebec (G. W. H. Norman), 521
—Cambrian succession: the general and economic geology of these systems, in portions of South Australia. By Ralph W. Segnit. Review by Louise Barton Freeman, 672
chert in Ontario (W. A. Tarr and W. D. Keller), 196
correlations, Birch–Slate Lakes district, Ontario (J. D. Bateman), 623
crystalline rocks, Montana (L. Horberg), 275
crystalline rocks of north-central Utah (A. J. Eardley and R. A. Hatch), 58
nomenclature, Birch–Slate Lakes district, Ontario (J. D. Bateman), 623
succession of the Mistassini region, Quebec (G. W. H. Norman), 514
Pre-Illinoian drift, Indiana, search for (W. D. Thornbury), 454
Pre-Oligocene surface, Yellowstone Valley, Montana (L. Horberg), 286
Pre-Pennsylvanian topography of Joliet limestone, northeastern Illinois (J H. Bretz), 384
Pre-Tertiary rocks, New Mexico (C. S. Denny), 75
rocks in Pacific Northwest (G. E. Goodspeed), 176
Pre-Wisconsin glaciation of Yellowstone Valley, Montana (L. Horberg), 295
Present-day fault activity in southern California (W. J. Miller), 411
Pressure, high, new measurements of the rigidity of rocks at (F. Birch and D. Bancroft), 752
range used in studies on rocks (F. Birch and D. Bancroft), 752
stylolites, a note on: discussion (E. S. Bastin), 214
-temperature curves in metamorphism of limestone and dolomite (N. L. Bowen), 267
Pressures and temperatures in deep well near Wasco, California (J. B. Lyons), 440
Principles of economic geology. By William H. Emmons. Review by E. S. Bastin, 446
Problems, geomorphic and glacial geology of the Yellowstone Valley, Park County, Montana (L. Horberg), 275
Procyon lotor (Linnaeus) in Herculaneum, Missouri, region (E. C. Olson), 44
Procyonidae in Herculaneum, Missouri, region (E. C. Olson), 44
Profiles, soil, in glacial drift in Indiana (W. D. Thornbury), 450
Progressive metamorphism of siliceous dolomite (N. L. Bowen), 235
metamorphism of siliceous limestone and dolomite (N. L. Bowen), 225
Pryor Mountains, Montana (R. T. Chamberlin), 682
Mountains, Montana, structure of (D. L. Blackstone, Jr.), 590
structure similar to ramp structure, Montana (D. L. Blackstone, Jr.), 616
Pulaski thrust sheet, Virginia (B. N. Cooper and J. C. Haff), 948

Quartz-biotite-diorite gneiss of Idaho batholith (A. L. Anderson and V. Hammerand), 573
origin of (A. L. Anderson and V. Hammerand), 584
gabbro of Idaho batholith (A. L. Anderson and V. Hammerand), 581
Quartzite in Idaho batholith (A. L. Anderson and V. Hammerand), 566

origin of, in Idaho batholith (A. L. Anderson and V. Hammerand), 583

Quaternary, early, and Tertiary features of Yellowstone Valley, Montana (L. Horberg), 283
time of faulting in southern California (W. J. Miller), 408

Quebec, thrust faulting of Grenville gneisses northwestward against the Mistassini series of Mistassini Lake (G. W. H. Norman), 512

Range, the Koolau, Oahu, the intrusive rocks of the leeward slope of (C. K. Wentworth and A. E. Jones), 975

Ranges and basins, development of, in Beartooth-Bighorn region (R. T. Chamberlin), 701

Rastall, R. H. Cited on sedimentary beds in England (J. B. Lyons), 443

Rate of faceting (J. H. Maxson), 723
of solution-faceting (J. H. Maxson), 744

Recent marine sediments. Parker D. Trask (ed.). Review by A. C. Tester, 328

Record of Lyonothamnus *in Death Valley, California, a* (D. I. Axelrod), 526

Reed, R. D. Cited on migration of dunes in southern High Plains (F. A. Melton), 125
Cited on Transverse Ranges, southern California (W. J. Miller), 407

Refraction of flowlines across boundaries between different media (M. K. Hubbert), 845
of fluid interface across a plane boundary between media of different permeabilities (M. K. Hubbert), 874

Regional extent and direction of present-day active sand movement in southern High Plains (F. A. Melton), 141
relations around Bighorn Basin (R. T. Chamberlin), 673
stresses in relation to fault features, southern California (W. J. Miller), 412
structural trends, Mammoth embayment, California (J. R. Chelikowsky), 430

Relation between depth and vesicularity (C. K. Wentworth and A. E. Jones), 992
between structure and vesicularity (C. K. Wentworth and A. E. Jones), 992
of vertical uplift to overthrusting, Pryor Mountains, Montana (D. L. Blackstone, Jr.), 615

Relationship between cleavage and composition of calcareous shales (E. C. H. Lammers), 305

Renfrew County, Ontario, chert in the Grenville marble of Ross township (W. A. Tarr and W. D. Keller), 196

Replacement dikes, dilation and (G. E. Goodspeed), 175

Retrogressive metamorphism of limestone and dolomite (N. L. Bowen), 265

Reversal of structural asymmetry in western Wyoming (R. T. Chamberlin), 679

Rhyolite ridges, departure of, from flow pattern of lava, Mammoth embayment, California (J. R. Chelikowsky), 434
tectonics of the, in the Mammoth embayment, California (J. R. Chelikowsky), 421, 423

Ridges mistaken for true balls, Lake Michigan (O. F. Evans), 498

Ries, H., *et al.* Conservation in the United States. Review by Louise Barton Freeman, 559

Rigidity of rocks at high pressure, new measurements of the (F. Birch and D. Bancroft), 752

Rio Grande of Santa Fe time, New Mexico (C. S. Denny), 96

River deposits, Santa Fe formation, New Mexico (C. S. Denny), 89

Roberts, Joseph K., and Robert O. Bloomer. Catalogue of topographic and geologic maps of Virginia. Review by L. C. Glenn, 219

Roberts, L. B. *Petrified wood composed of iron oxide*, 212

Rock Creek Canyon, Illinois (J H. Bretz), 338
flowage, folding, and foliate structures: studies for students (W. J. Mead), 1007
fragments, fluting and faceting of (J. H. Maxson), 717

Rocks, carbonate, thirteen steps in metamorphism of (N. L. Bowen), 255
at high pressure, new measurements of the rigidity of (F. Birch and D. Bancroft), 752

the intrusive, of the leeward slope of the Koolau Range, Oahu (C. K. Wentworth and A. E. Jones), 975
pre-Cambrian crystalline, of north-central Utah (A. J. Eardley and R. A. Hatch), 58
Rodentia in Herculaneum, Missouri, region (E. C. Olson), 46
Rome formation, Draper Mountain area, Virginia (B. N. Cooper and J. C. Haff), 946
phyllite, Draper Mountain area, Virginia (B. N. Cooper and J. C. Haff), 960
Roof blocks, detached, and slabs in Joliet limestone, northeastern Illinois (J H. Bretz), 348
Roofed cavities, Joliet limestone, northeastern Illinois (J H. Bretz), 344
Ross, C. S. Cited on metamorphism of sediments, Wasco, California (J. B. Lyons), 438
Ross township, Renfrew County, Ontario, chert in the Grenville marble of (W. A. Tarr and W. D. Keller), 196
Rotating currents, figure assumed by (C. W. Cooke), 208
Ruedemann, Rudolf, and Robert Balk (eds.). Geology of North America. Review by Louise Barton Freeman, 221
Ruptured asymmetric anticline with subsidiary thrusting, Pryor Mountains, Montana (D. L. Blackstone, Jr.), 606
Russell, I. C. Cited on lows and balls of Lake Michigan (O. F. Evans), 482, 492
Russell, J. S. Cited on wave of translation (O. F. Evans), 498, 504

Sage Creek fault zone, Montana (D. L. Blackstone, Jr.), 603
San Acacia area, New Mexico, Tertiary geology of (C. S. Denny), 73
Andreas fault, southern California (W. J. Miller), 386
Jacinto fault, southern California (W. J. Miller), 388
Joaquin Valley, California (J. B. Lyons), 436
Sand dunes, a tentative classification of, and its application to dune history in the southern High Plains (F. A. Melton), 113
Sandstone blocks, deformation of, in northeastern Illinois (J H. Bretz), 375
Sangamon interglacial stage in Indiana (W. D. Thornbury), 459
Santa Fe formation, New Mexico (C. S. Denny), 84
age and correlation of (C. S. Denny), 93
origin of (C. S. Denny), 94
structural relations of (C. S. Denny), 90
thickness of (C. S. Denny), 91
Santa Fe time, climate of, New Mexico (C. S. Denny), 99
Ynez fault, southern California (W. J. Miller), 389
Savage, T. E. Cited on subdivisions of Niagaran limestone of Illinois (J H. Bretz), 337
Sayles, Robert W. Cited on eolian limestones and interbedded fossil soils of Bermuda (A. S. Knox), 768
Scawt Hill, Ireland, metamorphic minerals at (N. L. Bowen), 226, 265
Schoewe, Walter H. Cited on formation of ridge-shaped ventifacts (J. H. Maxson), 735
Schriever, William, and F. A. Melton. Cited on hypothesis of origin of sand ridges and bays, South Carolina (C. W. Cooke), 205
Sciuridae in Herculaneum, Missouri, region (E. C. Olson), 47
Sculpture of rock fragments by stream erosion (J. H. Maxson), 718
of rock fragments by subaerial erosion (J. H. Maxson), 723
Sea-level, evidences of postglacial changes in, the peat deposits of Bermuda and (A. S. Knox), 767
Sections showing buried Illinoian drift, Indiana (W. D. Thornbury), 455
Sedimentary rocks, metamorphosed in north-central Utah (A. J. Eardley and R. A. Hatch), 63
Sedimentation of Little North Mountain, Virginia (R. S. Edmundson), 542
role of armored mud balls in (H. S. Bell), 1, 28
Sediments, deeply buried Eocene, near Ventura, California, metamorphism of the, and of sediments of the deep well near Wasco, California (J. B. Lyons), 436

from well near Wasco, California (J. B. Lyons), 437

Segnit, Ralph W. The pre-Cambrian—Cambrian succession: the general and economic geology of these systems, in portions of South Australia. Review by Louise Barton Freeman, 672

Series, Mistassini, of Mistassini Lake, Quebec, thrust faulting of Grenville gneisses northwestward against the (G. W. H. Norman), 512

Shales, calcareous, cleavage in (E. C. H. Lammers), 304

Shape of eddies and elliptical bays in South Carolina, the (C. W. Cooke), 205
of eddy compared with bays (C. W. Cooke), 210

Shapes and connections of solution cavities in Joliet limestone (J H. Bretz), 340

Sharp, Robert P. *Summer field courses in geology*, 310

Shaub, B. M. Cited on origin of stylolites (E. S. Bastin), 214

Shaw, E. W. Cited on loess and lake silts of southern Indiana (W. D. Thornbury), 460

Shear cleavage (W. J. Mead), 1010

Shelbyville moraine, Indiana (W. D. Thornbury), 454

Shore, eastern, of Lake Michigan, the low and ball of (O. F. Evans), 476

"Short Hills," Yellowstone Valley, Montana (L. Horberg), 288

Shrub-coppice dune cluster (complex) in southern High Plains (F. A. Melton), 134
dune (simple) in southern High Plains (F. A. Melton), 124

Sierra Nevada fault, southern California (W. J. Miller), 386

Significance of mineral relations of Idaho batholith (A. L. Anderson and V. Hammerand), 582
physical, of Darcy's law (M. K. Hubbert), 792

Silexite of Idaho batholith (A. L. Anderson and V. Hammerand), 581
origin of (A. L. Anderson and V. Hammerand), 584

Siliceous limestone and dolomite, progressive metamorphism of (N. L. Bowen), 225

Silurian formation, Little North Mountain, Virginia (R. S. Edmundson), 541

Simple dune forms in southern High Plains (F. A. Melton), 115

Slabs and detached roof blocks in Joliet limestone, northeastern Illinois (J H. Bretz), 348

Slichter, C. S. Cited on ground-water motion (M. K. Hubbert), 903, 904

Slickolites in Joliet limestone, northeastern Illinois (J H. Bretz), 353, 355

Slocom, A. W. Cited on Niagaran limestone, Illinois (J H. Bretz), 344

Slope, the leeward, of the Koolau Range, Oahu, the intrusive rocks of (C. K. Wentworth and A. E. Jones), 975

Smith, Stanley, *et al.* Index of Paleozoic coral genera. Review by Carey Croneis, 781

Soil conservation. By Hugh Hammond Bennett. Review by Louise Barton Freeman, 560
profiles in glacial drift in Indiana (W. D. Thornbury), 450

Solution cavities in the Joliet limestone of northeastern Illinois (J H. Bretz), 337

Solution-faceting (J. H. Maxson), 739
rate of (J. H. Maxson), 744

Solvent and time of solution of cleavage in calcareous shales (E. C. H. Lammers), 308

Soundings made across lows and balls, Lake Michigan (O. F. Evans), 489

Source book in geology, a. By Kirtley F. Mather and Shirley L. Mason. Review by Louise Barton Freeman, 107
—bordering lee dunes (complex) in southern High Plains (F. A. Melton), 134
—bordering lee dunes (simple) in southern High Plains (F. A. Melton), 122

South America, the Bogotá fault, Colombia (T. Clements), 660
Carolina, elliptical bays in, and the shape of eddies (C. W. Cooke), 205

Southern California, some features of faulting in (W. J. Miller), 385
High Plains, a tentative classification of sand dunes and its application to dune history in (F. A. Melton), 113

Indiana, weathered zones and glacial chronology in (W. D. Thornbury), 449
margin of the Absaroka Range, Wyoming, geology along the: discussion (C. M. Bauer), 324
Spilogale cf. *interrupta* (Rafinesque) in Herculaneum, Missouri, region (E. C. Olson), 45
Spurrite, formation of (N. L. Bowen), 232
Squamata in Herculaneum, Missouri, region (E. C. Olson), 41
Stearns, H. T. Geologic map and guide of Oahu, Hawaii. Review by Louise Barton Freeman, 672
Cited on geologic survey of Oahu (C. K. Wentworth and A. E. Jones), 977
Stearns, Norah Dowell. Cited on laboratory tests on physical properties of water-bearing materials (M. K. Hubbert), 919
Sternberg, C. W. Review of Characteristics of minable coal of West Virginia. By A. J. W. Headlee and John P. Nolting, Jr., 1024
Review of The physiography of Victoria. By E. Sherborn Hills, 1023
Stockdale, Paris B. Cited on impressed pebbles from European and Canadian localities (E. S. Bastin), 214
Straley, H. W. III. Review of Internal constitution of the earth. By B. Gutenberg (ed.), 108
Stratigraphy of Bogotá, South America (T. Clements), 663
and correlations in the Birch–Slate Lakes district, northwestern Ontario (J. D. Bateman), 619
of Draper Mountain area, Virginia (B. N. Cooper and J. C. Haff), 946
of Little North Mountain, Virginia (R. S. Edmundson), 537
and paleontology of the Lower Mississippian of Missouri, Part II. By various authors. Review by Raymond E. Janssen, 332
of Pryor Mountains, Montana (D. L. Blackstone, Jr.), 595
"Straw" stalactites (L. C. Huff), 643
Stream erosion as cause of sculpture of rock fragments (J. H. Maxson), 718
-faceting (J. H. Maxson), 721
-fluting (J. H. Maxson), 718
Structural asymmetry in western Wyoming, reversal of (R. T. Chamberlin), 679
geology of Pryor Mountains, Montana (D. L. Blackstone, Jr.), 596
section of deformed fill in cavity in Joliet limestone, northeastern Illinois (J. H. Bretz), 373
relations of Yellowstone Valley, Montana (L. Horberg), 276
relationships, Bogotá, South America (T. Clements), 666
section of Monserrate, South America (T. Clements), 667
sections of the San Acacia area, New Mexico (C. S. Denny), 78
significance of the Pryor relationships, Montana (D. L. Blackstone, Jr.), 612
Structure of Draper Mountain area, Virginia (B. N. Cooper and J. C. Haff), 946
of Farmington Canyon complex (A. J. Eardley and R. A. Hatch), 61
geologic, San Acacia area, New Mexico (C. S. Denny), 99
of Koolau Range, Hawaii (C. K. Wentworth and A. E. Jones), 977
of Little North Mountain, Virginia (R. S. Edmundson), 544
of Mistassini region, Quebec (G. W. H. Norman), 521
of the Pryor Mountains, Montana (D. L. Blackstone, Jr.), 590
of the rhyolite, Mammoth embayment, California (J. R. Chelikowsky), 427
Structures, foliate, folding, rock flowage and: studies for students (W. J. Mead), 1007
Studies on the Ice Age in India and associated human cultures. By H. de Terra and T. T. Patterson. Review by Louise Barton Freeman, 110
of profiles of soundings made across lows and balls, Lake Michigan (O. F. Evans), 489
for students: folding, rock flowage, and foliate structures (W. J. Mead), 1007
Stylolites, pressure, a note on: discussion (E. S. Bastin), 214
Subaerial erosion as cause of sculpture of rock fragments (J. H. Maxson), 723
Subaqueous ridges, migration of, Lake Michigan (O. F. Evans), 500
Submergence of Bermuda, topographical evidence of (A. S. Knox), 769
in modern time, evidence of, in Bermuda (A. S. Knox), 777

Substages of Wisconsin till in Indiana (W. D. Thornbury), 452
Summer field courses in geology (R. P. Sharp), 310
Surfaces, bare, of loose sand in complex dune forms, southern High Plains (F. A. Melton), 131
bare, of loose sand in simple dunes (F. A. Melton), 115
Swinnerton, A. C. Cited on caves of Bermuda (A. S. Knox), 770
Cited on ground-water motion (M. K. Hubbert), 927
Sykes Spring fault, Wyoming (D. L. Blackstone, Jr.), 603
Systems, dune, of different age in southern High Plains (F. A. Melton) 137

Tables of summer field courses in geology (R. P. Sharp), 313, 320
Taljaard, M. S. Cited on stream-faceted pebbles in South Africa (J. H. Maxson), 721
Tanupolama in Herculaneum, Missouri, region (E. C. Olson), 38
Tapirella in Herculaneum, Missouri, region (E. C. Olson), 38, 50
Tapiridae in Herculaneum, Missouri, region (E. C. Olson), 50
Tarr, R. S. Cited on postglacial submergence of Bermuda (A. S. Knox), 767
and W. D. Keller. *Chert in the Grenville marble, Ross township, Renfrew County, Ontario*, 196
Tayassuidae in Herculaneum, Missouri, region (E. C. Olson), 56
Tectonics of the rhyolite in the Mammoth embayment, California (J. R. Chelikowsky), 421
Temblor formation, California (J. B. Lyons), 436
Temperature of metamorphism of siliceous limestone and dolomite (N. L. Bowen), 226
range in study of effect of pressure on rigidity of rocks (F. Birch and D Bancroft), 752
Tentative classification of sand dunes and its application to dune history in the southern High Plains (F. A. Melton), 113
Terra, H. de, and T. T. Patterson. Studies on the Ice Age in India and associated human cultures. Review by Louise Barton Freeman, 110
Tertiary age of dikes in Pacific Northwest (G. E. Goodspeed), 175
age of Mammoth embayment, California (J. R. Chelikowsky), 431
basins of southwestern Montana (L. Horberg), 278
geology of the San Acacia area, New Mexico (C. S. Denny), 73
"lake beds," Yellowstone Valley, Montana (L. Horberg), 283
volcanic rocks (Miocene?), New Mexico (C. S. Denny), 76
Tester, A. C. Review of Recent marine sediments. By Parker D. Trask (ed.), 328
Theis, Charles V. Cited on ground-water motion (M. K. Hubbert), 902
Theory of ground-water motion, the (M. King Hubbert), 785
Thiem, G. Cited on method of measurement of permeability (M. K. Hubbert), 853
Thom, W. T., Jr., *et al.* Cited on alternating symmetry of Bighorn Range (R. T. Chamberlin), 680
Thomas, H. D., *et al.* Index of Paleozoic coral genera. Review by Carey Croneis, 781
Thornbury, William D. *Weathered zones and glacial chronology in southern Indiana*, 449
Thrust faulting, importance of, in southern California (W. J. Miller), 392
of Grenville gneisses northwestward against the Mistassini series of Mistassini Lake, Quebec (G. W. H. Norman), 512
Tilley, C. E. Cited on discovery of calcium orthosilicate (N. L. Bowen), 226
Time of solution and nature of solvent in cleavage in calcareous shales (E. C. H. Lammers), 309
Timiskaming subprovince, pre-Cambrian rocks of, Quebec (G. W. H. Norman), 514
Tonto Platform, Grand Canyon district (J. H. Maxson), 740
Topographical evidence of submergence of Bermuda (A. S. Knox), 769
Topography of Little North Mountain, Virginia (R. S. Edmundson), 535
Tower Falls, Yellowstone Park (L. Horberg), 285
"Transection type of blowout" dune in southern High Plains (F. A. Melton), 129

Transverse dune ridge (complex) in southern High Plains (F. A. Melton), 133
dune series in southern High Plains (F. A. Melton), 118
Ranges in southern California (W. J. Miller), 406
Trask, Parker D. (ed.). Recent marine sediments. Review by A. C. Tester, 328
Tremolite, formation of (N. L. Bowen), 237
Tricalcic silicate, formation of (N. L. Bowen), 255
Tuscarora sandstone, Little North Mountain, Virginia (R. S. Edmundson), 541
Types of dikes and sills, Oahu (C. K. Wentworth and A. E. Jones), 1004
Typical Grenville marble, Ontario (W. A. Tarr and W. D. Keller), 201

Uchi–Slate Lake unconformity, Ontario (J. D. Bateman), 632
Udden, J. A. Cited on solution-faceting of of rock fragments (J. H. Maxson), 739
Upland surface of crystalline rocks, Yellowstone, Valley, Montana (L. Horberg), 287
Upper Ordovician formations, Little North Mountain, Virginia (R. S. Edmundson), 540
Triassic age of "Potomac marble" (E. S. Bastin), 215
Urocyon sp. in Herculaneum, Missouri, region (E. C. Olson), 44
Utah, north-central, pre-Cambrian crystalline rocks of (A. J. Eardley and R. A. Hatch), 58

Validity, range of, of Darcy's law (M. K. Hubbert), 819
Valley, Death, California, a record of Lyonothamnus *in* (D. I. Axelrod), 526
of Virginia, shales in (E. C. H. Lammers), 304
Van Pelt, J. R. Cited on minor echelon folds (R. T. Chamberlin), 698
Variation of viscosity and specific conductivity for water with depth (M. K. Hubbert), 901
Varieties of foliate structures (W. J. Mead), 1009
Vaughan, F. E. Cited on faulting in southern California (W. J. Miller), 393
Väyrynen, Heikki. On the geology and tectonics of the Outokumpu ore field and region. Review by Louise Barton Freeman, 333
Velocity of shear waves at high pressure (F. Birch and D. Bancroft), 760
Ventura, California, metamorphism of the deeply buried Eocene sediments near, and of sediments of the deep well near Wasco, California (J. B. Lyons), 436
Verrill, A. E. Cited on postglacial submergence of Bermuda (A. S. Knox), 767, 769, 771, 777
Vertical movements of faults in southern California (W. J. Miller), 401
shear planes, Middle Rocky Mountain foreland area (R. T. Chamberlin), 704
Virginia, northern, origin of Little North Mountain in (R. S. Edmundson), 532
Volcanic rocks, Santa Fe formation, New Mexico (C. S. Denny), 90
Volcano-seismic crisis at Montserrat, 1933–37. By Frank A. Perrett. Review by C. H. Behre, Jr., 447

Wade, A. Cited on ventifacts in Nubian Desert (J. H. Maxson), 736
Waiakeakau Valley, Oahu (C. K. Wentworth and A. E. Jones), 986
Waldemar Christopher Brøgger, 1851–1940 (N. L. Bowen), 444
Wasco, California, metamorphism of sediments of the deep well near, and of the deeply buried Eocene sediments near Ventura, California (J. B. Lyons), 436
Washburne, C. W. Cited on relation of surficial folds to faults (D. L. Blackstone, Jr.), 616
Water table, the (M. K. Hubbert), 895
Wave of translation, Lake Michigan (O. F. Evans), 504
-tank studies at University of Oklahoma (O. F. Evans), 494
Weathered zones and glacial chronology in southern Indiana (W. D. Thornbury), 449
Weed, W. H. Cited on glacial features in Rocky Mountain (L. Horberg), 276
Well, the deep, near Wasco, California, metamorphism of sediments of, and and of the deeply buried Eocene sedi-

ments near Ventura, California (J. B. Lyons), 436
Weller, J. M. Cited on formation of artificial gypsum flowers (L. C. Huff), 657
Wentworth, Chester K. Ash formations of the Island, Hawaii. Review by Raymond E. Janssen, 111
and Austin E. Jones. *Intrusive rocks of the leeward slope of the Koolau Range, Oahu*, 975
Wheeler, W. H. Cited on relation between low and ball (O. F. Evans), 491
Cited on subaqueous ridges along British coast (O. F. Evans), 476, 480
"White Cliffs," Montana (L. Horberg), 284
Whitfield, C. J. Cited on migration of dunes (F. A. Melton), 117
Wilcox Eocene sand, Shreveport, Louisiana (L. B. Roberts), 212
Willard, Bradford. The Devonian of Pennsylvania. Review by Louise Barton Freeman, 784
Highway geology, Philadelphia to Pittsburgh. Review by Louise Barton Freeman, 335
Williamson, J. H. The geology of the Naseby subdivision, central Otago. Review by Louise Barton Freeman, 1022
Willis, Bailey. Cited on faulting in southern California (W. J. Miller), 393, 414, 415, 416
Cited on ramp structures in Dead Sea area (D. L. Blackstone, Jr.), 616
Willis, C. G. Cited on faulting in southern California (W. J. Miller), 399, 413
Wind erosion in sculpture of rock fragments (J. H. Maxson), 723
-faceting (J. H. Maxson), 734
-fluting in Death Valley, California (J. H. Maxson), 726
in conflict with vegetation (complex dune form) in southern High Plains (F. A. Melton), 134
in conflict with vegetation (simple dune form) in southern High Plains (F. A. Melton), 124
River Basin, Wyoming (C. M. Bauer), 327
River Basin, Wyoming (R. T. Chamberlin), 683
River Peneplain, Wyoming (C. M. Bauer), 325
River Range, Wyoming (C. M. Bauer), 325
—shadow dunes (simple) in southern High Plains (F. A. Melton), 120
—shadow lee dunes (complex) in southern High Plains (F. A. Melton), 133
"Windrift" dune (simple) in southern High Plains (F. A. Melton), 129
Wisconsin till in Indiana (W. D. Thornbury), 452
Wollastonite, formation of (N. L. Bowen), 227
Wood, H. O. Cited on faulting in southern California (W. J. Miller), 399
Wood, petrified, composed of iron oxide (L. B. Roberts), 212
Woodford, A. O. Review of On the different issues of the first geological map of England and Wales. By V. A. and Joan M. Eyles, 220
Cited on faulting in southern California (W. J. Miller), 394, 417
Cited on fluting and faceting of rock fragments (J. H. Maxson), 746
Woodward, Herbert P., John B. McCue, and John B. Lucke. Limestones of West Virginia. Review by Louise Barton Freeman, 333
Woody layers of peat in Bermuda, significance of (A. S. Knox), 775
Wright, J. F. Cited on stratigraphy of southeastern Manitoba (J. D. Bateman), 637
Wright, W. I. Cited on geologic sequence east of Slate Lake, Ontario (J. D. Bateman), 634
Wyoming, southern margin of the Absaroka Range, geology along the: discussion (C. M. Bauer), 324

Yellowstone Valley, Park County, Montana, geomorphic problems and glacial geology of the (L. Horberg), 275

Zenarthra in Herculaneum, Missouri, region (E. C. Olson), 45
Zones, weathered, and glacial chronology in southern Indiana (W. D. Thornbury), 449

8499 34